Final Report

Continuous, Wireless Monitoring of Sediment Flux within Streams on Military Installations

(ESTCP Project Number RC-200817)

Scott Hill, U.S. Army Aberdeen Test Center
Naiqian Zhang, Kansas State University
Ning Wang, Oklahoma State University
James Steichen, Kansas State University
Philip B. Woodford, Fort Riley
Hugh Westbury, Fort Benning

October 17, 2013

REPORT DOCUMENTATION PAGE

Form Approved
OMB No. 0704-0188

1. REPORT DATE *(DD-MM-YYYY)*	2. REPORT TYPE	3. DATES COVERED *(From - To)*
17-10-2013	Final Report	April 2008 to October 2013

4. TITLE AND SUBTITLE

Final Report: Continuous, Wireless Monitoring of Sediment Flux within Streams on Military Installations (ESTCP Project Number SI-200817)

5a. CONTRACT NUMBER
NA

5b. GRANT NUMBER
NA

5c. PROGRAM ELEMENT NUMBER
NA

6. AUTHOR(S)

Scott Hill, Carl Johnson, Steve McClung, Gerhard Grimm, Dr. Naiqian Zhang, Kevin X. Wang, Dr. Joseph Dvorak, Dr. Wei Han, Daniel Bigham, Dr. Linda Y. Zhang, Marvin Petingco, Darrell Oard, Dr. Ning Wang, Peyman Taher

5d. PROJECT NUMBER
SI-200817

5e. TASK NUMBER
NA

5f. WORK UNIT NUMBER
NA

7. PERFORMING ORGANIZATION NAME(S) AND ADDRESS(ES)

U.S. Army Aberdeen Test Center
Range Systems Technology Branch
400 Colleran Road
Aberdeen Proving Ground, MD 21005

Kansas State University
BAE Department
Seaton Hall, room 158
Manhattan, KS 66506

8. PERFORMING ORGANIZATION REPORT NUMBER
NA

9. SPONSORING / MONITORING AGENCY NAME(S) AND ADDRESS(ES)
U.S. Army Aberdeen Test Center
TEDT-AT-SLE
400 Colleran Road
Aberdeen Proving Ground, MD 21005

10. SPONSOR/MONITOR'S ACRONYM(S)
NA

11. SPONSOR/MONITOR'S REPORT NUMBER(S)
NA

12. DISTRIBUTION / AVAILABILITY STATEMENT
Approved for public release; distribution is unlimited

13. SUPPLEMENTARY NOTES
NA

14. ABSTRACT

A combined Suspended Solid Concentration (SSC)/flow velocity sensor and a three-tier wireless sensor network (WSN) were demonstrated at three military installations – Fort Riley, Fort Benning, and Aberdeen Proving Ground from 2010 to 2012. Twelve sensors were deployed to continuously monitored SSC. The SSC measurement range was found to be 0-5,000 mg/L and, in most cases, the SSC measurement error was limited within 10%. Fouling on optical lenses was reduced with an air-blast lens cleaning system embedded in the sensor, although maintenance of the system has presented a challenge. An algorithm for fouling and clogging correction was also developed for data post-processing. Data post-processing applied to a six-month SSC data showed that the sensor can be used in long-term natural water monitoring.

While measuring SSC, the sensor also measured flow velocity in the range of 0.125 – 4.5 m/s. In most cases, the error was limited below 20%. One of the velocity sensors was deployed at a USGS stream-gaging station. Through continuous velocity measurement over a one-year period, the measured point velocities were used to generate an index-rating curve, which was then used to estimate the mean velocity from measured point velocity. This experiment demonstrated the possibility of using both stage and point velocity measurements to provide better discharge estimation.

15. SUBJECT TERMS
Suspended Solid Concentration, sensor, water monitoring, flow velocity

16. SECURITY CLASSIFICATION OF:			17. LIMITATION OF ABSTRACT	18. NUMBER OF PAGES	19a. NAME OF RESPONSIBLE PERSON
a. REPORT	b. ABSTRACT	c. THIS PAGE	SAR	206	Scott A. Hill, TEDT-AT-SLE
Unclassified	Unclassified	Unclassified			19b. TELEPHONE NUMBER *(include area code)* (410) 278-1878

Standard Form 298 (Rev. 8-98)
Prescribed by ANSI Std. Z39.18

Table of Contents

List of Acronyms

ADC:	Analog-to-digital Converter
ADCP:	Acoustic Doppler Current Profiler
AERTA:	Army Environmental Requirements and Technology Assessments
AMI:	Advanced Manufacturing Institute
AnN:	Anita Leight Near
AnF:	Anita Leight Far
APG:	Aberdeen Proving Ground
ATC:	Aberdeen Test Center
BMP:	Best Management Practice
BRAC:	Base Realignment and Closure
CAD:	Computer-aided Design
CDMA:	Code Division Multiple Access
CF:	Compact Flash
CFD:	Computational Fluid Dynamics
CNC:	Computer Numerical Control
CV:	Coefficient of Variation
CWA:	Clean Water Act
DAQ:	Data Acquisition System
DC:	Direct Current
DLR:	Data Loss Rate
DoD:	Department of Defense
EPA:	Environment Protection Agency
ESTCP:	Environmental Security Technology Certification Program
FHSS:	Frequency Hopping Spread Spectrum
GA:	Georgia
GMS:	Global System for Mobile Communications
I/O:	Input/Output
IP:	Internet Protocol
IR:	Infra-red
KS:	Kansas
KSU:	Kansas State University
LED:	Light Emitting Diode
LK:	Little Kitten Creak
LRCN:	Long-range Cellular Network
LWSN:	Local Wireless Sensor Network
MATLAB:	Matrix Laboratory
MBC:	Meteor Burst Communication
MD:	Maryland
MRWN:	Mid-range Wireless Network
MTBF:	Mean Time Before Failures
NOF:	Number of Failures
NPDES:	National Pollutant Discharge Elimination System
NPS:	Non-point Source
NTU:	Nephelometric Turbidity Unit

ORA:	Orange
OSU:	Oklahoma State University
PCB:	Printed Circuit Board
PkN:	Pine Knot North
PkS:	Pine Knot South
PNO:	Percentage of Normal Operation
PT:	Phototransistor
PVC:	Polyvinyl Chloride
RMSE:	Root-mean-square Error
RSSI:	Received Signal Strength Indicator
SERDP:	Strategic Environmental Research Development Program
SSC:	Suspended Solids Concentration
TCP:	Transmission Control Protocol
TMDL:	Total Maximum Daily Load
TSS:	Total Suspended Solids
UpN:	Upatoi North
UpS:	Upatoi South
USGS:	United States Geological Survey
WC:	Wildcat Bridge
WebGIS:	Web-based Geographic Information System
WSN:	Wireless Sensor Network

List of Figures

List of Tables

Acknowledgement

The authors thank the U.S. Department of Defense's Environmental Security Technology Certification Program (ESTCP) for financial sponsorship of this project. Specific appreciation is extended to Dr. Jeffrey Marqusee, Executive Director and Dr. John Hall, Program Manager, Resource Conservation and Climate Change, and the ESTCP support office staff for their assistance with both technical and administrative matters throughout this project. Additional appreciation is extended to the U.S. Army installation staff at Fort Benning, GA and Fort Riley KS, and the staff at Anita C. Leight Estuary Center, Abingdon, MD for allowing us to demonstrate the technology at their sites.

The contributing authors of this report are:

Kansas State University

Dr. Naiqian Zhang, Professor

Kevin X. Wang, Graduate Research Assistant, Ph.D. Candidate

Dr. Joseph Dvorak, Former Graduate Research Assistant

Dr. Wei Han, Former Graduate Research Assistant

Daniel Bigham, Former Graduate Research Assistant

Dr. Linda Y. Zhang, Former Graduate Research Assistant

Marvin Petingco, Former Graduate Research Assistant

Darrell Oard, Former Engineering Technician

Oklahoma State University

Dr. Ning Wang, Associate Professor

Peyman Taher, Former Graduate Research Assistant

U.S. Army Aberdeen Test Center

Scott Hill, Principle Investigator

Carl Johnson, Associate Technologist

Steve McClung, Former Principle Investigator

Gerhard Grimm, Former Principle Investigator

Executive Summary

Training activities on ranges are adversely impacting the environment. Vehicle traffic on unpaved roads and tank trails causes extensive erosion that results in reduced water quality because of increased sediment loads. Currently, the Army does not have a way to continuously and directly monitor suspended solids concentration (SSC) in streams. In this demonstration project, twelve sensors that are designed to simultaneously measure SSC and flow velocity were deployed at three military installations – Fort Riley in Kansas, Fort Benning in Georgia, and Aberdeen Proving Ground in Maryland - through a three-tier wireless sensor network (WSN) to realize remote, Internet-based, continuous, long-term monitoring of sediment loads.

The objectives of the project included improvement of the sensor and the WSN, validating the accuracy, repeatability, and operability of the sensor in measuring SSC and flow velocity, and validating the functionality of the WSN.

The performance objectives for SSC measurement accuracy, repeatability, and operability were generally not achieved. The objective for SSC measurement accuracy was set to be ±10% or ±50 mg/L of actual SSC, whichever is greater. Within the 95% confidence interval, the highest prediction error for the validation data set was found to be -46.2% for SSCs larger than 500 mg/L and 290.9 mg/L for SSCs lower than 500 mg/L. The objectives for repeatability and operability ware set to be one half of that for accuracy. The actually achieved repeatability was lower than 12.9% for SSCs larger than 500 mg/L, and lower than 292 mg/L for SSCs lower than 500 mg/L. Data post-processing applied to a six-month SSC data showed that the actually achieved operability was 23.1% for SSCs greater than 500 mg/L and 234.5 mg/L for SSCs lower than 500 mg/L.

The performance objectives for flow velocity measurement were generally not achieved. The objective for measurement accuracy was set to be ±10% or ±0.01 m/s of actual flow velocity, whichever is greater. The objective for repeatability was set to be one half of that for accuracy. The error found in velocity measurement was less than 27.8%. The repeatability for velocity measurement was lower than 0.37 m/s.

The performance objectives for various tiers and components of the three-tier WSN were generally not achieved. The objectives for percentage of normal operation (PNO) and data loss rates (DLR) for individual components in the network were set to be 90% and 0.5%, respectively. The lowest PNO and highest DLR recorded were 55% and 8.83%, respectively.

During the demonstration, one of the velocity sensors was deployed at a USGS stream-gaging station in Pine Knot Creek at Fort Benning. Through continuous velocity measurement over a one-year period, the measured point velocities were used to generate an index-rating curve, which can be used to estimate the mean velocity from measured point velocity. The stage measurement provided by USGS and the estimated mean velocity were then used to estimate discharge using the “index-velocity method”. This experiment demonstrated the possibility of using both stage and point velocity measurements to provide better discharge estimation.

OBJECTIVES OF THE DEMONSTRATION

Previous studies have indicated that training activities on ranges are adversely impacting the environment. For example, installations have many miles of unimproved roads and tank trails. Vehicle traffic on these roads and trails typically causes extensive erosion that results in reduced water quality because of increased sediment loads. The Army is addressing these problems with a variety of Best Management Practices (BMPs) to control and minimize generation of sediment. Currently, the Army does not have a way to continuously and directly monitor SSC in streams. An inexpensive, long term SSC monitoring program is necessary to monitor the effectiveness of these BMPs. A wireless sensor network (WSN) that contains multiple sensors with the ability to directly measure both SSC and flow velocity will better enable installation managers to remotely monitor sediment discharge at strategic locations on a continuous, long-term basis, thus helping installations comply with State and Federal Clean Water Act and Total Maximum Daily Loads (TMDL) requirements.

Performance objectives of this project included accuracy and repeatability of the sensor in measuring sediment concentration and flow velocity, the operability of the sensor and its lens cleaning mechanism, and reliability of the components of a three-tier WSN examined through a long demonstration period. Most of the performance objectives were not completely met. Detailed analyses will be given in Chapter 6.

TECHNOLOGY DESCRIPTION

The technology being demonstrated consists of two parts: 1) an optical sensor that continuously measures suspended sediment concentration (SSC) in streams using visible and infrared (IR) lights and flow velocity using the cross-correlation method, and 2) a three-tier wireless sensor network to remotely transmit the SSC data from the sensor site(s) to the Internet. For the demonstration, 12 SSC/velocity sensors were deployed at three military installations – Fort Riley, Fort Benning, and APG, and a three-tier WSN was also deployed at these installations.

DEMONSTRATION RESULTS

In general, the accuracy of the SSC sensors deployed at various sensor sites did not meet the performance objective. Within the 95% confidence interval, the highest prediction error for the validation data set was found to be -46.2% for SSCs larger than 500 mg/L and 290.9 mg/L for SSCs lower than 500 mg/L.

The air-blast system reduced fouling on the sensor lenses. However, difficulties in maintaining the system has presented challenges for long-term field application

The flow velocity measurement of the sensor was found satisfactory when compared with a commercial ultrasonic meter. Installing one of the velocity sensors at a USGS stream-gaging station has allowed a study on the possibility of using both stage and point velocity measurements to provide better discharge estimation.

Components of the three-tier WSN were thoroughly examined during the demonstration. Percentage of Normal Operation (PNO) of individual components in the network was higher than 55%. Data loss in each tier of wireless transmission was below 8.83%.

IMPLEMENTATION ISSUES

Throughout the demonstration, SSC sensor calibration was found to be the most difficult issue for implementation. During the demonstration, a two-stage procedure was used for the calibration. The second stage of this procedure requires grab samples. In order to allow the sensor to measure SSC accurately within a wide range, a large amount of water samples with SSCs distributing within the desirable range need to be collected at the sensor site. This requires water samples to be taken during various rain events. The cost related to labor and transportation is very large.

In order to alleviate this concern, an alternative approach for the second stage of sensor calibration was developed since late 2011. The approach used a field sampler that continuously took water samples at various sediment concentrations and completes the sampling process within one to two hours. Detailed descriptions of this method are given in Appendix C.

Other implementation issues are related to deployment of the sensors in natural waters, including stream, lakes, rivers, and reservoirs. Securing the sensor in the water is always a challenge, especially during the high-flow season. Adding mechanical reinforcement usually alleviate the problem. However, for streams with sand/stone bottoms this may become extremely difficult.

The size of the stream needs to be considered when deploying the sensor. The general recommendation is that the sensor be deployed near a bank, perhaps within a distance of 20 ft. The maximum measurable SSC is 5,000 mg/L and the velocity sensor has a maximum measurable velocity of 5 m/s. These limits should not be exceeded.

1 INTRODUCTION

The overall objective is to further develop, demonstrate, and validate a suspended sediment concentration (SSC) sensor and wireless sensor network (WSN) for continuous, in-situ, real-time measurement and web-based, installation-scale, remote monitoring of suspended sediment fluxes and sediment loads. The technology to be demonstrated includes 1) a prototype SSC sensor that is insensitive to water color, sediment texture, and ambient light, 2) a flow-velocity measurement option on the SSC sensor, 3) a self-cleaning mechanism for sensor lenses to reduce the effect of biofouling; 4) a solar-powered, stand-alone wireless sensor node, and 5) a three-tier WSN to connect distributed sensors to the Internet for web-based data accessibility and management.

1.1 BACKGROUND

Previous studies have indicated that training activities on ranges are adversely impacting the environment. For example, installations have many miles of unimproved roads and tank trails. Vehicle traffic on these roads and trails typically causes extensive erosion that results in reduced water quality because of increased sediment loads. This is especially true at locations where an unimproved road or trail must traverse a stream or creek. Continued erosion can make trails impassable at crossing sites and result in environmental penalties for the installations. A projected increase in training activities and new construction at installations as a result of Base Realignment and Closure (BRAC) is expected to exacerbate the situation.

The Army is addressing these problems with a variety of Best Management Practices (BMPs) to control and minimize generation of sediment. An inexpensive, long term SSC monitoring program is necessary to monitor the effectiveness of these BMPs. Currently, the Army does not have a way to continuously and directly monitor SSC in streams. Current standard practice is to use in-situ turbidity measurements to estimate SSC, to perform automated monitoring with water samplers that are triggered during storm events, or to take grab samples. These methods are labor intensive and expensive, especially when sites are remote. Moreover, on-site water samplers or grab sampling can only provide intermittent measurements, often missing transient events when the potential for erosion is greatest. A WSN that contains multiple sensors with the ability to directly measure both SSC and flow velocity will better enable installation managers to remotely monitor sediment discharge at strategic locations on a continuous, long-term basis, thus helping installations comply with State and Federal Clean Water Act and Total Maximum Daily Loads (TMDL) requirements. It will also help installation personnel more quickly identify potential sediment problems. The SSC sensors can be deployed in streams where water flows onto an installation, and thereby help quantify sediment flux onto installations during storm events. These data could identify off-installation suspended sediment sources. They can also be deployed in places where the Army has jurisdiction and sole responsibility for monitoring large water bodies, such as along the Chesapeake Bay.

Prior to this ESTCP project, the Kansas State University (KSU) team, as a part of the Strategic Environmental Research Development Program (SERDP) project SI-1339 (Assessing the Impact of Maneuver Training on NPS Pollution and Water Quality, 2003-2006), developed a SSC optical sensor to continuously measure SSC in natural streams. Details of this development are given in Section 2.1.2.

1.2 OBJECTIVE OF THE DEMONSTRATION

Under this project, a prototype SSC sensor was further developed. The development effort added a stream flow velocity measurement capability and a self-cleaning capability to the sensor through a simple structural expansion. The project also developed a solar powered, stand alone, wireless sensor node design to improve field deployability, and an associated three-tier (WSN) designed to enable installation-scale SSC/flow velocity monitoring.

The overall objective was to demonstrate and validate the SSC/velocity sensor and the three-tier WSN for continuous, in-situ, real-time measurement and web-based, installation-scale monitoring of suspended sediment fluxes and sediment loads. The specific demonstration objectives included:

1. Add a stream flow-velocity measurement and a self-cleaning function to the SSC sensor through a simple structural expansion.
2. Develop a solar-powered, stand-alone, wireless sensor node mainly using off-the-shelf components to improve the field deployability.
3. Develop and deploy a three-layer WSN to enable installation-scale SSC/flow velocity monitoring.
4. Validate the accuracy of the sensor to measure SSC.
5. Validate the self-cleaning ability of the sensor.
6. Validate the ability of the sensor to measure flow.
7. Validate the functionality of the WSN for short and long range data transmission.
8. Validate the functionality of long-term, remote monitoring of sediment flux via the Internet and web-GIS.
9. Demonstrate the applicability of this technology in military training land and in an estuarine tidal environment.
10. Begin to transfer the technology by developing training tools and preparing the groundwork for disseminating the technology.

1.3 REGULATORY DRIVERS

The concern about suspended sediment in surface water stems from its adverse effects on aquatic plant and animal species.

The Federal Clean Water Act (CWA) was enacted by Congress to restore and maintain the health of surface waters. As required by EPA, the CWA developed water quality criteria, which established numerical maximum concentration levels for contaminants in discharges to surface waters. These criteria were used to develop regulatory requirements based on concentrations that will have an adverse impact on the qualities necessary for beneficial use of the surface waters. State and Federal CWA, and TMDL requirements have resulted in a need for this technology. Installations must comply with these State and Federal CWA and TMDL requirements. The CWA also created the National Pollutant Discharge Elimination System (NPDES) of permits that specified minimum water quality standards for discharged wastewaters and designates the types of pollutants to be regulated, including suspended sediments. Under the NPDES, point sources that discharge into waterways are required to obtain a permit for regulating their discharge. Each permit specifies effluent limitations for particular pollutants, and monitoring and reporting requirements.

Under Section 303(d) of the CWA and its implementing regulations, in addition to other pollutants, the Clean Water Act (CWA) requires a Total Maximum Daily Load (TMDL) for sediment be developed for those water bodies identified as impaired by the state where technology-based and other controls will not provide for attainment of water quality standards. A TMDL is a determination of the amount of a pollutant from point, nonpoint, and natural background sources, including a margin of safety, which may be discharged to a water quality-limited water body. TMDL have been established to address impairments of water quality caused by sediment. In addition, point source sediment loads are regulated under the NPDES program.

Finally, the sensor and WSN technology also address Army Environmental Requirements and Technology Assessments (AERTA) A (2.5.e) for Sustainable Army Live-Fire Range Design and Maintenance. This is a priority user need for the Army. The technology applies to similar user needs of the other services. Applications include all areas where sediment monitoring must be performed for water quality compliance purposes.

2 TECHNOLOGY/METHODOLOGY DESCRIPTION

2.1 TECHNOLOGY/METHODOLOGY OVERVIEW

2.1.1 Overview of Sensor and Wireless Network Technology

The technology being demonstrated consists of two parts: 1) an optical sensor that continuously measures suspended sediment concentration (SSC) and flow velocity in water using visible and infrared (IR) lights at three "feature" wavelengths, and 2) a three-tier wireless sensor network to remotely transmit the SSC data from the sensor site(s) to the Internet.

The optical sensor developed prior to this project ("third generation" sensor design) consisted of a watertight enclosure with three light emitting diodes (LED) and four phototransistors (PT) mounted in a channel running the length of the underside of the enclosure (Figure 2.1). Inside the enclosure were electronic components that controlled the LEDs and measured the PT signals. Optical sensors worked on the principle that the LEDs generated lights peaking at different wavelengths, which were then transmitted through or scattered and backscattered by sediment in the path of the beam. The transmitted, scattered, and backscattered lights were measured by the PTs, which converted the light intensities to current signals that were representative of the SSC. The three feature wavelengths selected were 1) 508 nm – blue-green, 2) 612 nm – orange, and 3) 768 nm – infrared (Stoll, 2004). For each LED, PTs were strategically placed at three angles from the incident light (180º, 90º, and 45º) to measure the transmitted, scattered, and backscattered lights, respectively.

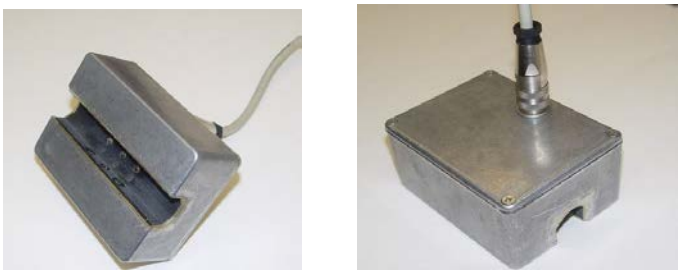

Figure 2.1 Top (right) and bottom (left) views of the "third generation" optical sensor. Note the channel on the bottom of the sensor enclosure.

Individual sensor nodes were deployed as part of a three–tier WSN to enable continuous, long-range SSC data transmission. The three-tier wireless communication network consisted of multiple local WSN (LWSN), a mid-range wireless network (MRWN), and a long-range cellular network (LRCN) (Figure 2.2).

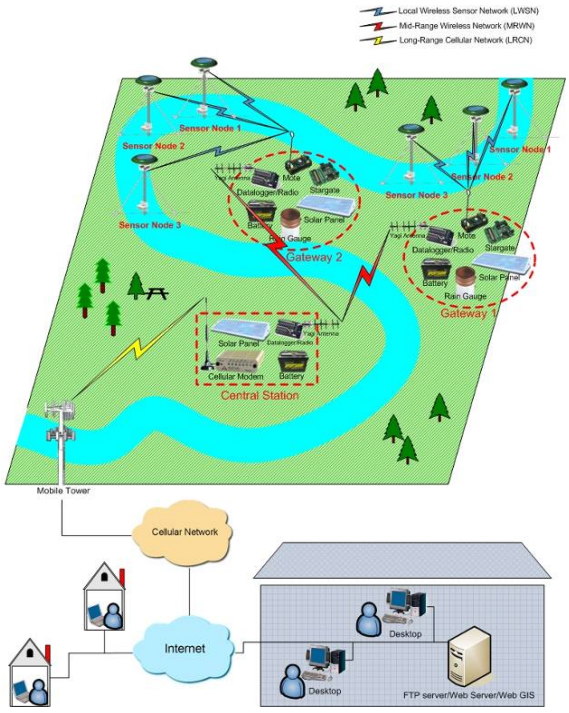

Figure 2.2 A figurative view of a three-tier wireless sensor network.

2.1.2 Chronological summary of the development of the technology prior to this project

The SSC optical sensor ("first generation" design) was originally developed at Kansas State University (KSU) as part of Strategic Environmental Research Development Program (SERDP) project SI-1339 (Assessing the Impact of Maneuver Training on NPS Pollution and Water Quality, 2003-2006). Design of the sensor was based on two assumptions: 1) SSC measurement errors caused by differences in water color may be removed by using multiple light sources at different "feature wavelengths"; and 2) SSC measurement errors caused by differences in soil texture may be reduced by using light detectors at multiple angles from the light source (Zhang et al., 2005). In 2006, prototype SSC sensors ("second generation" design) and WSN were installed and tested at several sites in Kansas and at a Low Water Stream Crossing site on Upatoi Creek at Fort Benning, GA (Zhang et al., 2007; Han et al., 2007, Zhang, 2009).

Several sensors and a two-tier WSN were installed at Little Kitten Creek in Manhattan, KS, in August 2006. After a period of debugging and refinement, the two-tier WSN successfully broadcast wireless SSC signals continuously. The two-tier network was similar to the three-tier WSN, except that it contained only two network tiers – a local wireless sensor network (LWSN) and a long-range cellular network (LRCN). The mid-range wireless network (MRWN) was not used at the Little Kitten Creek site because the network had only one gateway station and it had cellular coverage. In August 2007, two SSC sensors and a similar, two-tier wireless sensor network were deployed in an urban area of Kansas City as a part of a project on "Stormwater Best Management Practice (BMP) Evaluation and Design" (Han et al., 2007).

In a joint effort between KSU and ATC, four SSC sensors ("second generation" design) were installed in June 2006 at a low water stream crossing at Fort Benning, GA, where they

successfully monitored SSC at the low water stream crossing for eight months, with SSC being continuously monitored at 1-minute intervals. A WSN was not implemented at this site because remote data transmission was not an objective of the demonstration. This demonstration identified several issues related to deployment of the SSC sensor nodes at remote sites on Army training ranges. The most important issue was clogging and biofouling on optical lenses. A post-processing algorithm using MATLAB software was developed and implemented to correct the effects of clogging and biofouling on SSC data. The demonstration at Fort Benning also allowed comparisons between different designs of the SSC sensor. An open-bottom design proved to be the least susceptible to lens clogging and biofouling (Zhang et al., 2007, Zhang, 2009). Based on these findings, the "third-generation" sensor was designed.

2.1.3 Expected applications of the technology

The technology may be applied to remote monitoring of sediment transport and sediment load to assist studies of water erosion and wind erosion problems that are related to agricultural, construction, and military activities. The combined SSC and velocity sensor may be used to estimate discharge and sediment load at the watershed scale. It may also be used to estimate the life of reservoirs. For municipal water treatment plants, the sensor may be used to determine the optimal method for treatment, hence, reducing the treatment cost. The sensor may also be used in chemical plants to measure sediment in chemicals.

The WSN infrastructure may be used for large-scale, remote monitoring for other environmental and ecological studies, or studies related to climate changes.

2.2 TECHNOLOGY/METHODOLOGY DEVELOPMENT

Technology development conducted prior to the field demonstration under this ESTCP project included modification of the SSC/velocity sensor, design details of the three-tier WSN, and a WebGIS software package for data management, display, and query.

2.2.1 Sensor modification – the fourth generation design

The SSC sensors being prepared for the ESTCP demonstration ("fourth generation" design) used a new design which was a modification based on findings and lessons learned during the earlier experiments at Fort Benning, Little Kitten Creek, and Kansas City. Several modifications were made on the sensor: 1) a new case design that allowed air-blast cleaning and velocity measurement, 2) a printed circuit board (PCB) for sensor signal conditioning, processing and control. The PCB also interfaced with a thermocouple to continuously monitor water temperature and a rain gauge to monitor precipitation. With these modifications, data packets including measured SSC, flow velocity, water temperature and precipitation were transmitted to the WSN at programmable time intervals.

2.2.1.1 Structural modification of the sensor

The optical SSC sensors designed in 2005 ("third generation") were fabricated manually using an aluminum case (Figure 2.3a). In 2008 a new design ("fourth generation") was developed in collaboration with the KSU Advanced Manufacturing Institute. The new design used an acetal case (Figure 2.3b). The sensor body was manufactured on a Computer Numerical Control (CNC) turning center.

(a) **(b)**

Figure 2.3 Sensor designs (a) "third generation" (2005), (b) "fourth generation" (2008)

The optical sensor consists of a watertight enclosure with three light emitting diodes (LED) and four phototransistors (PT) mounted in a channel running the length of the underside of the enclosure (Figure 2.4). Inside the enclosure are electronic components that control the LEDs and translate the PT signals. Optical sensors work on the principle that the LEDs generate lights peaking at different wavelengths, which are then transmitted through or scattered and backscattered by sediment in the path of the beam. The transmitted, scattered, and backscattered lights are measured by the PTs, which convert the light intensities to current signals that are representative of the SSC. The three feature wavelengths being used are 1) 508 nm – blue-green, 2) 612 nm – orange, and 3) 768 nm – infrared (Stoll, 2004). For each LED, PTs are strategically placed at three angles from the incident light (180º, 90º, and 45º) to measure the transmitted, scattered, and backscattered lights, respectively.

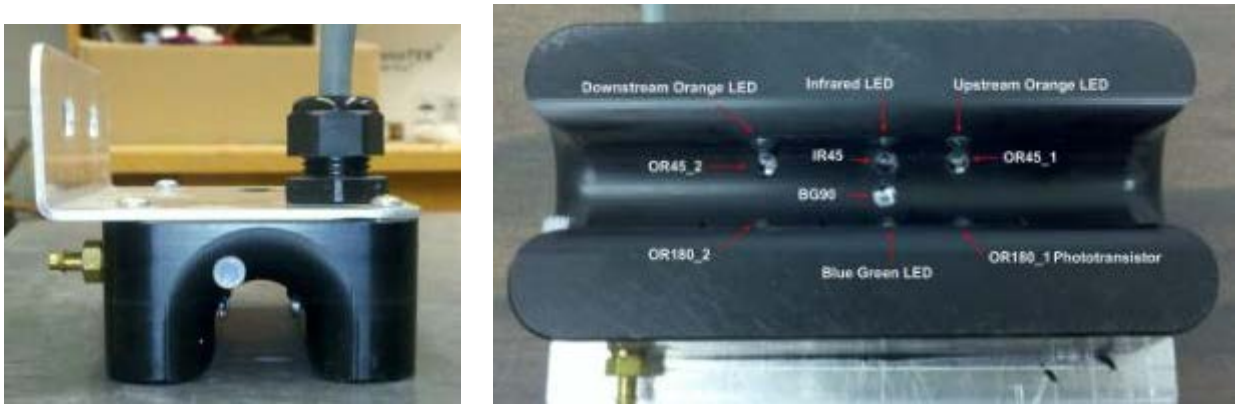

Figure 2.4 Side (left) and bottom (right) views of the Optical Sensor. Note the channel on the bottom of the sensor enclosure.

2.2.1.2 Velocity measurement

The velocity measuring function was added to the SSC sensor by a simple structural modification. Figure 2.5 shows the shape of the sensor and the position of the LEDs mounted into the sensor. When using the sensor for velocity measurement, only the orange LEDs and the corresponding phototransistors were used. The remaining blue-green and infrared LEDs and their phototransistors were only used for sediment monitoring. For each orange LED, there were two phototransistors in the same plane. One phototransistor was directly across from the LED at 180°, and the other was 45° from the LED. These phototransistors had a wide response range from 460 to 1080 nm with a maximum output at 850 nm. One orange LED/ phototransistors

combination was 4 cm downstream from the first orange LED/ phototransistors combination. Figure 2.6 shows the arrangement of the orange LEDs and phototransistors in the sensor. The infrared and blue-green LEDs and their corresponding phototransistors were not used in velocity measurement and, hence, not shown in this figure. Connections of the LEDs and phototransistors in the circuit are shown in Figure 2.7. The sensor contained internal passageways so that air could be forced into the sensor at a point and clean the LEDs and phototransistors.

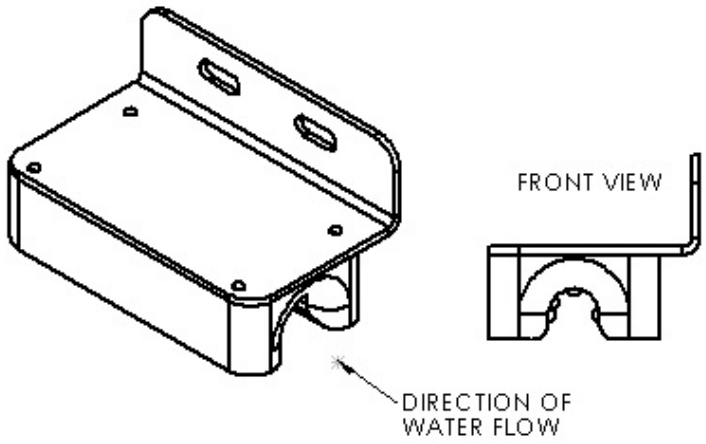

Figure 2.5 Soil Sediment and water velocity sensor ("fourth generation" design)

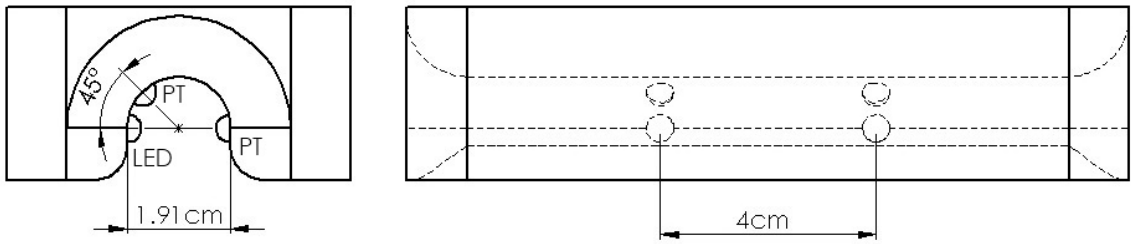

Figure 2.6 Orange LED and Phototransistor Arrangement in the Sensor (Infrared and Blue-Green LEDs and Corresponding Phototransistors not shown)

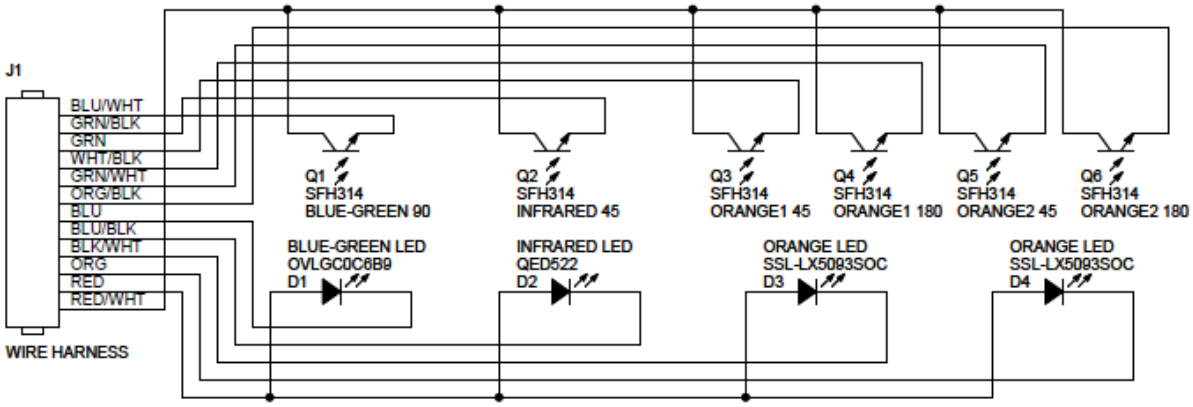

Figure 2.7 Sensor Circuit Schematic

In testing the fourth generation sensor, it became apparent that several improvements needed to be made to the sensor design. One area targeted for improvement was the shape of the sensor itself. Through a Computational Fluid Dynamics (CFD) analysis, the shape of the fourth generation sensor was changed to minimize the effect of the sensor body on the fluid velocity along the centerline of the U-shaped channel between the upstream and downstream LED/phototransistor pairs, where the velocity was measured. This simulation study resulted in the "fifth-generation" design of the sensor body, as shown in Figure 2.8 (Dvorak, 2012).

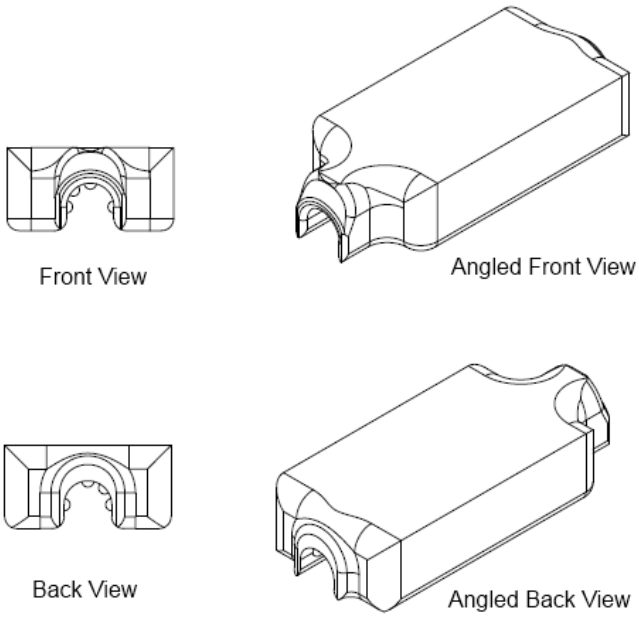

Figure 2.8 The body shape of the "fifth generation" sensor designed through a CFD analysis

2.2.1.3 Air-blast cleaning

Air passages were embedded in the sediment sensors for lens cleaning. The stretch-out views of the sensor tube with air outlets are shown in Figure 2.9.

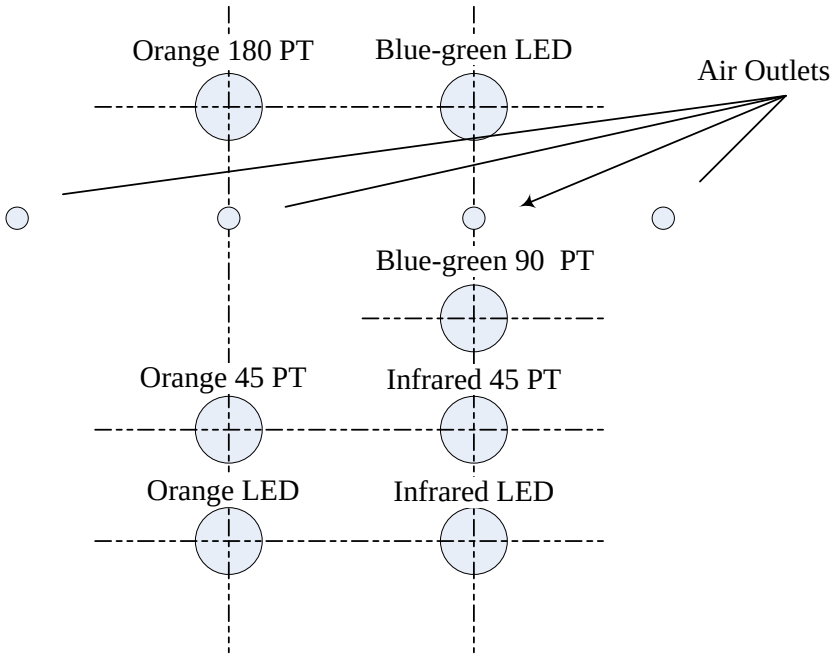

Figure 2.9 The stretch-out view of air outlets in the sensor tube with an acetal case.

A 12V air compressor equipped with a 3.5 liter air tank was used to generate pressurized air. A solenoid valve was controlled by the PCB to blast air into the sensor at programmable intervals to clean the sensor lenses (Zhang, 2009).

2.2.1.3.1 PCB Control Board

The sensor signals were sent to a solar-powered, wireless node consisting of a printed circuit board (PCB) (Figure 2.10), a data-acquisition board (MDA300, Crossbow Technology), a wireless mote (MICA2, Crossbow Technology), a rechargeable battery, and a mounting structure. The exact configuration of the wireless sensor node depended on the site where the sensor was deployed. The node was typically located on the channel bank, several meters away from the sensor. The rechargeable battery that provided power to the system was continuously trickle charged by the solar panel.

The PCB was an essential part of the sensor node. Functions of the PCB board included (1) voltage regulation, (2) mote and data acquisition, (3) sensor control, (4) sensor gain adjustment, (5) relay control, (6) signal conditioning for temperature measurement, and (7) interfaces. The electric circuit diagram of the PCB is shown in Figure 2.11.

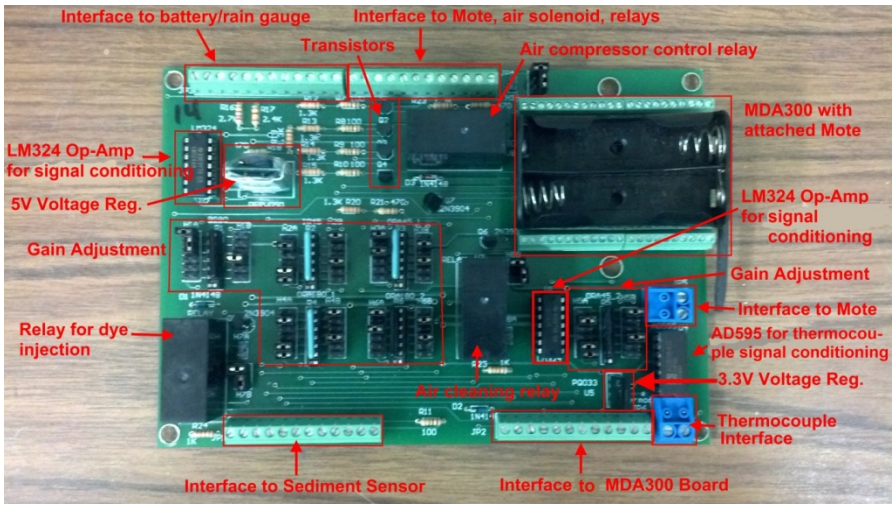

Figure 2.10 PCB control board

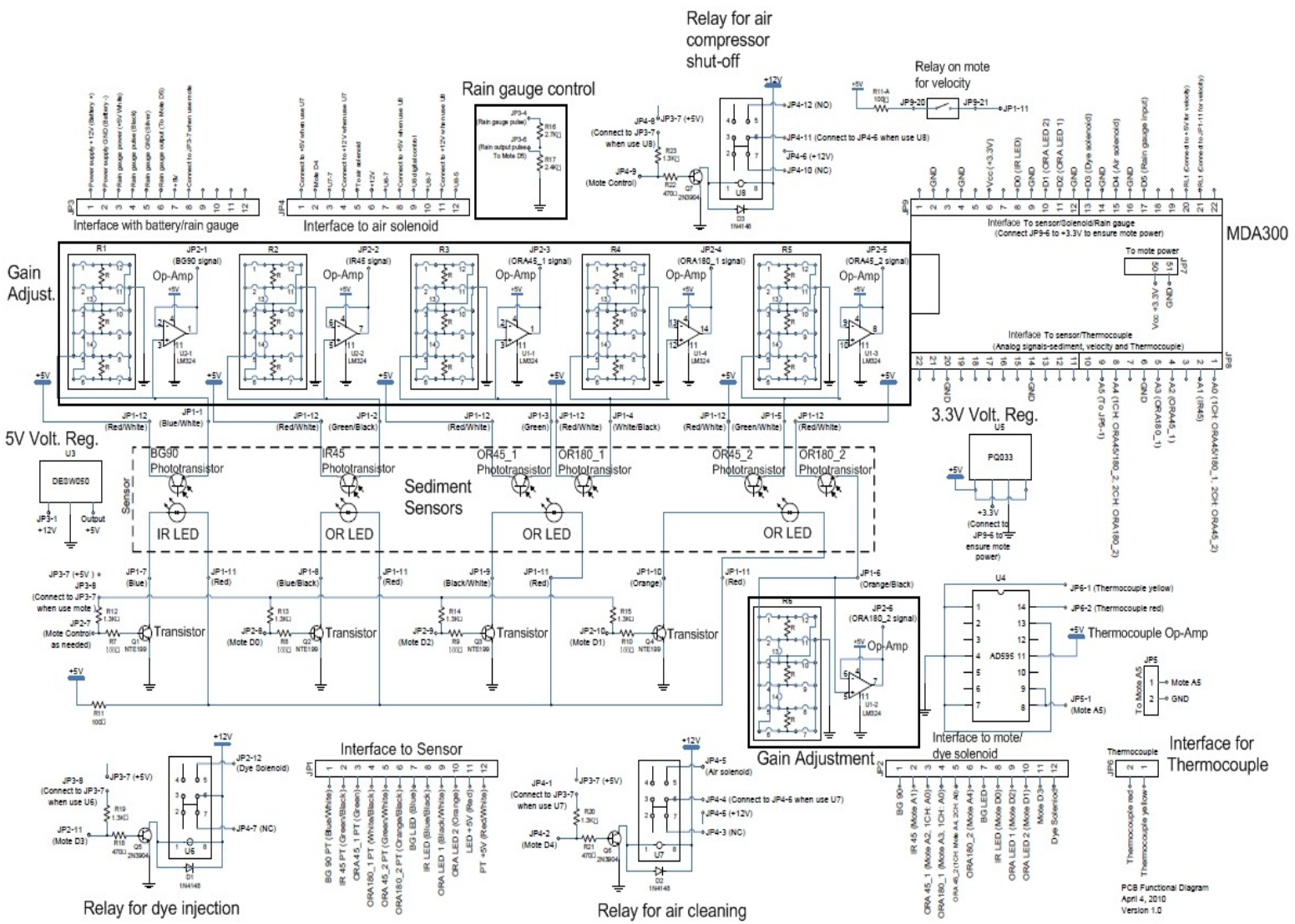
Relay for air compressor shut-off
Relay on mote for velocity
Rain gauge control
Interface with battery/rain gauge
Interface to air solenoid
MDA300
Gain Adjust.
Op-Amp
5V Volt. Reg.
3.3V Volt. Reg.
BG90 Phototransistor
IR45 Phototransistor
OR45_1 Phototransistor
OR180_1 Phototransistor
OR45_2 Phototransistor
OR180_2 Phototransistor
Sediment Sensors
IR LED
OR LED
Transistor
Gain Adjustment
Thermocouple Op-Amp
Interface to mote/ dye solenoid
Interface for Thermocouple
Relay for dye injection
Interface to Sensor
Relay for air cleaning
PCB Functional Diagram
April 4, 2010
Version 1.0

Figure 2.11 Functional Diagram of the PCB board

2.2.1.3.2 Voltage Regulation

The PCB board provided 3.3V power to the wireless mote (Micaz, Crossbow Technology Inc.) and the data acquisition board (MDA300, Crossbow Technology Inc.), and 5V power to the remaining components of the system – sediment sensors, control relays, rain gauge and temperature measurement.

2.2.1.3.3 Mote and Data Acquisition Board

The PCB board provided a 50 pin connector slot for the data acquisition board MDA300 to plug in. A Micaz mote can then be plugged into the MDA300 to control the sensor and relays. The MDA300 was equipped with a 6 Analog-to-digital converter (ADC) channels, 6 digital Input/Output (I/O) channels, a high-speed counter, 2.5V, 3.3V, and 5V external sensor excitations, and 2 relay controls.

2.2.1.3.4 Sensor Control

The PCB board served as the bridge between the data acquisition system (MDA300) and the sediment sensor. It provided power to the LEDs in a controlled time sequence, converted current signals from the phototransistors in the sediment sensors to voltage signals, and sent the voltage signals to the data acquisition board MDA300 for processing.

2.2.1.3.5 Gain Adjustment

The PCB board provided a gain adjustment circuit to each sediment sensor so that the gains of the current-to-voltage converters can be adjusted during the pre-calibration stage of the sensor to achieve similar gains among different sensors under the laboratory conditions. The gain adjustment was achieved by adjusting the resistor and jumper combination in order to achieve a desired resistance. The gain adjustment circuit is shown in Figure 2.12.

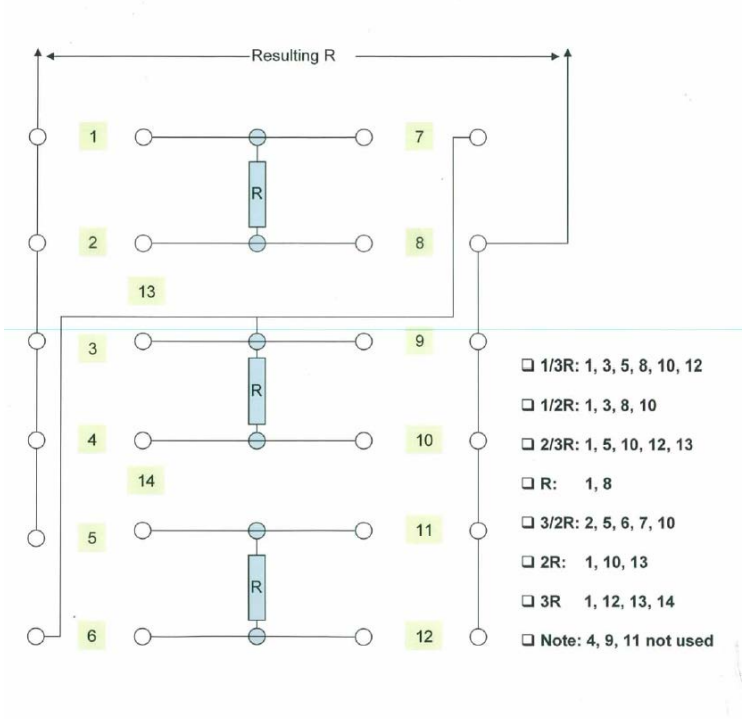

Figure 2.12 Gain adjustment to achieve desired resistance needed for calibration

After a six-pin resistor array with resistance of R plugged in the resistor socket, by selecting 2-6 from the 14 possible jumper connectors, nine different resistances, from 1/3 R to 3R, can be achieved.

2.2.1.3.6 Relays

The PCB board provided three separate Omron G2R-24 industrial relays to have the capability to control various devices. Two relays were used to control solenoid valves for air compressor and dye injection for velocity measurement. The third relay was used to prevent the air compressor from turning on when battery voltage was below 12V.

2.2.1.3.7 Temperature Measurement

The PCB board used an AD595 type-K thermocouple amplifier with cold junction compensation to measure water temperature.

2.2.1.3.8 Interfaces

The PCB board served as a general hub to provide interfaces between the mote/data acquisition system and several peripherals, including the sediment sensors, rain gauge, thermocouple, and solenoids to control air compressor and dye injector.

2.2.1.4 Sensor cover and mounting

2.2.1.4.1 Sensor mounting

A sensor installed in the stream was attached to a T-post which usually was driven into the thalweg of the stream (Figure 2.13). This was to help ensure that the sensor would always be submerged in water as long as the stream was flowing. Once the post was driven into the

streambed it was then cut off at water level to reduce the possibility of catching debris during high flow periods. The sensor was then attached to the post with the U-shaped channel of the sensor body parallel with the flow of the stream. Another post was driven 3-6 feet upstream from the sensor to act as a safety device to catch or divert large pieces of debris around the sensor (Bigham, 2012).

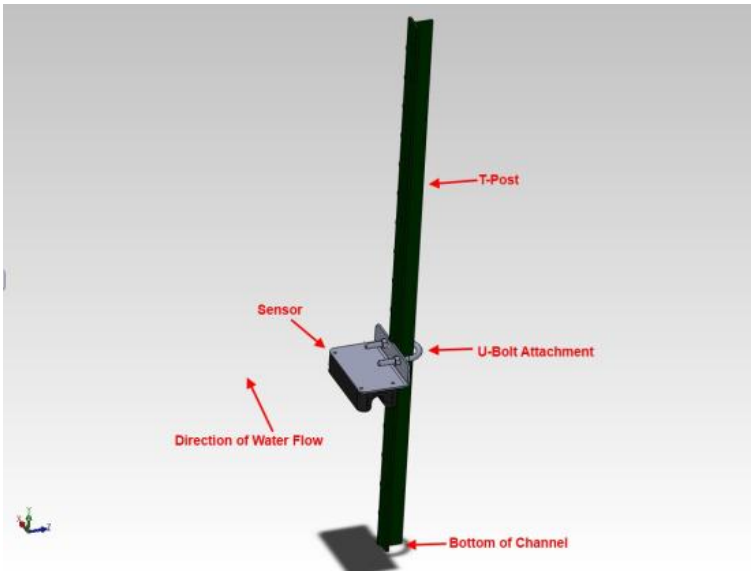

Figure 2.13 Installation of sensor in stream; the sensor is attached to a T-post.

2.2.1.4.2 Sensor cover

The optical SSC sensor has been found to be most accurate and have the least interference when placed in complete darkness (Zhang, 2009). This finding prompted the need to block the sensing area from ambient light. The upside-down U-shape of the sensor helped to block some, but not all light, causing skewed readings of the sensor during certain times in a day. This was improved by installing an aluminum cover plate on the T-post above the sensor itself.

Initial designs utilized a large, flat square plate (Figure 2.14). Through testing and real-world application, it was determined that these large plates caught a large amount of debris and caused a damming effect in the stream. A new pyramid type design (Figure 2.15) was then created to provide adequate light cover while diverting debris flowing down the stream and protecting the sensor. This cover had the front corner of the pyramid facing upstream to act as diversion plate to move debris such as limbs, leaves away from the sensor area. The cover was attached to a T-post that went through a hole in the cover and was attached using a U-bolt. This cover was also placed above the sensor as to not affect the sediment or velocity readings (Bigham, 2012).

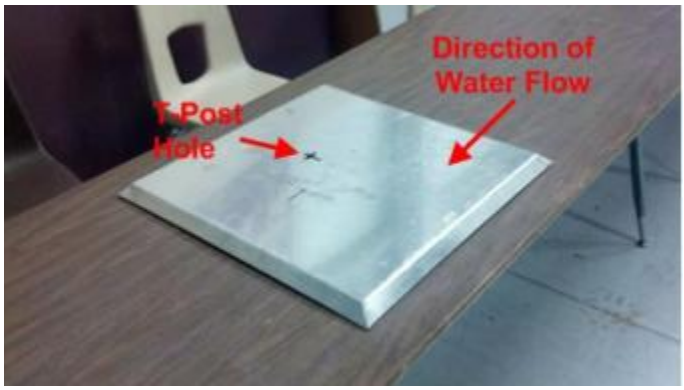

Figure 2.14 Initial sensor cover design

Figure 2.15 Top and bottom views of the new sensor cover design.

2.2.2 Three-tier wireless sensor network

2.2.2.1 Network Architecture

As the name implied, the three-tier WSN included three levels of networking: the local wireless sensor network (LWSN), the mid-range sensor network (MRSN) and the long-range cellular network (LRCN).

The LWSN was in charge of transmitting data from sensors to a gateway station. On this tier, the area that the wireless transmission had to cover was usually near a stream or under a bridge, surrounded by trees and other vegetation. The vegetation and water were generally hostile to wireless transmission because they often absorbed, refracted, or reflected the signals. Moreover, commercial cellular coverage in these areas were generally poor or nonexistent, and required short range wireless devices (up to 100 m) to relay sensor signals to a gateway station, where signals could be further relayed.

The MRSN relayed the data, through a moderately long distance (up to 16 km), from the signal-unfriendly sensor sites to a location with a satisfactory commercial cellular coverage. Because of

the longer transmission range, the MRSN allowed multiple LWSNs within a larger area to send data to the same central station, where they shared a single cellular service to transmit the data to the Internet. A repeater station could also be added to the MRSN to further enlarge its coverage area.

The last tier in the three-tier WSN was the LRCN. It used a commercial mobile wireless data service to further transmit data to the database server through the Internet. A "Web-GIS" system developed in this project gave access to the database via the Internet. A block diagram for the three-tier WSN system is shown in Figure 2.16.

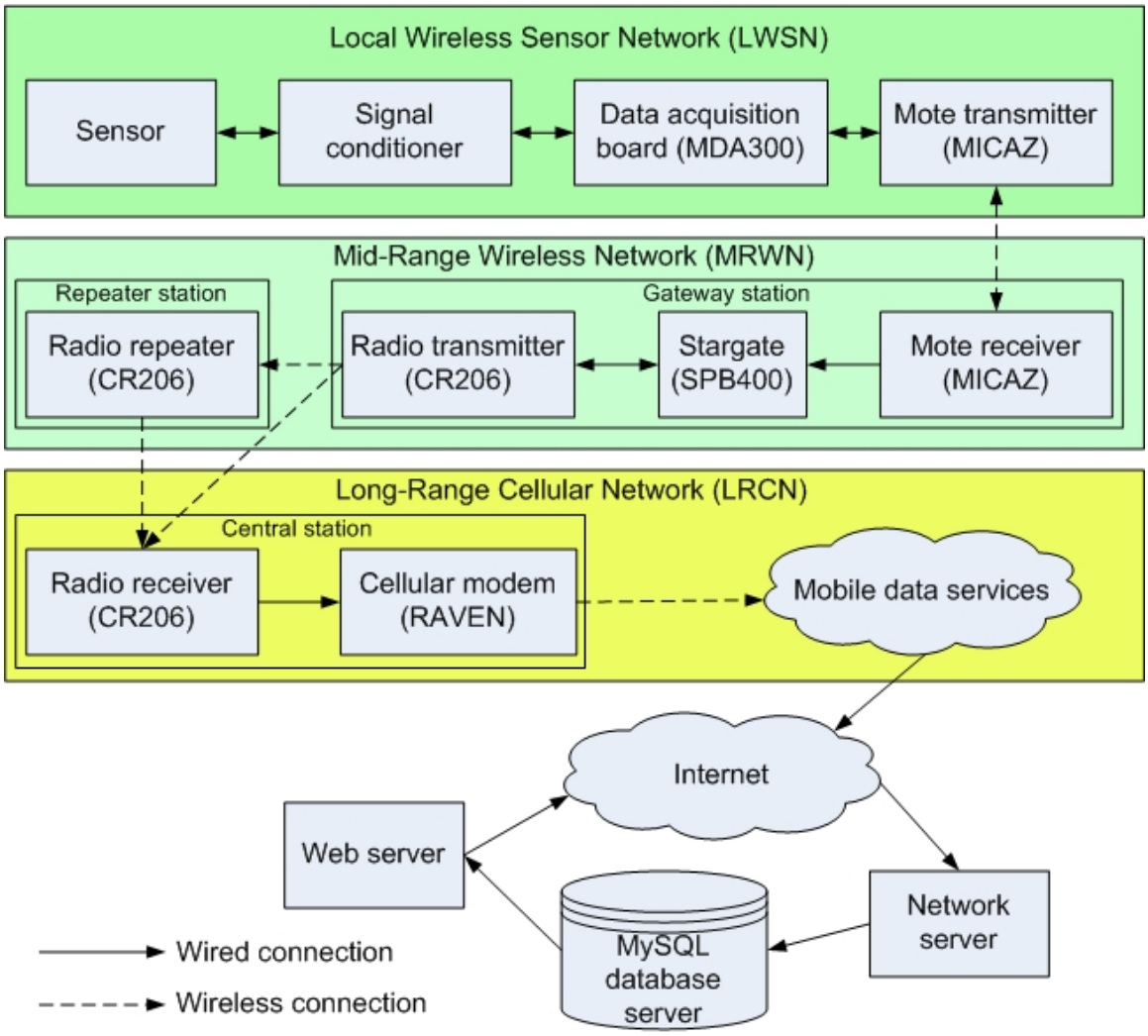

Figure 2.16 Block diagram for the three-tier WSN

A fully equipped sediment/velocity sensor node contained four modules. They were sensory module, sensor cleaning module, control and communication module, and power supply module. The sensory module included an optical sensor for SSC and velocity measurement, a dye bottle or canister for velocity measurement, a thermocouple for water temperature measurement, a rain gauge for precipitation measurement, and a metal cover to protect the light sensor from the ambient light. The sensor cleaning module included an air-blast or an ultrasonic device for automatic cleaning of the optical lenses. The control and communication module included a

mote, a data acquisition board, a printed circuit board (PCB) and a 2.4 GHz Yagi directional antenna. This module set the sampling rate of the sensor and the interval for sensor cleaning. It also sent the measurement data wirelessly to a mote mounted on the gateway station. These devices required considerable electrical power to operate, which was provided by the power supply module. The module included the solar panels and one or two deep-cycle, 12 V batteries. Depending on the location, terrain and distance to the gateway station, the height of the antenna tower for the sensor node varied between 1 and 3 meters. Some of the modules were placed in weather-proof enclosures for protection. Cables between the sensory module and the control and communication module were protected by polyvinyl chloride (PVC) pipes for outdoor deployment. The system configuration for a sensor node is illustrated in Figure 2.17 (Han, 2011).

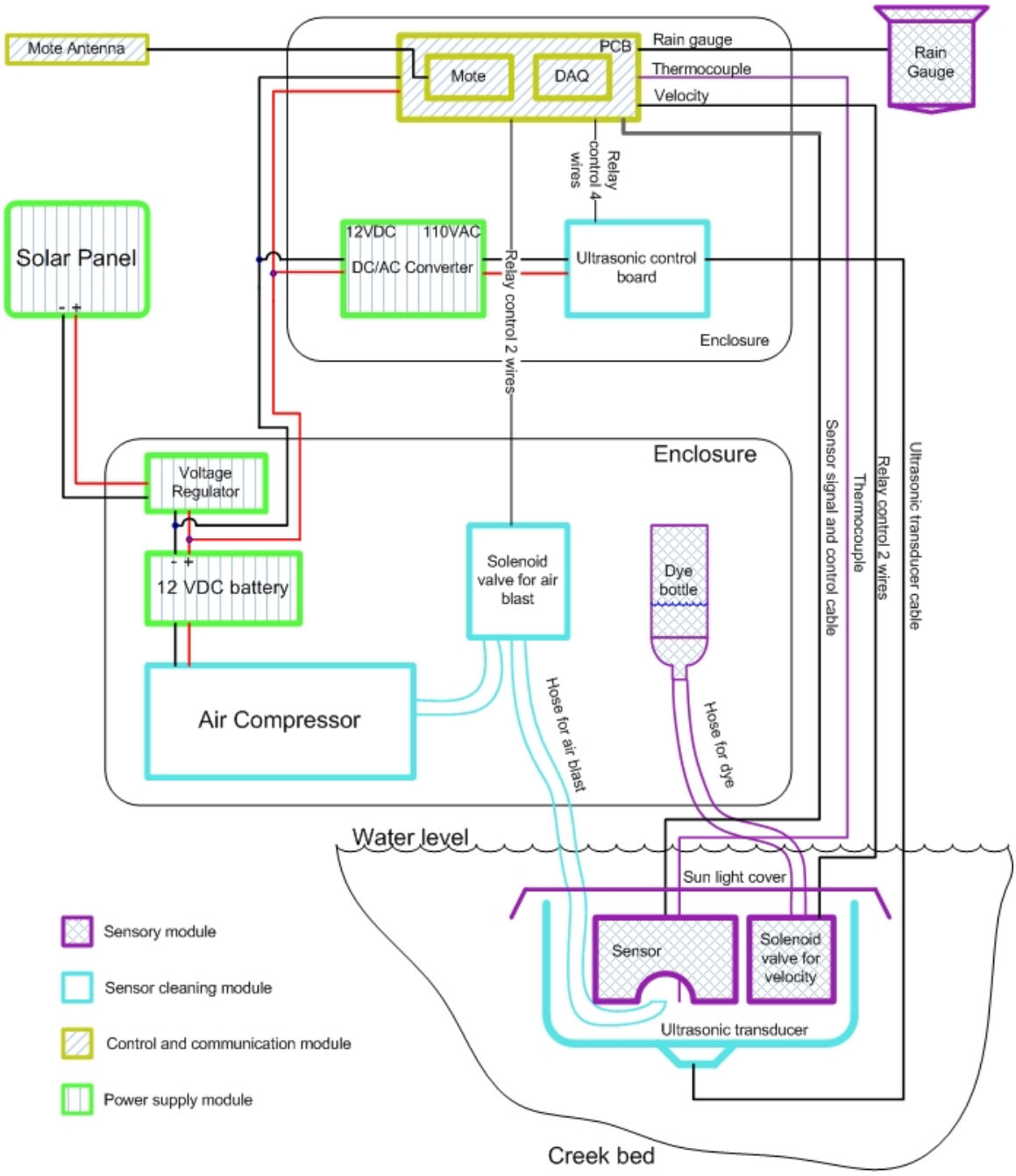

Figure 2.17 System configuration for a sensor node

2.2.2.1.1 Gateway station

The gateway station included three modules. The Stargate module was used for collecting data from connected sensor nodes, saving and parsing data, and sending data to a radio communication module. The radio communication module included a CR206 datalogger (CR206, Campbell Scientific Inc., Logan, UT) and an antenna tower. This module was responsible for sending data to the central station or a repeater station. The power supply module included a solar panel, a voltage regulator, and 12 VDC batteries.

A compact flash (CF) card was inserted in the Stargate to store the programs and the sensor data. The total space required to store the programs on the CF card was less than 120 MB. The storage spaces available on a 1 GB CF card to store the data and the time lengths the card can be used to store data under different scenarios are shown in Table 2.1.

Table 2.1 CF card capacity

Scenarios	Capacity needed to store one year of data	Years of usage for a 1 GB CF card
1 sensor node for sediment data only	0.1076 GB	8.1 years
1 sensor node for 1sediment and velocity data	0.1796 GB	4.9 years
2 sensor nodes for sediment data only	0.2152 GB	4.1 years
2 sensor nodes for both sediment and velocity data	0.2872 GB	3.1 years

The CR206 datalogger had an on-board 915 MHz, frequency hopping spread spectrum (FHSS) radio. The radio transmission range was 1.6 kilometers with 0 dBd, ¼ wave antenna (line-of-sight) and up to 16 kilometers (line-of-sight) with a high-gain antenna. The CR206's input channel configuration and small size were optimal for connecting a few sensors in an outdoor environment. It had a 9-pin, RS-232 interface for communication between the datalogger and a computer. It had 512 k byte flash memory formatted for 4 byte per data point. The program flash memory allowed a maximum storage of 6.5 k byte. The maximum operation speed was one scan per second. The communication protocol used for CR206 datalogger was PakBus. It was a packet-switched network protocol with routing capabilities. The CR206 datalogger used a 12 VDC power supply with an average current drain of 20 mA in a radio-always-on condition (Campbell Scientific, 2010a). The datalogger was used mainly as the mid-range radio device. It also measured the battery voltage of the power supply.

High-gain antennas for both the transmitter and the receiver were essential to obtaining high level of received signal strengths. A Yagi directional antenna was a high-gain device that can pick up very weak signals in a specific direction. The 900 MHz Yagi antenna had a manageable size and required a fairly simple installation.

An omni-directional antenna normally did not have higher gains on a particular direction than a Yagi directional antenna of similar sizes and costs; however, because an omni-directional antenna covered 360° surrounding areas, it had the advantage of transmitting and receiving signals from all directions simultaneously. Unlike the Yagi directional antenna which required accurate direction adjustments, the omni-directional antenna's installation was quite simple.

Under certain circumstances, when the numbers of transmitters were limited and the locations of the transmitters were known, 2-3 Yagi antennas with a signal splitter were used to replace an omni-directional antenna at the receiver end. The signal splitter at the receiver can split/combine signals for transmitters from different locations. Two types of antennas and a 2-way signal splitter are shown in Figure 2.18 (Han, 2011).

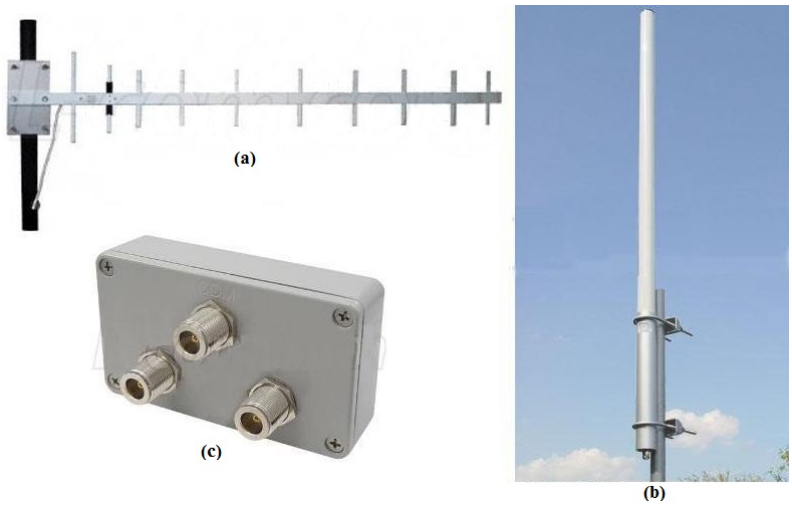

Figure 2.18 900 MHz antennas and signal splitter: (a) Yagi 14dBi directional antenna, (b) 8dBi omni-directional antenna (c) 2-way signal splitter

Figure 2.19 shows the system configuration for the gateway station.

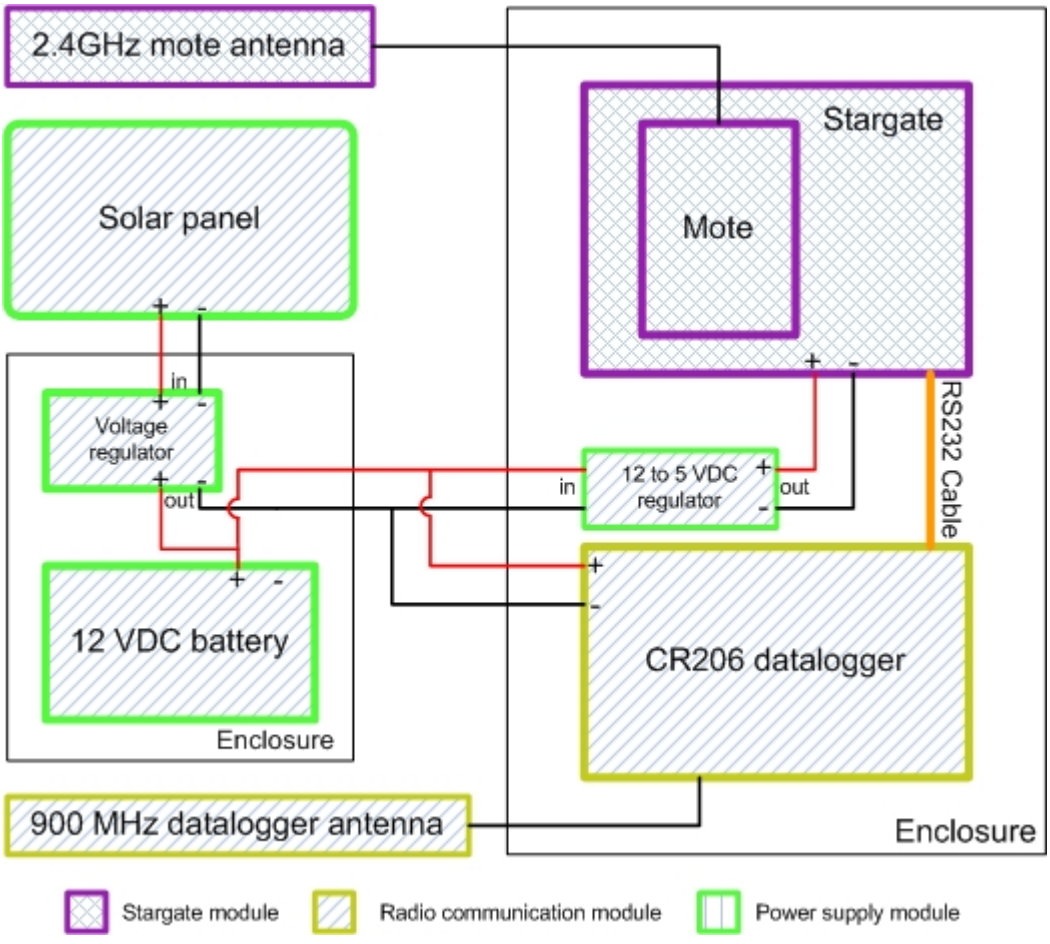

Figure 2.19 System configuration for the gateway station

2.2.2.1.2 Repeater station

The repeater station had only two modules: a radio communication module and a power supply module. It took the responsibility of receiving data packets from one or more gateway stations and forwarding them to the central station. If multiple repeaters were used to relay signals, a repeater station may receive data from or transmit them to another repeater station. Selection of the repeater location was very important. Ideally, the repeater station should be located on an upland area, with a good line-of-sight to the central station. For the repeater station, an omni-directional antenna was the common choice. However, Yagi antennas with a signal splitter were preferable. The power consumption at repeater station was generally very low (20 mA in average) and it required a small solar panel for recharging the battery.

2.2.2.1.3 Central station

A central station was the final data sink in a remote region. It included three modules: a radio communication module, a cellular modem module and a power supply module.

The cellular modem used was a Raven modem, model Raven XT (Sierra Wireless, Richmond, BC, Canada). It provided sophisticated remote monitoring and controlling functions. For Code Division Multiple Access (CDMA) cellular system, the modem used 800 MHz carrier frequency and, for a Global System for Mobile Communications (GSM) cellular system, the modem used 900 MHz carrier frequency. The average transmit/receive current drain at 12 VDC was 239 mA. It had a mini USB port and a RS232 port (Sierra Wireless, 2007). The Raven modem in the cellular modem module was connected to the CR206 datalogger in the radio communication module by a null modem RS-232 cable. There were different types of Raven modems manufactured for major cellular carriers in the US, such as AT&T, Verizon, and T-Mobile.

Before deployment, the Raven modem needed to be configured. This involved setting up the serial port, assigning the Internet Protocol (IP) address of the server computer, specifying the machine port on the server computer, choosing (Transmission Control Protocol (TCP), and disabling the TCP timeout. These configuration settings can be saved in the modem and do not need to be re-configured unless parameters were changed (Han, 2011).

2.2.3 WebGIS

A Web-based GIS software package was developed to manage the data received from the sensors through the three-tier WSN. The software package was built upon two databases – a cache database and an archive database, which were synchronized through a database synchronizer. The architecture of the data-access layer of the system is shown in Figure 2.20. The Web-based GIS was developed to meet the following requirements:

1. Facilitate representation of data in different forms (e.g., tabular and graphical).
2. Allow users to generate customized queries.
3. Provide functionality to export data to different formats.
4. View the location of sensors on maps for better understanding of the data.

The system also provided the following functions:

1. Daily summary report
2. General-purpose report
3. Alerts for low battery levels.

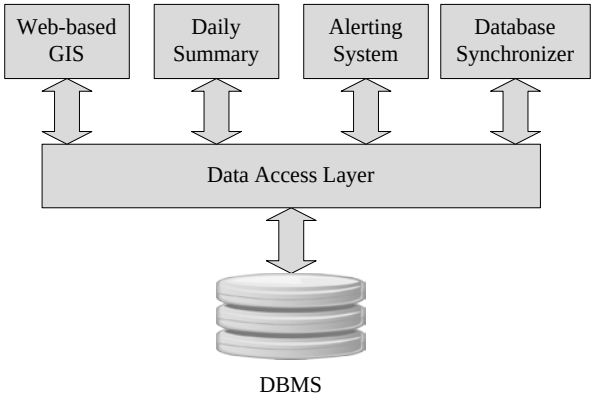

Figure 2.20 Data access layer architecture of the Web-based GIS

2.3 ADVANTAGES AND LIMITATIONS OF THE TECHNOLOGY

Two methods that are typically used to estimate SSC are 1) grab samples that are analyzed for turbidity or SSC, and 2) in-situ turbidity monitoring. Grab samples that are analyzed for turbidity provide an indirect measurement of SSC; the turbidity measurements must still be correlated to SSC using a correlation developed for the location where the sample was collected. Grab samples that are analyzed for SSC provide a direct measure of SSC. A disadvantage of this technique is that it is costly in terms of field work and lab processing, and it is time intensive. Grab samples do not have the temporal sampling resolution necessary to capture rapid intermittent flushes of suspended sediment during storms or other transient events, because the measurement is not continuous. They also lack the spatial resolution necessary to capture spatial variations in suspended sediment discharge across a channel (sediment samples collected at the same time across a channel can vary by a significant amount). Finally, the locations at which grab samples can be collected may be limited if sites are remote or otherwise inaccessible, or if sampling conditions are hazardous.

The optical sensors provide enhanced temporal and spatial resolution at a lower cost than grab samples. The optical sensors enable automated, continuous monitoring of SSC at reduced cost because they monitor SSC in-situ, thereby reducing the number of water samples that need to be collected and analyzed at offsite laboratories. They also provide improved temporal sampling resolution and enable the capture of rapid intermittent flushes of suspended sediment during storms and other transient events. They can therefore better monitor rapidly changing SSC, such as tidally affected water bodies, when vehicles ford a creek or stream, or during storm events. They can better determine irregular re-suspension of sediment, as in the case of boat passage. Depending on the number of sensors installed at a single location, they can provide enhanced spatial resolution (both horizontal and vertical) at that location. For example, they can be installed at several depths to provide depth profiles of SSC. Another advantage of optical sensors when compared to the grab sample technique is that they can be installed at many locations for real time monitoring over a large area. They can be installed at inaccessible locations, such as in marshes. They can perform real time monitoring under hazardous conditions, such as during storm events, when personnel cannot safely or easily go out to the sampling site to collect grab samples.

A limitation of the optical sensor is that it is susceptible to biofouling of the lenses. Biofouling is noticeable on the lenses after a very short time, and must be continually addressed. Another

limitation is that the optical sensor is vulnerable to damage by high flow conditions, flotsam, vandalism, or other damage. Perhaps the most challenging limitation of the optical sensor is the need for grab samples that cover a sufficient range of sediment concentration for a good, location-specific calibration. Although the number of grab samples needed for calibration is small, the wide range of sediment concentration covered by these samples may be difficult to achieve within a short period of time.

3 PERFORMANCE OBJECTIVES

The quantitative and qualitative performance criteria for the technology demonstration, along with related metric information, are summarized in Table 3.1, followed by detailed text description of each performance objective. Content of this section was basically identical to a similar section in the approved demonstration plan. As required, the results of assessment for the performance objectives are listed in this table, while detailed analyses are given in corresponding sections of Chapter 6.

Table 3.1 Performance Objectives

Performance Objective	Data Requirements	Success Criteria	Results
Quantitative Performance Objectives			
Accuracy in SSC measurement	SSC measured by sensor and laboratory analysis of grab samples	±10% or ±50 mg/L of actual SSC, whichever is greater.	For SSC>500 mg/L: Maximum error (95% confidence interval): -46.2% For SSC<500 mg/L: Maximum error (95% confidence interval): 291mg/L
SSC measurement range	SSC measurement by sensor and laboratory analysis of grab samples	0-10,000 mg/L	0-5,000 mg/L
Repeatability of SSC measurement	Repeated SSC measurements by sensor and laboratory analysis of grab samples obtained at the same time and location, under the same conditions	±5% or ±25 mg/L of actual SSC, whichever is greater.	for SSC>500 mg/L: ±12.9% for SSC<500 mg/L: ±292 mg/L
Operability of anti-fouling mechanisms and correction algorithm to compensate data deterioration due to fouling	SSC measured by sensor with anti-fouling mechanism and laboratory analysis of grab samples taken between manual lens cleanings	±10% or ±50 mg/L of actual SSC, whichever is greater	For SSC>500 mg/L 23.1% For SSC<500 mg/L 234.5 mg/L
Accuracy in flow velocity measurement	Flow velocity measured by sensor and flow meter	±10% or ±0.01 m/s of actual flow velocity, whichever is greater.	When using a commercial ultrasonic flow meter as reference: 27.75%
Flow velocity measurement range	Flow velocity measurement by sensor	0.01-5 m/s	0.125-4.5 m/s

	and flow meter		
Repeatability of flow velocity measurement	Repeated flow velocity measurements by sensor and flow meter at the same time and location, under the same conditions	±5% or ±0.005 m/s of actual flow velocity, whichever is greater.	Repeatability limit: 0.37 m/s
Reliability of the SSC/flow velocity sensor	Record of times a SSC/flow velocity sensor unexpectedly stops to normally measure SSC and flow velocity (downtime) and resumes normal operation after repair (uptime)	Greater than 90 % of the demonstration period, including high-flow season.	Percentage of normal operation (PNO): For SSC: 72.4% For velocity: 69.6%
Reliability of Local Wireless Sensor Network (LWSN)	Record downtimes and uptimes of each sensor	Greater than 90% of the demonstration period, including high-flow season.	PNO: 55.0%
Data loss rate of LWSN	Recorded data losses for each LWSN	Less than 0.5%	0.45%
Reliability of Mid-Range Wireless Network (MRWN)	Record of downtimes and uptimes of each LWSN	Greater than 90 % of the demonstration period, including high-flow season.	PNO: 64.7%
Data loss rate of MRWN	Recorded data losses for each MRWN	Less than 0.5%	(For both MRWN and LRCN) 8.83%
Reliability of Long-Range Wireless Network (LRCN)	Record of downtimes and uptimes of each LRCN	Greater than 90 % of the demonstration period, including high-flow season..	70.5%
Data loss rate of LRCN	Recorded data losses for each LRCN	Less than 0.5% s	(For both MRWN and LRCN) 8.83%
Reliability of Internet server	Record of downtimes and uptimes of the Internet server	Greater than 90 %.	98.1%
Reliability of Web GIS	Record of downtimes and uptimes of the Web GIS	Greater than 90 %	98.8%
Reliability of solar panel and charging circuit	Record of downtimes and uptimes of each solar panel and associated changing circuit	Greater than 90 % of the demonstration period, including high-flow season	74.1%

Reliability of alternative 1 for WSN - meteor-burst communication (MBC) system	Record of downtimes and uptimes of the MBC system	Greater than 70 % of the demonstration period, including high-flow season.	94%
Data loss rate of MBC	Record of data losses for the MBC	Less than 20%	1.1%
Reliability of alternative 2 for WSN - datalogger	Record of downtimes and uptimes of the datalogger	Greater than 90 % of the demonstration period, including high-flow season.	100%
Data loss rate of datalogger	Record of data lossesfor the datalogger	Less than 0.5%	0%
Qualitative Performance Objectives			
Degradation of sensor housing	Photograph, digital images	Minimal degradation or corrosion of sensor housing	Minimal degradation

In January, 2011, while requesting an extension for the demonstration, we added several qualitative and quantitative performance objectives. These new objectives are listed in **Table 3.2** and **Table 3.3**.

Table 3.2 Quantitative Performance Objectives added in January, 2011

Performance Objective	Data Requirements	Success Criteria	
Reliability of WSN components that deliver data to memory cards at the gateways	Record of events and durations of the events that cause complete loss of data, weather condition when these events occur	The number of such events is less than 10; the average and maximum duration of these events are less than 30 days and less than 15 days, respectively.	Number of events for a sensor site: 15 Average duration: 59 days Maximum duration: 91 days
Reliability of WSN components that deliver data from the gateways to the database server	Record of events and durations of the events during which the data is lost in the database server but is still stored in the memory cards at the gateways, weather condition when these events occur	Same as above	Number of events for a sensor site: 37 Average duration: 37 days Maximum duration: 186 days

Table 3.3 Qualitative Performance Objectives added in January, 2011

Performance Objective	Data Requirements	Success Criteria	
Ease of use of the technology	Record of troubleshooting by non electrical engineers in the team	Except the electronic circuits and mote/stargate programming, an engineering technician can troubleshoot and maintain the system and its components with an average time for fixing a component failure of one work day and an average time between the same failures of one month.	Skill level required: engineering technician with training for some components
System maintenance requirements	Time required to troubleshoot and repair system	Downtime during maintenance will not exceed an average of one work day to fix a component failure	6.5 hours (actual time spent after the technician arrived at the site)

3.1 ACCURACY IN SSC MEASUREMENT

This is the main performance objective for the SSC sensor. This performance objective not only can be used to assess the accuracy of the sensor, it also can be used to exam the sensor's ability to provide stable readings over a long period of time and under a wide range of water temperature variation.

To assess the accuracy of SSC measurement, grab samples were frequently collected at all experiment sites. The EPA procedure, SOP 2013, "Surface water sampling", was followed. To reduce the influence of spatial variation in sediment concentration on SSC measurement, 3-5 grab samples were collected near the sensor. The samples were analyzed for SSC at KSU Instrumentation and Control Laboratory following the EPA Method 160.2. The average SSC value of samples taken at each sensor location was used as the reference value.

The success criteria for SSC sensor accuracy are defined as "±10% or ±50 mg/L of actual SSC, whichever is greater". This definition can be interpreted as "±10% for SSC higher than 500 mg/L", and "±50 mg/L for SSC lower than 500 mg/L". We believe this is a truthful description of the sensor accuracy.

The concept of "95% confidence interval" was used to interpret error bands such as ±10% or ±50 mg/L. That is, when we say the measurement error was "within ±10% of the true SSC", we mean that, for a given true SSC, 95% of the sensor readings fell within ±10% of the true SSC value. Thus, one sensor reading with an error of larger than ±10% did not necessarily constitute to the failure of the sensor.

Signal drifting over time and due to temperature variation has been a concern. Opto-electronic components are known for their sensitivity to temperature. When optical sensors are placed in natural water, signals generated by the sensors vary with water temperature. These variations

would in turn cause errors in SSC measurement. Effect of water temperature on individual signals was studied through regression analyses of samples at similar SSC.

Influences of these factors are placed under the same umbrella of "SSC sensor accuracy". To emphasize this fact, a condition of "when water temperature is within 0-50^{o}C" is added to the metric of this performance objective.

3.2 SSC MEASUREMENT RANGE

The range of SSC measurement is limited by the optical detectors used in the sensor and associated signal conditioning circuits. This performance objective examines the effective SSC range that can be measured with sufficient accuracy. This success criterion can only be examined during the high-flow season, when samples of high SSC can be obtained.

3.3 REPEATABILITY OF SSC MEASUREMENT

This performance objective examines the stability of the sensor signals. It requires multiple sensor readings within a small time span (about one minute) when a grab sample is taken at the same location. Higher accuracy requirement is required for these readings - ±5% or ±25 mg/L of actual SSC, whichever is greater.

3.4 OPERABILITY OF ANTI-FOULING MECHANISMS AND CORRECTION ALGORITHM TO COMPENSATE DATA DETERIORATION DUE TO FOULING

We combine the hardware and software solutions for biofouling to this performance objective, because the effectiveness of lens cleaning mechanisms alone is difficult to examine quantitatively.

The cleaning mechanism was activated for ten seconds each hour. Signals acquired by the SSC sensor between the cleaning actions were analyzed and a proper correction algorithm was applied to these signals to remove the effect of fouling on signal deterioration. The corrected signals were used to calculate SSC, which was then used to compare with grab samples. The same success criteria for SSC accuracy were used for the corrected data.

3.5 ACCURACY IN FLOW VELOCITY MEASUREMENT

This is the main performance objective for the flow velocity function of the combined SSC/flow velocity sensor. Simultaneous SSC and flow velocity measurements can serve as the basis for estimating sediment fluxes at different discharge points, provided the cross-sectional areas at these points are known. This method can be used to compute sediment loading from the watershed above the measurement point. This approach would enable installation staff to assess two points on a stream (e.g., downstream of BMP's and/or training exercises) and estimate differences in sediment yields by using the sensor and by determining the cross-sectional flow areas at the two measurement points.

Both SSC and flow velocity were measured at Fort Riley and Fort Benning. For APG, because the sensors were placed in lakes with minimum water flow, only SSC was measured.

An open-channel flow meter placed at the same location, same depth, and same direction as the sensor was used to provide reference values for flow velocity measurements.

3.6 FLOW VELOCITY MEASUREMENT RANGE

For the correlation type of velocity measurement, the range of measurable flow velocity is determined by the sampling frequency and the amount of data needed for computation. Higher velocities require a higher sampling frequency. When this sampling frequency is used to measure extremely low velocities, the amount of data required may exceed the memory capacity and the computation may take extra time.

3.7 REPEATABILITY OF FLOW VELOCITY MEASUREMENT

This performance objective examines the stability of the flow velocity sensor. It requires multiple sensor readings within a small time span (about one minute) when the open-channel flow meter is taking readings at the same location and the same depth. Higher accuracy requirement is required for these readings - ±5% or ±0.005 m/s of actual flow velocity, whichever is greater.

3.8 RELIABILITY OF THE SSC/FLOW VELOCITY SENSOR

This performance objective is critical to the successful completion of the demonstration. For long-time, outdoor monitoring, reliability is an extremely important quality factor for the sensors. The sensors were deployed over a long span of time while being exposed to natural waters. The ability of the sensors to continuously measure SSC and flow velocity is therefore a critical factor.

We have great concerns over the reliability of the sensors and WSNs during the high-flow season. Past field experiences have shown that equipment damages from lightning strikes and loss of equipment due to flood conditions are very likely to occur. We believe that it is difficult to define this performance objective specifically for the high-flow conditions. Thus, we would like to use a single performance objective for all flow conditions.

The quantitative index for success criterion for this performance objective was defined as the "percentage of total time when an SSC/flow velocity sensor normally measures SSC and flow velocity within the demonstration period" ("Percentage of normal operation"). The actually recorded data were the times when a SSC/flow velocity sensor unexpectedly stops measuring SSC and flow velocity normally ("downtime") and the times when the normal operation is resumed after repair ("uptime")

The Percentage of normal operation (PNO) can then be calculated as

$$PNO = \frac{\sum(uptime)}{Length\ of\ demonstration\ period} \times 100 \qquad (1)$$

PNO can also be calculated using recorded number of failures (NOF) and the mean time before failures (MTBF)

$$MTBF = \frac{\sum(uptime)}{NOF} \qquad (2)$$

Thus,

$$PNO = \frac{MTBF \times NOF}{Length\ of\ demonstration\ period} \times 100 \qquad (3)$$

We used “90%”, not 95% or 98%, for the success criteria mainly because we were considering unexpected, or even disastrous situations during the high-flow season. In our minds, “90%” can be roughly translated to a month within a year. That is, we would leave up to a month-worth time each year to fix various problems and restore our systems (not including system interrupt due to hardware or software upgrading). It is expected that the sensor nodes and WSNs would have a higher reliability during low-or medium-flow seasons.

3.9 RELIABILITY OF LOCAL WIRELESS SENSOR NETWORK (LWSN)

The three “tiers” in the wireless sensor network worked under different environments. Thus, performances of the three WSN tiers need to be assessed separately. For each tier, two important indices – reliability and data loss - were used to assess its performance. A good reliability is indicated by infrequent system failure and minimum maintenance requirement. Reliable data transmission is indicated by low packet loss during transmission.

PNO is used to examine the reliability of LWSN. PNO was calculated for each LWSN throughout the entire demonstration period, including the high-flow seasons.

3.10 DATA LOSS RATE OF LWSN

Packet loss was detected by examining time stamp of each packet transmitted from a LWSN. Data loss rate was calculated only for the time periods when the LWSN was transmitting data normally.

3.11 RELIABILITY OF MID-RANGE WIRELESS NETWORK (MRWN)

Same as Section 3.9.

Because both the gateway station and central station used CF cards for data storage, failures occurring within the MRWN and LRCN can be easily distinguished. Thus, the number of failures occurring at MRWN can be quantified by examining the time stamps on the data stored in the CF memory card at each gateway station and that at the central station. The NOF and MTBF were then be calculated.

3.12 DATA LOSS RATE OF MRWN

Same as Section 3.10.

3.13 RELIABILITY OF LONG-RANGE WIRELESS NETWORK (LRCN)

Same as Section 3.9.

The time stamps examined were those attached to the data stored in the CF card at the central station and that attached to data received at the Internet server.

3.14 DATA LOSS RATE OF LRCN

Same as Section 3.10.

3.15 RELIABILITY OF INTERNET SERVER

Operability of the Internet server was assessed by counting number of times the Web server and WebGIS could not be opened, hang, or display erroneous data and recording the MTBF during the demonstration period. A log book was used to record these abnormal operating conditions.

3.16 RELIABILITY OF WEB GIS

Same as Section 3.15

3.17 RELIABILITY OF SOLAR PANEL AND CHARGING CIRCUIT

Reliability of the solar panels and charging circuits was assessed by NOF and MTBF for each sensor node, gateway station, repeater station, and central station. Battery voltages, which were included in all wirelessly transmitted data packets, were constantly checked. A log book was used to record these abnormal operating conditions.

3.18 RELIABILITY OF ALTERNATIVE 1 FOR WSN - METEOR-BURST COMMUNICATION (MBC) SYSTEM

Same as Section 3.9.

The MBC is not a stable data communication method. As a result, a higher failure rate was expected. We use 70% as the success criterion.

3.19 DATA LOSS RATE OF MBC

The MBC is not a continuous data communication method. As a result, a higher data loss rate was expected. We use 20% as the success criterion.

3.20 RELIABILITY OF ALTERNATIVE 2 FOR WSN – DATALOGGER

Same as Section 3.10.

Our past experience with dataloggers has been very positive. Thus, we expect a high reliability for this system.

3.21 DATA LOSS RATE OF DATALOGGER

Same as Section 3.10.

Our past experience with dataloggers has been very positive. Thus, we expect a low data loss rate for this system.

3.22 DEGRADATION OF SENSOR HOUSING

Material selection for sensors made for long-term, under-water use is important, although it is difficult to evaluate different materials quantitatively. Past laboratory experiment has shown that black polyethylene housing displayed significantly less biofouling and corrosion than metal housing with black paint, after both had been submerged in water for several days.

Another factor affecting our selection is the “machinability” of the materials. Polyethylene has been found difficult to machine because it is too soft. For the “fourth generation” sensor housing, a substitute plastic material – Acetal – was used. This material has a much higher hardness and is easy to machine.

We use visual inspection and digital images to qualitatively study housing degradation due to fouling and corrosion.

3.23 RELIABILITY OF DATA DELIVERY TO MEMORY CARDS

Among the three tiers of a three-tier wireless sensor network (WSN), the local wireless sensor network (LWSN) is responsible for sensor measurement and delivery of sensor data to the gateways, where the data are 1) relayed to the repeaters, central station and, finally, the database

server and 2) stored in memory cards at the gateway station. For a two-sensor gateway, a 1 GB memory card is capable of storing up to 4.6 years' of data. If the velocity raw data are also stored, the 1 GB memory card can record 2.7 years of data.

Reliable data storage in the memory cards is guaranteed as long as the key components in the LWSN are functioning. Components in the top two tiers of the WSN (the MRWN and LRCN) have no effects on memory card storage.

Key components in the LWSN that affect data storage in the memory cards include the sensor, the mote, cables connecting the sensor and the mote, antennas on the mote and the Stargate, and power supplies for the sensor, mote, and Stargate.

3.24 RELIABILITY OF DATA DELIVERY TO DATABASE SERVER

Failures occurring within the top two tiers of a three-tier WSN (MRWN and LRCN) cause data loss in the database server, but not in the memory cards installed in the gateways. Key components related to this type of data loss include the Stargate, datalloger/radio transceivers in the repeaters and the central station, cellular modem, antennas at the gateway stations, repeaters, and central station, and power supplies for these stations.

This performance objective examines the skill level required to troubleshoot and maintain the system and its components. We believe that an engineering technician with certain training should be able to troubleshoot the system and its major components except 1) the electrical circuits for sensor signal conditioning and control, and 2) programs for the microcontrollers on the motes and Stargates. The components they should be able to troubleshoot include the sensors and their fixtures/harness, dataloggers/radio transceivers, cellular modems, antennas, and power supplies.

3.25 EASY OF USE OF THE TECHNOLOGY

This performance objective examines the skill level required to troubleshoot and maintain the system and its components. We believe that an engineering technician with certain training should be able to troubleshoot the system and its major components except 1) the electrical circuits for sensor signal conditioning and control, and 2) programs for the microcontrollers on the motes and Stargates. The components they should be able to troubleshoot include the sensors and their fixtures/harness, dataloggers/radio transceivers, cellular modems, antennas, and power supplies.

3.26 SYSTEM MAINTENANCE REQUIREMENTS

This performance objective examines the downtime used for troubleshoot and repair the system and its components by an engineering technician.

4 SITE DESCRIPTION

4.1 SITE LOCATION AND HISTORY

The following nine criteria/requirements are established for demonstration site evaluation and selection:

1) Candidate sites should be located on Department of Defense (DOD) facilities, or affiliated with (and near) a DoD facility.
2) Demonstration sites should be accessible so that test equipment can be installed and maintained easily.
3) Demonstration sites should have continuous flowing water; the water depth should be sufficient so that SSC sensors are submerged most of the time. One of the sites should be in an estuarine tidal environment.
4) Candidate sites must have facility acceptance of the demonstration technology.
5) The Total Suspended Solids (TSS) should be sufficiently high in order for the sensor to be able to measure SSC concentration.
6) The various demonstration sites should be located in different geographical areas so that the sensors and WSN can be demonstrated under a variety of climactic conditions.
7) If possible, the demonstration sites should be close to existing water quality monitoring stations in order to be able to leverage SSC, flow, and weather data being collected at those stations.
8) Demonstration sites should be selected in areas where measured SSC data is meaningful and helpful to the installations to perform ongoing or planned water quality monitoring programs.
9) At least one location within each experiment site should have cellular coverage to serve as the central station for long range data transmission. The sites of central stations selected at the three experimental sites should have different types of topography so that the three-tier WSN can be demonstrated under different types of terrain.

A variety of candidate demonstration sites at several army installations were evaluated against these criteria, and the final site locations determined. The three Army installations selected were Fort Benning, GA, Fort Riley, KS, and Aberdeen Proving Ground (APG), MD. These installations are located in different geographical regions of the United States, which allowed the SSC sensor and WSN to be demonstrated under a variety of climactic conditions. One or more "sensor clusters" were installed at each installation, with each sensor cluster consisting of one or more optical sensors. Sensor clusters at each installation were integrated into a three-tier WSN. The sensor clusters and the number of sensors comprising each cluster are shown in Table 4.1. APG enabled testing of the sensor in an estuarine tidal environment. Fort Benning and Fort Riley enabled testing of the sensor and WSN on ranges under varying climactic conditions and with different types of topography. All three installations were very supportive of the demonstration test.

Table 4.1 Sensors deployed at the demonstration sites

Installations	Sensor Sites	Number of Sensors Deployed
Aberdeen Proving Ground, MD	Edgewood Rod and Gun Club (Gunpowder River Pier)	2
	Otter Point Creek (Anita Leight Estuary Center)	2
Fort Benning, GA	Pine Knot Creek	2
	Upatoi Creek	2
Fort Riley, KS	Little Kitten Creek	1
	Wildcat Creek	2
	Silver Creek	1

4.2 SITE CHARACTRISTICS

4.2.1 Fort Riley, Kansas

Fort Riley was selected as a desirable location for this project because of its close proximity to Kansas State University. This site can be classified under the Flint Hills Eco region, which is characterized by large rolling hills composed of shale and limestone. The average annual precipitation of the region is between 28-35 inches (Castle, 2007).The region is dominated by tallgrass prairie and remains mostly undeveloped in the study sites chosen. Three streams and four sensor sites where selected for this location. All of the streams used in this study are part of the Wildcat Creek basin.

4.2.1.1 Little Kitten Creek

Little Kitten Creek is a stable, perennial stream that drains a 1,900 acre watershed located on the western edge of Manhattan, KS (Castle, 2007). Little Kitten Creek is not located on the grounds of Fort Riley military training area, but for the purposes of this research it was included in the Fort Riley sensor location sites for easier referencing. The watershed and stream are highlighted in Figure 4.1.

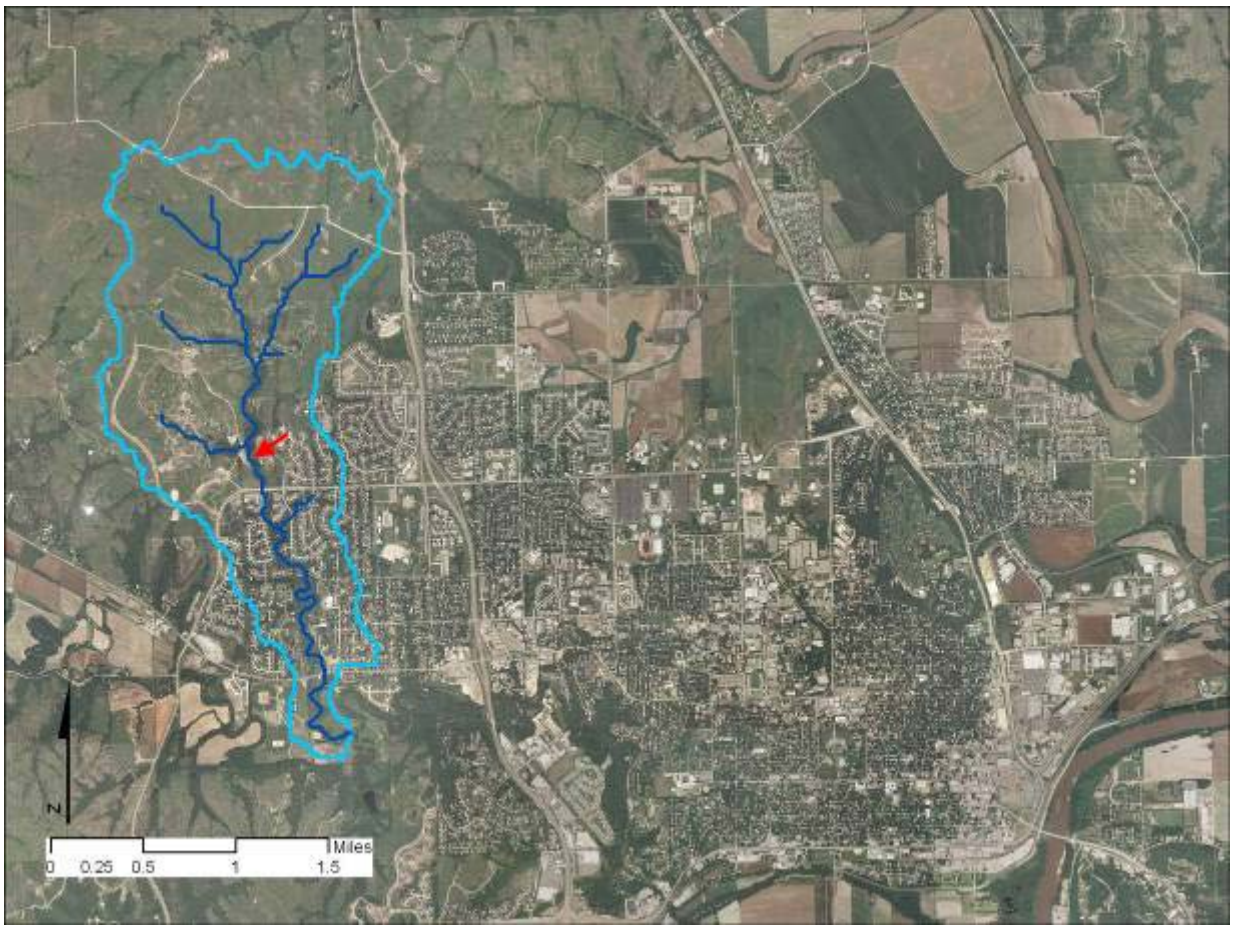

Figure 4.1 Little Kitten Creek Watershed. Sensor location denoted by red arrow. (Source: (Castle, 2007), edited by author)

The portion of the stream that is upstream from the sensor location is mostly undeveloped and is mostly dominated by groundwater seepage from the Flint Hills with stormwater runoff being added during storm events.

Usually the sensor was placed 6-12 inches from the bottom of the streambed. However at Little Kitten Creek the stream was not 6-8 inches deep at the site during normal flow so the sensor was placed 1-2 inches above the streambed but still submerged in the stream. Figure 4.2 displays the sensor placed in Little Kitten Creek.

Figure 4.2 Sensor installed in Little Kitten Creek, with velocity attachment and without cover.

4.2.1.2 Wildcat Creek

Wildcat Creek is a larger stream than Little Kitten Creek; this stream drains an 88 square mile area with its headwaters located 28 miles west of Manhattan, KS (Stutterheim, 1972). The portion of Wildcat Creek that was used in this study is directly south and southwest of the city of Keats, Kansas which is approximately 8 miles west of Manhattan. This study site is upstream from the entry of the Little Kitten Creek. This section of the stream also serves as the border between Fort Riley and private land.

Two sensors were installed in this stream approximately 1.3 miles apart from each other, measured on the stream channel. The names of these sensor sites used in this report are Wildcat Bridge and Wildcat Creek (Figure 4.3).

4.2.1.2.1 Wildcat Bridge

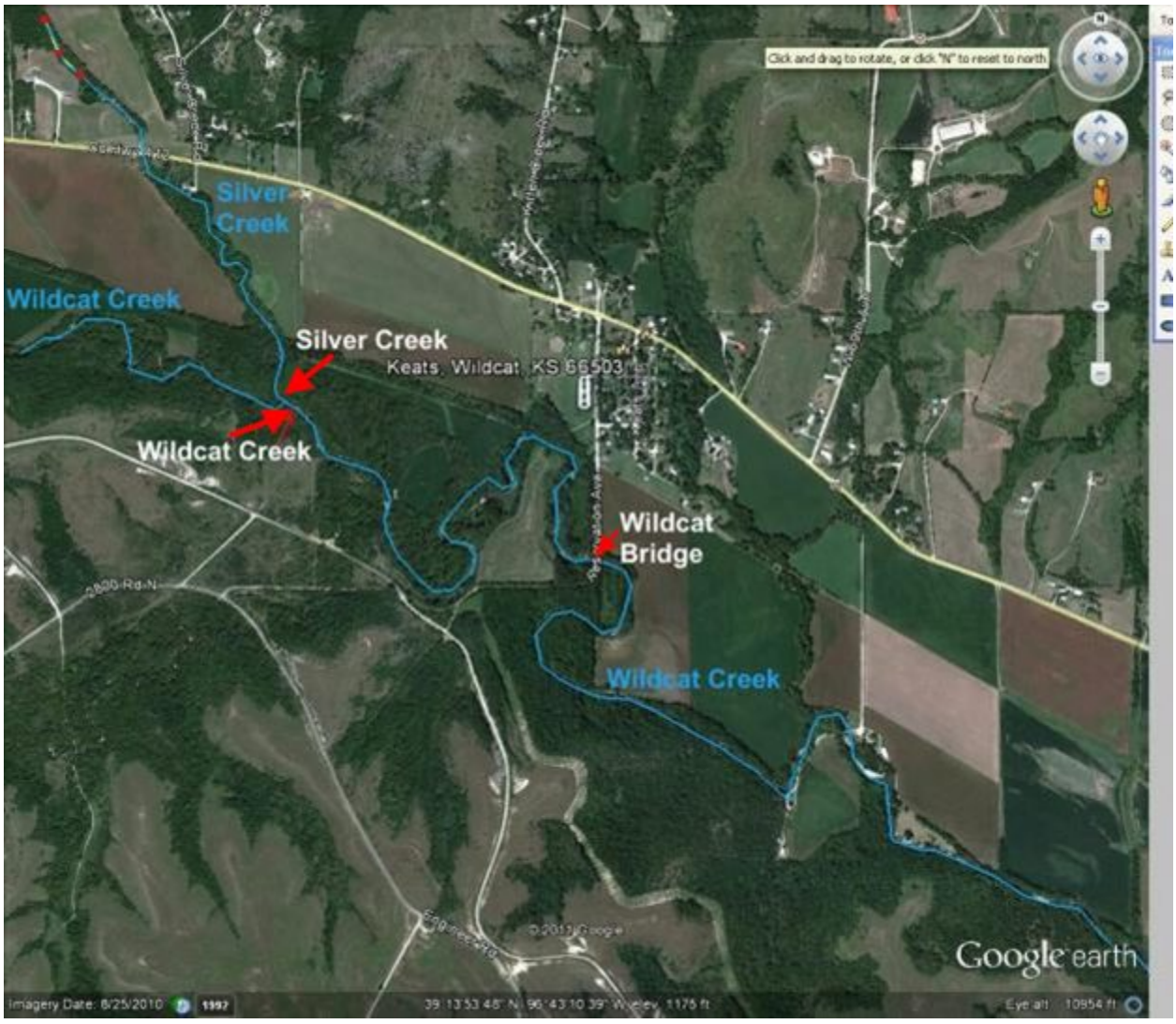

Figure 4.3 Wildcat Bridge, Wildcat Creek, and Silver Creek sensor sites. (Source: Google maps, edited by Author).

The Wildcat bridge sensor site was near an old military bridge that was directly south of Keats, KS. This can be seen in Figure 4.4 along with the other nearby sensor sites. The sensor was installed in the 3-6 foot deep portion of the stream. This depth created some difficulties for sensor calibrations. During periods of higher flow it was deemed unsafe to enter the middle of the stream channel. In order to properly gather calibration data the sensor was placed at the edge of the stream where it could be more easily accessed. After calibration was completed the sensor was then moved to the middle of the stream channel.

Figure 4.4 Wildcat Bridge sensor installed in stream with sensor name displayed.

4.2.1.2.2 Wildcat Creek

The Wildcat Creek site was located upstream from the Wildcat Bridge sensor. The sensor was initially placed in the riffle of the stream in a part of the channel that was between 2-8 inches deep in normal flow periods. During the summer of 2011, there was a very large rain event in the Wildcat Creek watershed causing considerable flooding for this stream. Because of the force of the flood event the streambed underwent some changes and the sensor site became a pool area of the stream, measuring 3-4 feet deep during normal flow periods.

During the flooding event some of the electronic components on the streambank also became damp and therefore needed to be replaced or fixed. After a period of troubleshooting it was determined to focus mainly on the Wildcat Bridge and Little Kitten sites. Although this site still transmitted data back to the database, the data it was sending no longer carried sediment information.

4.2.1.3 Silver Creek

Silver Creek is also a tributary of Wildcat Creek; this stream is approximately 7 miles long and drains a mostly undeveloped tallgrass ecosystem (Gustafson, 1999). The site for the sensor was located at the mouth of Silver Creek just upstream from the Wildcat Creek sensor site. Since this location was at the mouth of the stream, there was a large amount of streambed movement, burying the sensor in rocks on numerous occasions. This is because as the smaller, faster moving

stream enters the larger, slower moving Wildcat Creek, the velocity decreased, causing sediment and rocks to be deposited. This was especially true during periods of high flow. This was the same type of phenomena that happened when a stream entered a large pond or lake.

The sensor was moved from the newly formed rock bed to a new stream flow path several times. However, in the summer of 2011, there was a large rain event that buried the sensor once again, and the force of the water also broke the sensor cables and conduit, making the sensor dysfunctional. After this flood event the area went through a very dry period for the rest of the year and this stream stopped flowing altogether. As a result, this site was abandoned.

4.2.2 Fort Benning, Georgia

The second site that was chosen for this project was Fort Benning, Georgia. This military installation is located just south and east of Columbus, Georgia, near the Georgia-Alabama state line. This area is dominated by evergreen and deciduous forest and has rolling hill topography (Bourne & Graves, 2001). The average annual rainfall for this area is approximately 49 inches (U.S. Climate Data, 2011). This site has a different climate, soil type, and ecological makeup from the Fort Riley site and provides the study with data to improve versatility. Two different streams were chosen for this study site with two sensors installed in each stream.

4.2.2.1 Pine Knot Creek

Pine Knot Creek is located on the northeastern edge of Fort Benning; the sediment type is mostly sand so high sediment concentrations were seldom occurring. Pine Knot Creek is a tributary of the Upatoi River which will be discussed in the next section. There were two sensors installed at this site to measure the SSC. The sensors were installed approximately 15 feet apart from each other, with the northernmost sensor being installed near the bank of the stream and the southern sensor being installed in the middle and deepest part of the channel. Figure 4.5 displays both the Pine Knot and Upatoi River along with the location of the sensor sites.

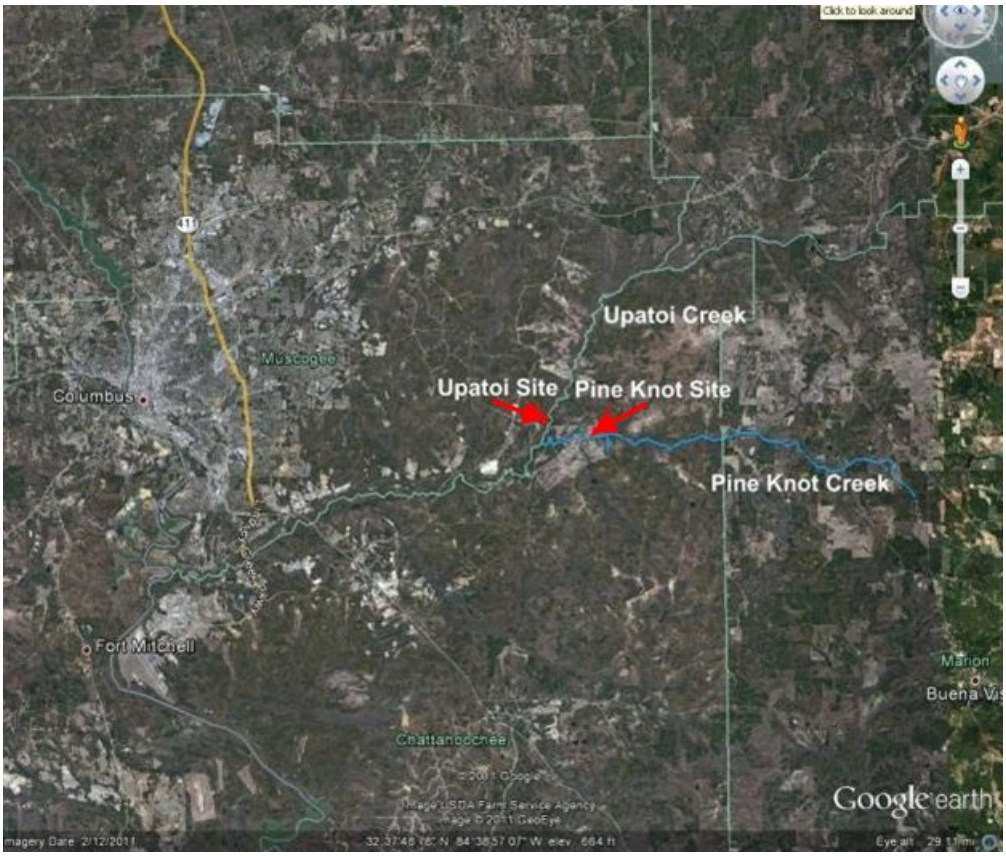

Figure 4.5 Ft. Benning stream sites with sensor location. (Source Google Earth, edited by Author)

The north sensor is referred to as Pine Knot North (PKN) while the south sensor Pine Knot South (PKS) in this report. The PKS sensor had the capability of measuring velocity as well as SSC. Figure 4.6 displays the sensors installed in the stream.

Figure 4.6 Pine Knot sensor site with labels displaying sensor names. Sensor covers are installed on both sensors.

4.2.2.2 Upatoi River

Upatoi Creek is a 35.5 mile long river that runs through Fort Benning before depositing in the Chattahoochee River (USGS, 2011).The section of this river where the sensors were installed was near the middle of the length of this river. The streambed of this river is mostly sand which tends to settle very quickly to the bottom of the stream. This caused some difficulty in obtaining high SSC samples. Both sensors at this site were installed approximately 15 feet apart from each other with one sensor being slightly north and east of the other sensor. In this report, the north sensor is referred to as Upatoi North while the south sensor Upatoi South. Figure 4.7 displays the sensors installed in the river with the sensor covers.

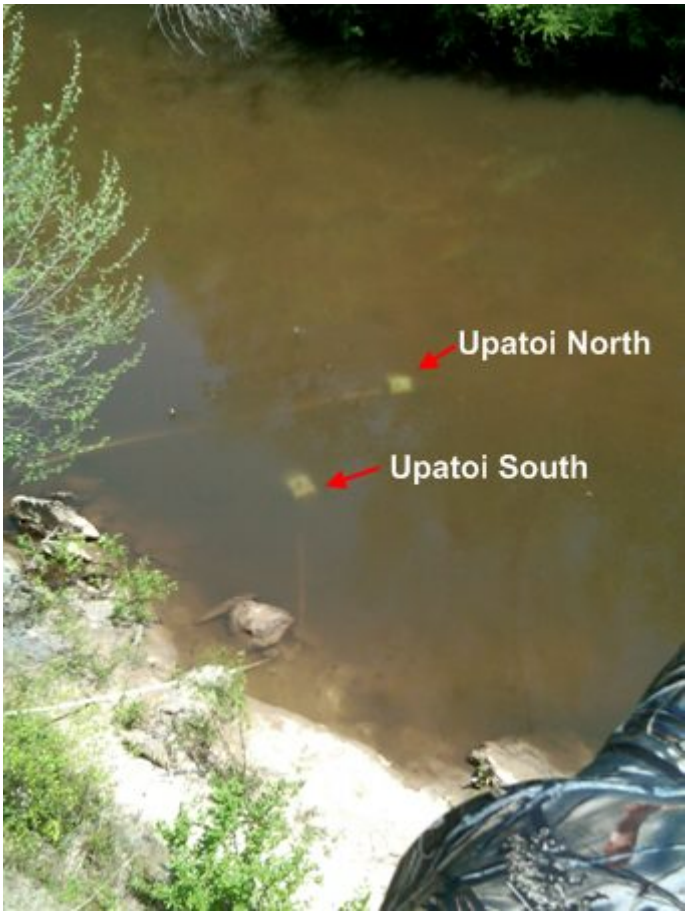

Figure 4.7 Upatoi sensor site displaying sensor name labels, sensor covers are installed on both sensors.

4.2.3 Aberdeen Proving Grounds, Maryland

The U.S. Army Aberdeen Proving Ground (APG) is located in Harford County, Md. The installation has about 72,000 acres, most of which are rangelands and water areas that are used for testing purposes. APG consists of two principal areas that are separated by the Bush River. The northern part is known as the Aberdeen Area and the southern part is known as the Edgewood Area. The northern boundary of APG is bounded by the Susquehanna River and the Chesapeake Bay. On the south it is bordered by the Gunpowder River and the Chesapeake Bay. APG has more than 103 miles of shoreline, with shoreline erosion occurring at significant rates in several areas. There are several marinas and other piers on the installation that are used for recreational activities such as boating. APG is actively involved in several environmental compliance, pollution prevention, conservation, and restoration programs. For example, the installation's Natural Resources Program has taken actions to stabilize vulnerable areas of shoreline and minimize erosion. Studies are continuing to evaluate shoreline areas and to monitor changes after storm events. APG also acts as a steward for those areas of the Chesapeake Bay within the proving grounds boundaries.

The ecological region of this area is defined as the outer coastal plain, mixed forest and is fairly developed (Doe III, Shaw, Bailey, Jones, & Marcia, 1999). The Eco region is characterized by

mostly flat topography with oak-hickory-pine forests being the natural vegetation (McNab & Peter, 1994). The rivers in this area are mostly stagnant with their flow coming from tidal influence. Two sites were selected for this location with two sensors installed at each site (Figure 4.8). The distance between the two sites is 8.1 km.

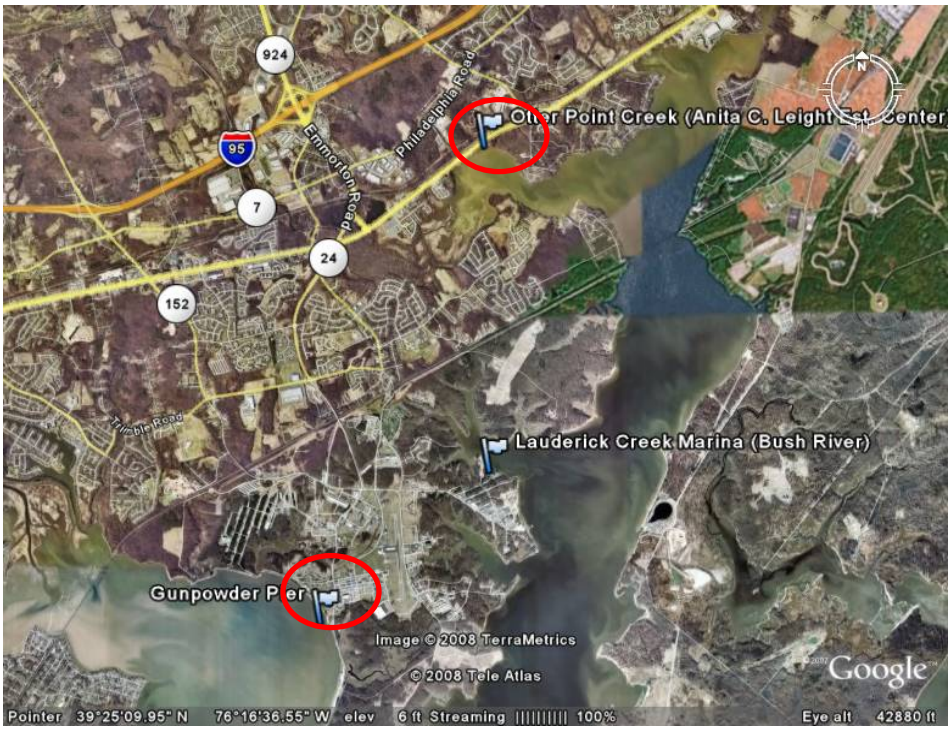

Figure 4.8 Overall locations of SSC sensor clusters at APG, MD.

4.2.3.1 Anita Leight Estuary

Anita Leight Estuary is part of a tidal cove that is part of the Chesapeake Bay. Fluctuations in SSC at this site are usually seen from tidal action and rain events. The area that drains into this sensor site is mostly developed with a small nature preserve directly east of the sensor site. Figure 4.9 displays the sensor location.

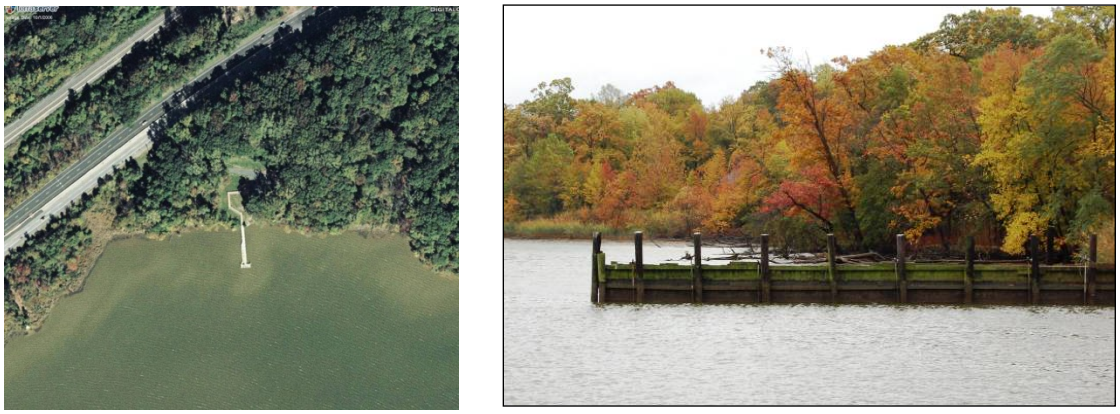

Figure 4.9 Anita Leight sensor site location. (Source: Google maps, edited by author)

Sensors at this site were attached to support posts of a boat dock. This type of set up was chosen because of the protection the dock offers along with the ease of access to the sensors. Sensor covers for this site were modified in a way that the sensors were attached to the covers and the covers were then attached to the dock using a bracket and lag bolts.

4.2.3.2 Gunpowder River

Much like the Anita Leight site, the Gunpowder River site is also part of the Chesapeake Bay system. This site is on the APG base and also has tidal fluctuations. Much of the area that drains into this river system is developed. The sensors at this site were attached to a boat dock as well using the same method as described in the Anita Leight section. Figure 4.10 displays the location of the Gunpowder sensor site.

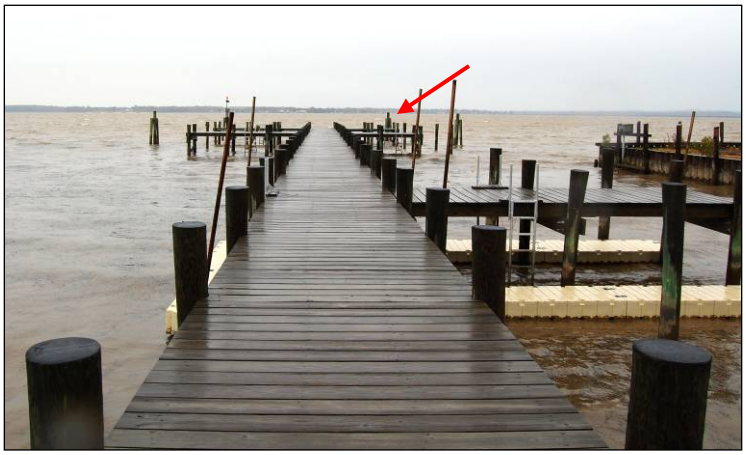

Figure 4.10 Gunpowder River sensor site

Initial calibration and testing of this sensor site was performed in the initial round of sensor deployment from 2009-2010. Some difficulties with data transmission were encountered during the test. Also one of the sensors at this site was hit by a boat and knocked off of its attachment to the boat dock. It was determined that, for the second round of calibration, the sensors at the Anita Leight was reinstalled while Gunpowder site was only used for data transmission testing.

5 TEST DESIGN

5.1 CONCEPTUAL TEST DESIGN

The experiment was designed to test 1) performance of the SSC sensor in long-term, remote monitoring of sediment in streams at three military installations, 2) performance of the integrated SSC/flow velocity sensor in measuring flow velocity in open streams, and 3) performance of the three-tier WSN in transmitting and managing SSC and velocity data measured at multiple location within three military installations over a long period of time. The experiment was accomplished by deploying components of the system – sensor nodes, gateway stations, repeater stations, and central stations at the installations. The SSC measurement was calibrated against grab samples collected at the sensor locations. The velocity measurement was calibrated against a commercial ultrasonic flow velocity sensor, and the three-tier WSN was examined on failures and data loss.

Tasks of the experiment included 1) lab testing of the flow velocity measurement capability and anti-fouling mechanism components added to the optical sensor, followed by field testing of the entire optical sensor node, and 2) lab and field tests of each tier of the three-tier WSN.

The demonstration proceeded through three phases. Phase 1 was further development of the sensor and software for communications between various wireless components at Kansas State University. Phase 2 included testing of the sensor and the three-tier network at a pilot experimental site located in Manhattan, Kansas, close to Kansas State University. Phase 3 was installation and operational testing of the sensors and the WSN in the field at the three military installations. Phase 3 started at Fort Riley, which was located very close to Kansas State University. This provided convenience to the researchers of KSU for installation, sampling, and maintenance of the sensors and WSN. Phase 3 then proceeded with installation at Fort Benning, followed by APG. Among the three phases, phases 1 and 2 were for pre-demonstration preparation. Only phase 3 was for demonstration.

During phase 3, we placed an SSC/flow velocity sensor at the Pine Knot sensor site where the “USGS 02341725 Pine Knot Creek Near EelBeeck, GA” stage monitoring station was located. The purpose of this arrangement was to compare the velocity data with USGS stage and discharge data and to study the possibility of using the point velocity measurement provided by our sensor to either help simplify the discharge estimation procedure or to provide better discharge estimates.

5.2 BASELINE CHARACTERIZATION AND PREPARATION

Characterization and site preparation activities that were performed prior to beginning demonstration testing included: 1) perform pre-calibration of the optical sensors, 2) determine the final locations of the individual gateway stations and central stations, and 3) installation of the optical sensor and ancillary components at the various demonstration sites.

5.2.1 Calibration of Optical Sensors

It was anticipated that the optical sensor signals would vary with the optical properties of the suspended sediment and the opto-electric components. For the best results, a calibration model needed to be developed for each sensor and for each location where the sensor was installed.

Calibration of the sensors consisted of two steps. The first step was "pre-calibration". The goal of pre-calibration was to select the gains of the current-to-voltage converters in the signal conditioning circuits so that the maximum sensor signals were achieved at a certain level of SSC. This level was selected to be 5,000 mg/L before sensors were deployed to the three installations in 2009.

The second step was to establish the calibration model for predicting sediment concentration from the sensor signals for each sensor at its location of deployment. To develop this model, a large number of grab samples within a wide range of sediment concentration were needed. Actual sediment concentrations of these samples were measured using the filtering and weighing method in laboratory. A regression analysis of the actual concentration against sensor signals was then conducted to produce the calibration model. Obviously, for a good model that could predict SSCs within a specific range, grab samples with SSCs evenly distributed within the range would provide the best results.

After the sensors were deployed to the three installations, it was found that the actually SSCs of the water samples taken from the sensor sites were generally low. With the exception of one grab sample taken during a rain event at the Silver Creek site, the maximum sediment concentration obtained from these samples was 232 mg/L, which was only about 1/20 of the expected range (Table 5.1). If calibration was limited to these grab samples, the effective measurement range would be very narrow. As a result, the measurement accuracy within a wider range of SSC would suffer greatly.

Table 5.1 Grab samples taken at the twelve sensor sites in 2009-2010

Sensor Location		Number of grab samples taken	Time period the grab samples were taken	Range of sediment concentration (mg/L)
Fort Riley	Little Kitten	19	3/24/2010 – 11/12/2010	5 – 160
	Wildcat Bridge	2	11/12/2010	12 – 14
	Wildcat Creek	6	3/29/2010 – 9/23/2010	15 – 203
	Silver Creek	5	9/10/2010 – 9/23/2010	64 – 803
Fort Benning	Pine Knot North	10	9/10/2009 – 6/30/2010	4 – 15
	Pine Knot South	10	9/10/2009 – 6/30/2010	6 – 12
	Upatoi North	9	9/10/2009 – 6/30/2010	3 – 15
	Upatoi South	12	9/10/2009 – 6/30/2010	3 – 10
APG	Anita Leight Near	14	10/19/2009 – 10/27/2010	16 – 126
	Anita Leight Far	9	10/19/2009 – 10/27/2010	10 – 232
	Gunpowder Near	9	10/19/2009 – 10/272010	19 – 201
	Gunpowder Far	9	10/19/2009 – 10/27/2010	16 – 124

Due to this situation, we requested a one-year extension for field demonstration (from 7/1/2011 to 6/30/2012) in March, 2011. In order to derive better prediction models, we decided to make the following changes:

1. Knowing that the actual sediment concentration range at the sensor locations was in general much lower than the range we assumed in pre-calibration, we adjusted the gains of the sensors so that the measurement ranges were reduced. This adjustment was accomplished in laboratory by replacing several resistors on the signal conditioning board. This gain adjustment will become a part of sensor calibration before a sensor is deployed to a specific site. It is performed only once for each sensor, and it is always done in the laboratory.
2. Increasing the number of grab samples taken from all sensor sites.

5.2.2 Determine locations of gateway, repeater, and central stations

After the final locations of the optical sensors were identified, the locations of the gateway stations needed to be determined at all sites. The gateway stations should be located within 100 meters of the sensor nodes for acceptable signal reception. The locations were determined by field inspections at the sensor sites for ease of access and minimum impacts on other ongoing activities at the sites. The selection was also coordinated with, and approved by installation personnel. The final locations of the gateway stations were field validated before the wireless network components were installed at the site. Validation was performed by measuring Received Signal Strength Indicator (RSSI) at the locations of the gateway stations to ensure that signals can be transmitted from each of the sensor sites to the gateway station. The locations of the gateway stations were determined using GPS and marked on an appropriately scaled map.

Based on the locations of the gateway stations, a final location for the central station was determined at each installation. Several possible locations for the central station were first identified using installation maps. These locations were then assessed during field inspections, and the best location determined. The candidate sites for the central station were evaluated on 1) strengths of signals received from the gateways at the central station as measured using a spectrum analyzer, 2) ability to transmit signals from the central station through the cellular network (i.e. cellular coverage at the central station), 3) ease of access, and 4) impacts to other ongoing activities. The final locations of the central stations were validated before the network components were installed through a survey. The survey validated the signal strengths as indicated by RSSI at each selected gateway stations and the central station and the strength of cellular signals at the central station. The field survey also determined if any additional repeater stations were required to transmit signals from the gateways to the central station. GPS locations of the repeater and central stations were determined and marked on an appropriately scaled map. Also, the final location of the central and repeater stations at each installation were approved by installation personnel.

5.2.3 Installation of Optical Sensors and Three-tier Wireless Network

The optical sensor nodes, gateway stations, repeater stations, and central stations were installed at all three test installations. The system was operational before demonstration tests began.

5.2.4 Installation of WSN alternatives – Meteor Burst Communication (MBC) and datalogger

The MBC system as an alternative of WSN was also installed at the central station of the Fort Riley site, sharing the lower two tiers of the WSN with the three-tier WSN.

MBC is a wireless communication method for long-distance data transmission. By utilizing the ionized trail of gases left from the entry and disintegration of the meteors, people are able to create communication networks between different points on Earth. In this study, the MBC technology was investigated as a possible alternative of the upper tier – the LRCN in the three-tier WSN system.

In the three-tier WSN using the MBC network as the LRCN, the central station included three modules: a radio communication module, a MBC radio module, and a power supply module. The radio communication module consisted of a CR1000 datalogger, an RF401 radio (Campbell Scientific), and a Yagi directional antenna. The RF401 radio was connected to the CR1000 datalogger to receive SSC data from the CR206 at the repeater station. The MBC radio module included an MCC545B radio (MeteorComm LLC) and a MBY-3 Yagi directional antenna. The MCC545B radio operated in the low-band VHF (41.61 MHz for transmitter and 40.67 MHz for receiver) region of the RF spectrum. Figure 5.1 shows the main devices in the MBC central station. The power supply module included a 200 W solar panel, a solar charge controller with 10 A current rating, and a 12 V deep cycle battery.

(a) (b) (c)

Figure 5.1 MBC central station devices: (a) CR1000, (b) RF401, (c) MCC545B radio

The MBC central station was installed close to the central station of Ft. Riley site. The MBC antenna was mounted at the top of a 10 ft steel conduit and pointed to the MBC master station at Tipton, MO, which is locates over 200 miles from Manhattan, KS. The central station received

the SSC data from the sensor node at the Wildcat Bridge site and transmitted the data to the master station. The MBC central station is shown in Figure 5.2.

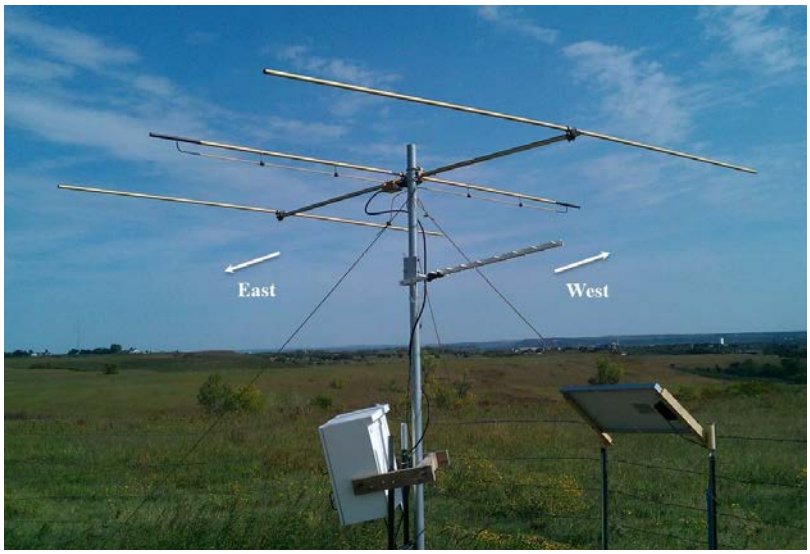

Figure 5.2 MBC central station

The raw data provided by the MBC master station consisted of four major components: header, data body, receiving time, and transmitter ID. Each complete SSC data packet included four pieces of raw data. The transmission time for each data packet can be calculated from the beginning and ending Rx time stamps. The maximum and average transmission time per data packet during the demonstration period is shown in Figure 5.3. The average time to transmit one data packet was within five minutes, and the maximum time was 51 minutes.

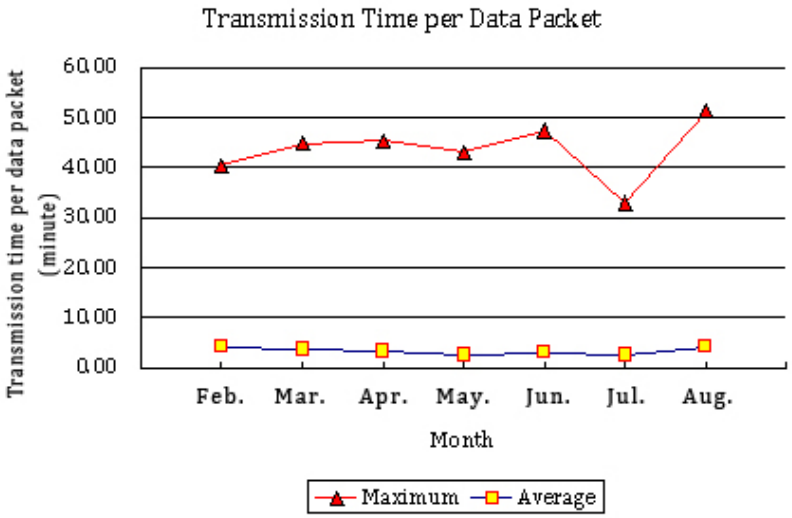

Figure 5.3 Transmission time per data packet for MBC

A datalogger-only option was considered as another alternative of the three-tier WSN. For this option, no wireless technology should be used. The SSC and velocity data should be stored in a

memory card at each sensor node, and be downloaded into a PC computer manually at a later time. Thus, the measurement cannot be done in real-time.

For the demonstration, we did not put an additional datalogger at a sensor site, because, based on our past experience with Campbell Scientific dataloggers, reliability of the dataloggers is not a concern. We did compare the costs related to the three alternatives, including the datalogger-only alternative. The results will be given in Chapter 7.

5.3 FIELD TESTING

The history of field testing is illustrated in a Gantt chart as shown in Figure 5.4.

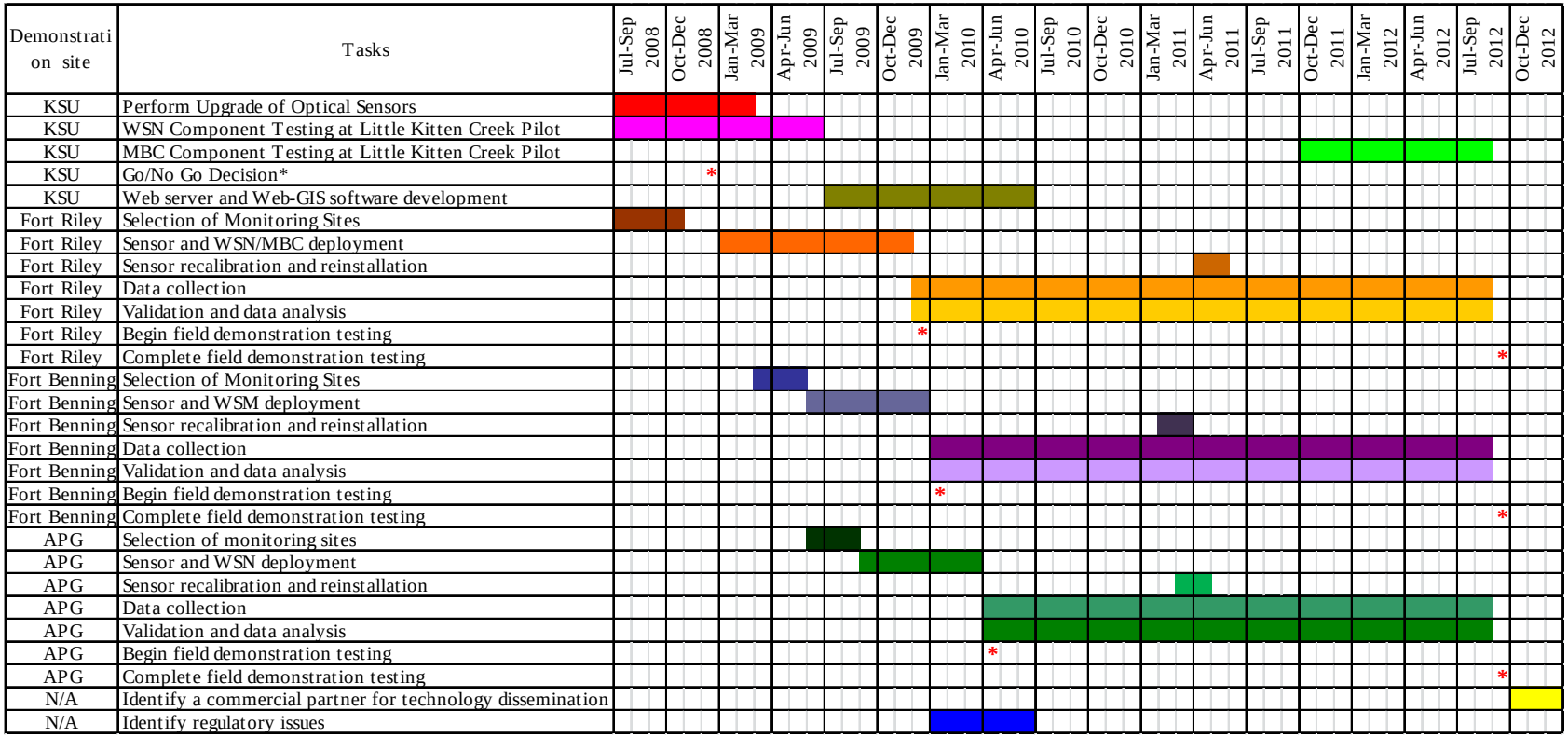

Figure 5.4 Actual schedule of the field test

Phase 1 - Further development of sensor and three-tier WSN

Phase 1 was conducted at Kansas State University. During this phase, the sensor was further improved by adding a stream flow velocity measurement and a self-cleaning mechanism through simple structural expansions. The velocity measurement function was tested in an enclosed circulation system and in a flume. A commercial ultrasonic, open-channel flow meter was used to calibrate the sensor. The KSU team worked with the Advanced Manufacturing Institute (AMI) of KSU to design a new prototype of the sensor using the Solidworks 3D Computer-aided Design (CAD) software, which allowed multiple sensors to be fabricated on (Computer Numerical Control (CNC) machine tools. While maintaining the basic optical structure, the new sensor prototype had the following advantages: 1) The sensor used acetal as the material to reduce corrosion, 2) The wiring chamber was filled with epoxy so that leakage problem can be completely avoided (as a result, the sensor became one-time use, disposable), 3) The CNC machine can precisely control the geometric positions and orientations of the optical components, and 4) Air passages for cleaning can be embedded in the sensor. Software for communication and control of the wireless motes, wireless data acquisition boards, datalogger/radio transceivers, and cellular modems was also completed during this stage.

Two options for sensor lens cleaning were designed and tested: an air-blast cleaning system and an ultrasonic cleaning system. The ultrasonic system was found to consume too much of the battery power, which made it not practical for field use. The air-blast cleaning system was tested in both laboratory and field. Sensors with acetal and aluminum cases were tested at 2-minute and 12-hour cleaning intervals to observe the performance of the cleaning system. Signal recovery due to sensor cleaning was studied and the cleanness of the optical lenses was visually observed to qualitatively evaluate the effectiveness of the cleaning system.

Phase 2 - Sensor and WSN test at the pilot experimental site

During the second stage, multiple sensors were deployed to the Little Kitten Creek pilot experiment site in Manhattan, Kansas. An LWSN was established between the sensors and a gateway station located on the bank of Little Kitten creek. Radio transceivers with Yagi and Omni antennas were installed at the gateway station, a repeater station, and a central station, all of which were located in Manhattan, Kansas. Receive Signal Strength Indicator (RSSI) was measured using a spectrum analyzer to help determine the locations of the gateway station, repeater, and central station.

Phase 3 - Sensor and WSN installation and test at the installations

During the third phase, multiple sensor nodes and WSNs were installed at Fort Benning, Fort Riley, and APG. At Fort Benning, a sensor node was selected near an United States Geological Survey (USGS) stream-gaging station. Data collection began when the optical sensor nodes and WSN became operational. Data packets consisting of SSC, flow velocity, water temperature, and precipitation were transmitted to the web servers at KSU and OSU. Project personnel at KSU and OSU remotely monitored the data being collected using a web server. Project personnel took site visits several times during the data collection period to inspect and maintain the sensors and WSN components, and to collect surface water grab samples. The sensor data were compared to the data obtained from grab sampling and flow measurement for calibration. Data

measured at three installations were displayed, archived, and analyzed at servers located at Kansas State University and Oklahoma State University to evaluate the functionalities of various sensors and wireless components. A Web-based GIS was developed to allow access and utilization of the monitoring data. A daily report that contained statistics of data collected during the previous day and alerts about low battery voltages was sent to the project personnel each morning at 6 am (central time) by the Web-based GIS system.

During the third phase, the MBC alternative was demonstrated at the Fort Riley site. The MBC system was used to replace the LRCS in the three-tier WSN.

Project personnel at KSU and OSU monitored the collected data on a daily basis through the daily report and alert report provided by the Web-based GIS. Personnel remotely accessed every optical sensor at all three test installations to assess the operability of the optical sensors and WSN and the quality of data transmission (packet loss and transmission error) from the daily reports generated by the Web-based GIS system and from the database.

During this stage, project personnel took several site visits to install the sensors and WSN, to debug and repair system problems, and to collect grab samples.

Table 5.2 summarizes the site visits project personnel took to Fort Benning and APG during the project.

Table 5.2 Sites visits to Fort Benning and APG

Sensor Network Maintenance Trips			
Location	Time period	People travelling	Purpose
Ft. Benning	27 May 2009 to 30 May 2009	Carl Johnson, Ning Wang, Naiqian Zhang	Site selection.
Ft. Benning	28 Jun 2009 to 2 Jul 2009	Wei Han, Darrell Oard, Carl Johnson, Dan Bigham, Naiqian Zhang	Install wireless sensor network.
Ft. Benning	3 Aug 2009 to 6 Aug 2009	Wei Han, Carl Johnson, Naiqian Zhang	Repair wireless sensor network.
Ft. Benning	9 Sep 2009 to 12 Sep 2009	Wei Han, Joseph Dvorak, Dan Bigham, Carl Johnson	Repair wireless sensor network.
APG	28 Sep 2009 to 3 Oct 2009	Wei Han, Dan Bigham, Joseph Dvorak, Carl Johnson	Install wireless sensor network.
Ft. Benning	21 Oct 2009 to 23 Oct 2009	Wei Han, Joseph Dvorak, Xu Wang	Repair wireless sensor network.

Ft. Benning	18 Nov 2009 to 19 Nov 2009	Wei Han, Carl Johnson	Repair wireless sensor network.
APG	2 Dec 2009 to 6 Dec 2009	Wei Han, Darrell Oard, Carl Johnson, Naiqian Zhang	Install new tower for wireless sensor network.
Ft. Benning	12 Apr 2010 to 17 Apr 2010	Dan Bigham, Joseph Dvorak, Xu Wang, Carl Johnson, Naiqian Zhang	Replace sensors and reactivate cellular service.
APG	23 May 2010 to 27 May 2010	Carl Johnson, Xu Wang, Naiqian Zhang	Reinstall one sensor and update the transmission program.
Ft. Benning	28 Jun 2010 to 1 Jul 2010	Carl Johnson, Joseph Dvorak, Xu Wang	Reinstall PCB with short circuit.
Ft. Benning	Sep 2010	Carl Johnson	Replace weak batteries, refill dye canisters, and remove vegetation for controlled burn
Ft. Benning	22 Feb 2011 to 24 Feb 2011	Joseph Dvorak, Dan Bigham	Uninstall sensors for calibration.
Ft. Benning	30 Mar 2011 to 1 Apr 2011	Carl Johnson, Joseph Dvorak, Dan Bigham, Xu Wang, Darrell Oard, Naiqian Zhang	Reinstall sensors and update transmission program.
APG	6 Apr 2011 to 9 Apr 2011	Carl Johnson, Dan Bigham, Xu Wang, Darrell Oard, Naiqian Zhang	Reinstall sensors at Anita site. Update the transmission program.
Ft. Benning	17 May 2011 to 20 May 2011	Joseph Dvorak, Xu Wang	Reinstall one sensor at Pine Knot site. Update the transmission program. Modify the power connection at Pine Knot site.
APG	7 Sept 2011 to 10 Sept 2011	Carl Johnson, Xu Wang	Reinstall one sensor at Anita site. Update the transmission program.

Ft. Benning	9 Oct 2011 to 12 Oct 2011	Dan Bigham	Collect water samples. Download data from CF card.
Ft. Benning	18 Dec 2011 to 21 Dec 2011	Dan Bigham, Joseph Dvorak, Xu Wang	Reinstall one sensor at Upatoi site. Collect water samples.
Ft. Benning	11 Apr 2012 to 14 Apr 2012	Marvin Petingco, Joseph Dvorak, Xu Wang, Darrell Oard, Naiqian Zhang	Calibrate all four sensors on site. Collect water samples.

Demobilization of Sensors and Wireless Network

After demonstration testing was completed, the sensors and wireless network components were dismantled at the APG site and returned to KSU. Up to date, the systems at the Fort Benning and Fort Riley sites still remain in place. We plan to dismantle these two sites in summer, 2013.

5.4 SENSOR CALIBRATION

This section discusses the procedures for calibrating the SSC and velocity sensors.

5.4.1 SSC sensor

Calibration of the SSC sensors was composed of two stages – a pre-calibration conducted in laboratory using formazin stock suspensions and a field calibration conducted in stream using grab water samples.

5.4.1.1 Pre-calibration

5.4.1.1.1 Test Stand

In order to properly measure the SSC in the streams the sensor/PCB board assembly needed to be pre-calibrated. This was performed using a test stand that would test the various functions of the sensor and the PCB board in the laboratory while mimicking real-world settings. The PCB boards and sensors could be attached to the stand quickly and the functionality of different field operations could be checked before being installed in an actual field setting. Figure 5.5 displays a picture of the test stand with all components labeled.

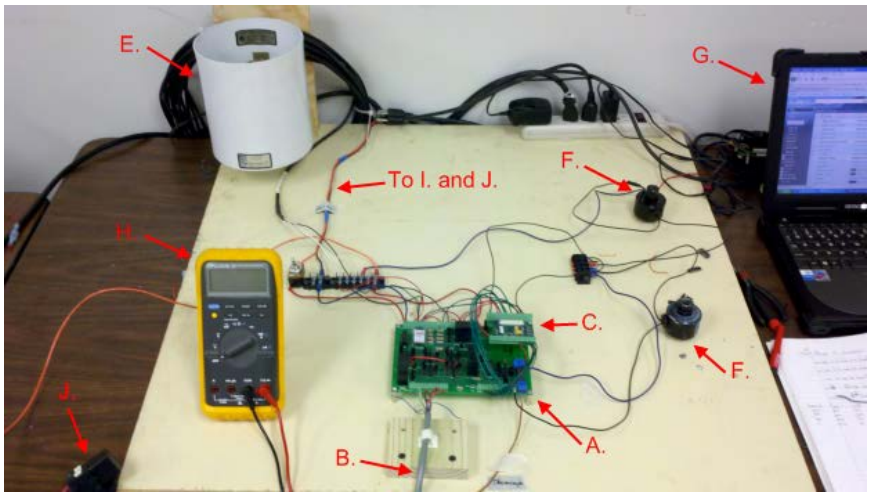

Figure 5.5 Test stand for testing PCB board and sensor assembly. The components are: A. PCB board; B. Suspended sediment sensor; C. MDA300; D. Crossbow mote (not in the picture); E. Rain gauge; F. Two solenoid valves; G. Laptop; H. Multimeter; I. 12V DC battery power (not in the picture); J. Voltage regulating relay.

5.4.1.1.2 Suspended Sediment Solution

In order for the sensor to be properly pre-calibrated it must be placed in solutions with known turbidities. The goal of the pre-calibration was to allow all sensors to yield about the same level of signals for the same turbidity. This would set the sensitivities of the sensors to an appropriate level.

Pre-calibration of the sensor was performed using formazin stock suspensions, following the EPA standard 2130B (EPA, 1999). The suspension was created using the following procedure:

- Dissolve 1.0 gram of hydrazine sulfate in filtered, de-ionized water and dilute it to 100 milliliters
- Dissolve 10.0 grams of hexamethylenetramine in filtered, de-ionized water and dilute it to 100 milliliters
- Mix the two resultant solutions and let the mixture stand for 24 hours after mixing at 24-26 °C to produce a 200 milliliter formazin suspension

This process was adjusted in order to create three separate 6000-milliliter formazin suspensions at various Nephelometric Turbidity Units (NTU), which were used in pre-calibration. Selection of the concentrations of these solutions was based on previously observed SSC and sensor readings at the locations where the sensors were installed.

Table 5.3 displays the concentrations of the stock formazin solutions used for calibration of the sediment sensors to be deployed at the three installations.

Table 5.3 Stock formazin concentrations used for calibration of suspended sediment sensor

Experimental site	*Ft. Riley, Kansas*	*Ft. Benning, GA*	*Aberdeen, MD*
Stock formazin concentrations	1200 NTU 800 NTU 400 NTU 0 NTU	1200 NTU 800 NTU 400 NTU 0 NTU	400 NTU 0 NTU

The solutions were placed in black boxes with lids in order to eliminate ambient light. During pre-calibration, the black box was placed on a magnetic stirrer (Fisher Scientific) and was stirred at a constant rate in order to maintain particle suspension and to keep a uniform concentration throughout the solution. Figure 5.6 displays the sensor housed in the black box assembly atop the stirrer.

Figure 5.6 Sensor assembly placed in black box (without lid) for pre-calibration in clean water.

5.4.1.1.3 Gain Adjustment

In order to adjust the signal levels of the sensors so that they can achieve a uniform level at the same stock formazin concentration, the gain of the current-to-voltage converters system must be adjusted.

For the sensors, the phototransistors placed at different angles from their associated LEDs had different trends in signal variation when the NTU concentrations changed. Therefore, using more than one angle would allow the sensor to measure SSC over a wider range of sediment loads (Zhang, 2009). Based on sensor design and previous research it was determined that the OR180 signal should reach its maximum value in clean water, because the 180 degree phototransistor was measuring transmitted light through the U-shape channel of the sensor. As the sediment concentration increased, the signal should decrease. On the other hand, the IR45 and OR45 signals should approach their minimum values in clean water because the 45 degree

phototransistors were measuring backscattered light. Thus, as the concentration increased, the signal from these phototransistors should also increase. The maximum level a signal was calibrated to was 1800 mV. This was determined based on previous sensor testing and knowledge of typical SSC of the area where the sensors were installed. Table 5.4 displays the average signal level for each location after calibration and Figure 5.7 demonstrates the signal variation trends.

Table 5.4 Average signal output (mV) of sensor/PCB board assembly after calibration

	IR45	*OR45*	*OR180*
Ft. Riley			
0 NTU	160	62	1858
400 NTU	976	854	822
800 NTU	1450	1098	559
1200 NTU	1793	1790	435
Ft. Benning			
0 NTU	167	44	1810
400 NTU	1044	833	746
800 NTU	1522	1469	506
1200 NTU	1917	1870	372
Aberdeen			
0 NTU	242	97	1739
400 NTU	1786	1818	766

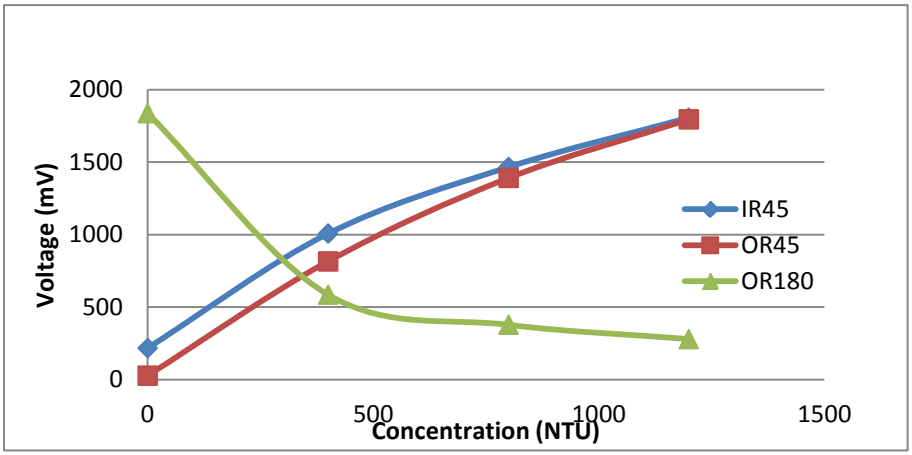

Figure 5.7 Pre-calibration curves of the sensors for Little Kitten Creek

5.4.1.1.4 Pre-calibration Procedure

The first step of pre-calibration was to mount the PCB board to the test stand and attach the wires properly. The sensor was wired to the PCB board. The solenoid valves and other attachments were also wired to the PCB board to imitate a real-world environment

The sensor was then placed inside the first of suspended sediment solutions and the pre-calibration program was run on the attached mote. The output signals from the sensor were then read and from this data the needed resistance was calculated and the gain was adjusted by choosing different jumper combinations as mentioned in Section 2.2.1.3.5. This procedure was repeated until all channels were calibrated to their proper gain.

5.4.1.2 Field calibration

Water sampling provided the base for the second stage of sensor calibration – the field calibration. Water sampling was also the core action for sensor validation. At all sensor sites, water sampling has been conducted throughout the experiment to provide sufficient numbers of grab samples for SSC sensor calibration and validation.

5.4.1.2.1 Grab sampling

Grab samples were taken in field following the following procedure.

5.4.1.2.2 Sensor Cleaning

Prior to taking each grab sample the sensor was cleaned manually using a cotton cloth or paper towel. The sensor was not removed from the T-post during cleaning. Sometimes in order to reach the sensor in the stream the cover needed to be removed in order to clean the lens. Before the sample was taken the cover was reattached in order to obtain more accurate results and reduce the effect of ambient light.

5.4.1.2.3 Sampling Process

Grab sampling was done most often during or shortly after rain events, as these were the periods of time when higher SSCs were observed. Each grab sample was taken at the height of the sensor in the stream directly in front of the sensor. The lid of the sampling container was kept on the container until the container was at the same height as the sensor then it was removed until the container was filled and placed back on the container. The sampling container used was a 120 mL sampling cup. The date, time, and location of the sample were then recorded to be used later for correlation with sensor signals. Any water samples not processed immediately when returned to laboratory were refrigerated until the laboratory analysis was started, usually within a few days of sampling. Samples shipped from other locations such as Aberdeen were next-day shipped cold in coolers of ice to keep the samples as cold as possible to prevent bacterial growth.

5.4.1.2.4 Sediment Concentration Measurement

SSCs of water samples were analyzed in laboratory following the following procedure.

5.4.1.2.5 Equipment

Weighing of the water samples and filters were done using a Mettler HK 160 balance (Mettler Instrument Corp.) which has a resolution of 0.1 mg and a max weight of 160 g. The weighing procedure was as follows:

- Turn on balance and allow the balance to warm up. It is important that no air drafts or floor vibrations were present.
- Tare scale to all zeroes on the digital display. Also should be displayed was a “+” symbol.

- Press the CAL button or lever. The button should be pushed gently so that the stability of the balance was not lost. CAL should appear on the digital display.
- Place calibration weight on the weighing pan. Dashes should be displayed on the output screen. The HK 160 used an internal 100 gram weight for calibration.
- When the digital display showed a value of 100 g, calibration was complete.

The filters used for this study were GN-6 Gridded 0.45 μm 47 mm filters (Pall Corporation); the water was pumped through the filter using a vacuum pump. Figure 5.8 displays the experimental set-up for water sampling analysis.

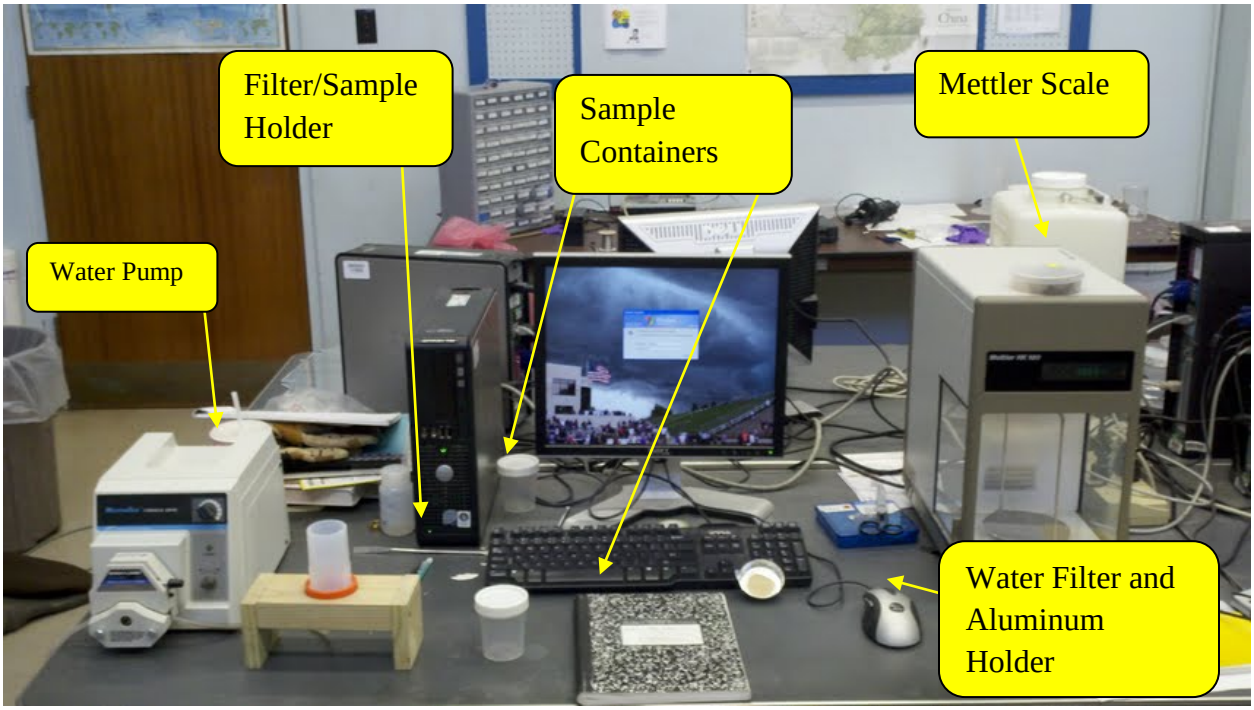

Figure 5.8 Water sampling analysis set-up

5.4.1.2.6 Procedure

Water samples were taken back to the laboratory where they were processed for SSC measurement by filtration. Analysis was typically done within 24 hours after the sample was taken; however samples that were not analyzed in this time frame were place in a refrigerator in accordance with the EPA guidelines for water sample measurement. SSC was calculated based on EPA method 160.2. The procedure used is as follows:

- Weigh the water sample together with its container and lid (M1); then weigh the dry, sterilized filter paper (S1).
- Place the filter paper in a holder and pour water sample in the container on top of the paper and turn on the vacuum pump.
- After filtration is complete, remove the filter and place it on the aluminum weighing dish.

- Place this along with the empty water sample container and lid in an oven at 105°C for 24 hours.
- After drying, weigh the container and lid together (M2); then weigh the dried filter paper with sediment (S2).

The following calculations were then performed to find the SSC in mg/L:

$$SSC = \frac{1x10^6(S_2 - S_1)}{M_1 - M_2}$$

where

SSC = suspended sediment concentration in mg/L

S_1 = mass of clean, dry filter paper

S_2 = mass of dried filter paper with sediment

M_1 = mass of water sample with container and lid

M_2 = mass of dried container and lid

The data was then matched up with the sensor signals in the online database recorded at the same time in order to find a correlation between sensor signal and SSC. Sensor signals were then plotted against measured concentrations to determine the relationship between the signals and SSC (Bigham, 2012).

5.4.2 Flow velocity measurements

Combined SSC/flow velocity measurement was demonstrated at two sensor site – the Little Kitten Creek site at Fort Riley and the Pine Knot Creek site, where the sensor was installed in the same cross section as the USGS stream gage 02341725.

5.4.2.1 Field test of the velocity sensor

The field tests compared the measurements of the fifth generation sensor to those from a commercial Flowtracker ultrasonic velocity sensor in an actual field installation. The goal was to determine if the sensor could properly detect the water velocity in real-world conditions where turbulent flow was present. This field test was conducted in Little Kitten Creek. Twenty six separate tests were conducted in Little Kitten Creek comparing these sensors. In each test, multiple measurements were taken with both sensors. While the presence of turbulence in the water meant that the instantaneous velocity measurements would not be identical, the experiment was based on an assumption that, during a given test, the average velocity measured by both sensors would be identical because the flow conditions experienced by both sensors were the same.

5.4.2.2 Test procedure

Before the test, a bracket was added to the fifth generation sensor to which the Flowtracker probe could be mounted. The bracket held the probe so that the Flowtracker was measuring the velocity

of a point 8 cm in front of the centerline of the fifth generation sensor. The Flowtracker could not be permanently mounted in the creek, so the bracket ensured that it could be placed at the exact same position for every test. When conducting tests the Flowtracker was installed on the bracket and was configured to sample for 40 seconds for each velocity measurement it produced. Tests were conducted at different times and on different days to catch different flow velocities that resulted from different flow conditions. During these comparison tests, the fifth generation sensor system was connected directly to a laptop that could control the measurements being made and record all the data. Using the laptop, the velocity measurement period for the fifth generation sensor was changed to less than 20 seconds. This allowed the fifth generation sensor to record many individual measurements during each of these field tests. While the fifth generation sensor was taking its set of measurements, the Flowtracker was continually commanded to take more velocity measurements at the same time. This produced a set of velocity measurements from each the Flowtracker and the fifth generation sensor that were taken at the same time and under the same flow conditions. It was attempted to obtain at least 15 good measurements from the Flowtracker and at least 30 good measurements from the fifth generation sensor.

The period when the fifth generation sensor was tested in the field was a relatively calm period in terms of weather events. Little Kitten Creek would not have naturally seen the variations that were needed to test the sensor at different velocities. To create different velocities for sensor calibration, the stream flow was altered to produce different flow rate. These alterations included placing rocks downstream from the sensor to slow the flow though the sensor, creating restrictions upstream for the same purpose and using sandbags to ensure the thalweg of the creek was directly in line with the sensor. On two occasions, sandbags were placed upstream to restrict and backup water. When these sandbags were removed, the backed up water resulted in increased discharge and velocity for long enough to take a consistent set of measurements. There was an initial surge for about a minute immediately after removing the sandbags so measurements from the sensors had to wait until this surge past. Using these methods, it was possible to generate different velocity levels in Little Kitten Creek for these tests. However, these methods were never close to producing the flow levels observed during rain events. The two highest velocities recorded in the creek both came from natural rain events, so the modifications to the stream flow only allowed the velocity range to be filled in with more tests (Dvorak, 2012).

5.4.2.3 Using USGS stage data and point velocity measurement to estimate discharge

The stage data recorded at the USGS 02341725 gaging station at Pine Knot Creek at Fort Benning was compared with the velocity data measured by the SSC/velocity sensor deployed at the same location. Both data were used to estimate the discharge using the “index-velocity method”. This method requires that two rating curves be developed. The first relates stage to area and the second relates the index velocity to the mean velocity of the water in the channel profile. The results of these ratings are mean velocity and cross sectional area which can be multiplied together to produce the discharge of the stream (Levesque and Oberg 2012).

The stage-area rating curve required for this method was developed using the USGS AreaComp program based on cross-section survey provided by USGS. For the index velocity rating curve, one half randomly selected USGS discharge estimates for the gage station were converted to mean velocities using corresponding stage measurements and the stage-area rating. These mean velocity readings were compared against the velocity readings provided by the velocity sensor to derive the index velocity rating.

5.4.3 Automatic lens cleaning

Fouling, including bio-fouling, on optical lenses has been a common problem for optical sensors exposed to various pollutants in water. Field experiments have shown that fouling effect caused signal deterioration (Figure 5.9). This can be observed from the fact that, each time the sensor was manually cleaned, the signals went back to their original levels. Usually, fouling of the sensor lenses caused the transmitted signal to decrease and the backscattered signal to increase. In order to maintain meaningful signals, the lenses need to be periodically cleaned.

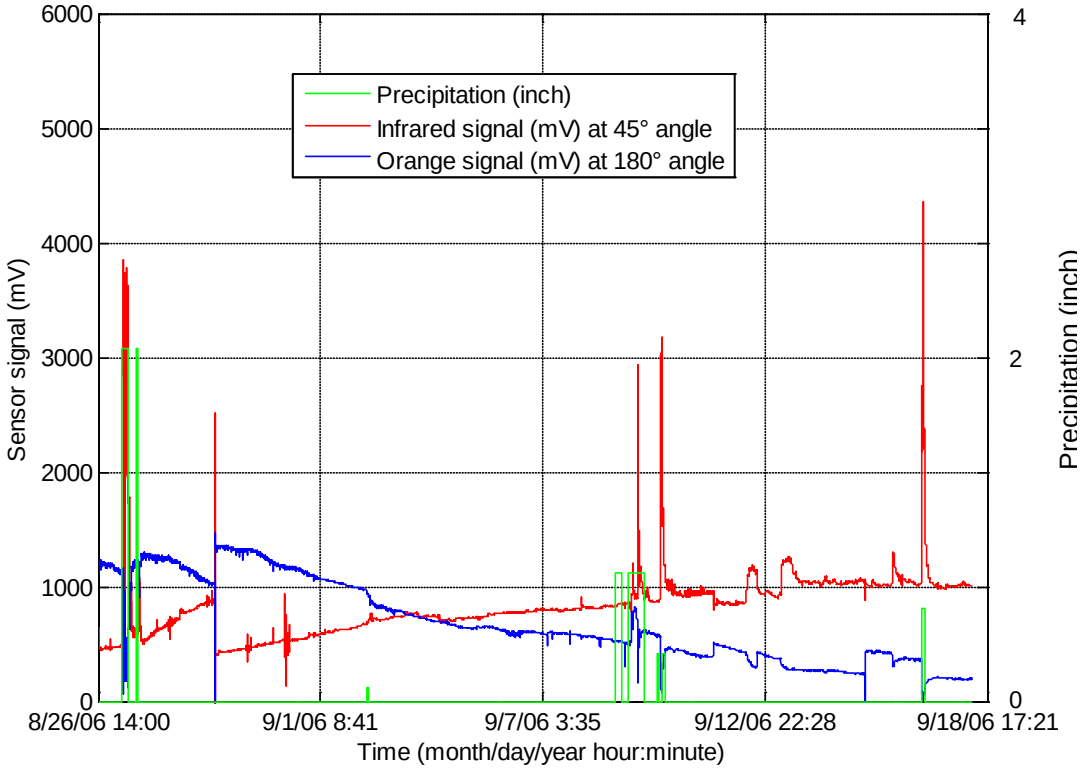

Figure 5.9 Signal deterioration due to fouling. Precipitation data source: www.weatherunderground.com.

The air-blast cleaning mechanism installed on the sensor body was proven to be effective in cleaning the lenses and restoring the signals through a series of indoor tests, which were conducted in 2008. Figure 5.10 shows the laboratory setup for the experiment. Pressurized air was generated by a 12V air compressor equipped with a 3.5 liter air tank and was regulated by a pressure reducing valve to 60 psi. The sensor was placed in a fish tank filled with was taken from Little Kitten site. A CR10X datalogger was programmed to turn on a solenoid valve for two seconds every 12 hours to clean the sensor.

Figure 5.10 Laboratory setup of the air-blast cleaning experiment.

The effect of the air-blast cleaning system was also tested in field.

5.4.4 Data post-processing to remove fouling effect

During data post-processing, correction algorithms were applied to restore the signals. The correction was done by determining the fouling trend through a regression analysis on peak signal values taken during no-rain periods. The fouling trend was then removed to restore the sensor signals. A MATLAB program was developed to complete the signal correction (Zhang, 2009). Although the fouling trend may differ from site to site and, hence, the regression curve may differ, the regression curve was automatically developed by the program and the same program can be used for different sites without modification.

Figure 5.11 shows the result of correction for the backscattering signal IR45 from the original signals shown inFigure 5.11. Figure 5.12 shows the sediment concentration measurement restored after the correction.

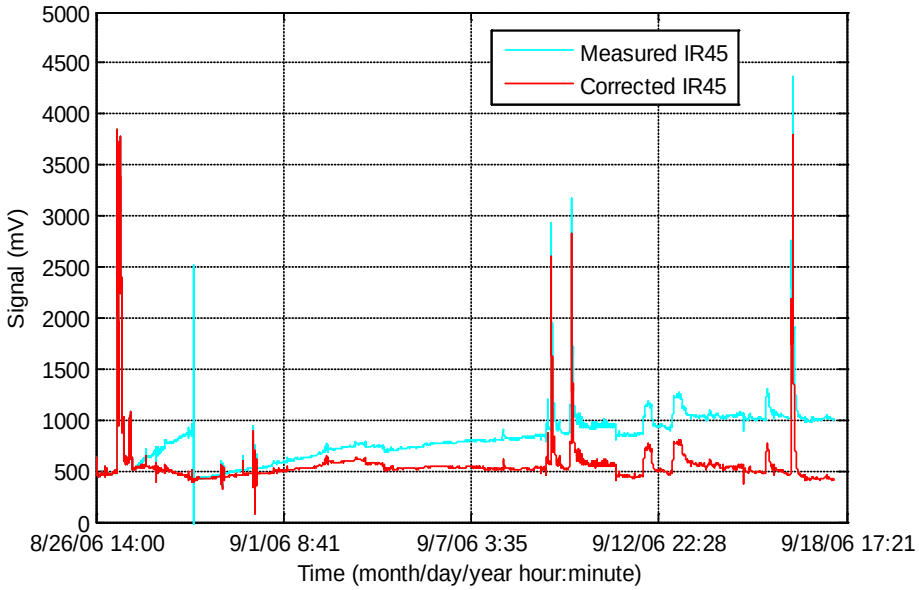

Figure 5.11 Backscattered signal (IR45) correction result.

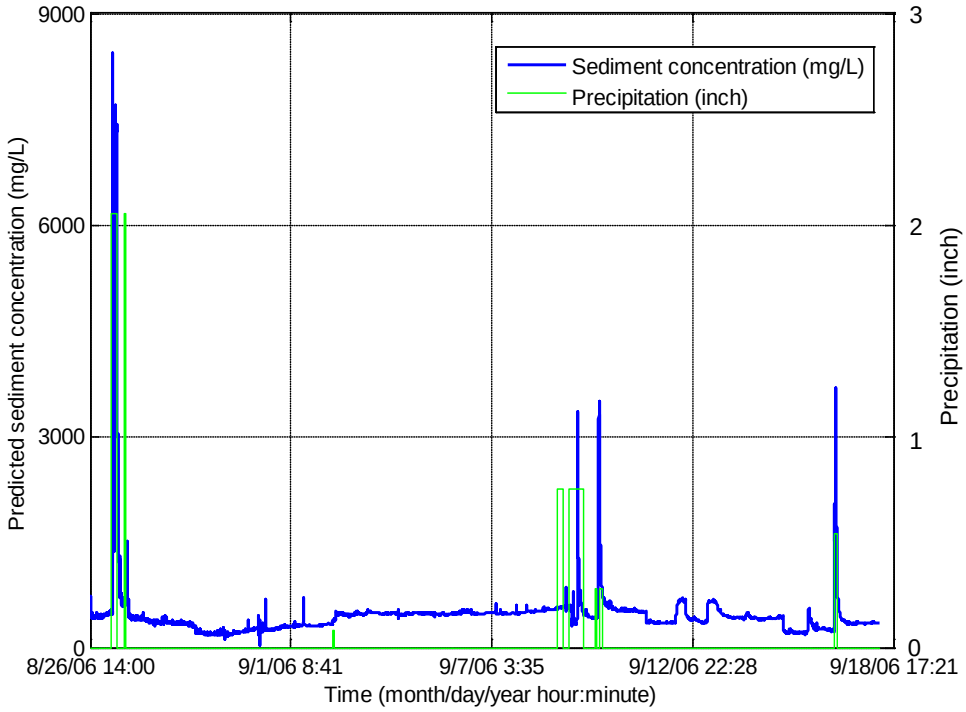

Figure 5.12 Sediment concentration data restored using the correction algorithm. Precipitation data source: www.weatherunderground.com.

6 PERFORMANCE ASSESSMENT

Performance of the system is assessed against each performance objective listed in Table 3.1.

6.1 ACCURACY IN SSC MEASUREMENT

Accuracy of the SSC sensor was assessed using grab samples collected at each sensor site. For each sensor, one half of the grab samples along with sensor signals received at sample collection times were used to establish "calibration models" to predict SSC from the sensor signals. The remaining half of the grab samples were then used for validation.

6.1.1 Calibration Models

Calibration models were established through statistical analyses on a site-by-site basis. This was done under the assumption that each sensor was unique and therefore required its own unique calibration model.

Each site had a certain number of samples taken within a certain SSC range. This was because different regions have different stream types, soil types, watershed management practices, and storm events. These differences along with the need to travel to each site made calibration for some sites somewhat difficult. Travel to some of the sites was costly and the timing of traveling to these sites can determine whether a high sediment flow period can be observed. Table 6.1 displays the sites, time periods in which the water samples were taken along with the SSC ranges observed.

Table 6.1 Water sample data displaying number of grab samples taken at each site, period samples were taken, and range of concentration of water samples

Sensor Location		Number of grab samples taken	Time period the grab samples were taken	Range of sediment concentration (mg/L)	Daily precipitation (inch)		
					Min.	Max.	Avg.
Fort Riley	Little Kitten	24	5/17/2011 – 11/08/2011	7.3 – 815.6	0.00	2.11	0.11
	Wildcat Bridge	17	5/20/2011 – 12/3/2011	8.0 – 4685.1	0.00	2.11	0.11
	Wildcat Creek	2	5/25/2011	106.7 – 116.3	1.07	1.07	1.07
	Silver Creek	2	5/25/2011	105.1– 190.3	1.07	1.07	1.07
Total		45	5/17/2011 – 12/3/2011	7.3 – 4685.1			
Fort Benning	Pine Knot North	14	4/1/2011 – 4/13/2012	2.9 – 27.9	0.00	3.28	0.10
	Pine Knot South	11	4/1/2011 – 4/13/2012	0.7 – 90.2	0.00	3.28	0.10
	Upatoi North	14	4/1/2011 – 4/13/2012	7.2 – 34.8	0.00	3.28	0.10
	Upatoi South	22	7/5/2011 – 4/13/2012	4.0 – 31.4	0.00	3.28	0.12
Total		61	4/1/2011 – 12/21/2011	0.7 – 90.2			
APG	Anita Near	25	4/28/2011 – 12/20/2011	2.43 – 461.4	0.00	1.02	0.08
	Anita Far	23	4/28/2011 – 12/21/2011	11.2 – 729.1	0.00	1.02	0.08
Total		48	4/28/2011 – 12/21/2011	2.43 – 729.1			
Grand Total		154					

Water samples taken at each site were divided into two sets – a calibration set and a validation set. This was done by 1) sorting the samples from each site by measured SSC in a descending order, and 2) taking the odd numbered samples as the calibration set and the remaining samples the validation set. Although this selection procedure was not completely random, it guaranteed that the ranges of the two data sets were similar.

The following sections describe the calibration models obtained for each site. The sensors provided three signals (IR45, OR45, and OR180) in each measurement. Statistical analyses were performed to determine the significance of each signal in predicting SSC. For each signal, the "on-off" value, which was the difference between a signal measured when an LED was turned on and that measured when it was turned off, was used as the predictor in the calibration model, because these values were not greatly affected by the ambient light. The three "on-off" signals were entered into a stepwise regression procedure in which insignificant predictors were eliminated to produce the most effective and simple linear model for predicting SSC.

Once the linear regression model for each site was determined, a second order polynomial regression model was tested to see if the model could be improved by adding some of the second-order terms. In some cases, based on the stepwise analyses, more than one signal was used to establish the calibration model.

6.1.1.1 Fort Riley Calibration Models

The Little Kitten and Wildcat Bridge sites were the first sites modeled for sediment prediction. The Wildcat Bridge sensor site had water samples within a much larger range of SSC than any other site. After running the statistical analysis it was determined that, among the three signals, OR180 signal was chosen as the best single predictor in a linear model for both the Little Kitten and the Wildcat Bridge sites (Figure 6.1 and Figure 6.2).

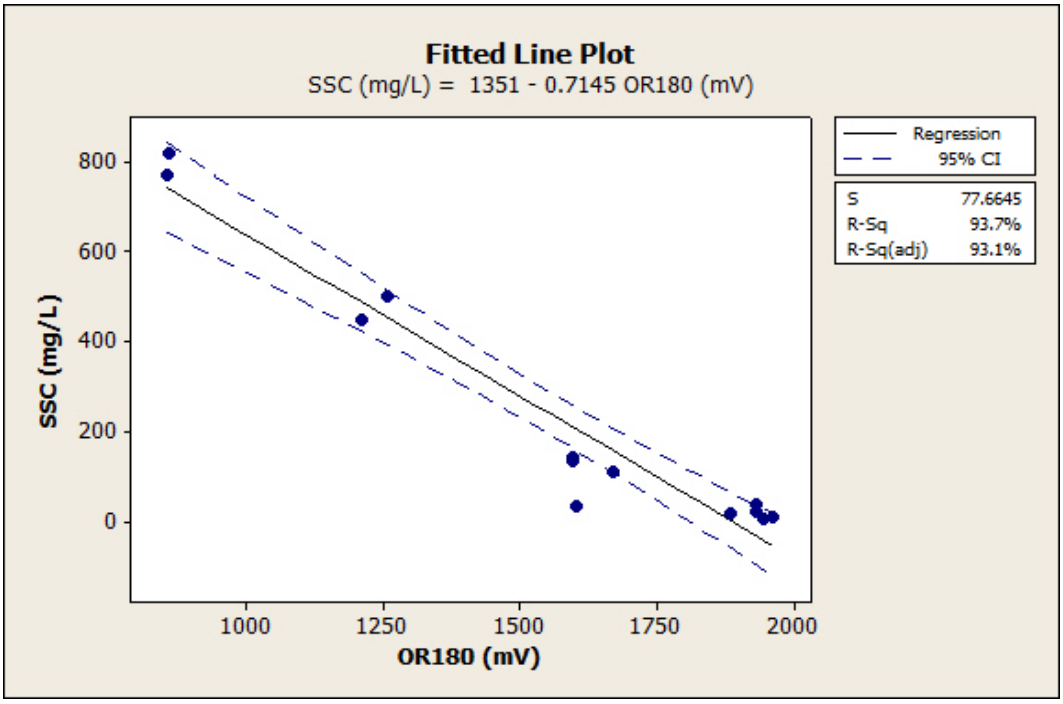

Figure 6.1 Regression model to predict the suspended sediment concentration using OR180 signal for Little Kitten Creek, Manhattan, KS

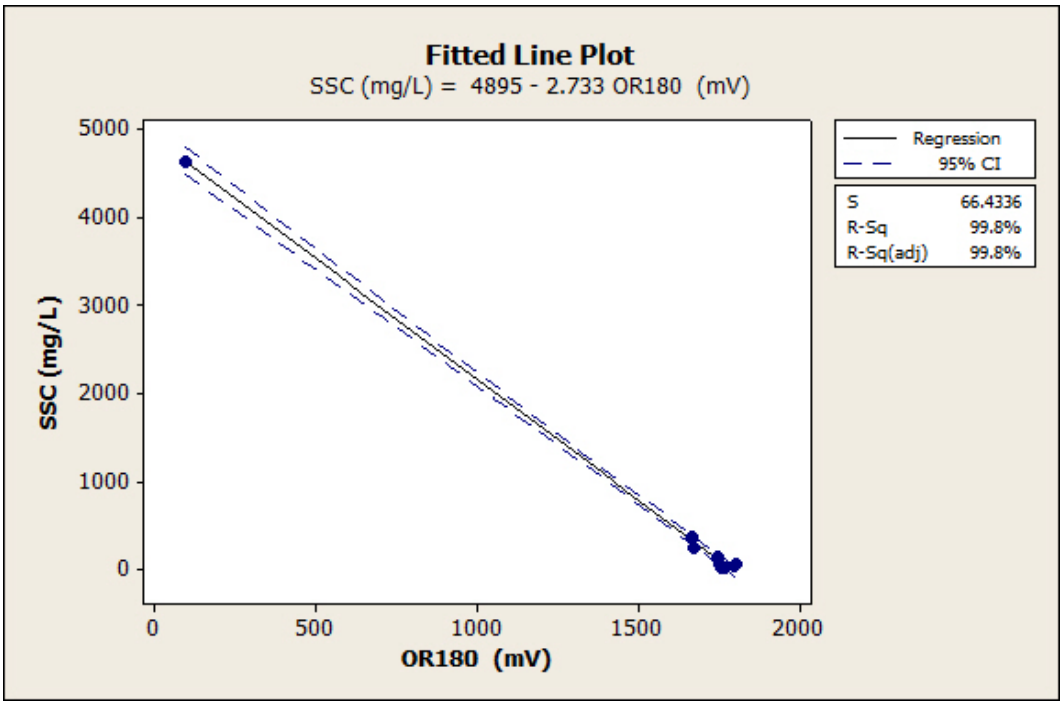

Figure 6.2 Regression model to predict the suspended sediment concentration using OR180 signal for Wildcat Bridge site location, Wildcat Creek, Ft. Riley, KS

Figure 6.3 and Figure 6.4 show the residual plots created for the best linear models for the Little Kitten and Wildcat Bridge sensors, respectively. These plots were generated by the Minitab software (Minitab Inc., 2012). The "normal probability plot" displays the sample data distribution against a theoretical normal distribution and is used to assess whether the sample data is normally distributed. A straight line indicates a good fit to a normal distribution. The next graph ("Versus Fits") plots the regression residuals against the model-fitted values. From this graph, trends of over- or under-prediction of the model within various SSC ranges (low, medium, and high) can be observed. The third graph ("Histogram") displays a histogram of residuals to show how the sample data fit the normal distribution. The final graph ("Versus order") displays the residuals plotted against time as the data was recorded. From this graph, temporal trend, such as "aging" of sensor electronic and optical components, in prediction error of the model can be observed.

From Figure 6.3, it can be seen that the sample data collected at the Little Kitten site was approximately normally distributed and no obvious temporal trend was observed. The "normal probability plot" follows the normal distribution line meaning that the samples taken are generally normally distributed, which is the ideal scenario in residual analysis. In addition, the "versus fits" graph for Little Kitten shows a trend of underestimating in the medium SSC range (200-400 mg/L), indicating that a higher order model may provide more accurate predictions.

For the Wildcat Bridge site (Figure 6.4), the "versus fit" graph has a skewness. This is because not many data points were gathered during the high sediment flow periods.

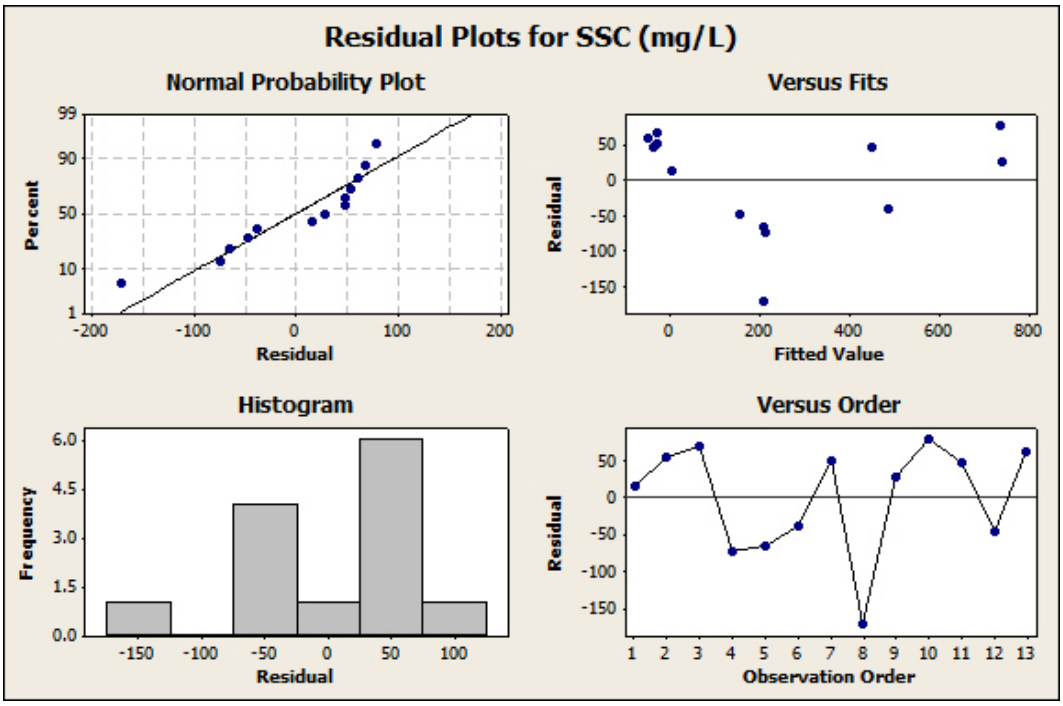

Figure 6.3 Residual plot of OR180 linear model for Little Kitten sensor site (source: Minitab)

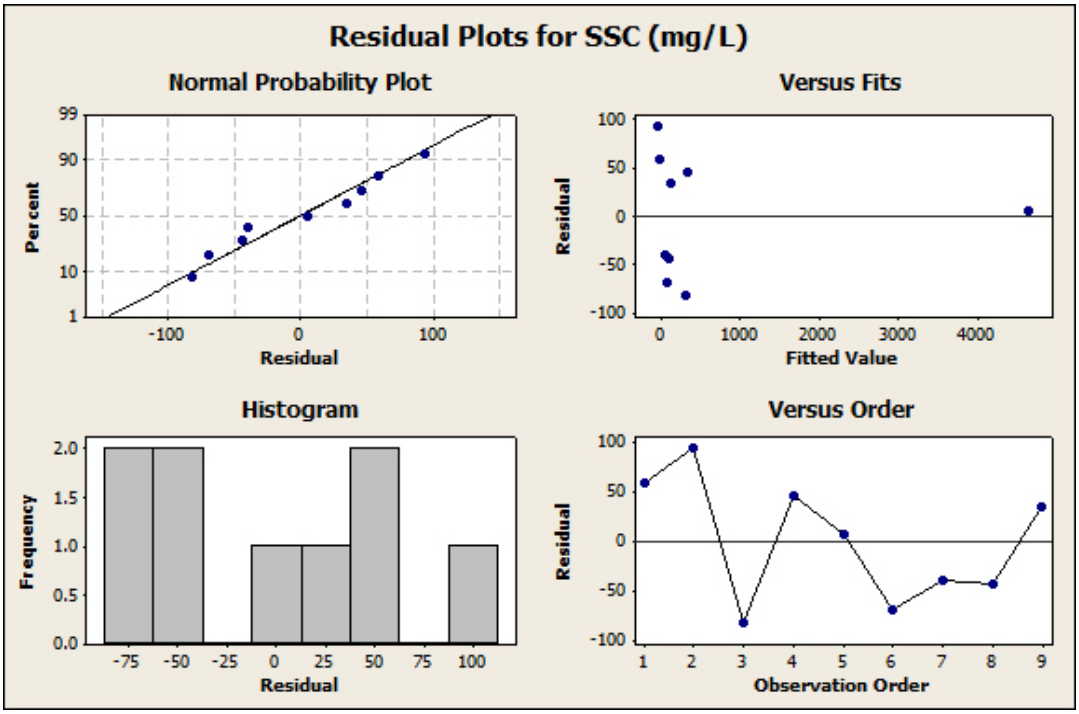

Figure 6.4 Residual plots of OR180 linear model for Wildcat Bridge sensor site (source: Minitab)

After testing the second order calibration model for the two sites using the stepwise procedure, it was found that the best second order polynomial model for Little Kitten was:

Concentration (mg/L) = 0.006*[IR45 (mV)]^2 – 2.43*IR45 (mV) – 0.255*OR180(mV) + 740.

On the other hand, the second-order polynomial model did not significantly improve the prediction model for Wildcat Bridge.

The second-order polynomial model for Little Kitten was evaluated using Minitab and is shown in Figure 6.5. Statistical analyses showed that this model was an improvement over the linear model when the R^2 and root mean square error (RMSE) values were considered. Table 6.2 displays the R^2 and RMSE values for the various models established for the Fort Riley sensors. Figure 6.6 - Figure 6.8 show SSC predicted using these models vs. actual SSC. The 95% confidence intervals for the predicted values are also given.

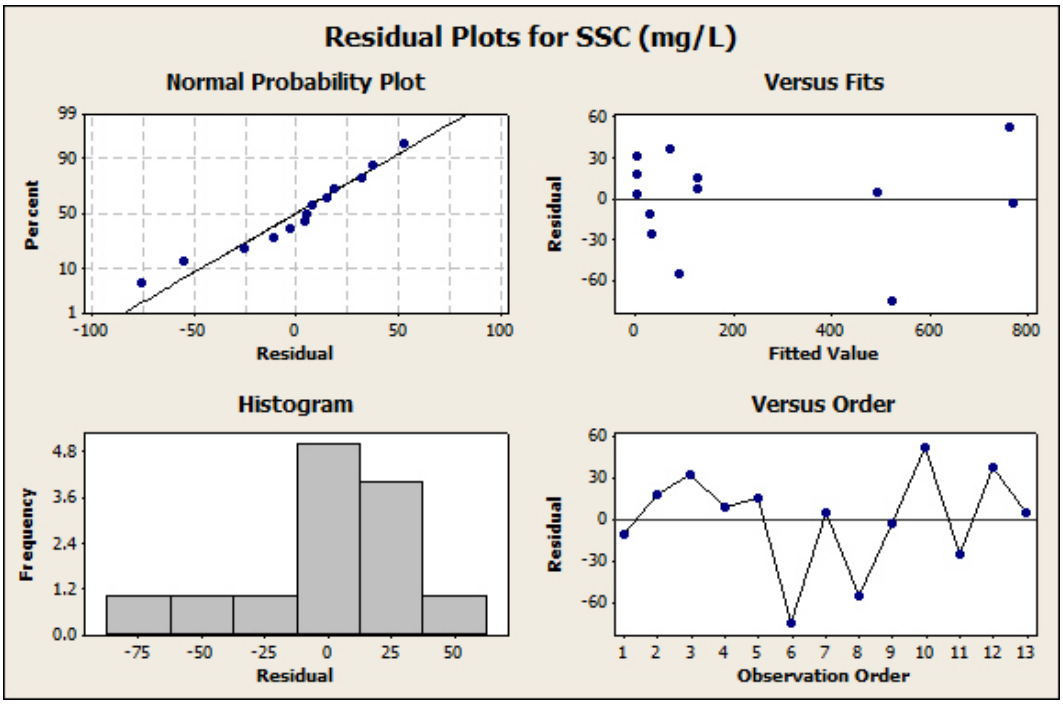

Figure 6.5 Residual plots of second-order polynomial prediction model for Little Kitten sensor site (source: Minitab)

Table 6.2 R^2 and RMSE values for calibration models used at the Fort Riley sensor sites

Sensor Site	Model Type	Signal(s)	R^2 Value	RMSE (mg/L)
Little Kitten	Linear	OR180	0.937	77.66
	2nd Order	IR45 and OR180	0.985	41.61
Wildcat Bridge	Linear	OR180	0.998	66.43

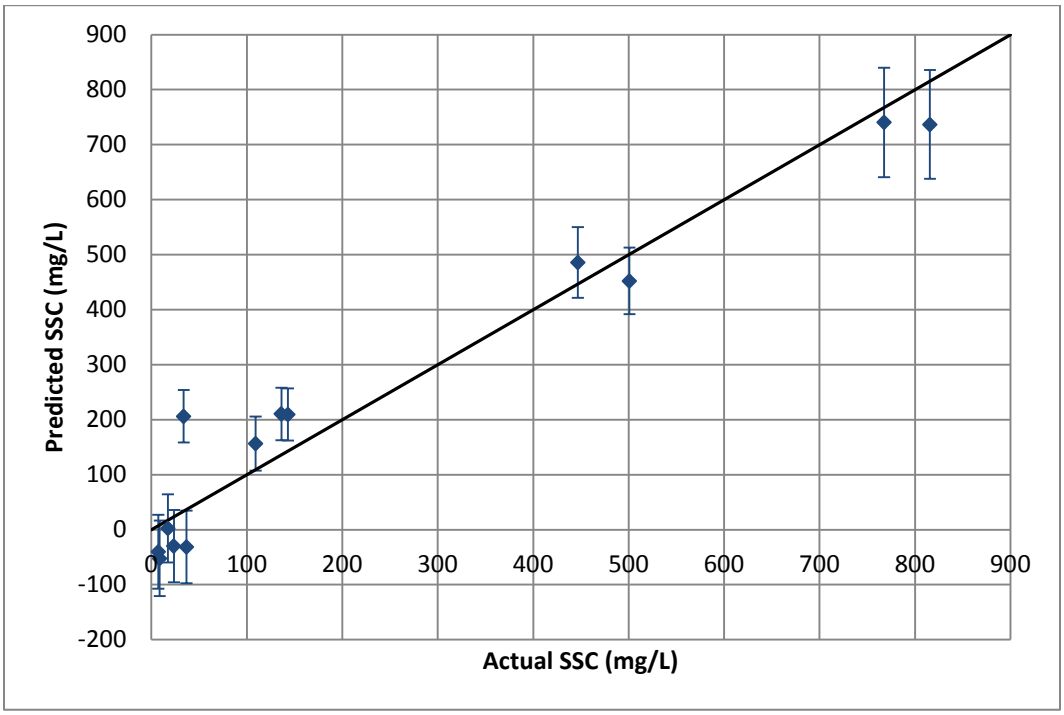

Figure 6.6 Predicted SSC vs. actual SSC for the Little Kitten sensor using OR180 linear calibration model

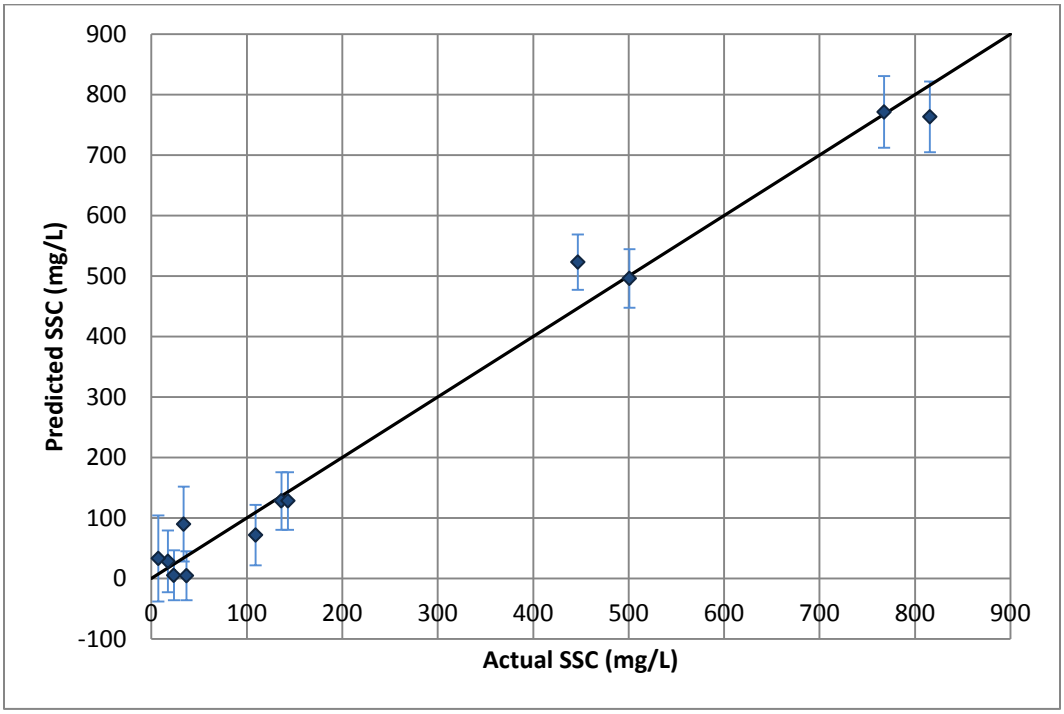

Figure 6.7 Predicted SSC vs. actual SSC for the Little Kitten sensor using a second-order polynomial calibration model

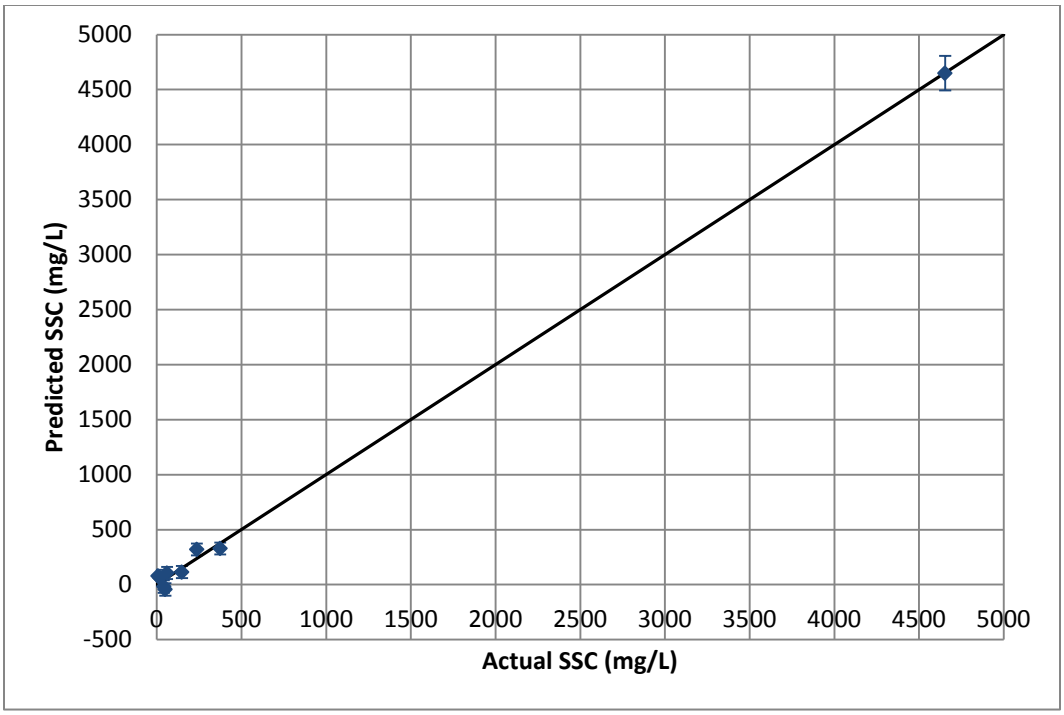

Figure 6.8 Predicted SSC vs. actual SSC for the Wildcat Bridge sensor using OR180 linear calibration model

6.1.1.2 Fort Benning Calibration Models

For the Fort Benning sensor sites, prediction models were established for three of the four sensors. For the Upatoi South sensor, a prediction model was not successfully established mainly due to problems with the sensor control board that caused sporadic sensor readings.

After performing statistical analyses on data from the three sensors and running the stepwise regression analysis for both linear and second-order models, it was determined that a linear model was most appropriate for all three sensors. Figure 6.9 –Figure 6.11 display the sample SSC against the signals measured at the sampling times for the three sensors at Fort Benning along with their lines of best fit.

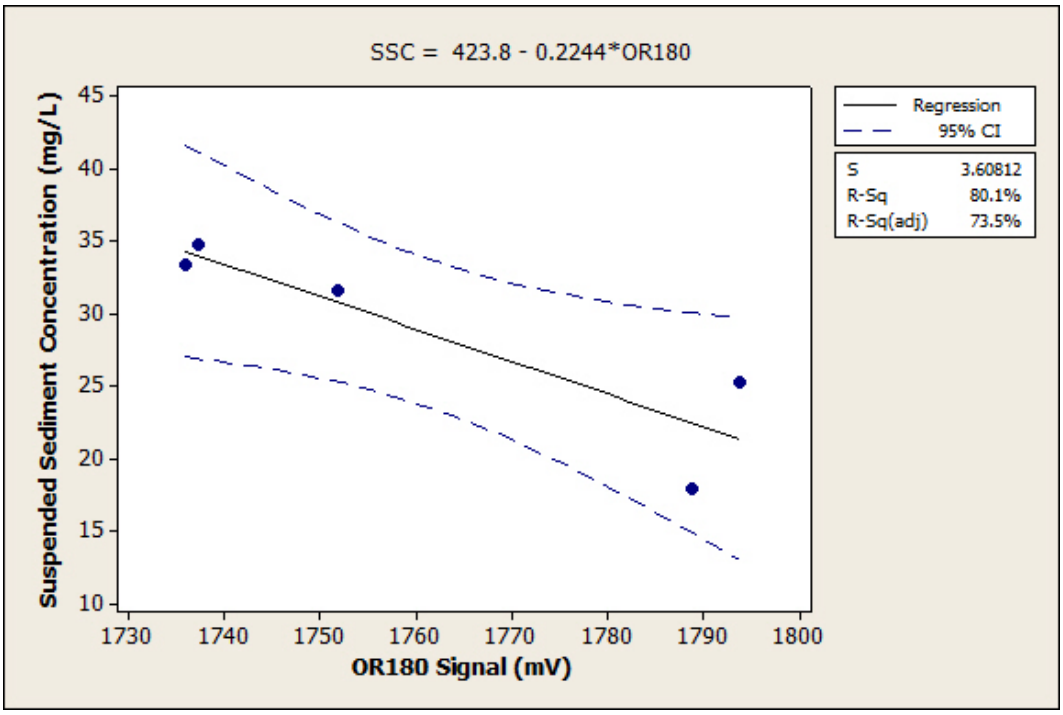

Figure 6.9 Regression model to predict the suspended sediment concentration using OR180 signal for Upatoi North site, Upatoi Creek, Ft. Benning, GA

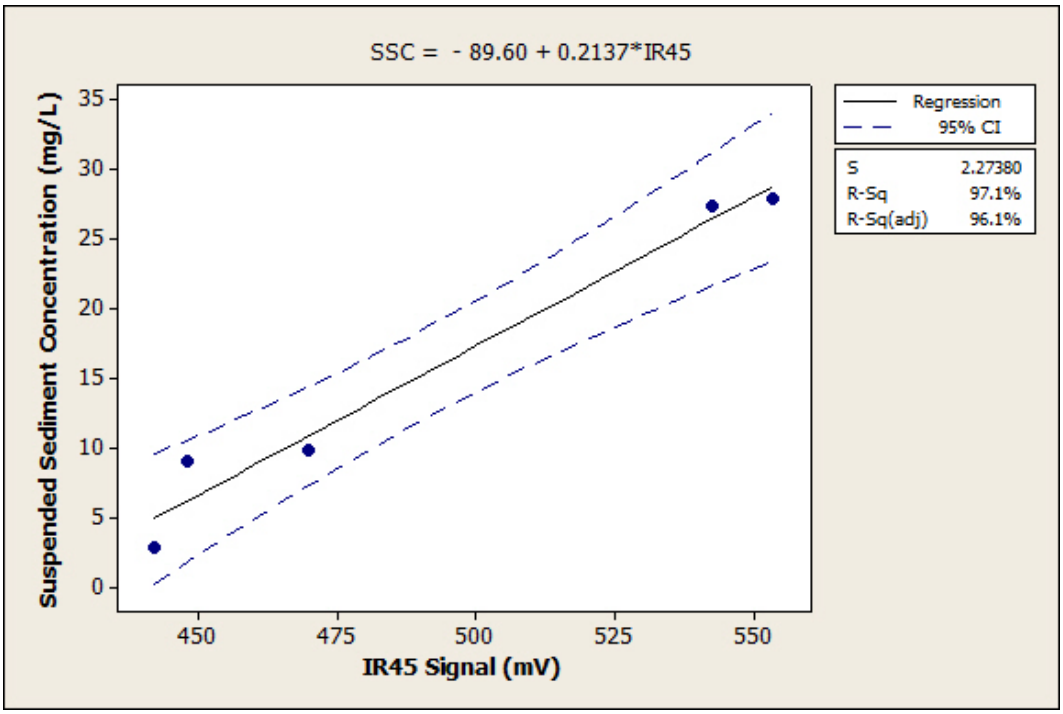

Figure 6.10 Regression model to predict the suspended sediment concentration using IR45 signal for Pine Knot North site, Pine Knot Creek, Ft. Benning, GA

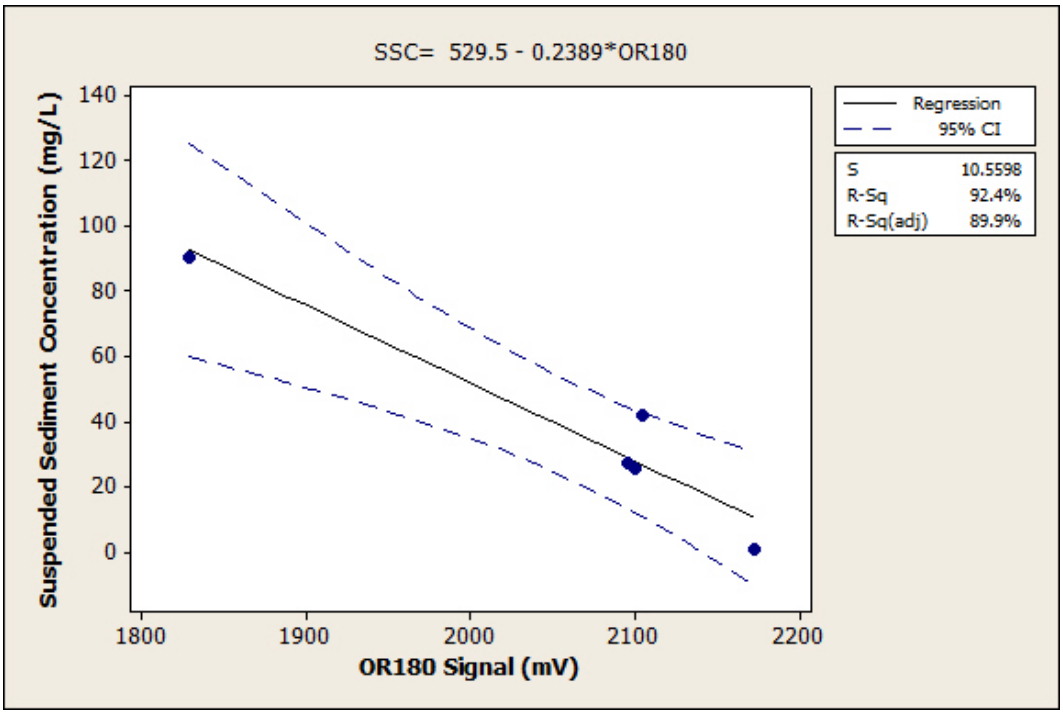

Figure 6.11 Regression model to predict the suspended sediment concentration using OR180 signal for Pine Knot South site, Pine Knot Creek, Ft. Benning, GA

The linear model determined to be the best fit for the Upatoi North sensor site is:

$$\text{Concentration (mg/L)} = -0.073*\text{OR45(mV)} - 0.336*\text{OR180 (mV)} + 633$$

The linear model determined to be the best fit for the Pine Knot North sensor site is:

$$\text{Concentration (mg/L)} = 0.159*\text{IR45(mV)} + 0.296*\text{OR45(mV)} - 96.3$$

The linear model determined to be the best fit for the Pine Knot South sensor site is:

$$\text{Concentration (mg/L)} = 0.178*\text{IR45(mV)} - 0.398*\text{OR180(mV)} + 795$$

R-squared and RMSE values for these models were tabulated in Table 6.3. In general, the range of SSC in Fort Benning was lower than those for the Fort Riley sites.

Table 6.3 R^2 and RMSE values for calibration models used at Fort Benning sensor sites

Sensor Site	Model Type		R^2 Value	RMSE
	Order	Signal(s) used		
Upatoi North	1	OR180	0.801	3.61
	1	OR45 and OR180	0.971	1.69
Pine Knot North	1	IR45	0.971	2.27
	1	IR45 and OR45	0.997	0.84
Pine Knot South	1	OR180	0.924	10.55
	1	IR45 and OR180	0.957	9.74

Statistical analyses were run on all three sites and residual plots were developed using Minitab in order to determine how the samples fit the normal distribution and how the prediction models predict SSC within different SSC regions and at different sampling times. The graphs of the residual analyses are displayed in Figure 6.12 - Figure 6.17.

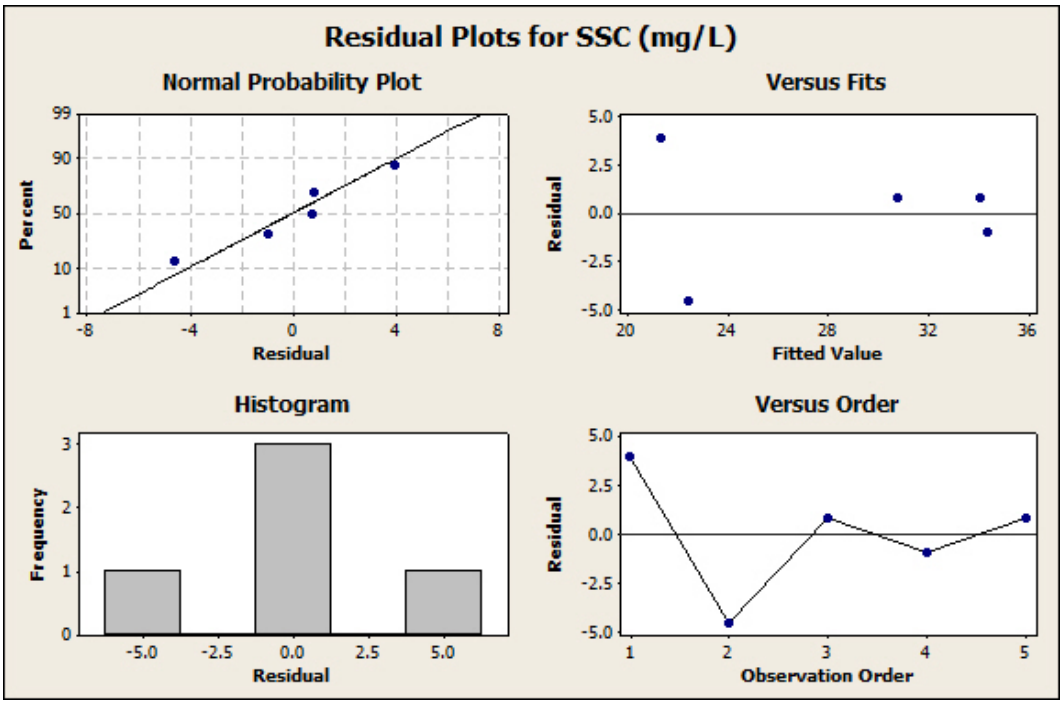

Figure 6.12 Residual plots of OR180 linear prediction model for Upatoi North sensor site (source: Minitab)

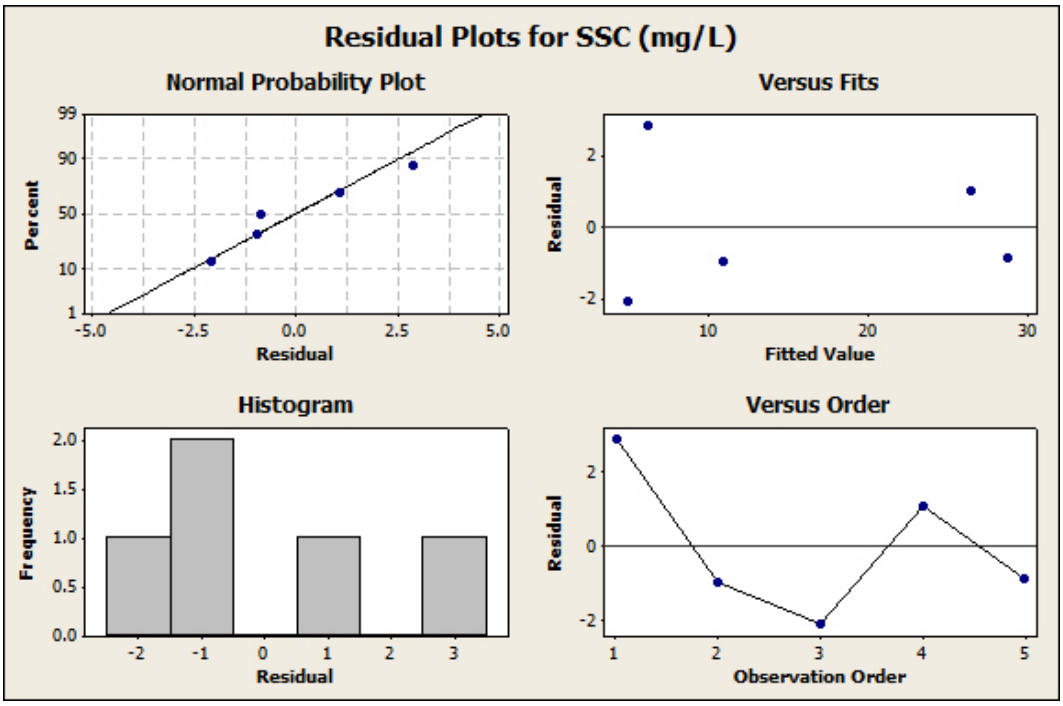

Figure 6.13 Residual plots of IR45 linear prediction model for Pine Knot North sensor site (source: Minitab)

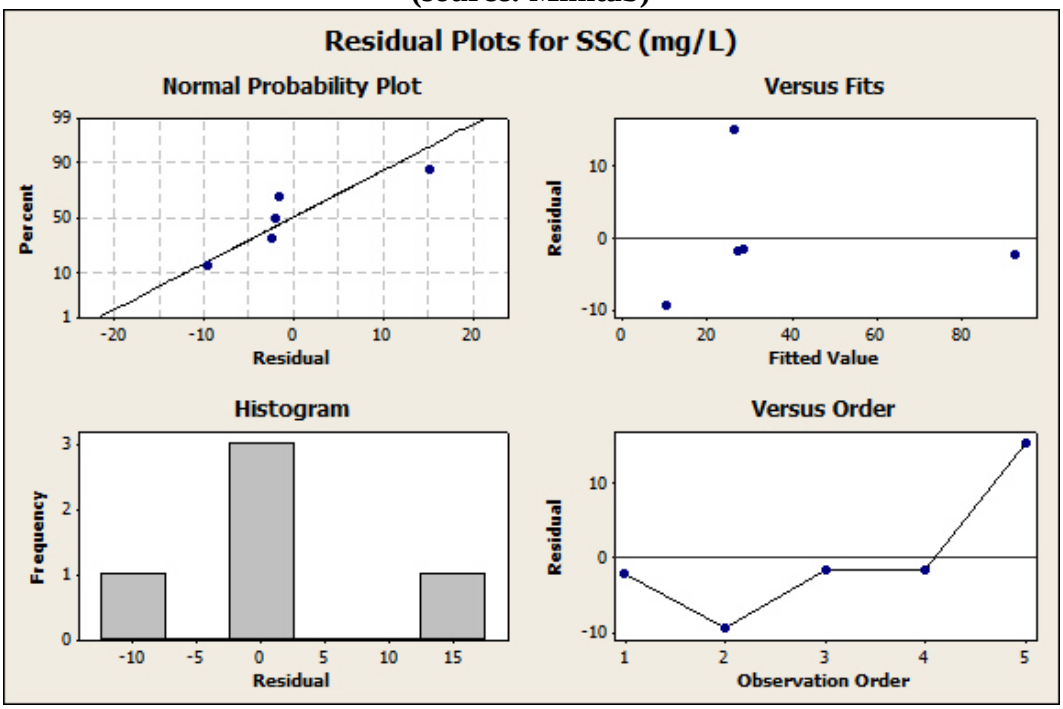

Figure 6.14 Residual plots of OR180 linear prediction model for Pine Knot South sensor site (source: Minitab)

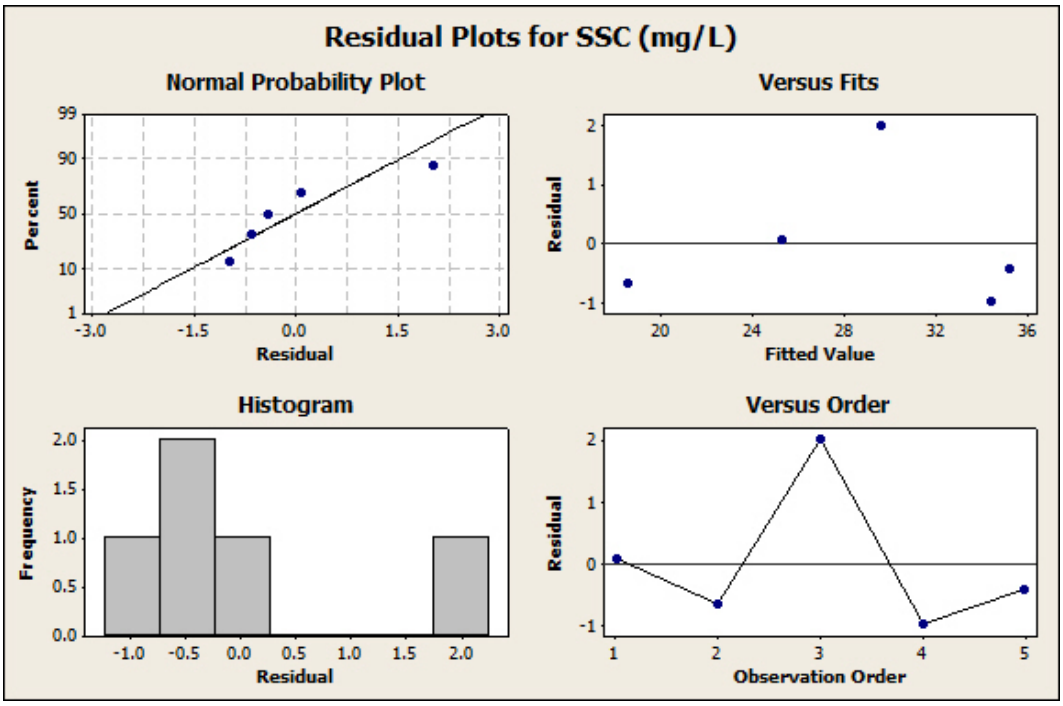

Figure 6.15 Residual plots of OR45-OR180 linear prediction model for Upatoi North sensor site (source: Minitab)

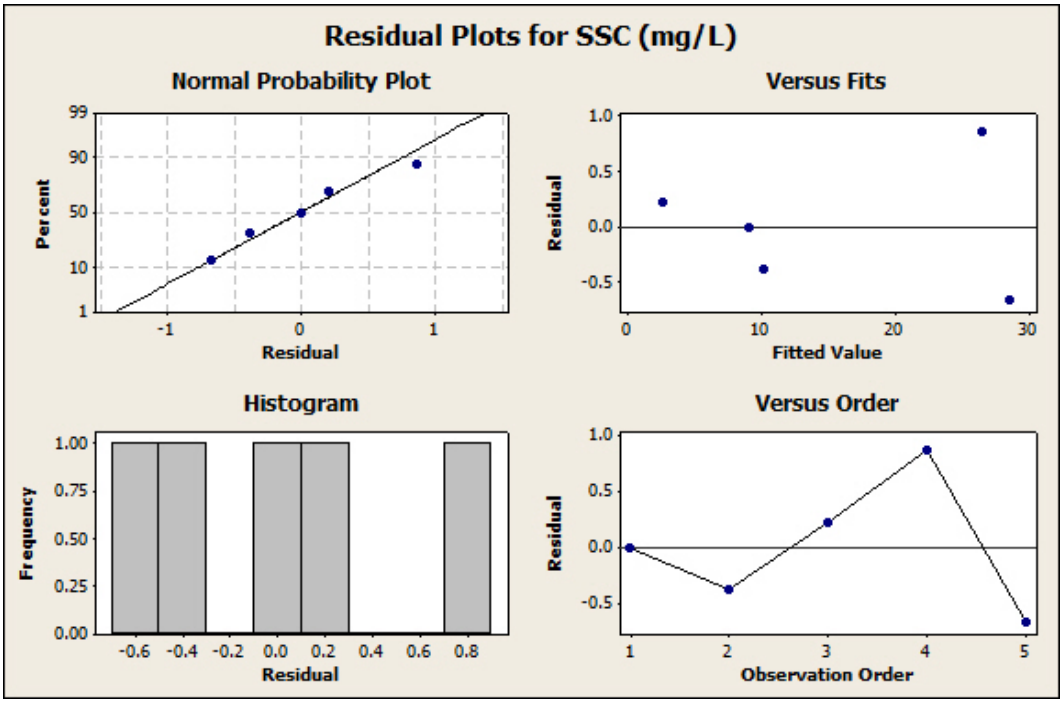

Figure 6.16 Residual plots of IR45-OR45 linear prediction model for Pine Knot North sensor site (source: Minitab)

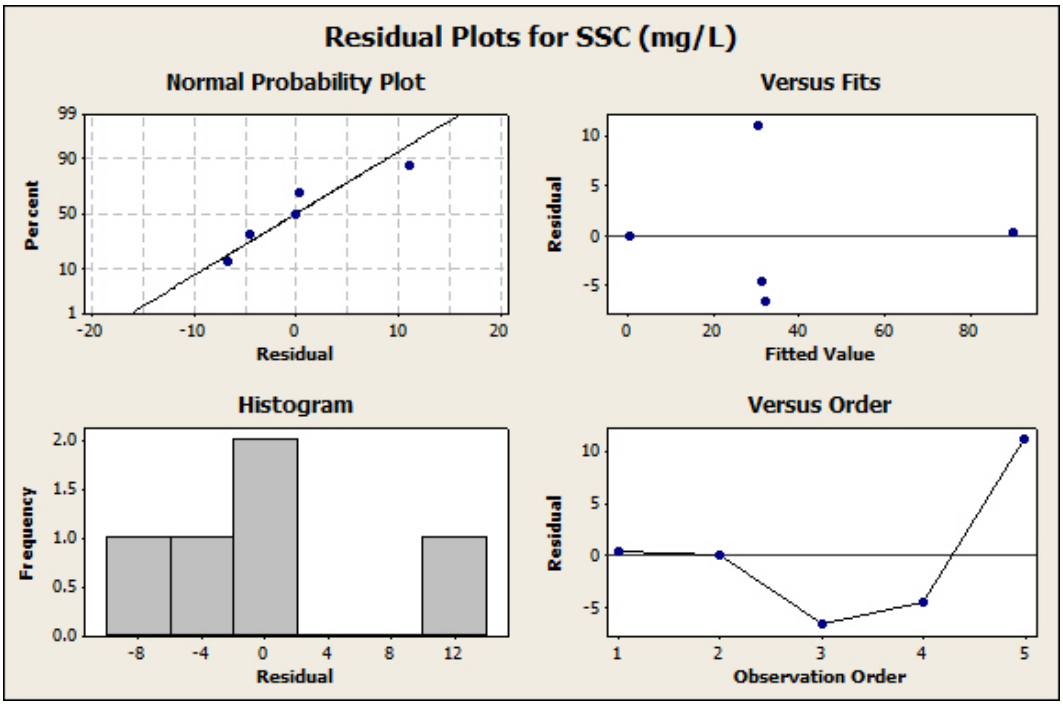

Figure 6.17 Residual plots of IR45-OR180 linear prediction model for Pine Knot South sensor site (source: Minitab)

From these graphs, it can be clearly seen that the smaller number of samples and narrower SSC range of the samples greatly affected the accuracy of these models. The normal probability plots for the PKS and UPN sensors show significant deviations from the straight lines. These deviations indicate the distribution of the samples was less normal, which was probably due to the small sample sizes.

The "versus fits" plot for the Pine Knot South sensor showed smaller prediction errors in the high and low ends of the measured SSC range. This trend, however, cannot be confirmed due to the small sample size. The SSC predicted using the regression models for the water samples are plotted against the SSC values measured using the filtering-weighing methods in Figure 6.18 - Figure 6.23 for the three sensor sites. In addition, the confidence interval for each predicted value is also shown.

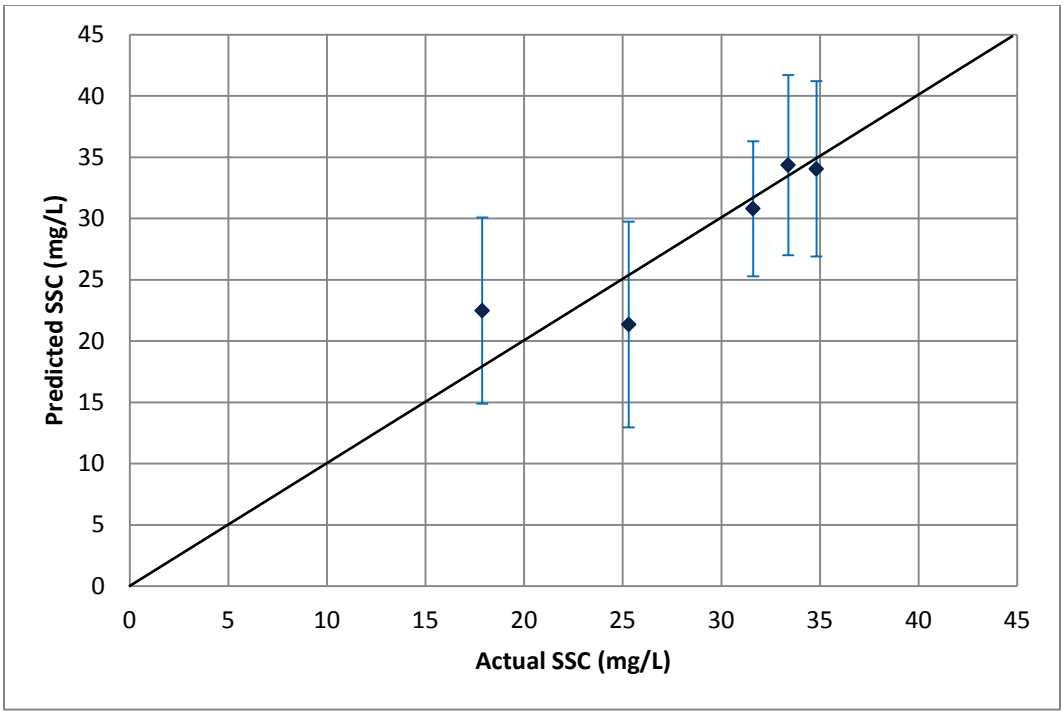

Figure 6.18 Predicted SSC vs. actual SSC for the Upatoi North sensor site using OR180 linear calibration model

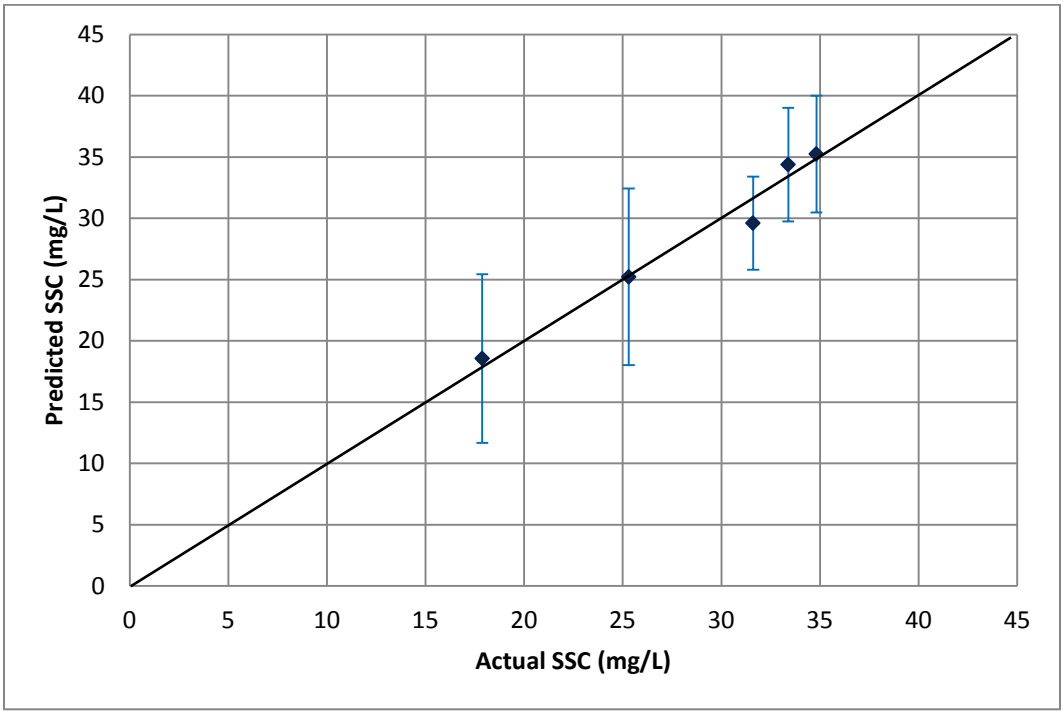

Figure 6.19 Predicted SSC vs. actual SSC for the Upatoi North sensor site using OR45-OR180 linear calibration model

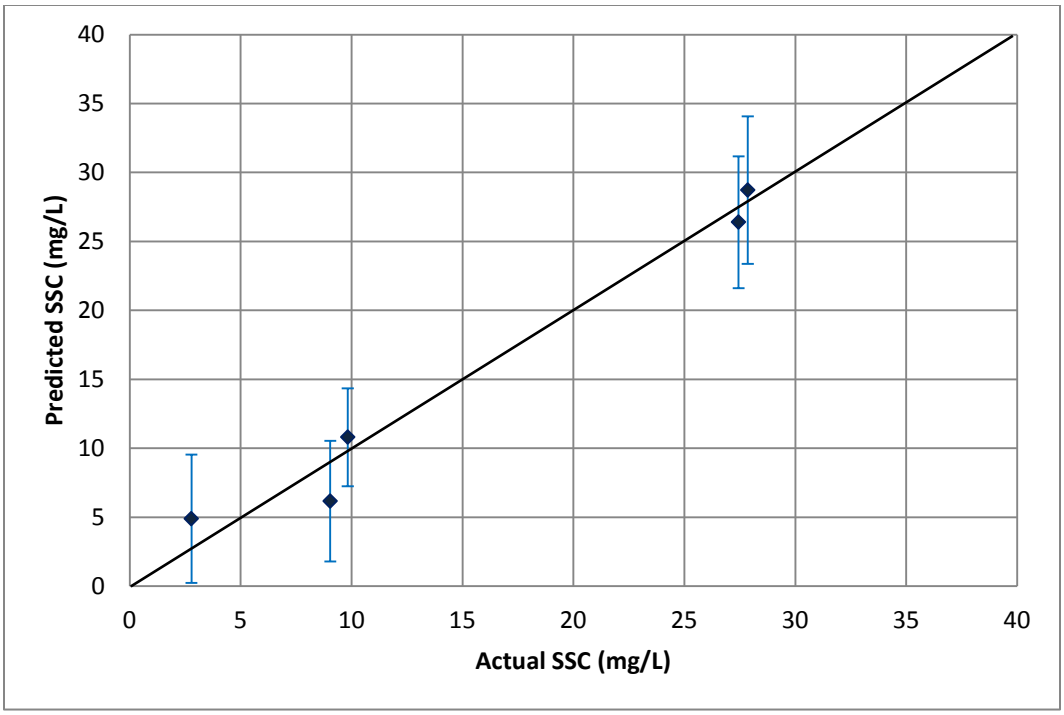

Figure 6.20 Predicted SSC vs. actual SSC for the Pine Knot North sensor site using IR45 linear calibration model

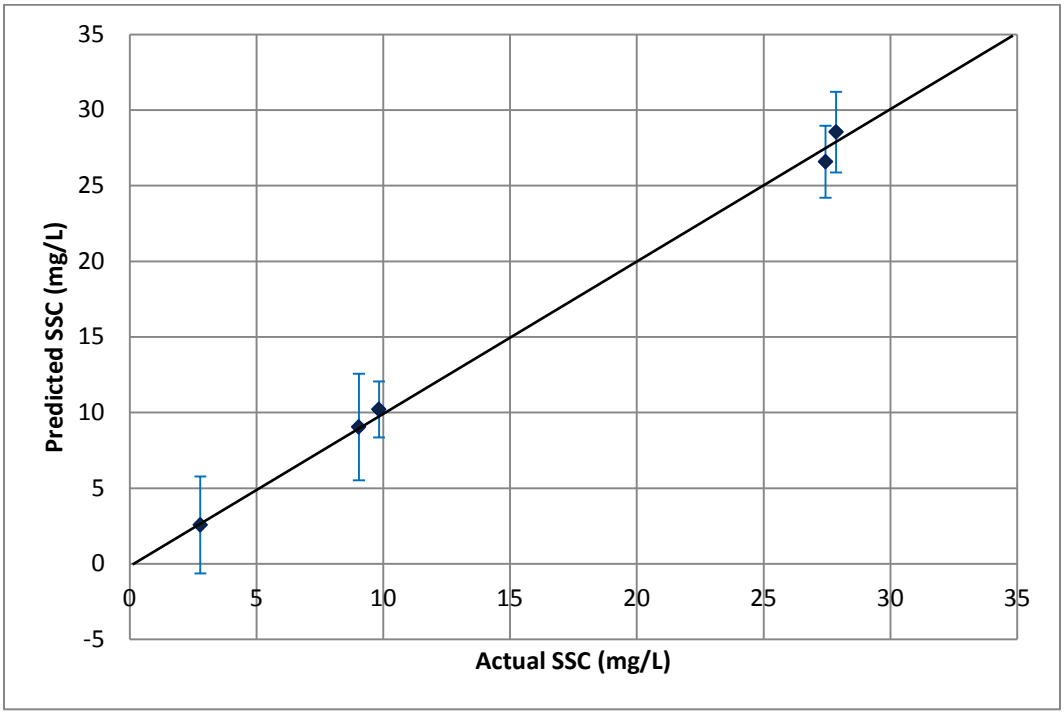

Figure 6.21 Predicted SSC vs. actual SSC for the Pine Knot North sensor site using IR45-OR45 linear calibration model

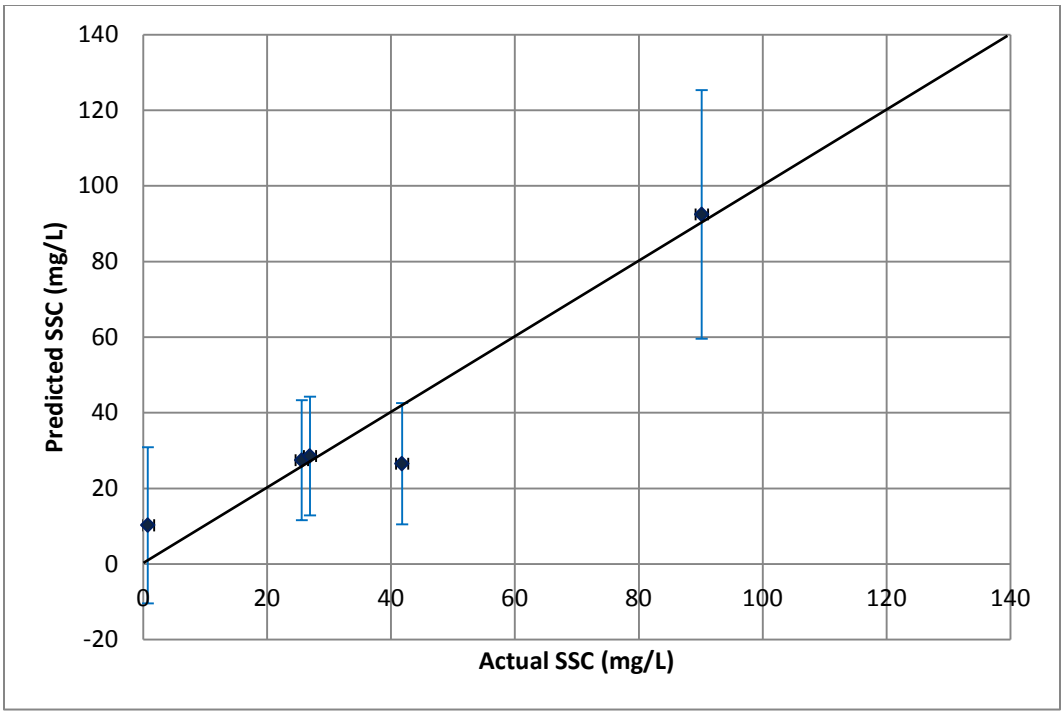

Figure 6.22 Predicted SSC vs. actual SSC for the Pine Knot South sensor site using OR180 linear calibration model

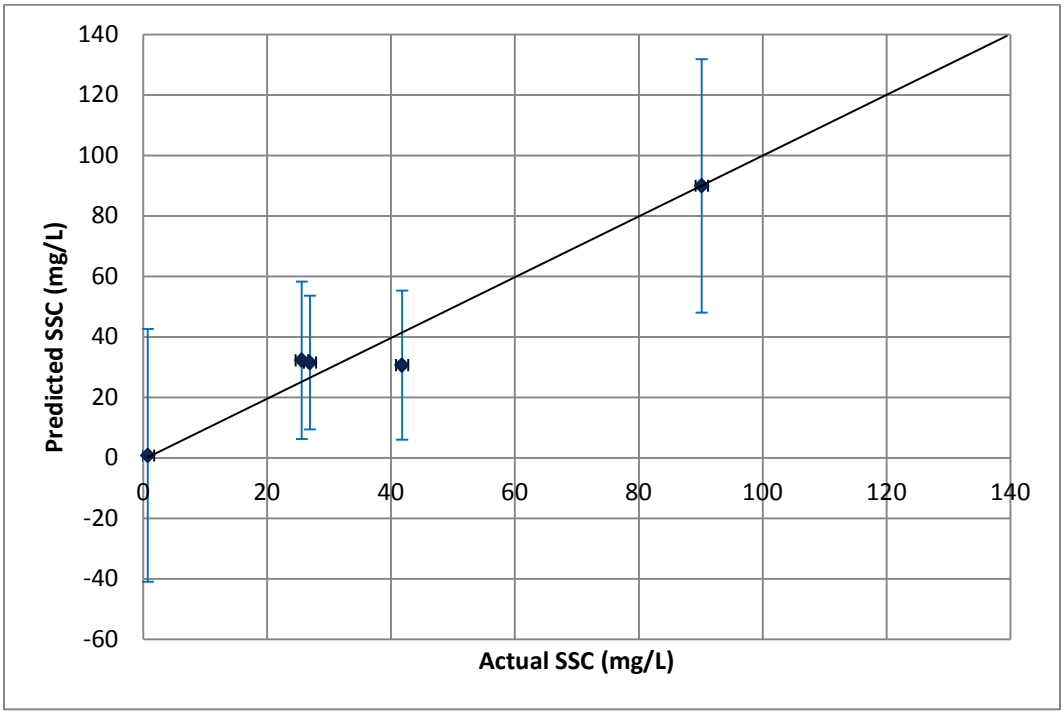

Figure 6.23 Predicted SSC vs. actual SSC for the Pine Knot South sensor site using IR45-OR180 linear calibration model

6.1.1.3 Aberdeen Proving Ground Calibration Models

Calibration was done for the two sensors installed in Anita Leigh Estuary. These two sensors, Anita Near and Anita Far, were placed 3 m from each other. During the demonstration, totally 48 water samples were taken from these two sensor sites. For some of the samples, corresponding sensor signals could not be matched due to hardware problems, including damage on the Stargate, damage on the PCB board, and gateway power loss (See Figures 11 and 12 in Appendix B). Some of the samples were not taken immediately after lens cleaning, because these samples were taken for other purposes, such as characterizing the baseline TSS conditions and observing the fouling effect. Several other samples were taken when the sensor was not completely submerged in water, probably due to low tide. As a result, only 24 samples (10 for the Anita Near site and 14 for the Anita Far site) were used for model calibration and validation.

Calibration models using a single signal as predictor were developed and the best single-variable prediction models were found to be OR45 for Anita Near and IR45 for Anita Far. Figure 6.24 and Figure 6.25 show the fitted line plots for the single-variable models of Anita Near and Anita Far, respectively.

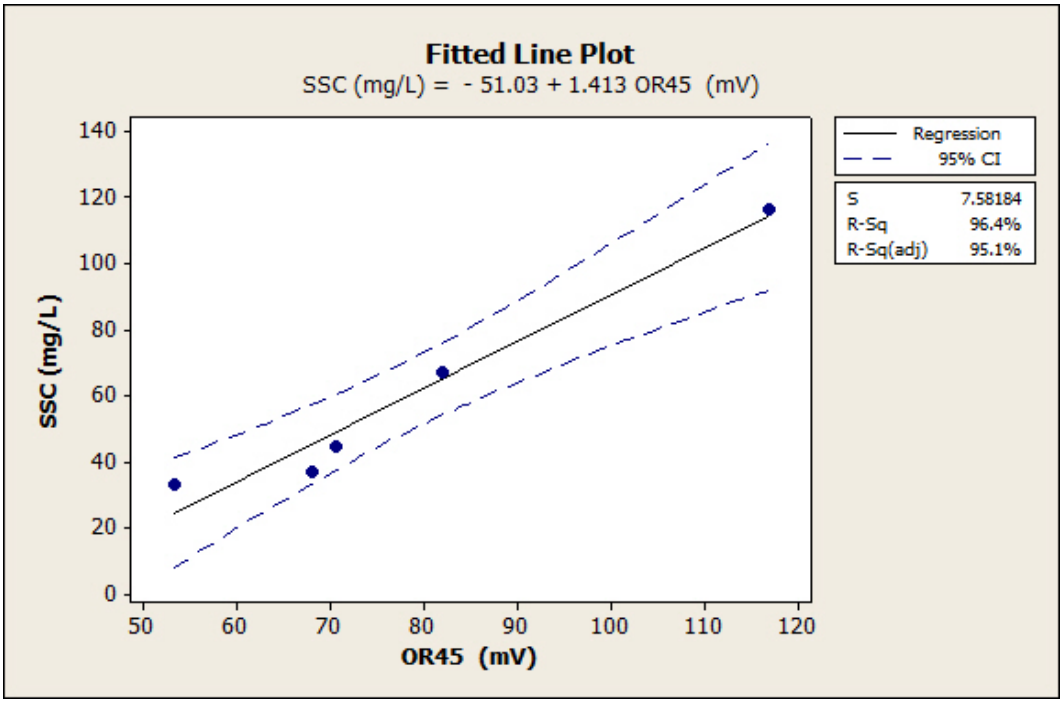

Figure 6.24 OR45 signal vs. suspended sediment concentration for the Anita Near site, Anita Leight Estuary, Edgewood, MD

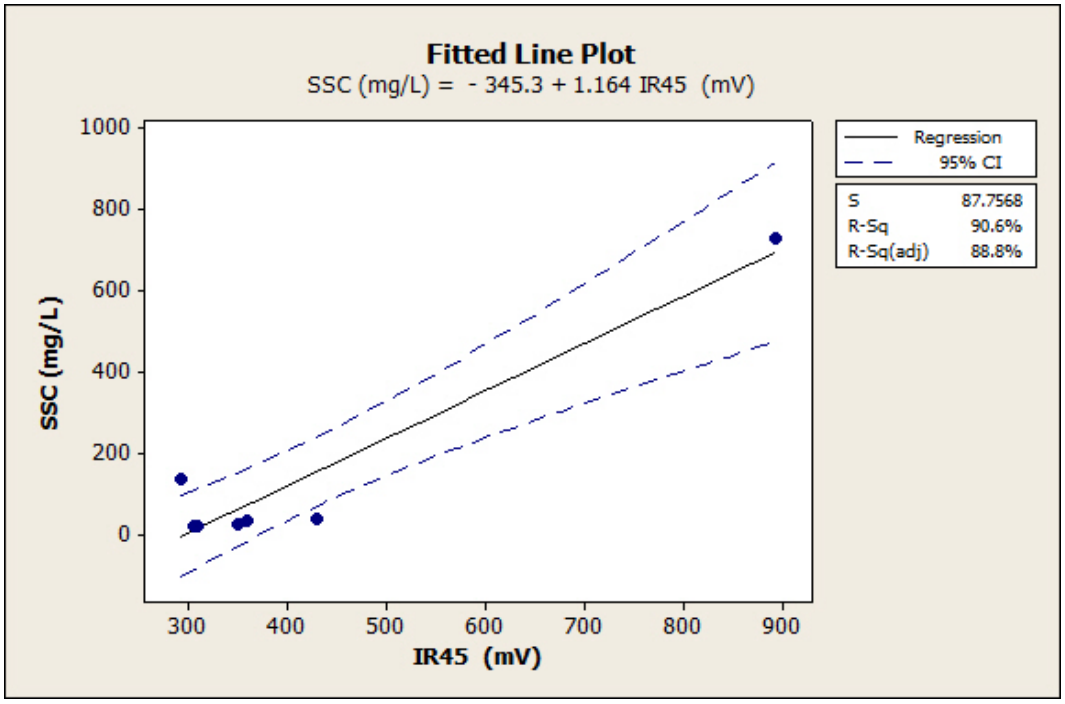

Figure 6.25 IR45 signal vs. suspended sediment concentration for the Anita Far site, Anita Leight Estuary, Edgewood, MD

The best single-variable linear prediction model for Anita Near and Anita Far are:

Anita Near: Concentration (mg/L) = -51.0 + 1.41*OR45(mV)

Anita Far: Concentration (mg/L) = -345 + 1.16*IR45(mV)

After running the stepwise regression analysis, a linear model using all three signals to predict SSC was found to be the best model for Anita Far. The linear model determined to be the best fit for Anita Far sensor site is:

Concentration(mg/L) = 899 + 0.24*IR45(mV) - 2.74*OR45(mV) - 0.23*OR180(mV)

These models were also analyzed using Minitab, as shown in Figure 6.26 - Figure 6.28.

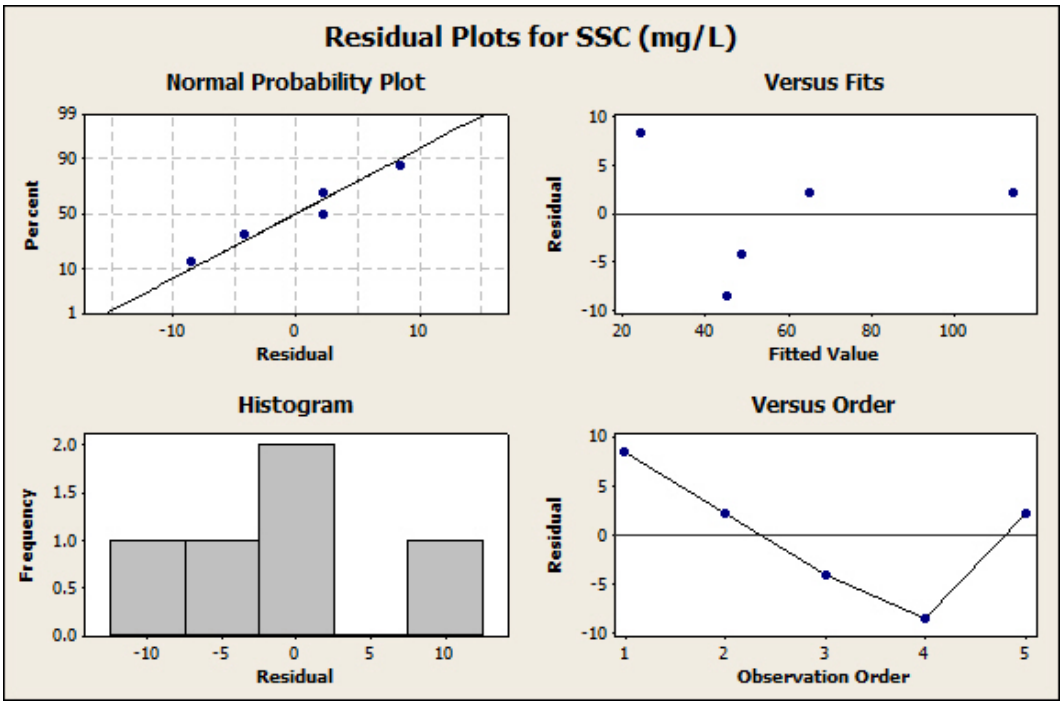

Figure 6.26 Residual plots of the OR45 linear prediction model for Anita Near sensor site (source: Minitab)

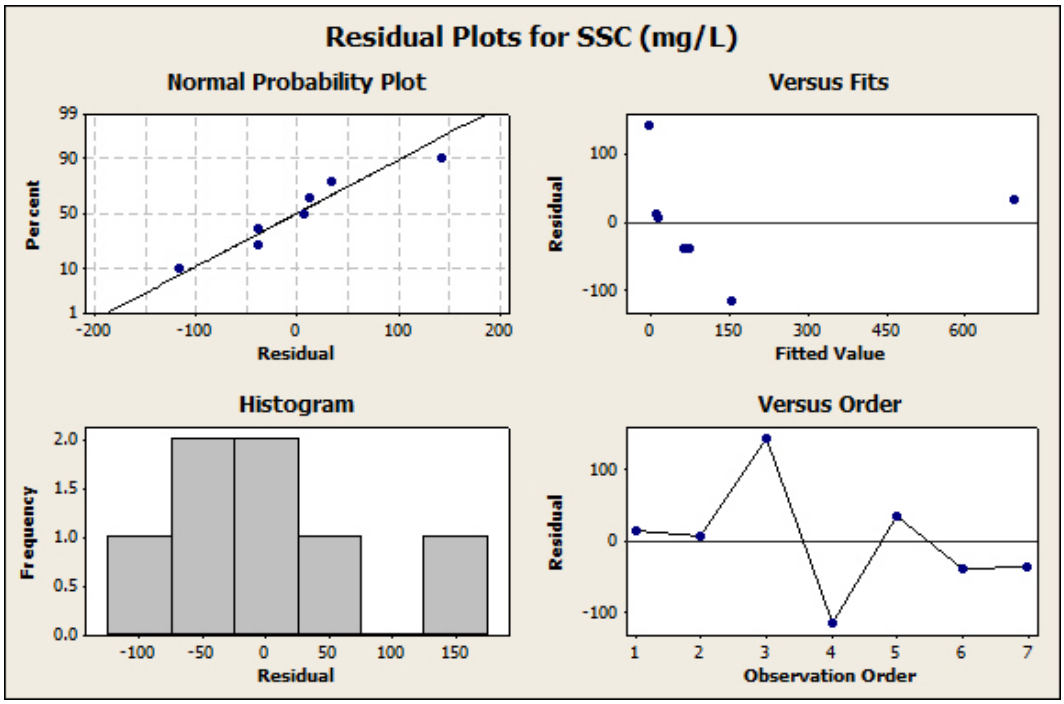

Figure 6.27 Residual plots of the linear prediction model for Anita Near sensor site using IR45 signal (source: Minitab)

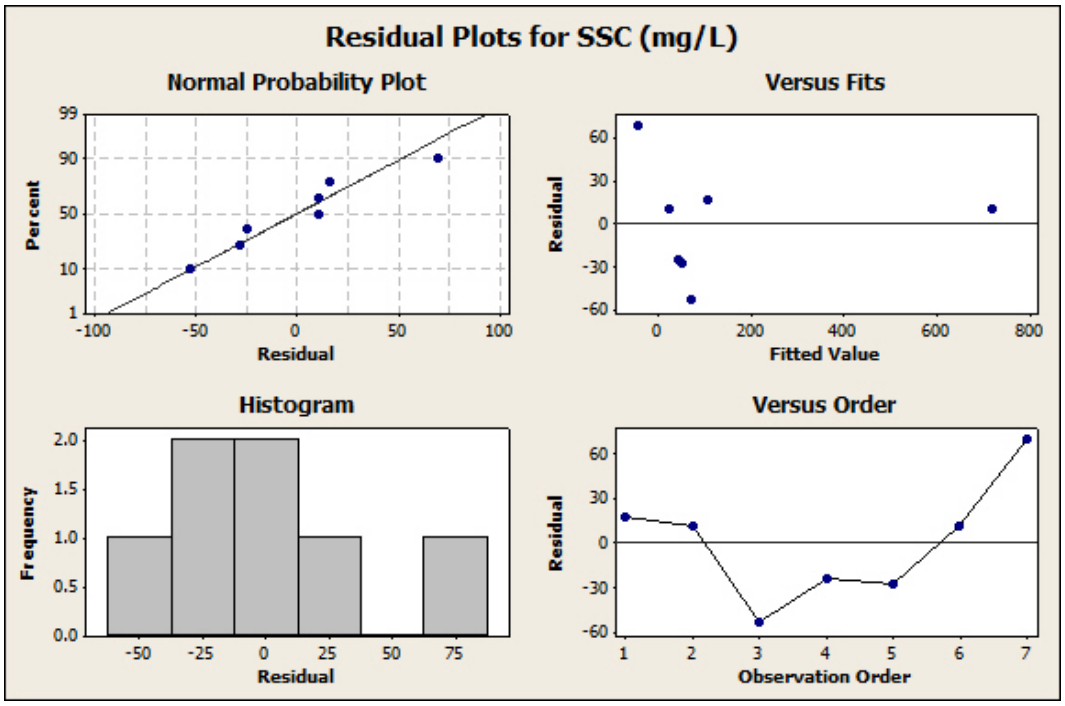

Figure 6.28 Residual plots of the linear prediction model for Anita Far sensor site using all signals (source: Minitab)

Table 6.4 displays the R^2 and RMSE values for the calibration models at the Aberdeen sites. From this table it can be observed that the R^2 and RMSE values were improved by including more signals as the predictors for the Anita Far site.

Table 6.4 R^2 and RMSE values for calibration models used at Aberdeen sensor sites

Sensor Site	*Model Type*	*Signal(s)*	*R^2 Value*	*Root MSE*
Anita Near	Linear	OR45	0.964	7.58
Anita Far	Linear	OR45	0.906	87.8
	Linear	IR45, OR45 and OR180	0.977	56.5

The SSC predicted using the best models for the two sites were compared with the SSC measured using the filtering-weighing methods for the grab samples. The results of this comparison are displayed in Figure 6.29, Figure 6.30, and Figure 6.31. The 95% confidence intervals for the predicted values are also shown.

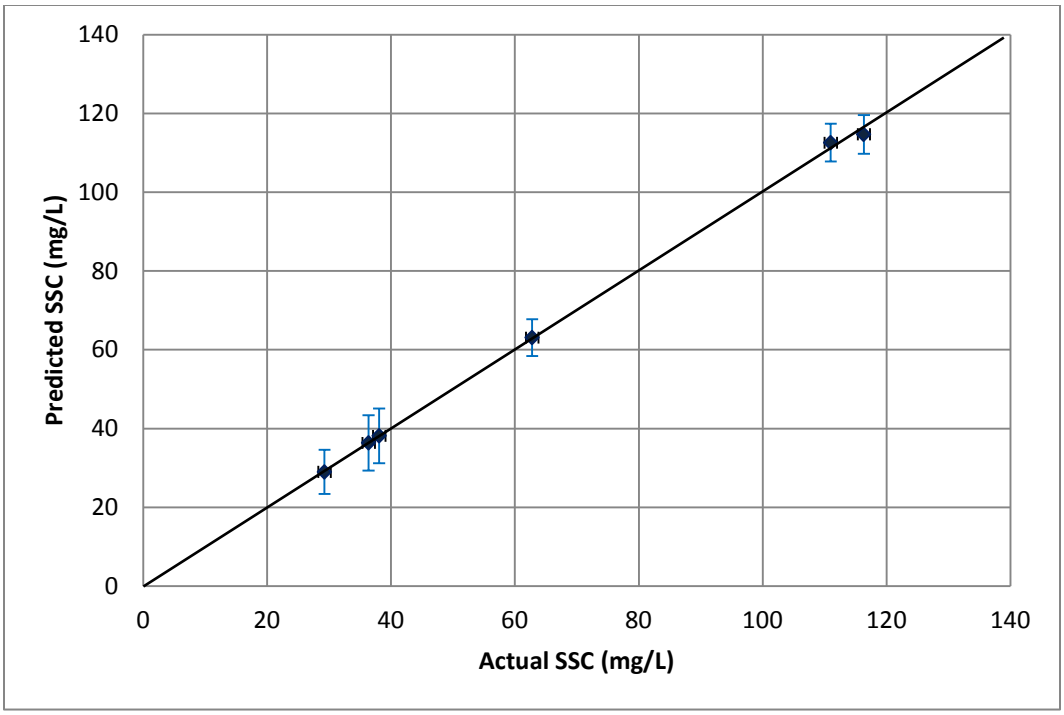

Figure 6.29 Predicted SSC vs. actual SSC for the Anita Near sensor site using the OR45 signal for a linear calibration model (source:minitab)

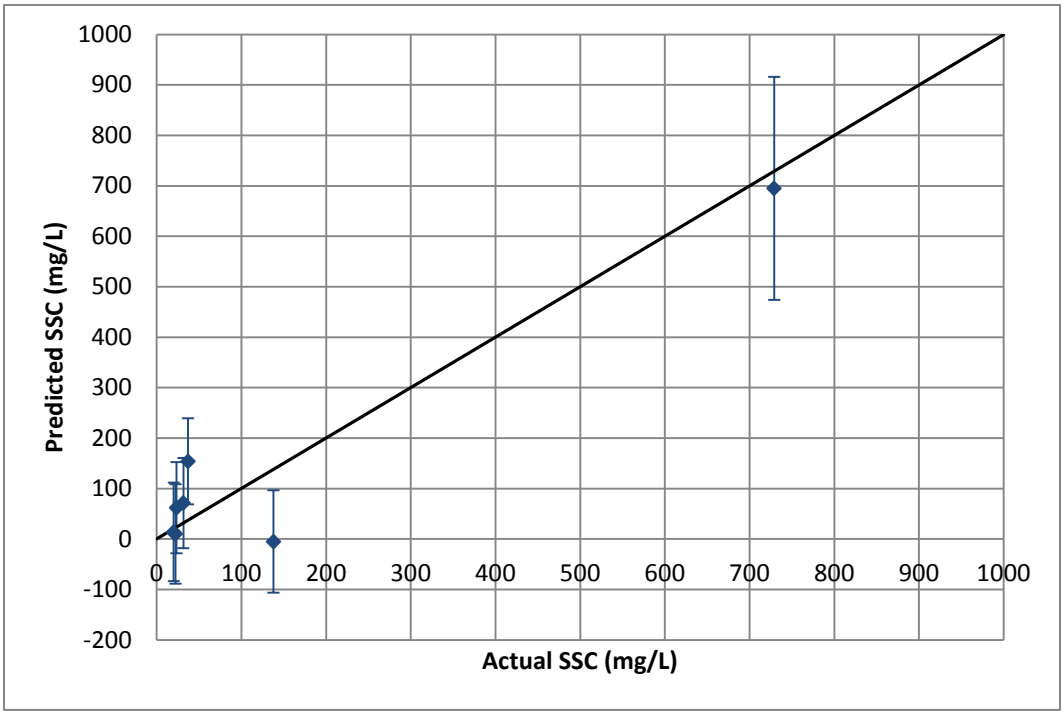

Figure 6.30 Predicted SSC vs. actual SSC for the Anita Far sensor site using IR45 signal for a linear calibration model (source:minitab)

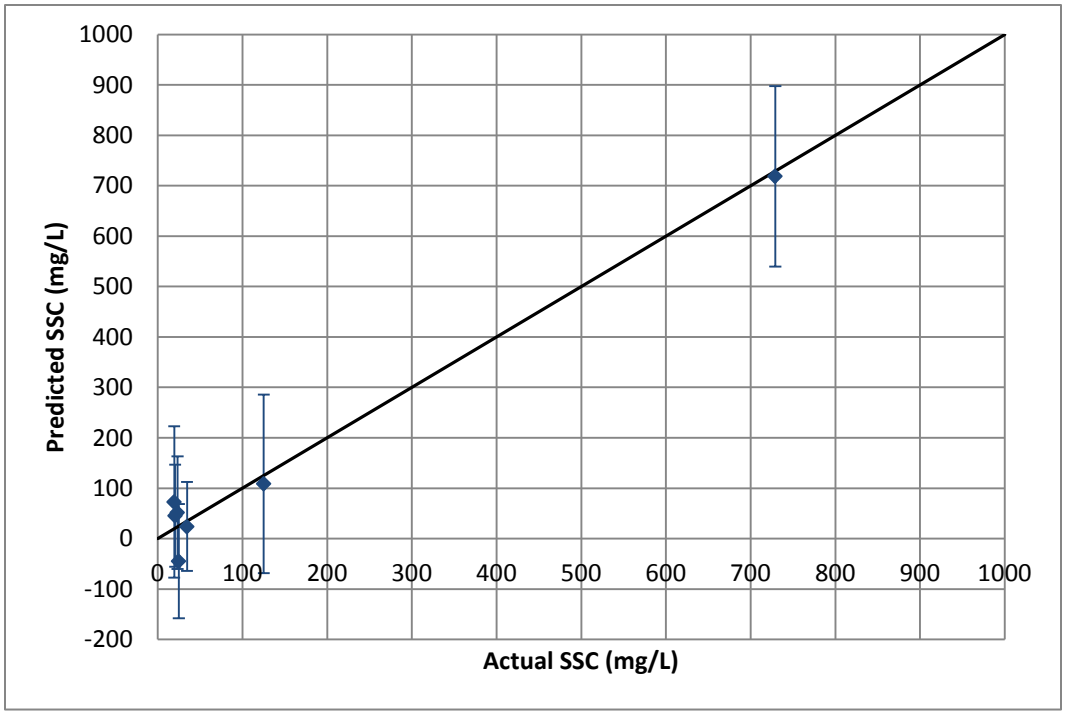

Figure 6.31 Predicted SSC vs. actual SSC for the Anita Far sensor site using all signals for a linear calibration model (source:minitab)

6.1.2 Model Validation

After the calibration models were developed, models were validated. Validation analysis was performed on the models except for Upatoi South where there was no significant calibration models obtained.

Half of the water samples taken at a site were used in validation. The calibration data set was entered into Minitab to establish a calibration model through regression. The validation data set was then entered into the calibration model to see how it fits in the calibration model. RMSE values were calculated for both calibration and validation data sets.

Two measures of accuracy are presented below. One is the maximum error in predicting the SSC which was the maximum absolute difference between the actual SSC and the predicted SSC. The second measure determined the maximum error using the 95% confidence interval. The differences between the actual SSC and the upper limit of predicted SSC (at 95% confidence interval) and between the actual SSC and the lower limit of predicted SSC were computed and the larger among these two was reported as the maximum error. A positive difference indicated over-prediction and a negative difference under-prediction. Obviously, the second measure is stricter in evaluating the sensor accuracy.

For the accuracy of each model in SSC measurement, a success criteria of $\pm$10% or $\pm$50mg/L of actual SSC (whichever is greater) was used for evaluation.

6.1.2.1 Fort Riley Sites

Figure 6.32 - Figure 6.34 show predicted SSCs for both the calibration and validation data sets against the actual SSCs for the Fort Riley sites. Also shown in the plots are the 95% confidence intervals for the validation data.

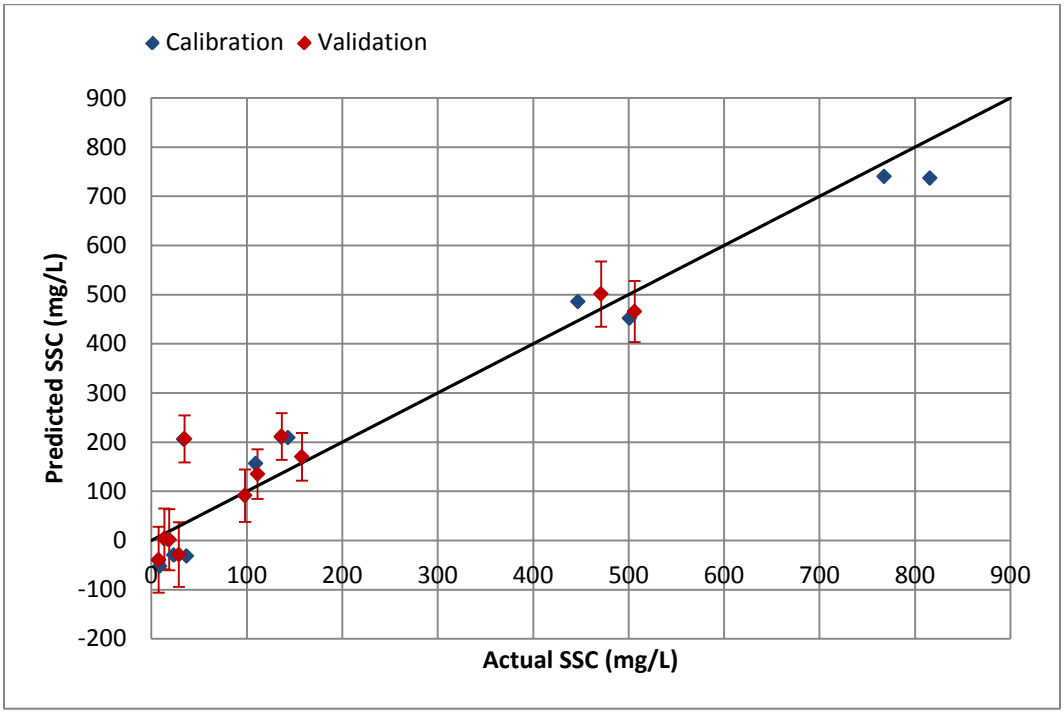

Figure 6.32 Predicted SSC vs. actual SSC of the calibration and validation data sets for the Little Kitten sensor site using OR180 linear calibration model

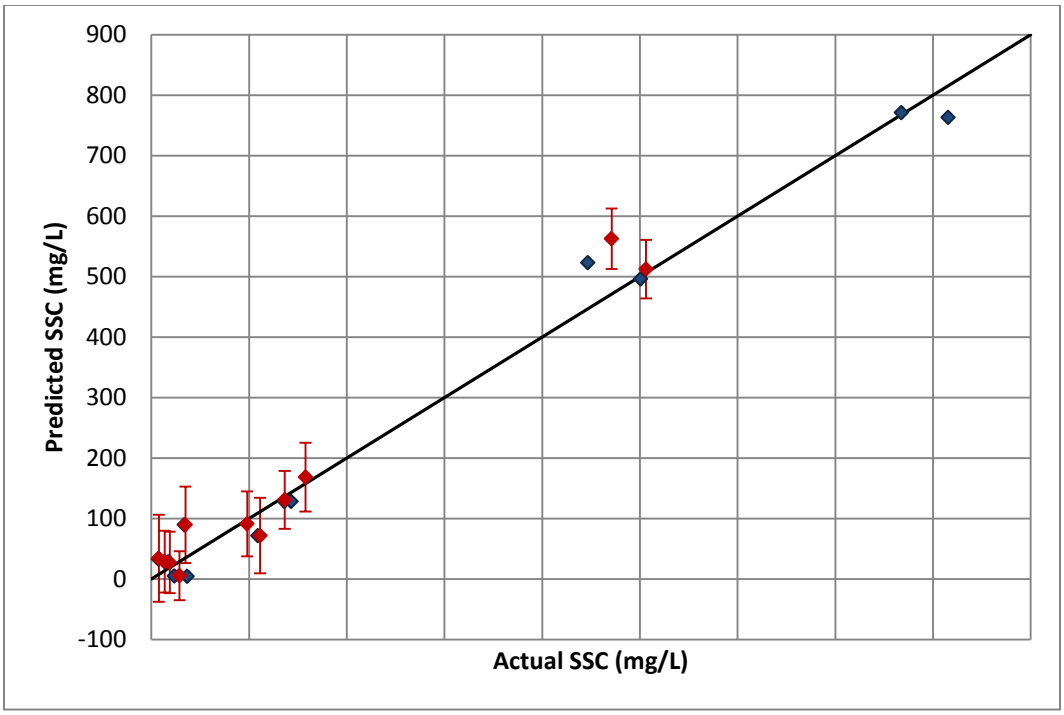

Figure 6.33 Predicted SSC vs. actual SSC of the calibration and validation data sets for the Little Kitten sensor site using second-order calibration model

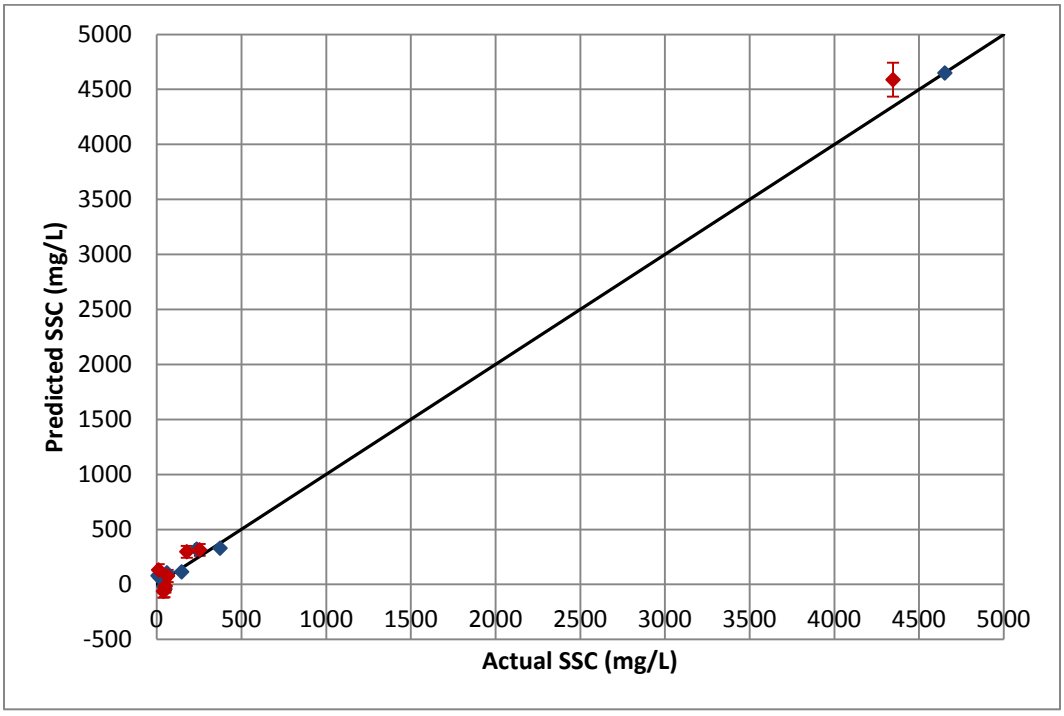

Figure 6.34 Predicted SSC vs. actual SSC of the calibration and validation data sets for the Wildcat Bridge sensor site using OR180 linear calibration model

The Little Kitten site had a measurement range of 0-500 mg/L while Wildcat Bridge site had 0-4000mg/L.

Table 6.5 and Table 6.6 show the accuracies of each model for calibration data and validation data, respectively.

It can be seen that the sensors at Little Kitten site failed to meet the success criteria for the entire range when the second measure (considering the 95% confidence interval) was used. On the other hand, Wildcat Bridge just failed to meet the criteria for range below 500 mg/L (though not too far from ±50mg/L) and was good for SSC measurement above 500mg/L with a maximum error in measurement of about -3.5% at 95% confidence interval. The results for the validation data set is similar (Table 6.6).

Table 6.5 SSC Measurement Range and Accuracy for Calibration Data in Fort Riley sites.

Site (Range)	Model Type		Maximum Error (Measure 1)		Maximum Error (95% confidence interval) (Measure 2)	
	Order	Signal(s) used	≤ 500mg/L (mg/L)	>500mg/L (%)	≤ 500mg/L (mg/L)	>500mg/L (%)
Little Kitten (7.3 – 815.6 mg/L)	1	OR180	172	-9.7	220	-21.8
	2	IR45, OR180	76	-6.5	122	-13.6
Wildcat Bridge (8.0 – 4685.1 mg/L)	1	OR180	-94	-0.1	-152	-3.5

Table 6.6 SSC Measurement Range and Accuracy for Validation Data in Fort Riley sites.

Site (Range)	Model Type		Maximum Error (Measure 1)		Maximum Error (95% confidence interval) (Measure 2)	
	Order	Signal(s) used	≤ 500mg/L (mg/L)	>500mg/L (%)	≤ 500mg/L (mg/L)	>500mg/L (%)
Little Kitten (7.6 – 506.3 mg/L)	1	OR180	172	-8.0	220	-20.3

	2	IR45, OR180	92	1.2	142	10.8
Wildcat Bridge (8.0 – 4685.1 mg/L)	1	OR180	118	5.6	173	9.1

6.1.2.2 Fort Benning sites

Figure 6.35 - Figure 6.40 show predicted SSC of both the calibration and validation data sets against the actual SSC for the Fort Benning sites. Also included in the plot is the 95% confidence interval of each data point used for validation. The SSC ranges observed at the Fort Benning sites were lower than those observed at the Fort Riley sites.

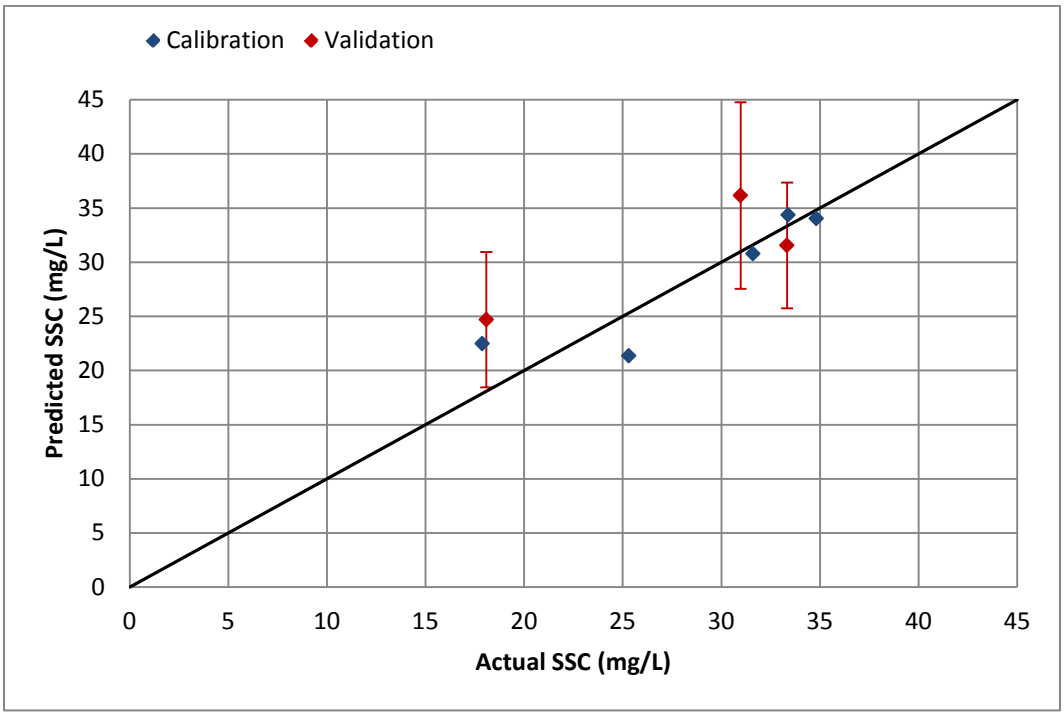

Figure 6.35 Predicted SSC vs. actual SSC of the calibration and validation data sets for the Upatoi North sensor site using OR180 linear calibration model

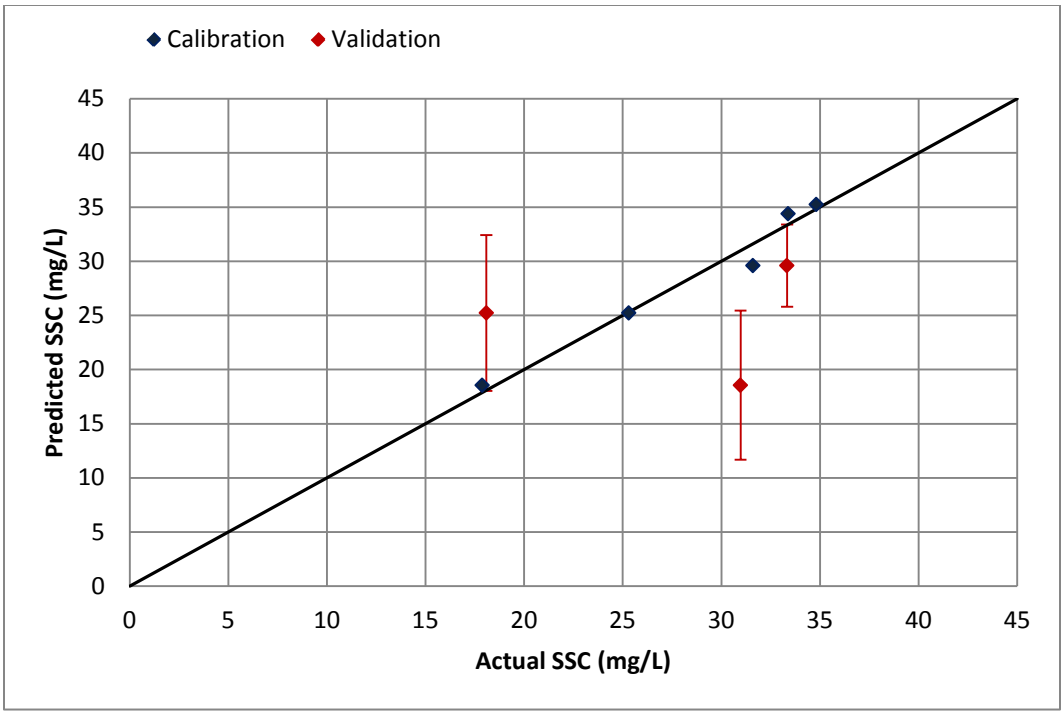

Figure 6.36 Predicted SSC vs. actual SSC of the calibration and validation data sets for the Upatoi North sensor site using OR45-OR180 linear calibration model

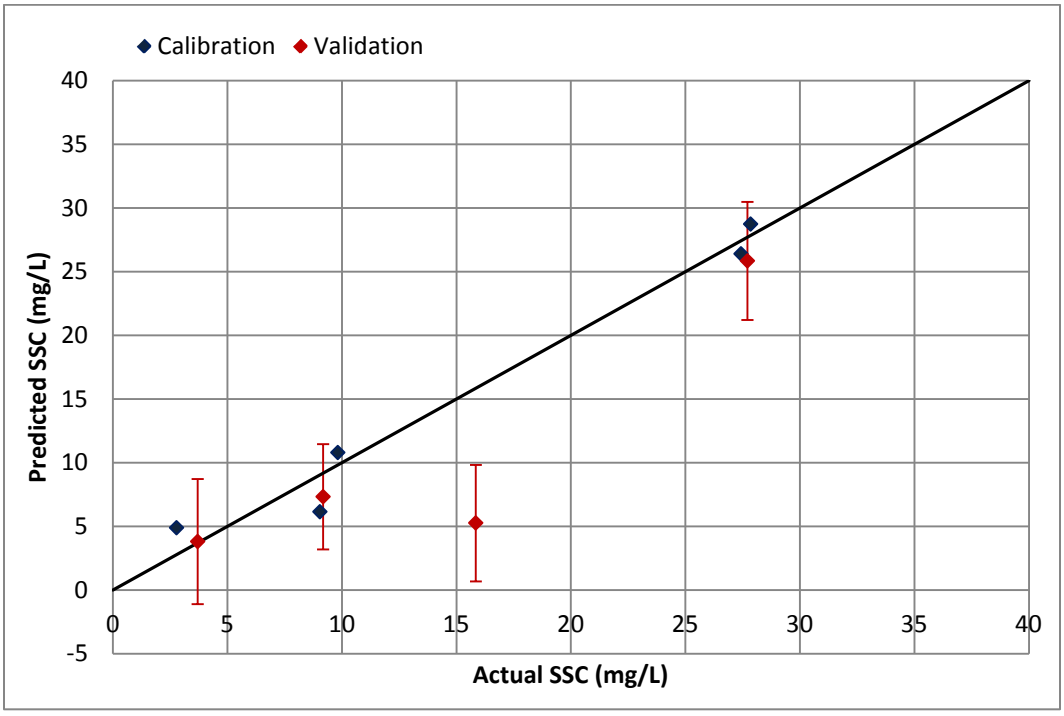

Figure 6.37 Predicted SSC vs. actual SSC of the calibration and validation data sets for the Pine Knot North sensor site using IR45 linear calibration model

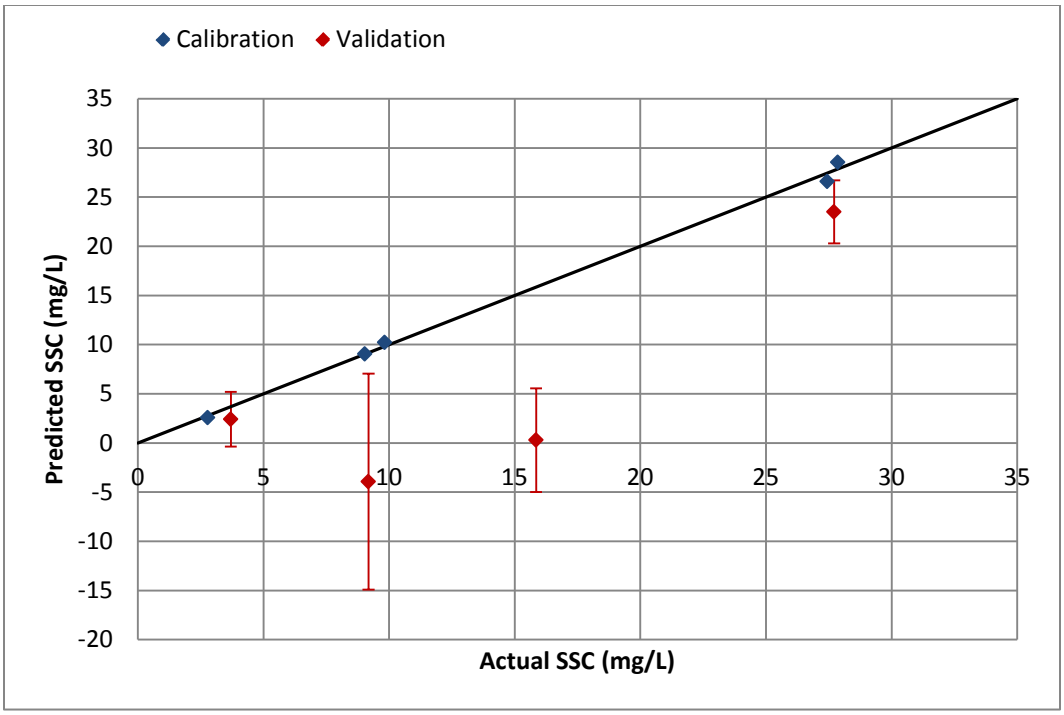

Figure 6.38 Predicted SSC vs. actual SSC of the calibration and validation data sets for the Pine Knot North sensor site using IR45-OR45 linear calibration model

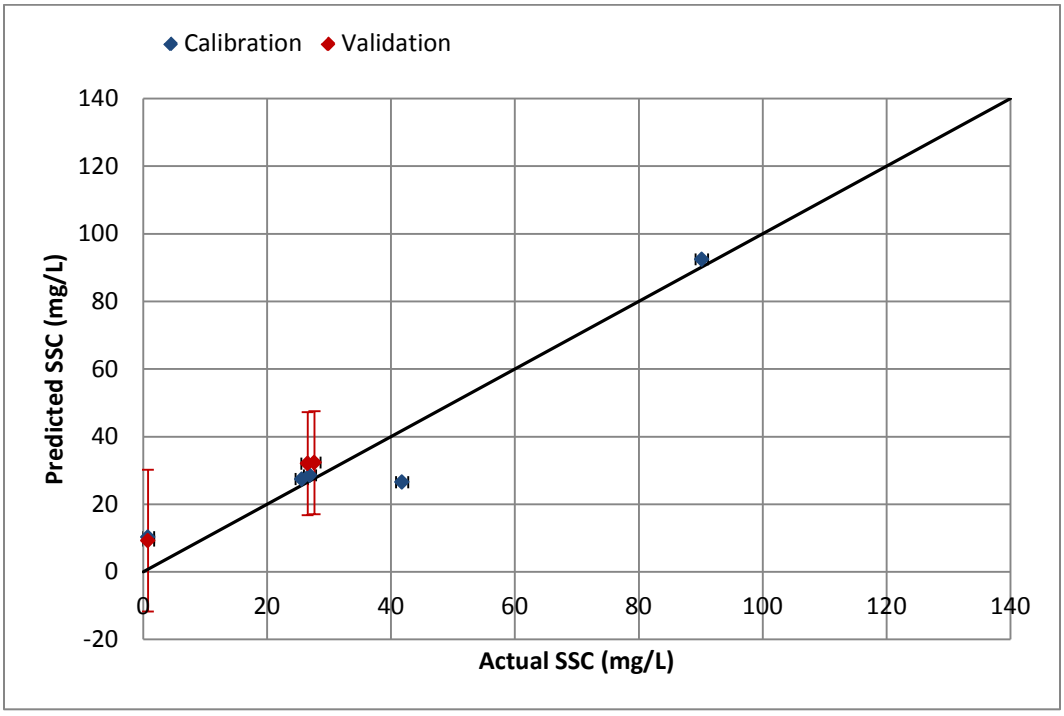

Figure 6.39 Predicted SSC vs. actual SSC of the calibration and validation data sets for the Pine Knot South sensor site using OR180 linear calibration model

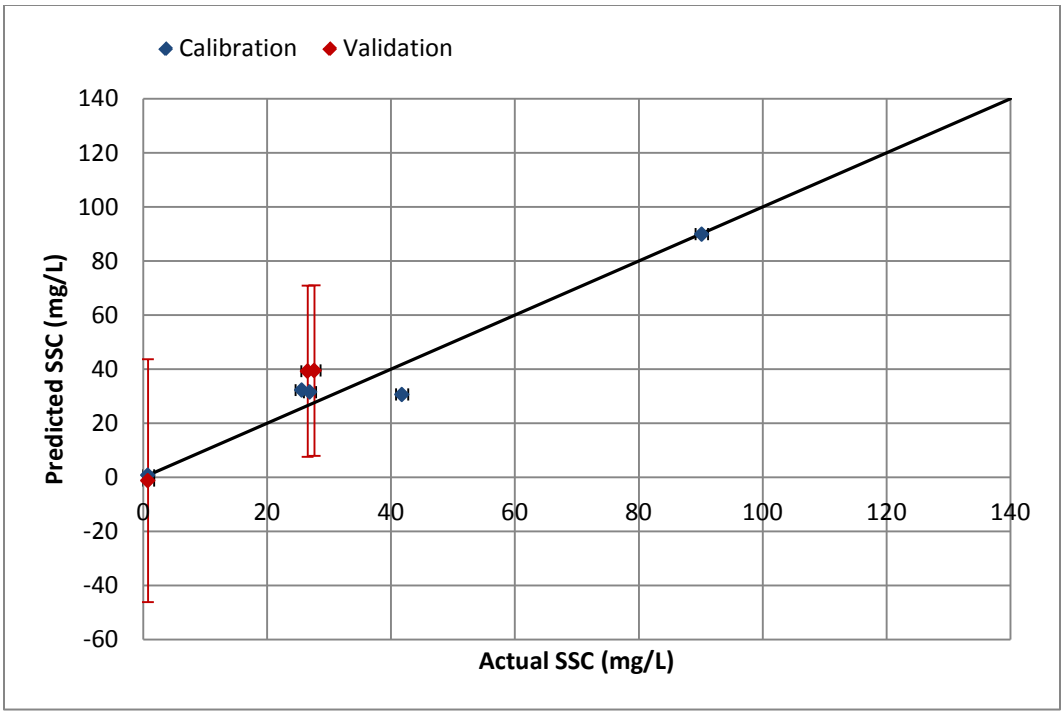

Figure 6.40 Predicted SSC vs. actual SSC of the calibration and validation data sets for the Pine Knot South sensor site using IR45-OR180 linear calibration model

Table 6.7 and

Table 6.8 show the accuracy of each model in each site for calibration and validate data sets, respectively. All the models in the three sites of Fort Benning passed the success criterion for measurement accuracy at 95% confidence interval.

Table 6.7 SSC Measurement Range and Accuracy for Calibration Data in Fort Benning sites.

Site (Range)	Model Type		Maximum Error (Measure 1)	Maximum Error (95% confidence interval) (Measure 2)
	Order	Signal(s) used	$\leq$ 500mg/L (mg/L)	$\leq$ 500mg/L (mg/L)
Upatoi North (17.9 – 34.8 mg/L)	1	OR180	4.6	-12.4
	1	OR45, OR180	-2.0	7.6
PineKnot North (2.8 – 27.9 mg/L)	1	IR45	-2.9	-7.3
	1	IR45, OR45	-0.9	3.5
PineKnot South (0.7 – 90.2 mg/L)	1	OR180	-15.3	35.1
	1	IR45, OR180	-11.1	-42.0

Table 6.8 SSC Measurement Range and Accuracy for Validation Data at Fort Benning sites.

Site (Range)	Model Type		Maximum Error (Measure 1)	Maximum Error (95% confidence interval) (Measure 2)
	Order	Signal(s) used	≤ 500mg/L (mg/L)	≤ 500mg/L (mg/L)
Upatoi North (18.1 – 33.3 mg/L)	1	OR180	6.6	13.8
	1	OR45, OR180	-12.4	-19.3
PineKnot North (3.7 – 27.7 mg/L)	1	IR45	-10.6	-15.2
	1	IR45, OR45	-15.6	-24.1
PineKnot South (0.8 – 27.6 mg/L)	1	OR180	8.5	29.5
	1	IR45, OR180	12.7	-47.0

6.1.2.2 Aberdeen Proving Grounds sites

Figure 6.41 and Figure 6.42 show predicted SSC for both the calibration and validation data sets against the actual SSC for the Anita Near and Anita Far sites. Also included in the plot is the confidence interval of each data point used for validation

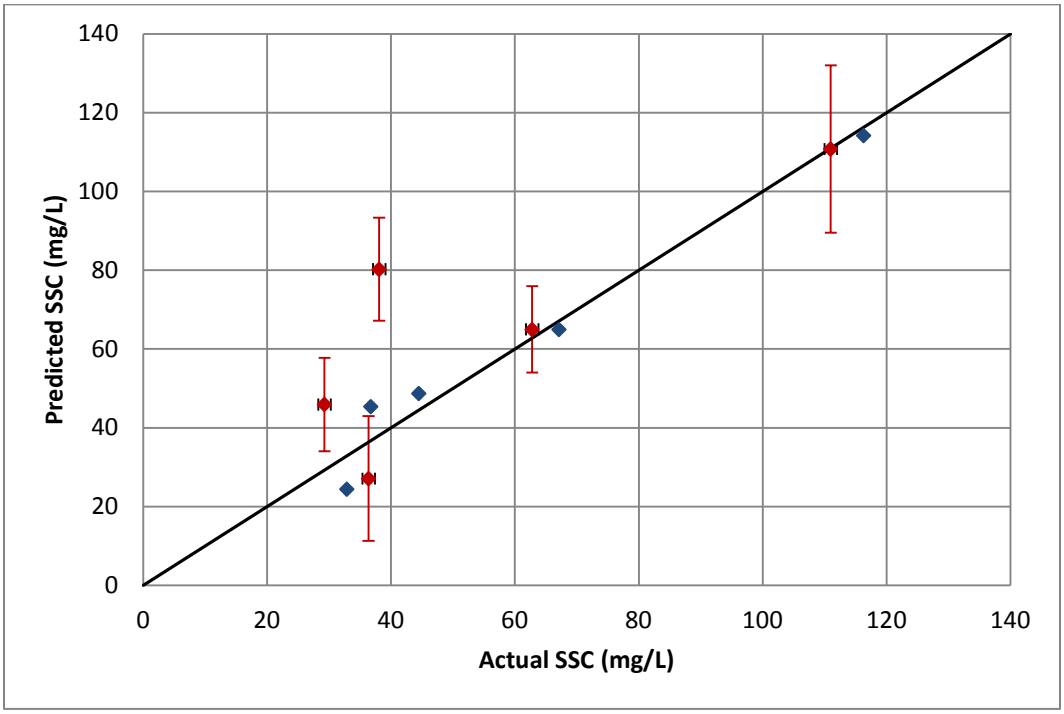

Figure 6.41 **Predicted SSC vs. actual SSC of the calibration and validation data sets for the Anita Near sensor site using OR45 linear calibration model**

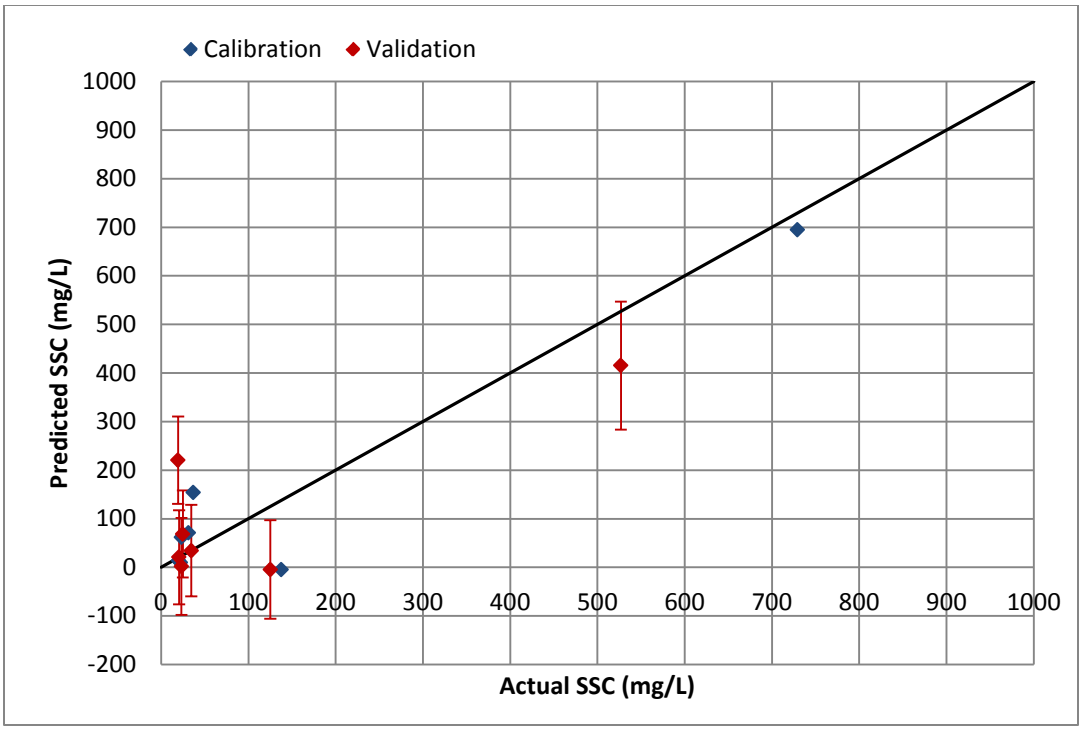

Figure 6.42 Predicted SSC vs. actual SSC of the calibration and validation data sets for the Anita Far sensor site using IR45 linear calibration model.

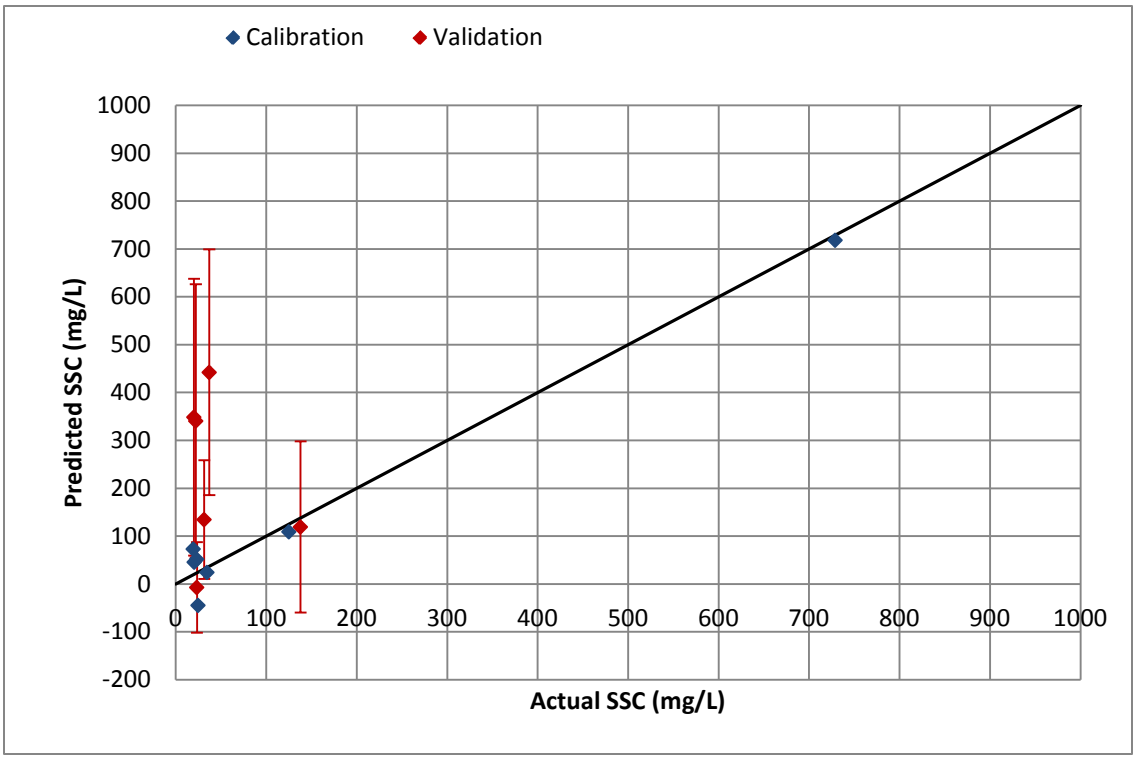

Figure 6.43 Predicted SSC vs. actual SSC of the calibration and validation data sets for the Anita Far sensor site using all signals linear calibration model.

Table 6.9 and **Table 6.10** show the accuracy of measurement for the calibration and validation data sets, respectively. Considering the maximum error at 95% confidence interval (measure 2), Anita Near passed the success criteria for SSC less than 500 mg/L in the calibration part but failed in the validation. On the other hand, Anita far models failed the success criteria for the entire range for both calibration and validation.

Considering the maximum error in prediction (measure 1), Anita Near passed the criteria for both calibration and validation. Anita Far failed to meet the success criteria for both calibration and validation for SSC of 500mg/L and below. On the contrary, for SSC greater than 500mg/L, Anita Far models passed the success criteria in calibration but failed in validation.

The accuracy of prediction models may have been affected by the fact that SSC samples were not normally distributed. The small number of samples actually used in calibration and validation may also contribute to the failures.

Table 6.9 SSC Measurement Range and Accuracy for Calibration Data in Aberdeen Proving Grounds sites.

Site (Range)	Model Type		Maximum Error (Measure 1)		Maximum Error (95% confidence interval) (Measure 2)	
	Order	Signal(s) used	≤ 500mg/L (mg/L)	> 500mg/L (%)	≤ 500mg/L (mg/L)	> 500mg/L (%)
Anita Near (32.9 – 116.3 mg/L)	1	OR45	8.6	n/a	-25.0	n/a
Anita Far (20.1 – 729.1 mg/L)	1	IR45	-142.9	-4.7	-244.2	-35.0
Anita Far (19.4 – 729.1 mg/L)	1	IR45, OR45, OR180	-69.4	-1.4	203.8	-26.0

Table 6.10 SSC Measurement Range and Accuracy for Validation Data in Aberdeen Proving Grounds sites.

Site (Range)	Model Type		Maximum Error (Measure 1)		Maximum Error (95% confidence interval) (Measure 2)	
	Order	Signal(s) used	≤ 500mg/L (mg/L)	> 500mg/L (%)	≤ 500mg/L (mg/L)	> 500mg/L (%)
Anita Near (29.3 – 111.0 mg/L)	1	OR45	42.2	n/a	55.3	n/a
Anita Far (19.4 – 526.8 mg/L)	1	IR45	201	-21.2	290.9	-46.2

Anita Far (20.1 – 137.9 mg/L)	1	IR45, OR45, OR180	405.3	n/a	662.0	n/a

Table 6.11 summarizes the accuracy of SSC measurements for all sensor sites. Results reported in this table were only for the validation data sets. It is safe to say that for the Upatoi North, Pine Knot North, Pine Knot South and Anita Near sites, the sensors have passed the success criteria for SSC below 500 mg/L. However, because of the low range of SSC, the measurement accuracy was not satisfactory.

For sites like Little Kitten, Wildcat Bridge, Anita Near, and Anita Far where the success criteria were not met, lack of evenly distributed samples within the SSC range affected the prediction models. For instance, the Wildcat Bridge site had clustered samples below 100mg/L, but was lacking samples within the mid-range of SSC.

Overall, the best models in each site used either IR45 or OR180 signals, or combination of these two. Linear model was also found to be generally more accurate in predicting SSC.

Table 6.11 Summary of SSC Measurement Range and Accuracy (for validation data sets only)

Site (Range)	Model Type		Maximum Error (Measure 1)		Maximum Error (95% confidence interval) (Measure 2)	
	Order	Signal(s) used	≤ 500mg/L (mg/L)	>500mg/L (%)	≤ 500mg/L (mg/L)	>500mg/L (%)
Little Kitten (0 – 500 mg/L)	2	IR45, OR180	91.6	1.2	142.0	10.8
Wildcat Bridge (0 – 4000 mg/L)	1	OR180	117.8	5.6	173.2	9.1
Upatoi North (0 – 35 mg/L)	1	OR180	6.6		13.8	
PineKnot North (0 – 30 mg/L)	1	IR45	-10.6		-15.2	
PineKnot South (0 – 90 mg/L)	1	OR180	8.5		29.5	
Anita Near (0 – 120 mg/L)	1	OR45	42.2		55.3	
Anita Far (0 – 700 mg/L)	1	IR45	201.0	-21.2	290.9	-46.2

6.2 SSC MEASUREMENT RANGE

As demonstrated at the Wildcat Bridge sensor, SSCs of higher than 4,000 mg/L was successfully measured using the sensor. The range of SSC measurement was mainly determined by the gain of the current-to-voltage converter in the signal-conditioning circuit of the sensor, which was adjustable and was selected during the sensor pre-calibration based on expected SSC range. A previous study has shown that 5,000 mg/L was not difficult to achieve (Figure 6.44).

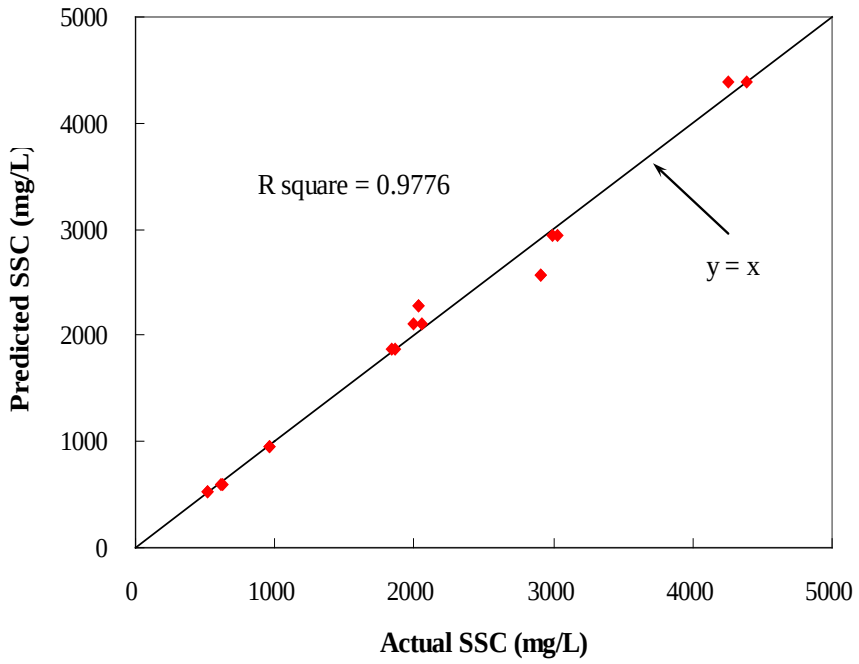

Figure 6.44 SSC measurement range (Zhang, 2009)

6.3 REPEATABILITY OF SSC MEASUREMENT

The stability of the sensor signals is of much importance to reliable SSC measurement. In this study, two randomly selected sets of multiple sensor signals, each taken within a small time span (10 minute) from each sensor site were used to analyze the repeatability. Because the sensors were programmed to take two measurements every minute, the number of sensor readings taken within this time period was about 20. Within this time span, the SSC was assumed to be constant.

The coefficient of variation for each set of signals was computed and is shown in Table 6.12. In general, it can be observed that the OR180 signal for all sensors gave the lowest coefficient of variation (CV), indicating a higher stability. The IR45 signals had low CV for almost all sites except for Wildcat Bridge, Upatoi North and Anita Far. On the other hand, the OR45 signals seemed to have the highest variability. This finding explains why in most cases, the best SSC prediction model was the one that used solely or in combination with the OR180 signal.

Table 6.12 Coefficient of variation of the three sensor signals from each sensor site.

Sites	*Sample 1*			*Sample 2*			*Average*		
	IR45	OR45	OR180	IR45	OR45	OR180	IR45	OR45	OR180
LK	0.05	0.08	0.01	0.02	0.07	0.01	0.04	0.07	0.01
WC	0.07	0.20	0.01	0.04	0.15	0.08	0.05	0.17	0.04
UpN	0.08	0.10	0.02	0.08	0.12	0.02	0.08	0.11	0.02
UpS	0.04	0.20	0.02	0.04	0.18	0.07	0.04	0.19	0.05
PkN	0.04	0.23	0.01	0.02	0.12	0.03	0.03	0.17	0.02
PkS	0.02	0.13	0.01	0.03	0.09	0.10	0.03	0.11	0.06
AnN	0.08	0.08	0.10	0.02	0.08	0.09	0.05	0.08	0.10
AnF	0.05	0.13	0.14	0.10	0.09	0.07	0.08	0.11	0.10
Average	0.05	0.14	0.04	0.04	0.11	0.06	0.05	0.13	0.05

The confidence interval calculated for the SSC predicted from the 20 signals was also calculated for each data set. The repeatability limit was calculated using the following equation:

$$r = t * \sqrt{2} * s_r$$

where: t = two-tailed student t value at 95% confidence level

s_r = standard deviation

r = repeatability limit

At 95% confidence level, the t-value for twenty measurements was 2.08.

Table 6.13shows the standard deviation, coefficient of variation, and repeatability limit (at 95% confidence level) of each measurement considered. The success criteria for repeatability limit were $\pm$ 5% or $\pm$25 mg/L, whichever is larger. The repeatability limits that did not pass the success criteria are colored red. From the table, it can be observed that larger repeatability limits were found at higher SSC readings.

Table 6.13 Repeatability limits for the SSC prediction models.

Site	*Model*	*Sample*	*Measured SSC (mg/L)*	*Sd (mg/L)*	*CV*	*Repeatability Limit*	
						(mg/L)	(%)
LK	OR180 model	1	183.6	14.6	0.08	43	
		2	94.5	6.5	0.07	19	
	IR45-OR180	1	184.6	14.4	0.08	42	
	2nd order	2	75.5	7.8	0.10	23	
WC	OR180 model	1	141.3	99	0.7	292	
		2	1835	80.4	0.04		12.9%
UpN	OR180 model	1	35	8.1	0.23	24	
		2	27.8	8.2	0.29	24	
	OR45-OR180	1	34.7	11.6	0.33	34	
	model	2	25.9	13.1	0.5	39	
PkN	IR45 model	1	8.8	4.0	0.46	12	
		2	25.3	4.4	0.17	13	
	IR45-OR45model	1	8	5.1	0.63	15	
		2	25.1	6.3	0.25	19	
PkS	OR180 model	1	29.6	6.5	0.22	19	
		2	30.2	6.8	0.23	20	
	IR45-OR180model	1	35.6	11	0.31	32	
		2	37.5	12.1	0.32	36	
AnN	All signals	1	55.4	14.6	0.26	43	
		2	37.4	11.9	0.32	35	

6.4 OPERABILITY OF ANTI-FOULING MECHANISMS AND CORRECTION ALGORITHM TO COMPENSATE DATA DETERIORATION DUE TO FOULING

Figure 6.45 shows the results of laboratory test of the air-blast system. The signals shown in this figure were measured during a 40-day period. Figure 6.46 gives a close-up view of the first four day's data. The effect of the air-blast system can be clearly observed from the sharp spikes on the IR45 and ORA180 signals. From Figure 6.45, it can also be seen that signal deterioration accelerated about 28 days after the experiment started, indicating that, the cleaning mechanism could only maintain the lenses clean for a limited period of time, beyond which the mechanism had only a limited effect on reducing lens fouling.

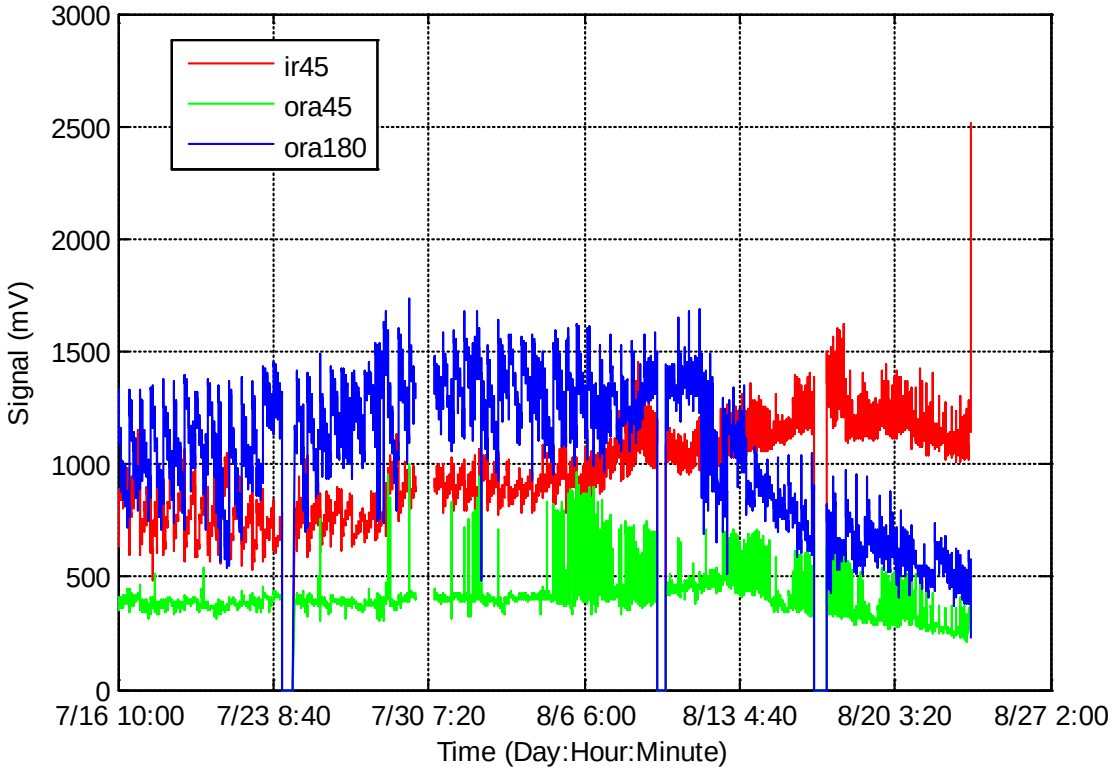

Figure 6.45 A 40-day laboratory test on air-blast cleaning.

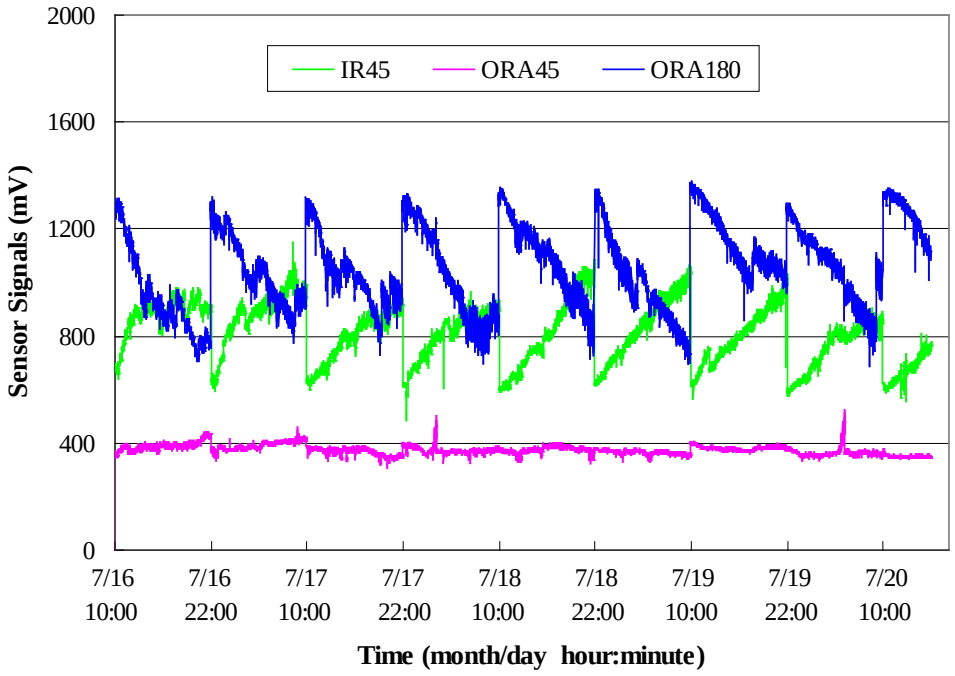

Figure 6.46 A close-up view of the first four days' data.

Figure 6.47 compares two sensors, one with air-blast cleaning and one without. Both sensors were left in stream water for 16 days. The effectiveness of the air-blast cleaning system can be easily observed.

Sensor with air-blast cleaning

Sensor without air-blast cleaning

(a)

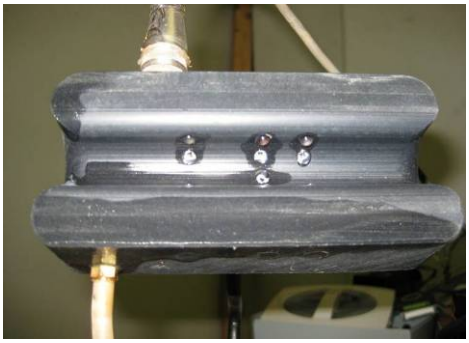

Sensor with air-blast cleaning

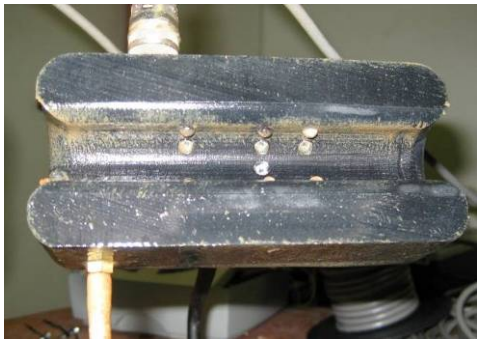

Sensor without air-blast cleaning

(b)

Figure 6.47 Photographs comparing sensors with and without air-blast cleaning after a 16-day cleaning experiment (November 26 ~ December 12, 2008): (a) side view; (b) bottom view.

Maintenance of the air blast system has been a challenge. The life span of the air compressor seemed to be within several months. The large electric power required to run the air compressor often caused system power down. In order to solve this problem, a relay circuit was added to the PCB board so that whenever the battery voltage dropped below a threshold, the air compressor was not allowed to kick off. This would give a higher priority to more critical components, such as the sensor and the signal transmission devices, when power was not sufficient. After the air compressor was installed, the air hose often detached from the compressor, especially during strong storms. Frequent maintenance was required to change the air compressor, to replace voltage regulators, and to replace plastic tubing. Usually after these repairs the air blast system still did not work as well as it did after the initial installation.

With the ability to keep the sensor lenses clean for a certain period of time, the air-blast system allowed longer intervals between manual cleanings. However, because the effectiveness of the system was limited, fouling would eventually find a way to deteriorate the signals, although the cleaning system helped reduce the rate of deterioration. To further reduce the effect of fouling on long-term SSC monitoring, a post-processing data correction algorithm was developed at the early stage of the project, and was further improved during the field demonstration. The

improved algorithm featured more universal signal restoration caused by fouling and clogging, faster computation, and the ability to handle long-term field data.

Figure 6.48 shows data collected during a six-month period (May 1 – October 31, 2011) from the Little Kitten sensor site. Figure 6.49 gives a close-up view of the first month's data (May, 1012). The raw ORA 180 signal was first filtered using a moving-average method. It was then corrected to remove the effects of fouling and clogging.

Several time blocks within this half-year period showed no raw data in the figure. This was due to problems related to failures in power supply, sensor, or communication within the LWSN tier. The significant signal drop during the first half of May was clearly due to fouling, because the sensor was not cleaned after its reinstallation in late April until May 17. The three steep increases in the signal that occurred on May 3, May 4, and May 14 were not due to lens cleaning. They probably were good examples of natural removal of clogging, which may have been leaves or other debris that were stacked in the sensor channel, hence blocking the light.

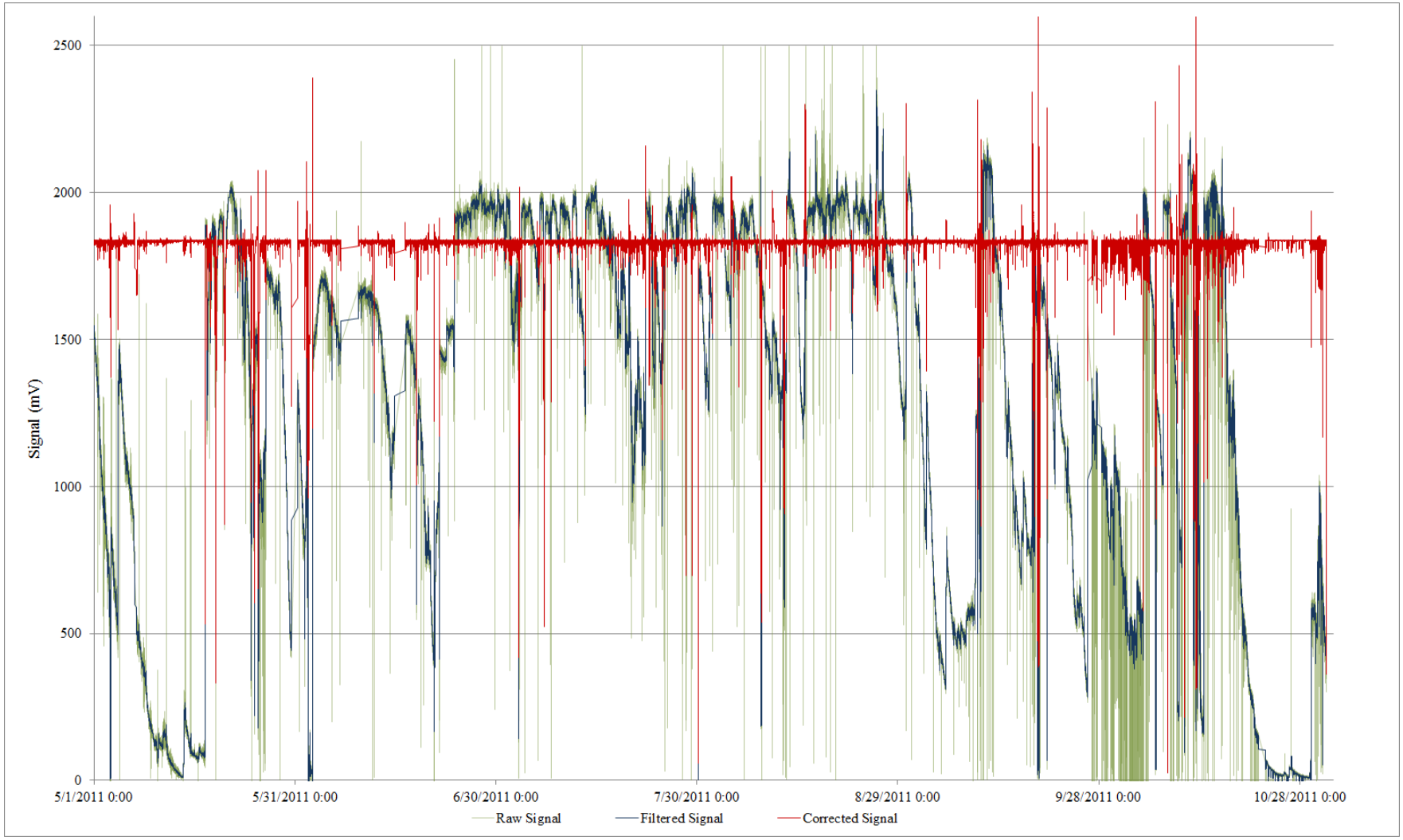

Figure 6.48 The ORA 180 signal collected for the sensor at the Little Kitten site during a six-month period – from May 1 to October 31 of 2011. The signal was first filtered and then corrected for fouling and clogging.

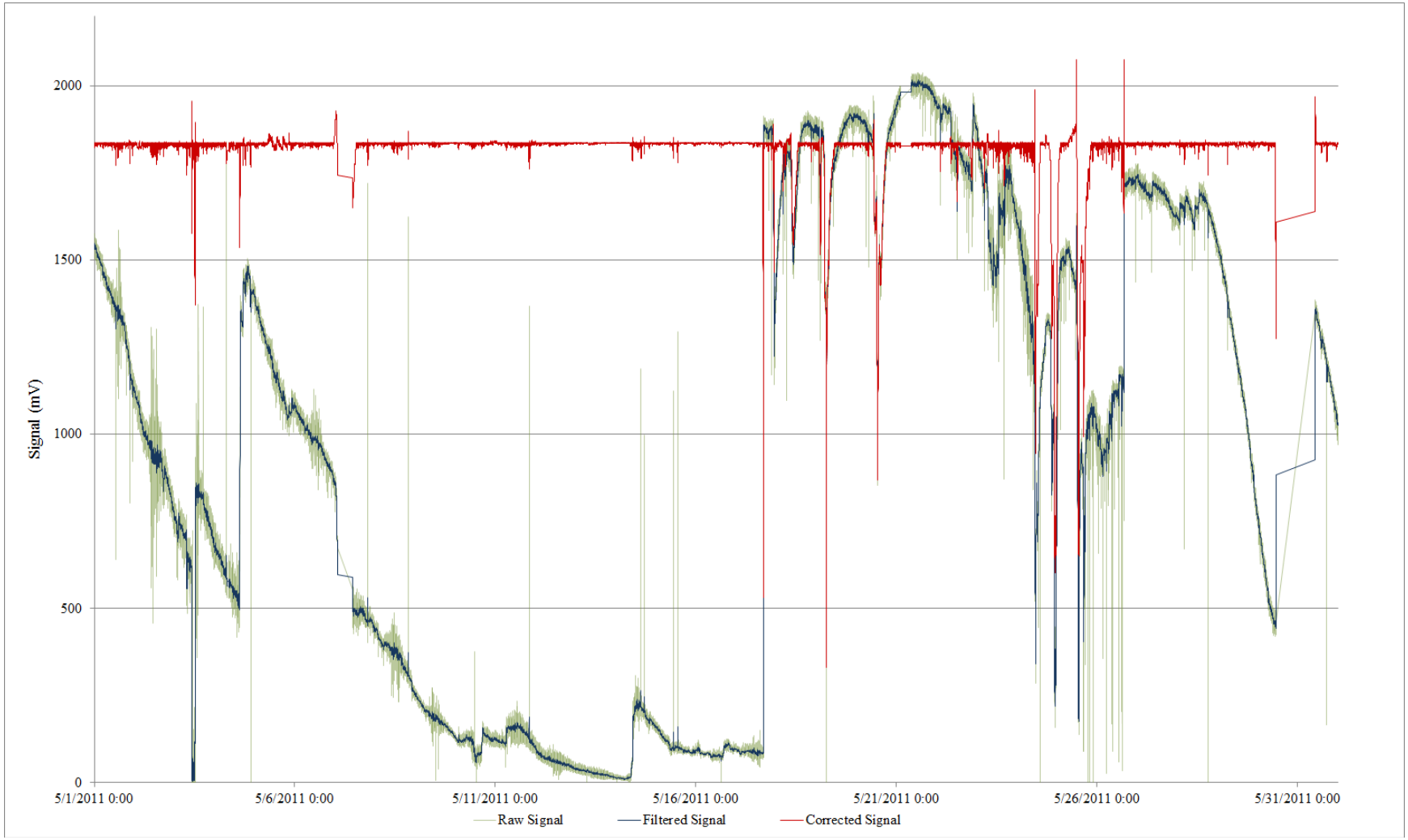

Figure 6.49 A close-up view of the first month's data (May, 2011)

The correction algorithm not only corrected the signals against fouling and clogging, it also calculated the SSC based on the corrected signals. Figure 6.50 shows the SSC calculated based on the fouling/clogging corrected ORA 180 signals for the six month period (May 1 – October 31, 2011). Grab samples taken and precipitation received within this period are also shown in the figure. Figure 6.51 is a close-up view of the first month's data (May, 2011).

The SSCs measured from the fouling/corrected ORA 180 signals are compared against the actual SSCs of the grab samples taken during this period of time in Table 6.14. Also shown in the table are measurement errors calculated in mg/L for SSCs below 500 mg/L or in percentage for SSCs higher than 500 mg/L.

Table 6.14 Comparison of SSC measured from the fouling/clogging corrected signals against the actual SSC for the grab samples collected in May, 2011, at the Little Kitten sensor site

Actual SSC (mg/L) (grab samples)	Measured SSC (mg/L) (from corrected ORA 180 signal)	Error (mg/L)	Error (%)
13.54	42.51	29.0	
17.32	41.82	24.5	
18.73	64.71	46.0	
23.59	14.01	-9.6	
28.80	22.18	-6.6	
33.85	0	-33.8	
34.75	0	-34.7	
36.75	17.98	-18.8	
136.24	219.82	83.6	
136.48	217.32	80.8	
143.07	215.51	72.4	
446.77	676.86	230.1	
471.08	705.58	234.5	
500.89	616.68		23.1
506.32	639.01		26.2
767.66	811.13		5.7
815.63	811.3		-0.5
Mean		53.6	13.6

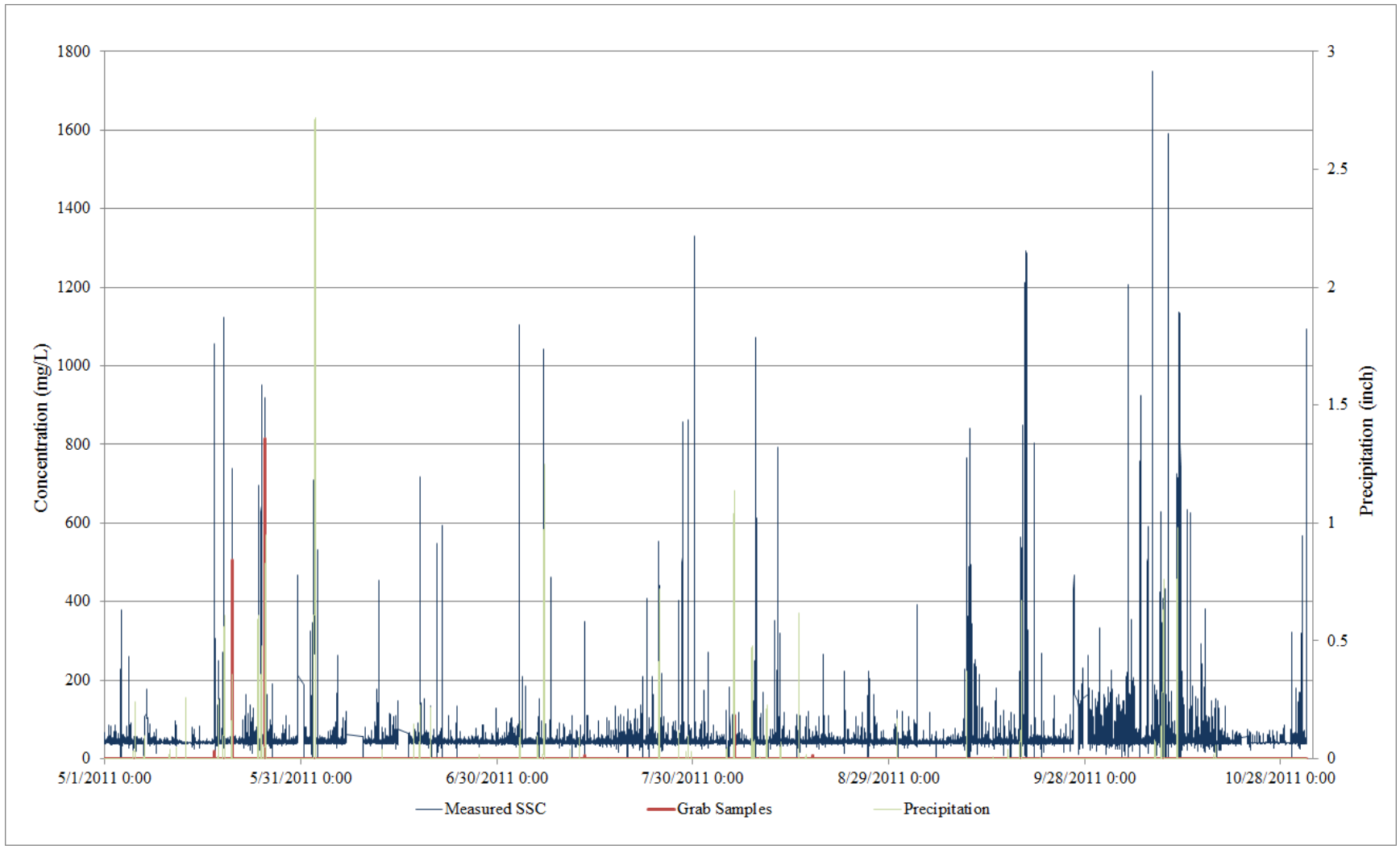

Figure 6.50 SSC measured using the clogging/fouling corrected ORA 180 signals during the May-October period at the Little Kitten site

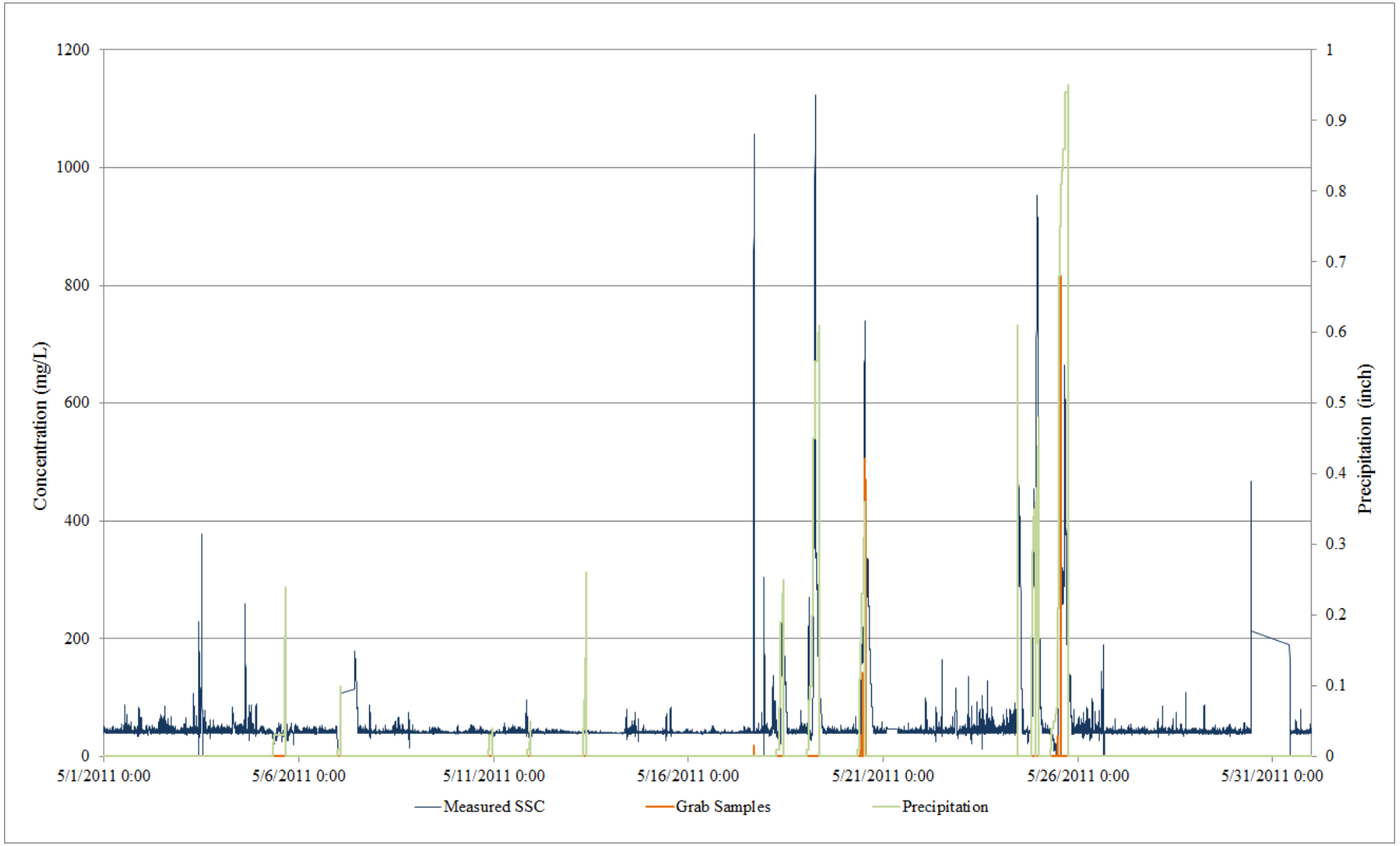

Figure 6.51 A close-up view of the SSC measurement shown in Figure 6.50 with only the first month's data (May, 2011) displayed.

6.5 ACCURACY IN FLOW VELOCITY MEASUREMENT

6.5.1 Field test of velocity sensor

This section reports the results of the field test described in Section 5.4.2. Velocities measured using the Flowtracker ultrasonic sensor and the fifth generation velocity sensor at the Little Kitten sensor site are plotted against each other in Figure 6.52. Each point on this graph represents a single test that yielded multiple velocity measurement readings from both sensors. The locations of the points on the graph indicate the average readings from the sensors. In addition, 95% confidence intervals for each measurement are shown in the form of error bars around each point. The horizontal error bars indicate the confidence intervals for the Flowtracker measurements, while the vertical the velocity sensor measurements. A linear relationship between the measurements across the entire velocity range tested, from about 0.25 m s-1 to about 1.66 m s-1, is apparent.

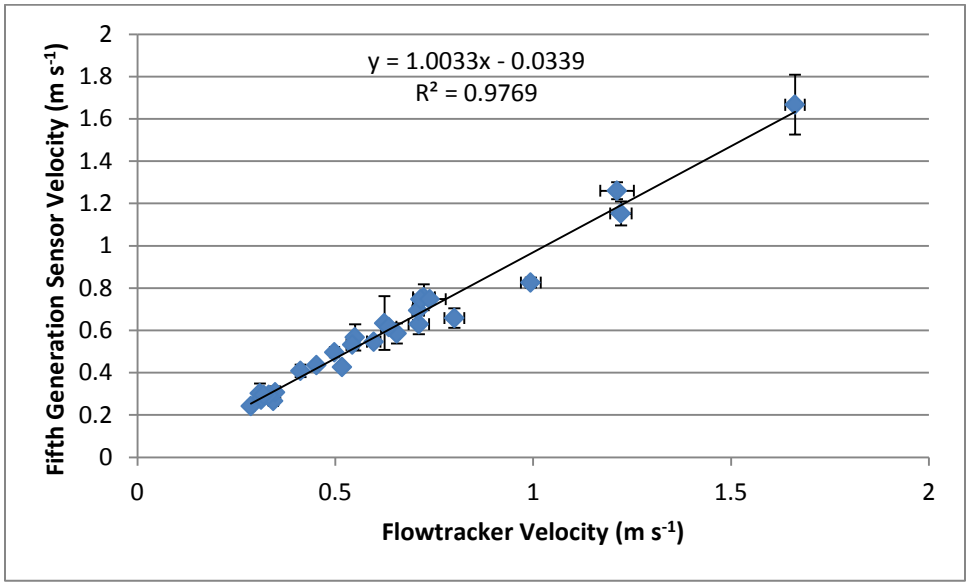

Figure 6.52 Comparison of Velocities Measured by the 5th Generation Sensor and the Flowtracker with 95% Confidence Intervals

Table 6.15 lists statistics of the field test data. The abbreviations in the table are explained below:

- S.D. – standard deviation
- C.L. – confidence limit
- t-value – student t-value
- Rep limit – repeatability limit
- U.L – upper limit of 95% confidence interval
- L.L. – lower limit of 95% confidence level

Table 6.15 Accuracy and repeatability of 5th generation velocity sensor

Run	Size	Mean	S.D.	C.L.	t-value	Rep. limit	U.L.	L.L.	%Error with Flowtracker Mean Velocity as Reference	
									U.L.	L.L.
1	11	1.15	0.084	0.056	2.20	0.261	1.21	1.10	-1.05	10.27
2	33	0.28	0.038	0.014	2.03	0.110	0.30	0.27	-4.68	13.44
3	21	0.61	0.076	0.035	2.08	0.224	0.65	0.58	-8.89	18.65
4	19	0.59	0.099	0.048	2.09	0.292	0.63	0.54	-3.51	18.01
5	48	0.55	0.062	0.018	2.01	0.175	0.56	0.53	-5.43	11.42
6	13	0.56	0.113	0.069	2.16	0.347	0.63	0.49	0.60	21.36
7	26	0.40	0.051	0.021	2.06	0.149	0.42	0.38	1.45	8.59
8	28	0.27	0.048	0.019	2.05	0.139	0.29	0.25	-16.88	27.75
9	25	0.30	0.039	0.016	2.06	0.113	0.31	0.28	-10.20	19.43
10	16	0.54	0.040	0.022	2.12	0.121	0.56	0.52	1.92	5.92
11	17	0.69	0.085	0.044	2.11	0.254	0.74	0.65	4.02	8.33
12	27	0.73	0.107	0.042	2.05	0.311	0.78	0.69	7.24	4.47
13	37	0.27	0.022	0.007	2.03	0.063	0.28	0.26	-10.92	15.56
14	42	0.27	0.029	0.009	2.02	0.083	0.28	0.26	-11.69	17.50
15	43	0.29	0.025	0.008	2.02	0.072	0.30	0.28	-9.91	14.58
16	44	0.24	0.017	0.005	2.02	0.048	0.25	0.24	-13.54	17.12
17	40	0.43	0.032	0.010	2.02	0.091	0.44	0.42	-15.69	19.62
18	24	0.62	0.031	0.013	2.06	0.009	0.63	0.60	-0.92	5.02
19	41	0.30	0.036	0.011	2.02	0.102	0.31	0.28	-3.68	10.77
20	73	0.53	0.037	0.009	1.99	0.105	0.54	0.52	-0.47	3.66
21	15	0.66	0.084	0.046	2.13	0.253	0.70	0.61	-12.04	23.65
22	52	0.75	0.047	0.013	2.01	0.133	0.76	0.73	6.35	-2.70
23	128	0.75	0.132	0.023	1.98	0.370	0.77	0.72	4.38	1.88
24	60	0.50	0.022	0.006	2.00	0.063	0.50	0.49	0.86	1.44
25	72	0.82	0.095	0.022	1.99	0.267	0.84	0.80	-15.08	19.55
26	51	0.44	0.028	0.008	2.01	0.078	0.44	0.43	-1.97	5.40
27	3	1.67	0.057	0.141	3.18	0.256	1.81	1.53	8.81	8.19
28	24	1.26	0.095	0.040	2.06	0.277	1.30	1.22	7.28	-0.66

With an assumption that the Flowtracker ultrasonic sensor measured the true velocities without any error, the 95% confidence interval for the 5th generation velocity sensor was found to be from ±1.44% to ±27.75% within the velocity range of 0.25- 1.66 m s^{-1}. On the other hand, if the 5th generation velocity sensor measured the true velocities without any error, the 95% confidence

intervals of the Flowtracker sensor varied from ±2.45% to ±33.17% within the same velocity range, indicating that the two sensors measured flow velocity at about the same accuracy.

This comparison also indicates that, since we did not have a more accurate instrument to provide a good reference to assess the accuracy of our sensor, we cannot provide a more solid conclusion about the measurement accuracy of the 5th generation sensor.

6.5.2 Predicting discharge using point velocity measurement

During this study, we placed an SSC/flow velocity sensor at a Pine Knot sensor site where the "USGS 02341725 Pine Knot Creek Near EelBeeck, GA" stage monitoring station was located. The purpose of this arrangement was to compare the velocity data with USGS stage and discharge data and to study the possibility of using the point velocity measurement provided by our sensor to either help simplify the discharge estimation procedure or to provide better discharge estimates.

6.5.2.1 USGS methods of Estimating Discharge

For many years the USGS has estimated stream discharge in rivers and streams across the United States mainly using two methods – the stage-discharge method and index velocity method (Olson and Norris 2007).

6.5.2.1.1 Stage-discharge method

The stage-discharge method used continuous stage measurement to estimate discharge using a site-specific, stage-discharge rating curve. Figure 6.53 shows such a curve for the Pine Knot site where both the USGS stream gaging station and our velocity sensor were located. To obtain this rating curve, discharge was measured using the "mid-section" method. This measurement needs to be repeated every six to eight months, because changes in the channel shape caused by events like erosion or land use changes would change this relationship (Olson and Norris 2007).

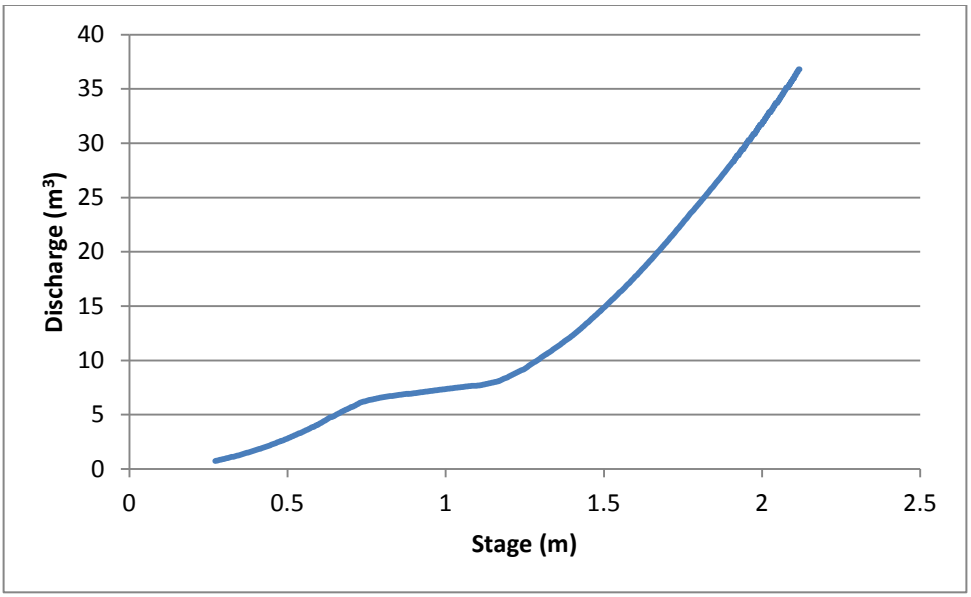

Figure 6.53 Stage-Discharge Rating Curve for USGS streamgage 02341725 on Pine Knot Creek in Fort Benning, Ga. (U. S. Geoligical Survey 2011)

6.5.2.1.2 Index-velocity method

The index-velocity method utilizes continuous records of both stage and an index velocity to estimate discharge. This method requires that two rating curves be developed. The first relates stage to area and the second relates the index velocity to the mean velocity of the water in the channel profile. The results of these ratings are mean velocity and cross sectional area which can be multiplied together to produce the discharge of the stream (Levesque and Oberg 2012).

6.5.2.2 Estimating discharge from point velocity and stage readings

In this study, since the sensor installed in Pine Knot Creek provided velocity measurement at a single fixed point, the index velocity method was used to estimate the discharge from the sensor's velocity measurement. The stage-area rating curve required for this method was developed using the USGS AreaComp program based on cross-section survey provided by USGS (Figure 6.54). The resulting stage-area curve is shown in Figure 6.55.

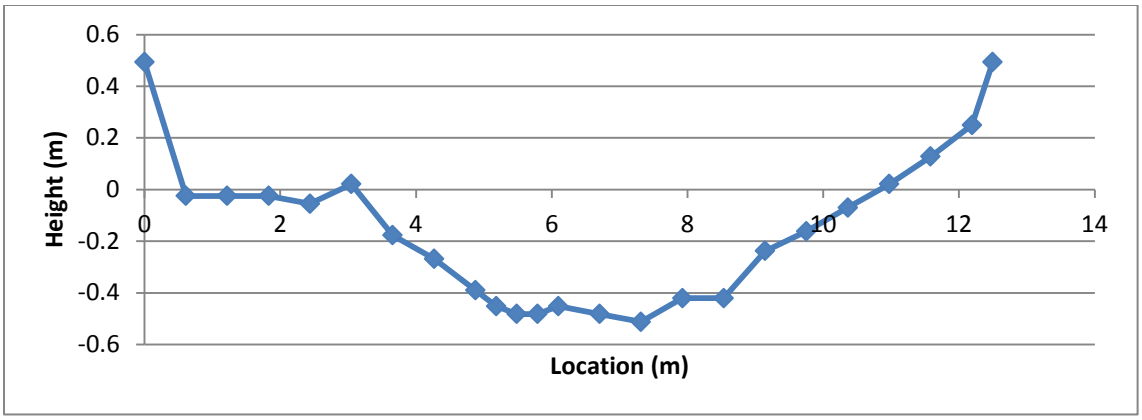

Figure 6.54 Cross Section of Pine Knot Creek at Sensor and Gaging Station Location used as the Standard Cross Section (U. S. Geological Survey 2012)

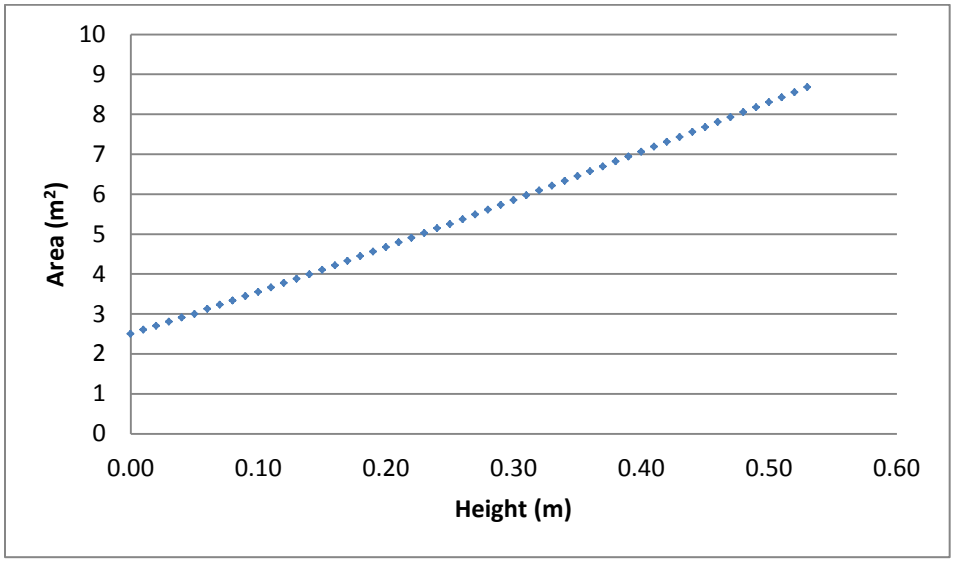

Figure 6.55 Stage-Area Rating for Pine Knot Creek

The next step in the index velocity method was creation of the index rating, which relates the index velocity to the mean velocity. Normally this is done by manually taking many separate discharge measurements using an acoustic Doppler current profiler (ADCP) or the mid-section method and comparing them to the index velocity. These discharge measurements need to cover the entire range and types of flows for the site. Unfortunately, at Pine Knot only three separate discharge measurements were made with the mid-section method while the index velocity sensor was operating. These did not cover the full range of flows and were insufficient to generate an index rating curve.

However, the USGS had previously measured discharges within a wide range of flows and created a stage-discharge curve for the station at the site. From this, they have been providing discharge estimates at the cross section every fifteen minutes. In a departure from the standard index velocity application, one half randomly selected USGS discharge estimates for the gage station were converted to mean velocities using corresponding stage measurements and the stage-area rating.

The velocity sensor installed in Pine Knot Creek took four velocity measurements each hour with each measurement separated by thirty seconds. All good measurements from a single hour were averaged together to produce the velocity estimate from the sensor for that hour. The hourly velocity measurements were further smoothed using a 24-hour moving average to produce the index velocity. A regression analysis provided a linear equation between the mean velocities and index velocities measured at the same time and, thus, the index rating curve (Figure 6.56).

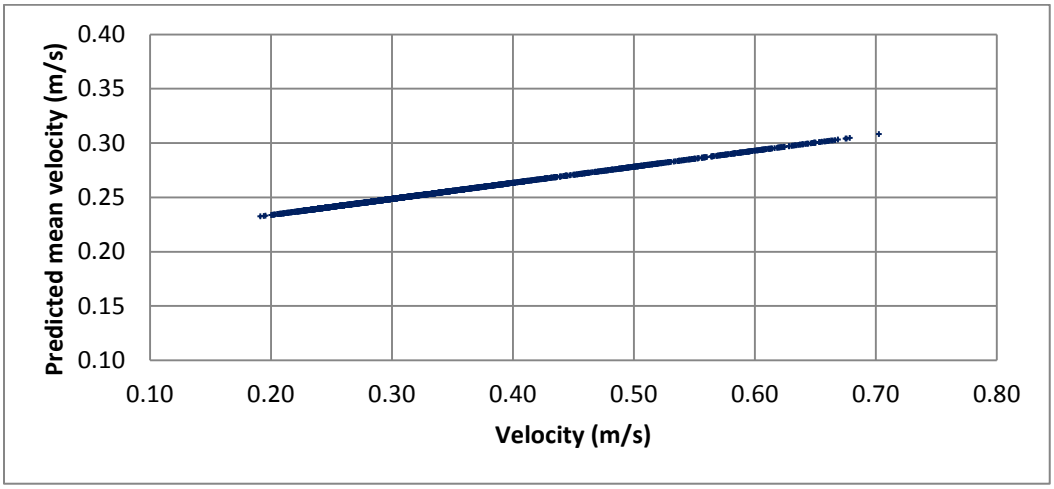

Figure 6.56 The index-rating curve that relates point velocity measurement to mean velocity for Pine Knot Creek

After both the stage-area and the index rating curves were created, the second half of the velocity and stage measurement data, which were not selected when creating the curves, were used to produce discharge estimates. First, the stages measured by the gage station were used with the stage-area rating to estimate areas. Next the mean velocities were determined by the index velocities measured by the sensor and the index rating curve. Multiplying the mean velocities and the areas resulted in the discharge estimates, which were used to compare with the USGS discharge estimates for validation. Figure 6.57 compares the estimated discharges against discharges reported by USGS.

A statistical analysis showed that, for the validation data set, the 95% confidence interval for the discharge estimate using the velocity sensor was $\pm 1.03 m^3/s$. It is clear that, for both the calibration and validation data sets, higher discharges (above $2 m^3/s$) were slightly underestimated.

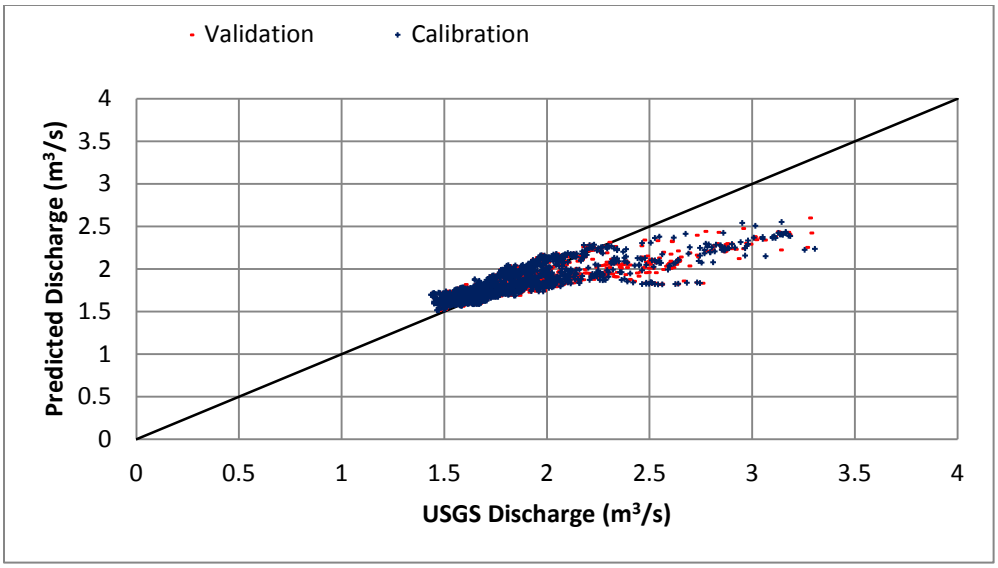

Figure 6.57 Estimating discharge from point velocity and stage measurement for Pine Knot Creek

This experiment demonstrated the possibility of using both stage and point velocity measurements to estimate discharge. Further experiments may help validate and further refine the method proposed in this report.

6.6 FLOW VELOCITY MEASUREMENT RANGE

As indicated in Section 6.5, the range of velocity tested in field was from 0.25 to 1.66 m s^{-1}. This was because we could not find a higher velocity at the sensor locations during the entire span of field test. We did, however, test the velocity sensor in a closed circulation system in laboratory to a much wider range - from 0.125 to 4.5 m s^{-1}. Figure 6.58 compares the measured velocities against true velocities. The mean percent error obtained on the validation data set was below 10% (Figure 6.59).

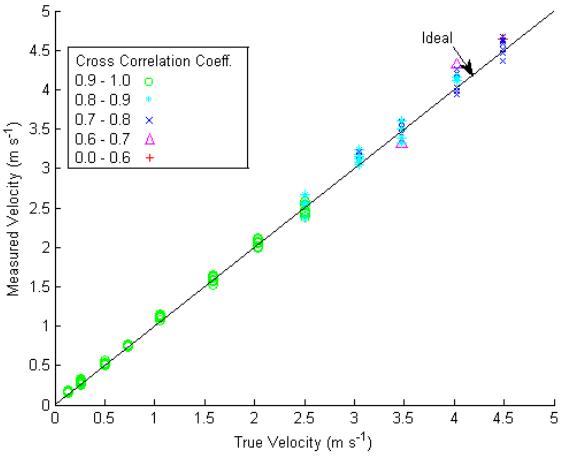

Figure 6.58 Measured against true velocities for the validation data set

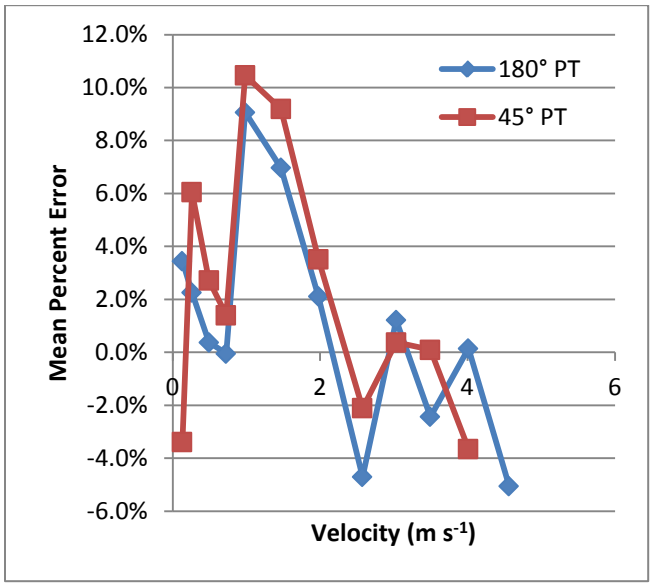

Figure 6.59 Mean Percent Error of Measurements in the Validation Data

6.7 REPEATABILITY OF FLOW VELOCITY MEASUREMENT

The method to assess the repeatability of the flow velocity measurement was the same as that described in Section 6.3. For the 5th generation velocity sensor, the 95% repeatability limit was found to be between 0.048 and 0.37 m/s, with a mean value of 0.173 m/s (Table 6.15).

6.8 RELIABILITY OF THE SSC/FLOW VELOCITY SENSOR

Working status of the major components of the three-tier WSN was recorded in an on-line logbook shared by the team. These components included sensors, sensor nodes, LWSNs, MRWNs, LRCNs, power supply units, memory cards, WebGIS, and database server. Issues that caused down times were also recorded. These records are summarized in Figures 1-12 in Appendix B.

Table 6.16 summarizes the data related to reliabilities, including the uptimes, downtimes, and PNOs, for all sensors. Issues that caused sensor down times included sensor and gateway power loses, PCB board damages, sensor cable damages, and sensor buried in streambed.

Table 6.16 Reliability of SSC sensor.

Sensors	*Demonstration period (Days)*	*Uptime (Days)*	*Downtime (Days)*	*PNO*
Little Kitten Creek	1005	909	96	90.4%
Wildcat Bridge	1005	941	64	93.6%
Wildcat Creek	700	591	109	84.4%
Silver Creek	486	372	114	76.5%
Upatoi North	974	910	64	93.4%

Upatoi South	974	910	64	93.4%
Pine Knot North	974	767	207	78.8%
Pine Knot South	974	767	207	78.8%
Gunpowder Near	275	237	38	86.2%
Gunpowder Far	275	208	67	75.6%
Anita Near	609	443	166	72.4%
Anita Far	884	645	239	73.0%

Table 6.17 summarizes the data related to reliabilities, including the uptimes, downtimes, and PNOs, for the velocity sensors. Issues that caused sensor down times included sensor power off, debris blocking the flow, disconnected dye hose, and empty dye bottles, as shown in Figure 6.60 and Figure 6.61.

Table 6.17 Reliability of flow velocity sensor

Sensors	Demonstration period (Days)	Uptime (Days)	Downtime (Days)	PNO
Little Kitten Creek	175	120	55	69.6%
Pine Knot South	310	257	124	82.9%

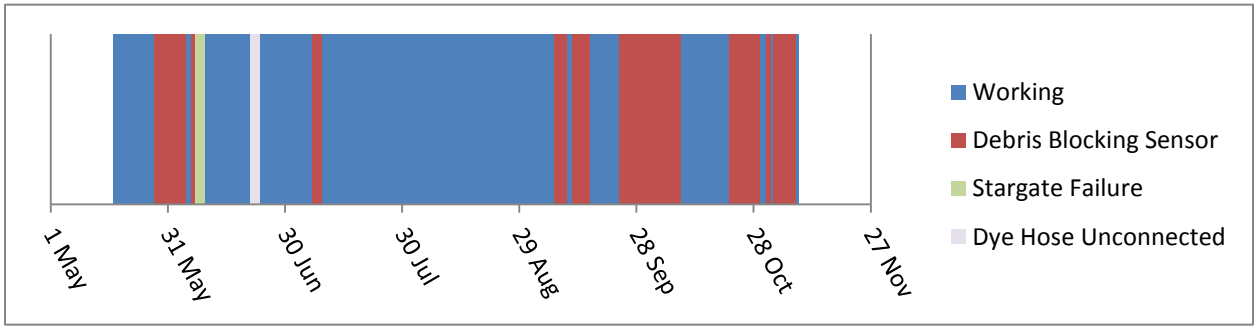

Figure 6.60 Velocity sensor working history – Little Kitten, Fort Riley

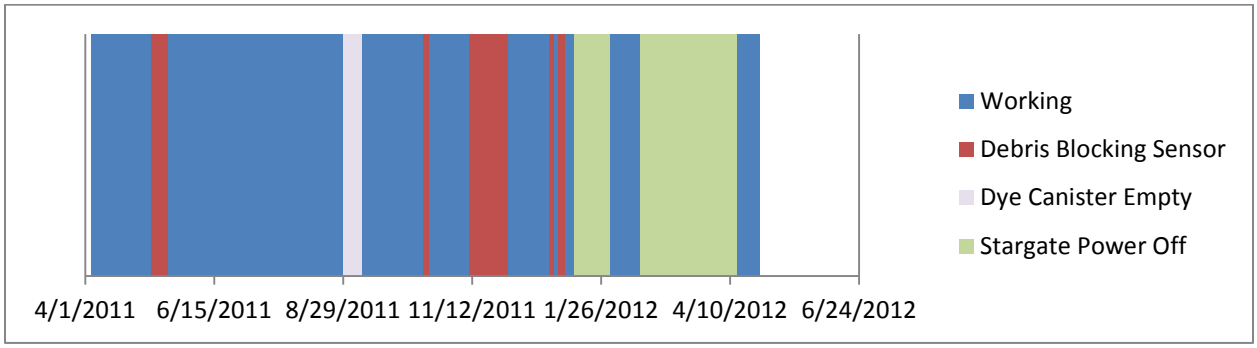

Figure 6.61 Velocity sensor working history – Pine Knot Creek, Fort Benning

6.9 RELIABILITY OF LOCAL WIRELESS SENSOR NETWORK (LWSN)

Table 6.18 summarizes the statistics related to reliabilities, including the uptimes, downtimes, and PNOs, for all LWSNs. Issues that caused LWSN down times included sensor and gateway power loss, unexpected Stargate reboot, gateway program updrade, Stargate damaged by ants, and Stargate replacement.

Table 6.18 Reliability of LWSN

Sensors	*Demonstration period (Days)*	*Uptime (Days)*	*Downtime (Days)*	*PNO*
Little Kitten Creek	1005	876	129	87.2%
Wildcat Bridge	1005	913	92	90.9%
Wildcat Creek	700	474	226	67.7%
Silver Creek	486	365	121	75.1%
Upatoi North	974	727	247	74.6%
Upatoi South	974	727	247	74.6%
Pine Knot North	974	536	438	55.0%
Pine Knot South	974	536	438	55.0%
Gunpowder Near	275	189	86	68.7%
Gunpowder Far	275	189	86	68.7%
Anita Near	609	438	171	71.9%
Anita Far	884	640	244	72.4%

6.10 DATA LOSS RATE OF LWSN

Calculation of the data loss rate for the LWSN tier was based on the data downloaded from the CF card and imported to the database server.

Issues related to data loss in the LWSN tier, as indicated by "n/a" in Table 6.19, included sensor uninstallation (for repair of recalibration), gateway station power loss, unexpected Stargate reboot, Stargate damage by ants, Stargate replacement, and CF card out of storage space (only for the Upatoi Creek site where a smaller (512 kB) CF card was used) .

As the sensor sampling rate for SSC measurement was two samples per minute, each sensor would generate 2,880 samples per day under normal operations. After the data in the CF card was imported to the database server, the number of samples stored in the CF card for each day (Q_i) was counted. Thus, the dataloss rate (*DLR*) for the LWSN within a month (with *N* days) can be calculated as

$$DLR = \frac{\sum_i^N Q_i}{2{,}880 \times N} \times 100\%$$

The average data loss rate of the LWSN during the entire demonstration period (

Table 6.20) can be calculated as

$$DLR_{avg} = \frac{\sum DLR}{Number\ of\ normal\ working\ months} \times 100\%$$

Table 6.19 LWSN data loss rate of 12 sensors during the demonstration period

	LittleKitten Cr.	Wildcat Br.	Wildcat Cr.	Silver Cr.	Upatoi N.	Upatoi S.	PineKnot N.	PineKnot S.	Gunpowder N.	Gunpowder F.	Anita N.	Anita F.
2009-09	n/a	0.10%	n/a	n/a								
2009-10	n/a	0.03%	n/a	n/a								
2009-11	n/a	0.07%	0.10%	0.07%								
2009-12	0.66%	0.03%	0.03%	0.14%								
2010-01	0.69%	0.03%	0.10%	n/a	n/a	n/a	0.14%	0.24%				
2010-02	1.71%	0.07%	0.14%	0.10%	n/a	n/a	n/a	n/a				
2010-03	0.66%	0.14%	0.14%	0.14%	n/a	n/a	n/a	n/a				
2010-04	0.17%	0.03%	0.17%	0.17%	0.24%	0.14%	0.28%	0.31%	0.69%	0.66%	0.07%	0.10%
2010-05	0.69%	0.07%	0.14%	0.10%	0.10%	0.03%	n/a	n/a	0.17%	0.17%	0.03%	0.14%
2010-06	0.35%	0.03%	0.07%	0.14%	0.03%	0.03%	n/a	n/a	0.24%	0.24%	0.07%	0.17%
2010-07	0.69%	0.14%	0.17%	0.24%	0.03%	0.03%	0.03%	0.07%	0.14%	0.14%	0.03%	0.07%
2010-08	0.69%	0.03%	0.14%	0.03%	0.07%	0.07%	0.03%	0.07%	0.35%	0.38%	0.07%	0.21%
2010-09	0.17%	0.03%	0.10%	0.10%	0.03%	0.03%	0.03%	0.03%	0.49%	0.45%	0.14%	0.28%
2010-10	0.34%	0.03%	0.07%	0.07%	0.07%	0.07%	0.10%	0.10%	0.17%	0.14%	0.14%	0.10%
2010-11	0.24%	0.03%	0.03%	0.14%	0.03%	0.03%	0.14%	0.14%	0.14%	n/a	0.07%	0.07%
2010-12	0.69%	0.03%	0.14%	0.03%	0.03%	0.03%	0.17%	0.17%	0.17%	0.42%	0.17%	0.17%
2011-01	0.17%	0.03%	0.17%	0.10%	0.07%	0.07%	0.14%	0.14%	n/a	n/a	n/a	n/a
2011-02	0.34%	0.03%	0.10%	0.07%	0.03%	0.03%	0.03%	0.03%	n/a	n/a	n/a	n/a
2011-03	0.34%	0.03%	n/a	0.03%	0.03%	0.03%	0.10%	0.10%	n/a	n/a	n/a	n/a
2011-04	n/a	n/a	n/a	n/a	0.03%	0.03%	0.03%	0.03%	n/a	n/a	0.17%	0.03%
2011-05	1.71%	0.03%	0.01%	n/a	0.03%	0.03%	0.03%	0.03%	n/a	n/a	n/a	n/a
2011-06	0.69%	0.07%	0.14%	n/a	0.03%	0.07%	0.03%	0.03%	n/a	n/a	0.03%	0.03%
2011-07	0.69%	0.03%	n/a	n/a	0.03%	0.03%	0.03%	0.03%	n/a	n/a	0.03%	0.03%
2011-08	0.34%	0.14%	n/a	n/a	0.03%	0.03%	0.03%	0.03%	n/a	n/a	n/a	0.03%
2011-09	0.34%	0.07%	0.14%	n/a	0.03%	0.03%	0.03%	0.03%	n/a	n/a	0.03%	0.03%
2011-10	0.34%	0.03%	0.10%	n/a	0.03%	0.03%	0.03%	0.03%	n/a	n/a	0.03%	0.03%
2011-11	0.03%	0.03%	n/a	n/a	n/a	n/a	0.03%	0.03%	n/a	n/a	0.03%	0.03%
2011-12	0.03%	0.03%	n/a	n/a	0.03%	0.03%	0.03%	0.03%	n/a	n/a	0.03%	n/a
2012-01	0.03%	0.03%	n/a	n/a	0.07%	0.07%	0.07%	0.07%	n/a	n/a	0.03%	n/a
2012-02	0.03%	0.03%	n/a	n/a	n/a	n/a	0.03%	0.03%	n/a	n/a	0.03%	n/a
2012-03	0.03%	0.03%	n/a	n/a	n/a	n/a	n/a	n/a	n/a	n/a	0.03%	n/a
2012-04	0.17%	0.03%	n/a	n/a	0.03%	0.03%	0.03%	0.03%	n/a	n/a	0.03%	n/a
2012-05	0.34%	0.07%	n/a	n/a	0.03%	0.03%	0.07%	0.07%	n/a	n/a	0.03%	n/a
2012-06	0.17%	0.03%	n/a	n/a	0.03%	0.03%	0.03%	0.03%	n/a	n/a	0.03%	n/a
2012-07	n/a	0.03%	n/a	n/a	0.07%	0.07%	0.03%	0.03%	n/a	n/a	0.03%	n/a
2012-08	n/a	0.03%	n/a	n/a	0.03%	0.03%	0.03%	0.03%	n/a	n/a	0.03%	n/a
Average	0.45%	0.05%	0.11%	0.10%	0.05%	0.04%	0.06%	0.07%	0.28%	0.33%	0.06%	0.10%

Table 6.20 Data loss rate of LWSN

Data loss rate of LWSN			
Ft. Riley site (2009 Sep. - 2012 Aug.)			
Little Kitten Creek	Wildcat Bridge	Wildcat Creek	Silver Creek
0.45%	0.05%	0.11%	0.10%
Ft. Benning site (2010 Jan. - 2012 Aug.)			
Upatoi North	Upatoi South	Pine Knot North	Pine Knot South
0.05%	0.04%	0.06%	0.07%
APG site (2010 Apr. - 2012 Aug.)			
Gunpowder Near	Gunpowder Far	Anita Near	Anita Far
0.28%	0.33%	0.06%	0.10%

6.11 RELIABILITY OF MID-RANGE WIRELESS NETWORK (MRWN)

Table 6.21 summarizes the statistics related to reliabilities, including the uptimes, downtimes, and PNOs, for all MRWNs. Issues that caused MRWN down times included unexpected datalogger reboot, repeater station power loss, central station power loss, antenna problems, and errors in the datalogger program.

Table 6.21 Reliability of MRWN

Sensors	*Demonstration period (Days)*	*Uptime (Days)*	*Downtime (Days)*	*PNO*
Little Kitten	1005	991	14	98.6%
Wildcat Bridge	1005	980	25	97.5%
Wildcat Creek	700	694	6	99.1%
Silver Creek	486	482	4	99.2%
Upatoi North	974	888	86	91.2%
Upatoi South	974	888	86	91.2%
Pine Knot North	974	888	86	91.2%
Pine Knot South	974	888	86	91.2%
Gunpowder Near	275	178	97	64.7%
Gunpowder Far	275	178	97	64.7%
Anita Near	609	578	31	94.9%
Anita Far	884	853	31	96.5%

6.12 DATA LOSS RATE OF MRWN

Since a data storage device (e.g. CF cards) was not installed in the MRWN tier, we cannot distinguish the data losses between the MRWN and LRCN tiers. The data loss rate calculation for the MRWN and LRCN tiers was based on records of the data received by the database server.

Issues that caused data loss within the MRWN and LRCN tiers, as indicated by "n/a" in Table 6.22, included unexpected reboot of the datalogger at the gateway station, errors in the datalogger program, repeater station power loss, central station power loss, changes in antenna orientation, and cellular service interruption.

As the SSC sensors were programmed to take two samples per minute, each sensor should generate 2,880 samples per day. When the MRWN and LRCN tiers were working normally, data that was wirelessly transmitted from the gateway stations to the database server each day (Q_i) was counted. The discrepancy between 2,880 and Q_i was the total number of data lost within the day. However, a part of the data loss was attributed to the LRCN. Removing this part of data loss from the total data loss gave the data loss that occurred within the MRWN and LRCN tiers:

$$DLR = \frac{\sum_i^N Q_i}{\sum_i^N 2{,}880 \times (1 - DLR_{i,LWSN})} \times 100\%$$

Hence, the average data loss rate of MRWN and LRCN during the demonstration period (Table 6.23) can be calculated as

$$DLR_{avg} = \frac{\sum DLR}{Number\ of\ normal\ working\ months} \times 100\%$$

Table 6.22 MRWN and LRCN data loss rate of 12 sensors during demonstration period

	LittleKitten Cr.	Wildcat Br.	Wildcat Cr.	Silver Cr.	Upatoi N.	Upatoi S.	PineKnot N.	PineKnot S.	Gunpowder N.	Gunpowder F.	Anita N.	Anita F.
2009-09	n/a	3.91%	n/a	n/a								
2009-10	n/a	0.97%	n/a	n/a								
2009-11	n/a	2.43%	3.56%	3.45%								
2009-12	5.10%	1.45%	3.19%	3.60%								
2010-01	3.92%	1.32%	3.87%	n/a	n/a	n/a	2.24%	1.82%				
2010-02	3.98%	2.75%	4.78%	4.65%	n/a	n/a	n/a	n/a				
2010-03	11.01%	4.76%	4.90%	4.86%	n/a	n/a	n/a	n/a				
2010-04	7.60%	1.25%	4.98%	4.77%	7.04%	0.91%	9.75%	8.24%	9.75%	9.70%	2.24%	3.01%
2010-05	4.93%	12.47%	45.50%	45.60%	5.00%	0.15%	n/a	n/a	2.30%	4.65%	1.76%	3.80%
2010-06	1.70%	2.65%	70.21%	70.10%	1.97%	0.21%	n/a	n/a	4.73%	6.25%	2.95%	5.30%
2010-07	1.84%	2.43%	25.24%	35.21%	0.96%	0.25%	0.94%	1.95%	3.45%	5.12%	1.71%	2.23%
2010-08	6.37%	18.60%	22.37%	22.14%	2.20%	0.95%	1.24%	2.23%	13.76%	13.65%	3.60%	6.67%
2010-09	5.80%	4.65%	7.25%	7.71%	0.54%	0.24%	1.74%	1.76%	15.80%	16.10%	7.13%	8.01%
2010-10	6.59%	3.12%	6.24%	5.95%	1.21%	1.19%	n/a	n/a	3.05%	4.57%	7.17%	6.99%
2010-11	7.35%	2.28%	5.65%	5.66%	0.74%	0.73%	n/a	n/a	9.38%	n/a	2.11%	2.36%
2010-12	7.68%	2.02%	5.25%	5.30%	n/a	n/a	n/a	n/a	9.43%	10.56%	6.33%	6.59%
2011-01	3.99%	0.36%	3.75%	3.35%	n/a	n/a	n/a	n/a	n/a	n/a	n/a	n/a
2011-02	0.70%	0.63%	0.67%	0.69%	n/a	n/a	n/a	n/a	n/a	n/a	n/a	n/a
2011-03	0.36%	0.61%	n/a	0.83%	n/a	n/a	n/a	n/a	n/a	n/a	n/a	n/a
2011-04	n/a	n/a	n/a	n/a	1.89%	0.19%	0.40%	0.14%	n/a	n/a	5.90%	1.81%
2011-05	1.27%	1.29%	1.72%	n/a	1.55%	0.83%	1.42%	0.87%	n/a	n/a	n/a	n/a
2011-06	1.94%	3.86%	1.27%	n/a	1.27%	1.17%	0.77%	1.31%	n/a	n/a	0.02%	0.01%
2011-07	3.82%	4.86%	n/a	n/a	1.56%	0.50%	0.73%	1.16%	n/a	n/a	0.01%	0.01%
2011-08	3.30%	15.66%	n/a	n/a	0.82%	0.79%	0.47%	1.12%	n/a	n/a	n/a	0.01%
2011-09	3.08%	5.21%	5.07%	n/a	0.74%	0.73%	0.19%	0.77%	n/a	n/a	0.81%	0.78%
2011-10	2.33%	5.35%	4.86%	n/a	0.68%	0.70%	0.18%	0.82%	n/a	n/a	0.53%	0.16%
2011-11	0.71%	2.01%	n/a	n/a	n/a	n/a	0.58%	0.09%	n/a	n/a	0.19%	0.14%
2011-12	0.11%	0.34%	n/a	n/a	0.53%	0.50%	0.69%	0.54%	n/a	n/a	0.02%	n/a
2012-01	0.65%	1.03%	n/a	n/a	3.43%	2.44%	2.48%	2.30%	n/a	n/a	0.19%	n/a
2012-02	0.34%	0.79%	n/a	n/a	n/a	n/a	0.49%	0.02%	n/a	n/a	0.10%	n/a
2012-03	1.40%	1.46%	n/a	n/a	n/a	n/a	n/a	n/a	n/a	n/a	0.21%	n/a
2012-04	1.22%	2.58%	n/a	n/a	2.06%	1.13%	1.51%	1.53%	n/a	n/a	0.04%	n/a
2012-05	1.10%	2.70%	n/a	n/a	2.36%	2.89%	2.59%	2.15%	n/a	n/a	0.01%	n/a
2012-06	2.66%	4.97%	n/a	n/a	0.85%	0.83%	0.78%	0.27%	n/a	n/a	0.23%	n/a
2012-07	n/a	1.41%	n/a	n/a	n/a	n/a	0.74%	0.20%	n/a	n/a	0.62%	n/a
2012-08	n/a	2.96%	n/a	n/a	n/a	n/a	0.93%	0.42%	n/a	n/a	0.56%	n/a
Average	3.43%	3.58%	11.52%	13.99%	1.87%	0.87%	1.47%	1.41%	7.96%	8.83%	1.85%	2.99%

Table 6.23 Data loss rate of MRWN and LRCN

Data loss rate of MRWN & LRCN			
Ft. Riley site (2009 Sep. - 2012 Aug.)			
Little Kitten Creek	Wildcat Bridge	Wildcat Creek	Silver Creek
3.43%	3.58%	11.52%	13.99%
Ft. Benning site (2010 Jan. - 2012 Aug.)			
Upatoi North	Upatoi South	Pine Knot North	Pine Knot South
1.87%	0.87%	1.47%	1.41%
APG site (2010 Apr. - 2012 Aug.)			
Gunpowder Near	Gunpowder Far	Anita Near	Anita Far
7.96%	8.83%	1.85%	2.99%

6.13 RELIABILITY OF LONG-RANGE WIRELESS NETWORK (LRCN)

Table 6.24 summarizes the statistics related to reliabilities, including the uptimes, downtimes, and PNOs, for all LRCNs. Issues that caused LRCN down times included central station power loss and cellular service interruptions.

Table 6.24 Reliability of LRCN

Sensors	*Demonstration period (Days)*	*Uptime (Days)*	*Downtime (Days)*	*PNO*
Little Kitten Creek	1005	981	24	97.6%
Wildcat Bridge	1005	981	24	97.6%
Wildcat Creek	700	687	13	98.1%
Silver Creek	486	478	8	98.4%
Upatoi North	974	687	287	70.5%
Upatoi South	974	687	287	70.5%
Pine Knot North	974	687	287	70.5%
Pine Knot South	974	687	287	70.5%
Gunpowder Near	275	255	20	92.7%
Gunpowder Far	275	255	20	92.7%
Anita Near	609	578	31	94.9%
Anita Far	884	853	31	96.5%

6.14 DATA LOSS RATE OF LRCN

As discussed in Section 6.12, because no data storage devices (e.g. CF cards) were installed in the MRWN tier, we cannot distinguish the data losses between the MRWN and LRCN tiers. Both Table 6.22 and Table 6.23 reflected overall data loss occurring in these two tiers.

6.15 RELIABILITY OF INTERNET SERVER

Table 6.25 summarizes the statistics related to the reliability, including the uptime, downtime, (Percentage of Normal Operation (PNO), and Number of Failures (NOF), for the Internet server. The only issue that caused the Internet serve down time was server reboot due to system update.

Table 6.25 Reliability of Internet server

Demonstration period (Days)	*Uptime (Days)*	*Downtime (Days)*	*PNO*	*NOF*	*MTBF (Days)*
1005	996	9	98.1%	9	111

6.16 RELIABILITY OF WEB GIS

Table 6.26 summarizes the statistics related to the reliability, including the uptime, downtime, PNO, and NOF, for the Web-based GIS. The issues that caused the Web-based GIS down time were server reboot and network communication interruptions.

Table 6.26 Reliability of Web GIS

Demonstration period (Days)	*Uptime (Days)*	*Downtime (Days)*	*PNO*	*NOF*	*MTBF (Days)*
1005	993	12	98.8%	12	83

6.17 RELIABILITY OF SOLAR PANEL AND CHARGING CIRCUIT

Table 6.27 summarizes the statistics related to reliabilities, including the uptime, downtime, PNO, and NOF, for the solar panels and their related charging circuits used at all the sensor sites, gateway stations, repeater stations, and central stations within the three-tier WSN. The issues that caused the power down included broken power cable, snow on solar panels, regulator failure, power overload (e.g. excessive current drawn by the air compressors), short circuit in the PCB board, and water entering the battery case.

Table 6.27 Reliability of solar panel and charging circuit

Location of solar panel and charging circuit	*Demonstration period (Days)*	*Uptime (Days)*	*Downtime (Days)*	*PNO*
Sensor node and gateway station at Little Kitten Creek	1005	969	36	96.4%
Repeater station at Cico Tank	1005	998	7	99.3%
Sensor node and gateway station at Wildcat Bridge	1005	966	39	96.1%
Sensor node and gateway station at Wildcat and Silver Creek	700	643	57	91.9%
Repeater station at Above Keats	1005	982	23	97.7%
Central station at Colbert Hill	1005	994	11	98.9%
Sensor nodes at Upatoi	974	921	53	94.6%
Gateway station at Upatoi	974	921	53	94.6%
Sensor nodes at Pine Knot	974	879	95	90.3%

Gateway station at Pine Knot	974	885	89	90.9%
Repeater station on Buena Vista Rd.	974	974	0	100.00%
Central station on Buena Vista Rd.	974	920	54	94.5%
Sensor nodes at Gunpowder	275	244	31	88.7%
Gateway station at Gunpowder	275	240	35	87.3%
Sensor nodes, gateway and central station at Anita	609	451	158	74.1%

6.18 RELIABILITY OF ALTERNATIVE 1 FOR WSN - METEOR-BURST COMMUNICATION (MBC) SYSTEM

The MBC system was demonstrated from Feb. 15 to Aug. 31 in 2012. Table 6.28 summarizes the statistics related to the reliability, including the uptime, downtime, and PNO, for the MBC system. The issues that caused the downtime included MBC service interruption (Apr. 3 – Apr. 4, 2012) and MBC central station power lost (Aug. 1 – Aug.10, 2012) (Figure 6.62).

Table 6.28 Reliability of MBC system

Demonstration period (Days)	*Uptime (Days)*	*Downtime (Days)*	*PNO*
199	187	12	94.0%

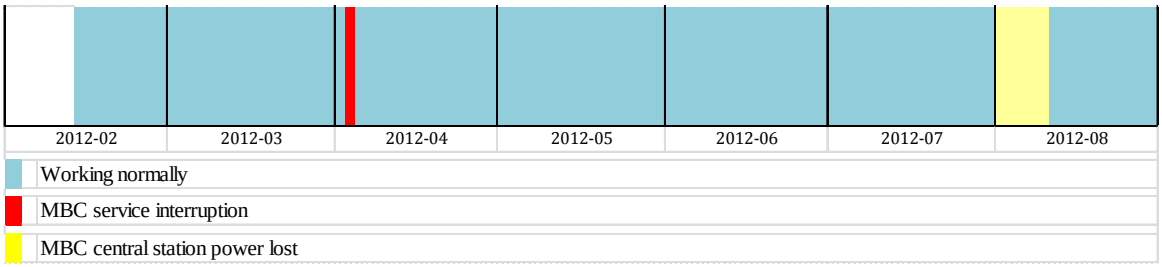

Figure 6.62 MBC system working history

6.19 DATA LOSS RATE OF MBC

As the sensor sampling rate was two samples per minute, each sensor should generate 2,880 samples per day. However, the MBC radio can send only one sample data every five minutes. Thus, the number of samples received in the database from the MBC server should be 288 each day. When the MBC system was working normally, the number of samples received in the database (Q_i) was counted. The discrepancy between 288 and Q_i was the total number of data

lost within the day. Since a part of the data loss was attributed to the LRCN, this part of data loss should be removed from the total data loss:

$$DLR = \frac{\sum_i^N Q_i}{\sum_i^N 288 \times (1 - DLR_{i,LWSN})} \times 100\%$$

Thus, the average data loss rate of MBC system during the entire demonstration period (Table 6.29) can be calculated as

$$DLR_{avg} = \frac{\sum DLR}{Number\ of\ normal\ working\ months} \times 100\%$$

Table 6.29 Data loss rate of MBC

Item	*Month*							*Average*
	Feb.	Mar.	Apr.	May	Jun.	Jul.	Aug.	
Data loss rate	0.69%	0.69%	0.69%	1.39%	1.39%	2.08%	0.69%	1.1%

6.20 RELIABILITY OF ALTERNATIVE 2 FOR WSN – DATALOGGER

Since we did not actually test this alternative during demonstration, we used the records of our previous experiments at Fort Riley and Fort Benning to provide the results. Our records showed that the datalogger never had a downtime, thus, the reliability was 100%

6.21 DATA LOSS RATE OF DATALOGGER

For the same reason as described in Section 6.20, we used our records from previous experiments. The data loss rate was 0%.

6.22 DEGRADATION OF SENSOR HOUSING

Figure 6.63 compares a new sensor with two sensors that have been deployed in natural water for two years. It can be seen that the brackish water at APG only created a thin layer of salt on the surface of the housing, whereas the stream water at Fort Riley developed a significant amount of deposit on the surface. The functionality of the sensors, however, was not affected.

(a)

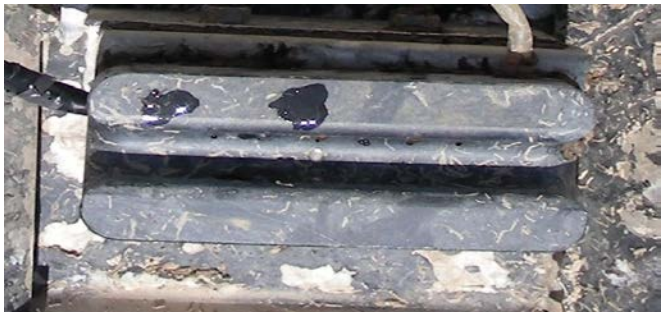

(b)

(c)

Figure 6.63 Sensor housing degradation: (a) before deployment, (b) after two years of deployment at the APG site, (c) after two years of deployment at the Fort Benning site

6.23 RELIABILITY OF DATA DELIVERY TO MEMORY CARDS

Table 6.30 summarizes the statistics related to reliabilities of data delivery to memory cards, including the uptimes, downtimes, PNO, and NOFs for all sensors. The maximum durations of the events all occurred for the Fort Benning sites. This was due to the late maintenance trip we took, considering the cost related to the trips.

Table 6.30 Reliability of data delivery to memory cards

Sensors	*Demonstration period (Days)*	*Uptime (Days)*	*Downtime (Days)*	*PNO*	*No. of Events*	*Average Duration (Days)*	*Max Duration (Days)*
Little Kitten Creek	1005	967	38	96.2%	10	4	15
Wildcat Bridge	1005	959	46	95.4%	10	5	16
Wildcat Creek	700	649	51	92.7%	3	17	18
Silver Creek	486	429	57	88.3%	2	29	39
Upatoi North	974	829	145	85.1%	3	48	91
Upatoi South	974	829	145	85.1%	3	48	91
Pine Knot North	974	678	296	69.6%	5	59	90
Pine Knot South	974	678	296	69.6%	5	59	90
Gunpowder Near	275	220	55	80.0%	9	6	21
Gunpowder Far	275	190	85	69.1%	9	9	50
Anita Near	609	448	161	73.6%	11	15	91
Anita Far	884	650	234	73.5%	15	16	91

6.24 RELIABILITY OF DATA DELIVERY TO DATABASE SERVER

Table 6.31 summarizes the statistics related to reliabilities of data delivery to the database server, including the uptimes, downtimes, PNO, and NOFs for all sensors. Again, the maximum durations of the events all occurred for the Fort Benning sites. This was due to the late maintenance trip we took, considering the cost related to the trips.

Table 6.31 Reliability of data delivery to database server

Sensors	*Demonstration period (Days)*	*Uptime (Days)*	*Downtime (Days)*	*PNO*	*No. of Events*	*Average Duration (Days)*	*Max Duration (Days)*
Little Kitten Creek	1005	929	76	92.4%	36	2	15
Wildcat Bridge	1005	913	92	90.9%	37	2	16
Wildcat Creek	700	633	67	90.4%	12	6	18
Silver Creek	486	418	68	86.0%	8	9	39
Upatoi North	974	493	481	50.6%	13	37	141
Upatoi South	974	493	481	50.6%	13	37	141
Pine Knot North	974	449	525	46.1%	16	33	186
Pine Knot South	974	449	525	46.1%	16	33	186
Gunpowder Near	275	185	90	67.3%	17	5	21
Gunpowder Far	275	155	120	56.4%	15	8	50
Anita Near	609	417	192	68.5%	14	14	91
Anita Far	884	618	266	69.9%	19	14	91

6.25 EASY OF USE OF THE TECHNOLOGY

Table 6.32 lists the skill level and training required to troubleshoot and maintain the system and its components.

Table 6.32 Skill level required to troubleshoot and maintain the system

Maintenance type	*Skill level required*
Sensor field calibration	Engineering technician
Sensor node maintenance	Engineering technician
Power supply maintenance	Engineering technician
Cellular modem troubleshoot & repair	Engineering technician
Datalogger troubleshoot & repair	Engineering technician (training required)
Stargate troubleshoot & repair	Engineering technician (training required)
Datalogger program download	Engineering technician (training required)
Stargate program update and data download	Engineering technician (training required)
MBC radio maintenance and data download	Engineering technician (training required)
Sensor circuits maintenance	Bachelor of electrical engineering
Software maintenance	Bachelor of electrical or computer engineering
Database server maintenance	Bachelor of electrical or computer engineering
Web GIS server maintenance	Bachelor of electrical or computer engineering

6.26 SYSTEM MAINTENANCE REQUIREMENTS

Table 6.33 lists the mean time used for troubleshoot and repair the system and its components by an engineering technician.

Table 6.33 Maintenance time required for an engineering technician

Failure type	*Time required (Hour)*		*Total time required (Hour)*
	Troubleshoot	**Repair**	
Power lost	0.1	1.0	1.1
Sensor node damaged	0.5	6.0	6.5
Stargate damaged	0.5	0.5	1.0
Datalogger damaged	0.2	0.5	0.7
Cellular modem damaged	0.2	0.5	0.7
Cellular service halt	0.5	0.3	0.8
Database server halt	0.5	0.3	0.8
Web GIS server halt	0.5	0.3	0.8
Mote program error	0.5	1.0	1.5
Stargate program error	0.5	2.0	2.5
Datalogger program error	0.5	1.0	1.5
Database server program error	0.5	0.5	1.0

7 COST ASSESSMENT

7.1 COST MODEL

Costs related to the SSC sensor/WSN technology demonstration were fully tracked. The types of costs that were tracked included procurement (capital) costs, labor costs, cost of installation, and training, start-up costs, operational costs, maintenance costs, and costs for documentation and laboratory analytical service.

Table 7.1 Cost Model for SSC Sensor and WSN Technology

Cost Category	Data Tracked During Demonstration	
Sensor Procurement	Cost of sensor conceptual design, CAD design, fabrication, assembly, and individual components	
	Initial cost	$828
Sensor Calibration Stage 1	Cost for sensor calibration Stage 1 in laboratory	
	Calibration set-up	$1,000
	Programming and data acquisition	$300
	Total	$1,300
Sensor Calibration Stage 2	Cost for sensor calibration Stage 2, field sampling	
	Travel for grab sampling	$1,000
	Sample filtering	$400
	Data analysis - regression	$200
	Total	$1,600
Sensor node procurement	Cost of components required for a single Sensor Node and assembly	
	Sensor cleaning module	$167
	Control and communication module	$446
	Power supply module	$567
	Assembly	$200
	Total	$1,380
Gateway procurement	Costs of components required for a single Gateway Station and assembly	
	Stargate	$747
	Radio communication module	$900
	Power supply	$395
	Assembly	$200
	Total	$2,242

Repeater Station procurement	Costs of components required for a single Repeater Station and assembly	
	Radio communication module	$900
	Power supply	$395
	Assembly	$200
	Total	$1,495
Datalogger station procurement	Costs of components of datalogger station and assembly	
	Datalogger	$1,105
	Assembly	$100
	Total	$1,205
Sensor node installation	Labor and material required to install.	
	Lab technician, 9h	$450
	Site preparation	$100
	Material (PVC pipe, enclosure,T-post)	$250
	Total	$800
Gateway Installation	Labor and material required to install.	
	Lab technician, 6h	$300
	Site preparation	$100
	Material (steel conduit, enclosure)	$200
	Total	$600
Repeater Station Installation	Labor and material required to install.	
	Lab technician, 4h	$200
	Site preparatory	$100
	Material (steel conduit, enclosure)	$200
	Total	$500
Cellular service Central Station installation	Labor and material required to install.	
	Lab technician, 6h	$300
	Site preparation	$100
	Material (steel conduit, enclosure)	$200
	Total	$600
MBC Central Station installation	Labor and material required to install	
	Lab technician, 9h	$450
	Site preparation	$100
	Material (steel conduit, enclosure)	$200
	Total	$750
Datalogger station installation	Labor and material required to install	

	Lab technician, 2h	$100
	Site preparation	$100
	Material (steel conduit, enclosure)	$200
	Total	$400
Startup Costs	Labor and miscellaneous material required to start-up integrated SSC/WSN until steady state (trouble free) operation is achieved.	
	Lab technician, 40h	$2,000
	Server computer	$800
	Total	$2,800
Sensor Node Operational costs	Recurring costs required to operate a single Sensor node.	
	Lab technician, 10h per year	$500
Gateway and Central Station Operating costs.	Recurring costs required to operate a single Gateway and Central Station. Cost for renting commercial cellular data service	
	Annual charge (variable on cellular service provider and data flow usage)	$720
Gateway and MBC Central Station Operating Costs	Recurring costs required to operate a single Gateway and MBC Central Station. Cost for renting MBC data service	
	Annual charge (for research only)	$365
Permits/Regulatory Requirements	Labor required to obtain any permits and space renting	
	Field technician, 4h	$200
	Total	$200
Sensor Consumable Items	Type and rate of consumable items used during field demonstration.	
	Power supply (battery and solar charging voltage regulator only), 4 per site per year	$500
	Dye for velocity measurement, 4 bottles/year	$1,000
	Total	$1,500
Gateway, Central Station, MBC, and Datalogger Consumable Items	Type and rate of consumable items used during field demonstration.	
	Power supply (battery and solar charging voltage regulator only), 1 per site per year	$100
Sensor Node Maintenance	Frequency of required maintenance.	
	Regularly, 4 per year	

	Unscheduled, 12 per year	
	Labor and material per maintenance action	
	Lab technician, 4h Vehicle mileage, (assuming 20 miles round trip) Material (mechanical tools, paper towel, wires, etc.)	$200 $10 $100
	Total	$310
Gateway and Central Station Maintenance	Frequency of required maintenance.	
	Regularly, twice per year Unscheduled, 12 per year	
	Labor and material per maintenance action	
	Lab technician, 2h Vehicle mileage, (assuming 20 miles round trip) Material (multimeter, portable computer)	$100 $10 $100
	Total	$210
Gateway and MBC Central Station Maintenance	Frequency of required maintenance	
	Regularly, twice per year Unscheduled, 12 per year	
	Labor and material per maintenance action	
	Lab technician, 2h Vehicle mileage, (assuming 20 miles round trip) Material (multimeter, portable computer)	$100 $10 $100
	Total	$210
Datalogger Station Maintenance	Frequency of required maintenance	
	Regularly, twice per year Unscheduled, 12 per year	
	Labor and material per maintenance action	
	Lab technician, 1h Vehicle mileage, (assuming 20 miles round trip) Material (multimeter, portable computer)	$50 $10 $100
	Total	$160
Manual sampling	Labor and material per manual sampling	

	Lab technician, 0.5h	$25
	Vehicle mileage, (assuming 20 miles round trip)	$10
	Material (sampling bottles, wader)	$2
	Total	$37
Sample analysis	Cost of laboratory analysis per sample	
	Lab technician, 0.5h	$25
	Material	$15
	Total	$40
Instrument and tools	Cost of measurement instruments and tools	
	Ruggedized laptop	$450
	Ultrasonic velocity meter	$7,500
	Spectrum analyzer	$17,600
	Water sampler	$1,400
	Total	$26,950

7.1.1 Sensor Procurement.

Sensor procurement costs include all capital costs related to the procurement of a single optical sensor. The initial cost for producing a single sensor will be much higher than that produced through mass production.

7.1.2 Sensor Calibration Stage 1.

The cost for stage 1 of sensor calibration includes the costs for laboratory setup and time needed to calibrate the sensor and to develop the program for data acquisition to data handling.

7.1.3 Sensor Calibration Stage 2.

The cost for stage 2 of sensor calibration includes the costs for labor and travel to collect grab samples, laboratory SSC measurement of the samples using the filtering-weighing method, and the time needed to run the statistical analysis to establish the calibration curve.

7.1.4 Sensor Node Procurement.

Sensor node procurement costs include all capital costs related to the procurement of the equipment installed at the sensor node for the demonstration test. It would not include the cost of a rain gage since this is not a part of the sensor node. A sensor node is comprised of the sensor control and communication module (PCB board, DAQ board, wireless mote, and antenna), the sensor cleaning module (air compressor, solenoid valve, and relay), and the power supply module (solar panel, battery, and voltage regulator).

7.1.5 Gateway Station Procurement.

Gateway station procurement costs include all capital costs associated with equipment installed at a single gateway. A Gateway Station is comprised of a Stargate (with wireless mote), the radio communication module (datalogger and antenna), and the power supply module.

7.1.6 Repeater Station Procurement.

Repeater station procurement costs include all capital costs associated with equipment installed at a single repeater. A Repeater Station is comprised of a radio communication module (datalogger, and antenna), and the power supply module.

7.1.7 Cellular Service Central Station Procurement.

Cellular service Central Station Procurement costs include all capital costs associated with equipment installed at the Central Station. They do not include costs associated with operating the central station. A cellular service Central Station is comprised of a cellular modem, the radio communication module, and the power supply module.

7.1.8 Alternative Configurations – MBC Central Station Procurement.

MBC Central Station costs include all capital costs associated with equipment installed in field. They do not include costs associated with operating the MBC Central Station. An MBC Central Station is comprised of the MBC communication module (MBC radio, datalogger, and antenna) and the power supply module.

7.1.9 Alternative Configurations – Datalogger Station Procurement.

Datalogger station costs include all capital costs associated with equipment installed in the field to replace the Gateway Station. They do not include costs associated with operating the datalogger station. A datalogger station is comprised of the datalogger and extended storage module.

7.1.10 Installation of Sensor Node.

Sensor node installation costs include all costs associated with installation of a single sensor node. These costs would include labor costs associated with installation of the sensor node, site preparation costs, and equipment costs, etc.

7.1.11 Installation of Gateway.

Gateway installation costs include costs associated with installation of a single Gateway. These costs would include labor costs associated with installation of the Gateway, any site preparation costs, equipment costs, etc.

7.1.12 Installation of Gateway.

Repeater Station installation costs include costs associated with installation of a single repeater. These costs would include labor costs associated with installation of the Repeater Station, any site preparation costs, equipment costs, etc.

7.1.13 Installation of Cellular Service Central Station.

Installation costs for the cellular service Central Station include all costs associated with installation of a single Central Station. These costs would include labor costs, site preparation costs, equipment costs, etc.

7.1.14 Installation of MBC Central Station.

Installation costs for the MBC Central Station include all costs associated with installation of a single MBC Central Station. These costs would include labor costs, any site preparation costs, consulting cost if necessary, etc.

7.1.15 Installation of Datalogger Station.

Installation costs for the Datalogger station include all costs associated with installation of a single datalogger station to replace the Gateway Station. These costs would include labor costs, any site preparatory costs, consulting cost if necessary, etc.

7.1.16 Startup costs.

System startup includes all activities required to bring the integrated SSC sensor/WSN system (i.e. sensor nodes, Gateway, Central Station) on-line until the integrated system reaches the operational stage. Costs include all costs to bring a sensor node, gateway, and central station online. These costs include labor, equipment, and calibration costs.

7.1.17 Sensor Node Operating Costs.

Operating costs for a single sensor node consist of all recurring costs necessary to operate the sensor node. Operating costs are expected to be minimal. It is expected that the SSC sensor will need to be pulled out of the water and recalibrated on a periodic basis. The cost for recalibrating the sensor is mainly the labor cost. There are no other recurrent costs that have been identified at this time.

7.1.18 Gateway Station and Central Station Operating Costs.

Operating costs for the Gateway Station and Central Station consist of all recurring costs necessary to operate the Gateway and Central Station. Operating costs are expected to be minimal, and will consist of usage fees for the cellular network.

7.1.19 Gateway Station and MBC Central Station Operating Costs.

Operating costs for the MBC and datalogger alternatives consist are expected to be minimal, and will likely consist of usage fees for the MBC data service.

7.1.20 Permits/regulatory requirements.

Permits/regulatory requirement costs would include the estimated labor costs to prepare application forms to obtain required permits.

7.1.21 Sensor Consumable Items.

The most likely parts to be replaced would be the battery. For velocity measurement, blue dye will need to be replaced on a regular basis (about 4 bottles per year).

7.1.22 Gateway, Central Station, MBC, and Datalogger Consumable Items.

There are no consumable items identified at a Gateway, Central Station, MBC, and datalogger that will need to be replaced on a regular basis.

7.1.23 Sensor Node Maintenance.

The type and frequency of any maintenance performed at individual sensor node(s) will be recorded. There are two types of maintenance actions that will be tracked: 1) regularly scheduled maintenance and 2) unscheduled maintenance actions. Regularly scheduled maintenance at the sensor nodes will be performed when the sensor is pulled out of the water and recalibrated. The sensor node(s) will be inspected and individual components replaced if they are damaged. Any severed or frayed wires will be replaced, and loose or corroded connections fixed. Labor hours and material items and costs per maintenance action will be tracked. Unscheduled maintenance actions will be performed as required. Labor hours and material (replacement) items and costs per unscheduled maintenance action will also be tracked.

7.1.24 Gateway and Central Station Maintenance.

There are two types of maintenance actions at the Gateway and Central Station: 1) regularly scheduled maintenance and 2) unscheduled maintenance. Regularly scheduled maintenance consisted of periodic site visits to the Gateway site(s) and Central Station to ensure that they have not been tampered with. Individual components of the Gateway or Central Station were inspected and replaced if damaged. Any severed or frayed wires were replaced, and loose or corroded connections fixed. Unscheduled maintenance actions were performed only when they were needed. Costs for these maintenances include labor hours and materials.

7.1.25 Gateway and MBC Central Station Maintenance.

Same as 7.1.20.

7.1.26 Datalogger Station Maintenance.

Same as 7.1.20.

7.1.27 Manual Sampling.

Costs for manual sampling included labor hours, transportation, and material cost.

7.1.28 Sample analysis.

Grab sample analysis was a recurring cost.

7.1.29 Measurement instruments and tools.

Costs for instruments required for site measurement (ruggedized laptops, dataloggers, flow meters, water samplers, and spectrum analyzers, etc.) and tools require d for troubleshooting and repair.

7.2 COST DRIVERS

For the sensor, installation and maintenance are the major cost drivers. The installation cost is dependent on the site characteristics. Installing the sensor and associated gateway station/solar power system in narrow streams with dense vegetative covers usually requires much greater cost on labor and materials. Usually, more frequent maintenance trips to these sensor sites would also add significant cost.

For the WSN, the need for repeater stations is often a major cost driver. This is especially true for rural sensor sites where no cellular coverage is available. Directly providing cellular devices to each LWSN would eliminate the need for MRWN, hence reducing the cost for hardware and initial installation. However, recursive charges for continuous data services by the cellular companies may eventually even out this saving.

7.3 COST ANALYSIS AND COMPARISON

The most popular technologies for measuring suspended sediment concentration (SSC) are grab sampling followed by laboratory analysis.

In order to collect the grab samples, a technician must travel to the field and manually collect water samples at the site(s) of interest. Depending on the number of sites and the distance that needs to be travelled, this can take hours or even days. Samples are typically sent to an off-site laboratory for gravimetric analysis.

Table 7.2 compares costs related to four options for SSC monitoring. The first option is the SSC sensor and three-tier WSN that has been demonstrated through this project. Option 2 (“Alternative 1”) replaces the top tier of the three-tier WSN with the MBC technology. An obvious drawback of this option is that only 1/10 of the SSC data can be transmitted and stored. Option 3 (“Alternative 2”) avoids all wireless technologies and places a datalogger with sufficient memory space at each sensor. Obviously, this option cannot provide “real-time” data.

The fourth option (“Alternative 3”) is the traditional grab sampling and consequent laboratory analysis without using any of the sensing and WSN technologies. The cost for this option is based on an assumption that at least one grab sample is taken every hour, which would total

8,760 samples for a year, and it would require 8,760 trips to the site to take the samples and transport them to the laboratory. Thus, while proving very few samples, especially when compared to the 2,880 SSC readings per day we obtain from our technology, this option would take a very high labor cost. Of course if this is done consistently throughout the year, it still can be considered "long-term" monitoring.

The last option ("Alternative 4") uses an automatic pump sampler, such as the popular ISCO sampler. The sampler can be programmed to take samples either by preset times or upon rain event triggering. Since the sampler contains multiple sample containers (24 for a typical ISCO sampler), and it can be triggered by water level, which is in turn triggered by rain events, much less samples would be needed. Assuming 30 rain-triggered events having an average duration of one day each within a year, if 24 samples are taken for each event, the total number of water samples taken by the sampler within a year would be 720. If, in addition, two base flow samples are taken each month, the total number of samples would add up to 744. On the other hand, because the sampler can hold multiple samples (24 in the case of the ISCO sampler), the number of trips required for sampling would be reduced to 54 (30 to take samples and reset the sampler after each rain event and 24 to take base-flow samples). Savings from the reduced requirement for travel would be great. Although this option cannot provide "real-time" and "continuous" data, the data it provides may be meaningful and sufficient for many applications.

Table 7.2 Cost Comparison between Different Technologies

	Three-tier WSN (2,880 samples per day)	Alternative 1 MBC at Central Station (288 samples per day)	Alternative 2 Sensor and datalogger only (2,880 samples per day)	Alternative 3 Manual sampling (24 samples per day)	Alternative 4 Pump sampler (30 rain events, 24 samples per rain event, plus 24 base-flow samples)	Notes
Sensors	$9,936	$9,936	$9,936	$0	$0	12 sensors per site
Sensor nodes	$16,560	$16,560	$16,560	$0	$0	12 sensor nodes totally
Gateway Station	$13,452	$13,452	$0	$0	$0	6 Gateway Station totally
Repeater Station	$4,485	$4,485	$0	$0	$0	3 Repeater Station

						totally
Central Station	$6,210	$10,980	$0	$0	$0	3 Central Stations totally
Datalogger station	$0	$0	$14,460	$0	$0	12 dataloggers totally
Sensor node installation	$9,600	$9,600	$9,600	$0	$0	12 sensors totally
Gateway installation	$3,600	$3,600	$0	$0	$0	6 Gateway Station totally
Repeater installation	$1,500	$1,500	$0	$0	$0	3 Repeater Station totally
Central Station installation	$1,800	$2,250	$0	$0	$0	3 Central Stations totally
Datalogger station installation	$0	$0	$4,800	$0	$0	1 datalogger per sensor
Startup costs	$2,800	$2,800	$0	$0	$0	
Sensor node operational costs	$6,000	$6,000	$6,000	$0	$0	12 sensors total
Gateway and Central Station operational costs	$2,160	$1,095	$0	$0	$0	3 Central Stations totally
Permits Regulatory requirement	$200	$200	$200	$200	$200	
Sensor Consumable Items	$5,930	$5,930	$5,930	$0	$0	
Gateway, Cental Station,	$100	$100	$100	$0	$0	

MBC, and datalogger consumable items						
Sensor node maintenance	$3,720	$3,720	$3,720	$0	$0	12 times per year
Gateway, Cental Station, MBC, and datalogger maintenance	$420	$420	$320	$0	$0	Twice per year
Labor and transportation for sampling	$0	$0	$0	$324,120[1]	$1, 998[2]	[1]:8,760 trips [2]:54 trips annually
Sample analysis	$0	$0	$0	$350,400[3]	$29,760[4]	[3]:8,760 samples [4]:744 samples annually
Pump sampler	$0	$0	$0	$0	$6,000	
Pump sampling station	$0	$0	$0	$0	$500	Power module and case
Instrument and tools	$26,950	$26,950	$26,950	$26,950	$26,950	
Total	$115,423	$119,578	$98,576	$701,670	$65,408	

8 IMPLEMENTATION ISSUES

8.1 SSC SENSOR CALIBRATION ISSUE

The biggest concern we had with the SSC sensor was difficulties in collecting water samples that cover a sufficiently wide range of sediment concentration for calibration. If the two-stage calibration procedure requires a long-term, field collection of water samples, especially during the raining season, this sensor may not find wide acceptance among the potential users.

In order to alleviate this concern, we started to think about an alternative approach for the second stage of sensor calibration since late 2011. The approach was to develop a continuously operated field sampler that continuously takes water samples at various sediment concentrations and completes the sampling process within one to two hours. From late 2011 to early 2012, we held several brainstorming meetings and in February, 2012, we actually designed and fabricated the sampler. We then used this sampler at six sensor sites, two at Fort Riley and four at Fort Benning. A detailed description of the system and field test results are given in Appendix C.

We recommend using the sampler for stage 2 of sensor calibration because 1) The sampler allows the sensor to be calibrated in the same stream where it is deployed. This would ensure similar water and soil conditions between calibration and actual measurement. 2) Use of this sampler would greatly reduce the time and effort needed to take grab samples and avoid the long wait for significant precipitation events to cover the desirable SSC measurement range.

When using the sampler for calibration, 10-12 SSC levels need to be created by adding local soil into the circulation system, and 3-4 replicated measurements are recommended for each SSC level. A regression analysis will then be conducted to allow prediction of SSC from single or multiple sensor signals.

The sampler we designed and fabricated is large and heavy (due to the pump and its driver – a gasoline engine), thus inconvenient for use in streams. A smaller sampler needs to be designed to make it easier to handle.

8.2 SSC/VELOCITY SENSOR DEPLOYMENT ISSUES

For practical uses, the SSC/velocity sensor is always deployed in natural waters, including stream, lakes, rivers, and reservoirs. Securing the sensor in the water is always a challenge, especially during the high-flow season. We've had several experiences when the sensor was partially or completely damaged by water flow. Adding mechanical reinforcement usually alleviate the problem. However, for streams with sand/stone bottoms this may become extremely difficult.

While being deployed in stream, the SSC/velocity sensor has the following connections to the PCB control board which is located on the bank near the sensor: 1) Signal wires to transmit the analog signals from the sensor to the PCB and control wires to transmit digital signals from the PCB to the sensor for LED illumination control, 2) Air hose to lead pressurized air to the sensor for cleaning, 3) Thermocouple wires to measure water temperature, and 4) (If velocity is

measured) dye hose to lead color dye to the sensor. These connectors/hoses should be placed in a single conduit for protection.

The size of the stream needs to be considered when deploying the sensor. The general recommendation is that the sensor be deployed near a bank, perhaps within a distance of 20 ft. This recommendation is mainly based on concerns of the conduit length and the depth of the water. The velocity sensor has a maximum measurable velocity of 5 m/s. If the water velocity is expected to exceed this limit, the sensor should not be deployed. The maximum measurable SSC is 5,000 mg/L. Therefore, the sensor should not be deployed in stream with expected SSC higher than 5,000 mg/L.

During demonstration, we had several experiences where the sensor was buried by sands in locations where the water depth was sufficiently large when the sensor was first deployed. These experiences taught us that, when selecting sensor locations, history of topography changes of the locations should be considered.

9 REFERENCES

ASTM D3977-97 (2007). http://www.astm.org/Standards/D3977.htm

Bigham, D. 2012. Calibration and Testing of a Wireless Suspended Sediment Sensor. A Master's thesis, Manhattan, Kansas: Kansas State University, Department of Biological and Agricultural Engineering.

Brakensiek, D.L., H.B. Osborn, and W.J. Rawls. 1979. Field manual for research in agricultural hydrology. Agriculture Handbook No. 224, Sience and Education Administration, USDA.

Clifford, N.J., K.S. Richards, R.A. Brown, and S.N. Lane. 1995. Laboratory and field assessment of an infrared turbidity probe and its response to particle size and variation in suspended sediment concentration. Hydrological Sciences Journal 40(6):771-791.

Csuros, M. Environmental Sampling and Analysis Lab Manual, Lewis Publishers, CRC Press LLC, Boca Raton, FL 1997.

Davies-Colley, R.J., and D.G. Smith. 2001. Turbidity, suspended sediment, and water clarity: A review. J. American Water Resources Association 37(5): 1085-1101.

Dvorak, J. 2012. An optical water velocity sensor for open channel flows. A PhD dissertation, Manhattan, Kansas: Kansas State University, Department of Biological and Agricultural Engineering.

Han, W. 2011. Three-tier wireless sensor network infrastructure for environmental monitoring. A PhD dissertation, Manhattan, Kansas: Kansas State University, Department of Biological and Agricultural Engineering.

Han, W., N. Zhang, Y. Zhang. 2007. A remote, real-time sediment-runoff monitoring system using a wireless sensor network and GPRS. ASABE Paper No. 073079. St. Joseph, Mich.: ASABE.

Riley, S.J. 1998. The sediment concentration-turbidity relation: Its value in monitoring at Ranger Uranium Mine, Northern Territory, Australia. Cantena. 32: 1-14.

Stoll, Q. M. 2004. Design of a Real-time, Optical Sediment Concentration Sensor. MS thesis. Manhattan, Kansas: Kansas State University, Department of Biological and Agricultural Engineering.

Zhang, N., Y. Zhang, J. Steichen, D. Oard, P. Woodford, P. Barnes, and S. Hutchinson. 2005. Real-time monitoring of sediment concentration at a low-water stream crossing using a unique sediment sensor. Poster on the Partners in Environmental Technology Technical Symposium & Workshop, November 29-December 1, 2005, Washington, D.C.

Zhang, Y. 2009. An optical sensor for in-stream monitoring of suspended sediment concentration. A PhD dissertation, Manhattan, Kansas: Kansas State University, Department of Biological and Agricultural Engineering.

Zhang, Y., N. Zhang, G. Grimm, C. Johnson, D. Oarrd, and J. Steichen. 2007. Long-term field test of an optical sediment-concentration sensor at low-water stream crossings (LWSC). ASABE Paper No. 072137. St. Joseph, Mich.: ASABE.

Appendices

Appendix A: Points of Contact

POINT OF CONTACT Name	ORGANIZATION Name Address	Phone Fax E-mail	Role in Project
Scott Hill	US Army Aberdeen Test Center, 400 Colleran Road, Aberdeen Proving Ground, MD 21005	Phone: 410-278-1878 Fax: 410-278-1589	PI
Naiqian Zhang	BAE Department, Kansas State University, Seaton Hall, room 158, Manhattan, KS	Phone: 785-532-2910 Fax: 785-532-5825 Email: zhangn@ksu.edu	Co-PI Lead Scientist
Ning Wang	BAE Department, Oklahoma State University, Ag Hall, room 112 Stillwater, OK	Phone: 405-744-2877 Fax: 405-744-6059 Email: ning.wang@okstate.edu	Co-PI Lead Scientist
Carl Johnson	US Army Aberdeen Test Center400 Colleran Road, Aberdeen Proving Ground, MD 21005	410_278-1274 Fax: 410-278-1589	Co-PI

Appendix B: Sensor working histories

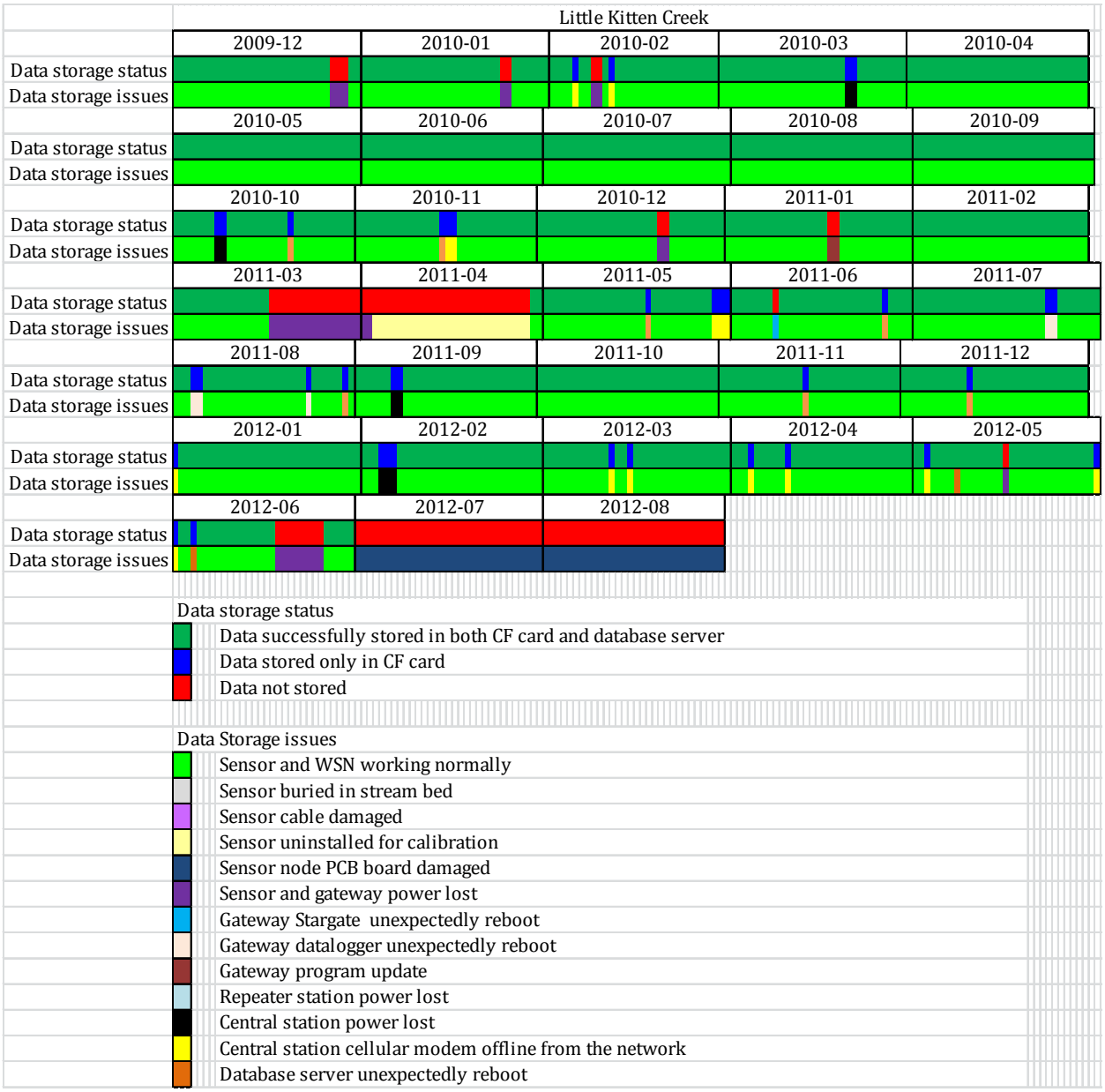

Figure 1. Sensor working history – Little Kitten Creek

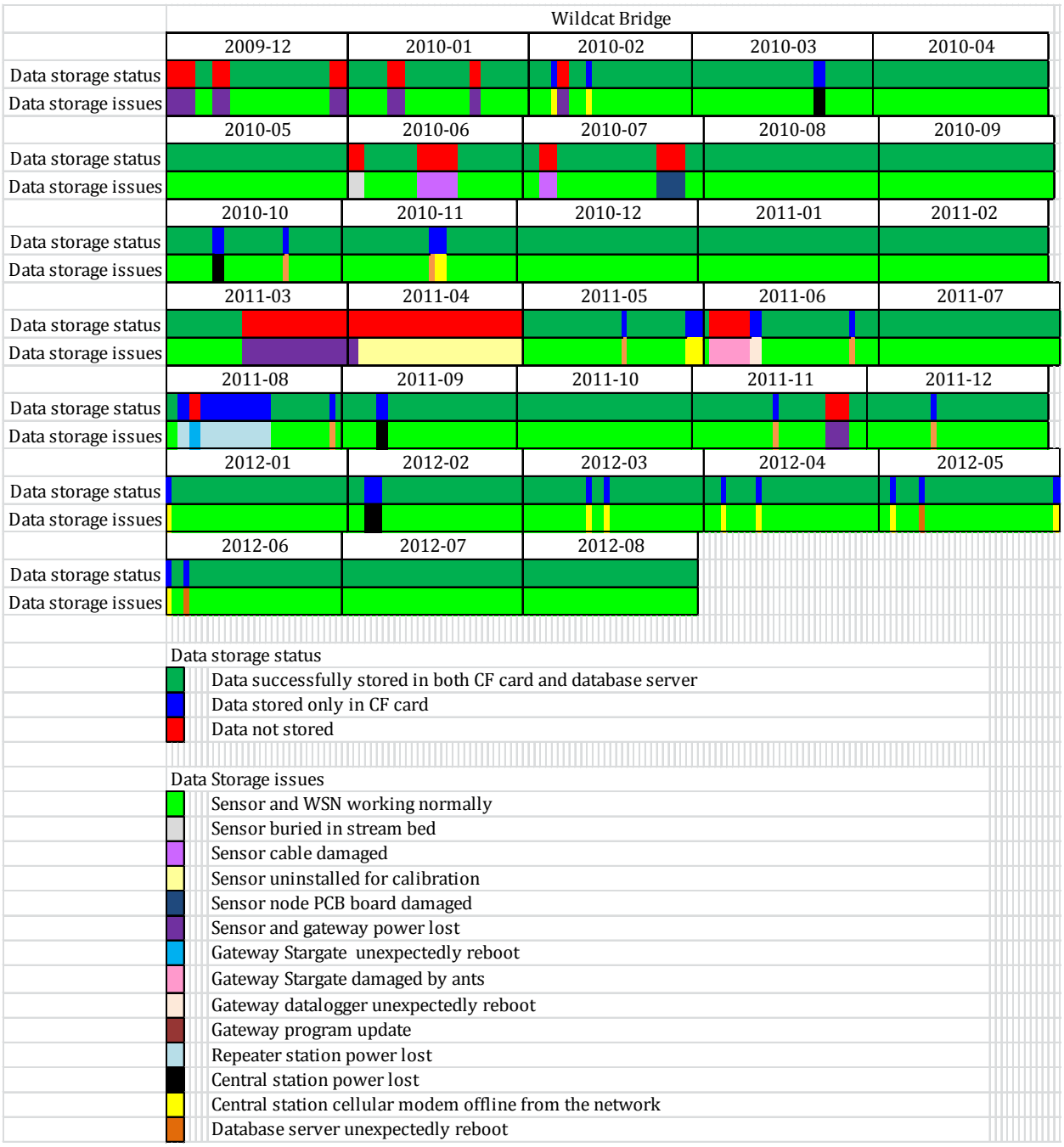

Figure 2. Sensor working history – Wildcat Bridge

Figure 3. Sensor working history – Wildcat Creek

Figure 4. Sensor working history – Silver Creek

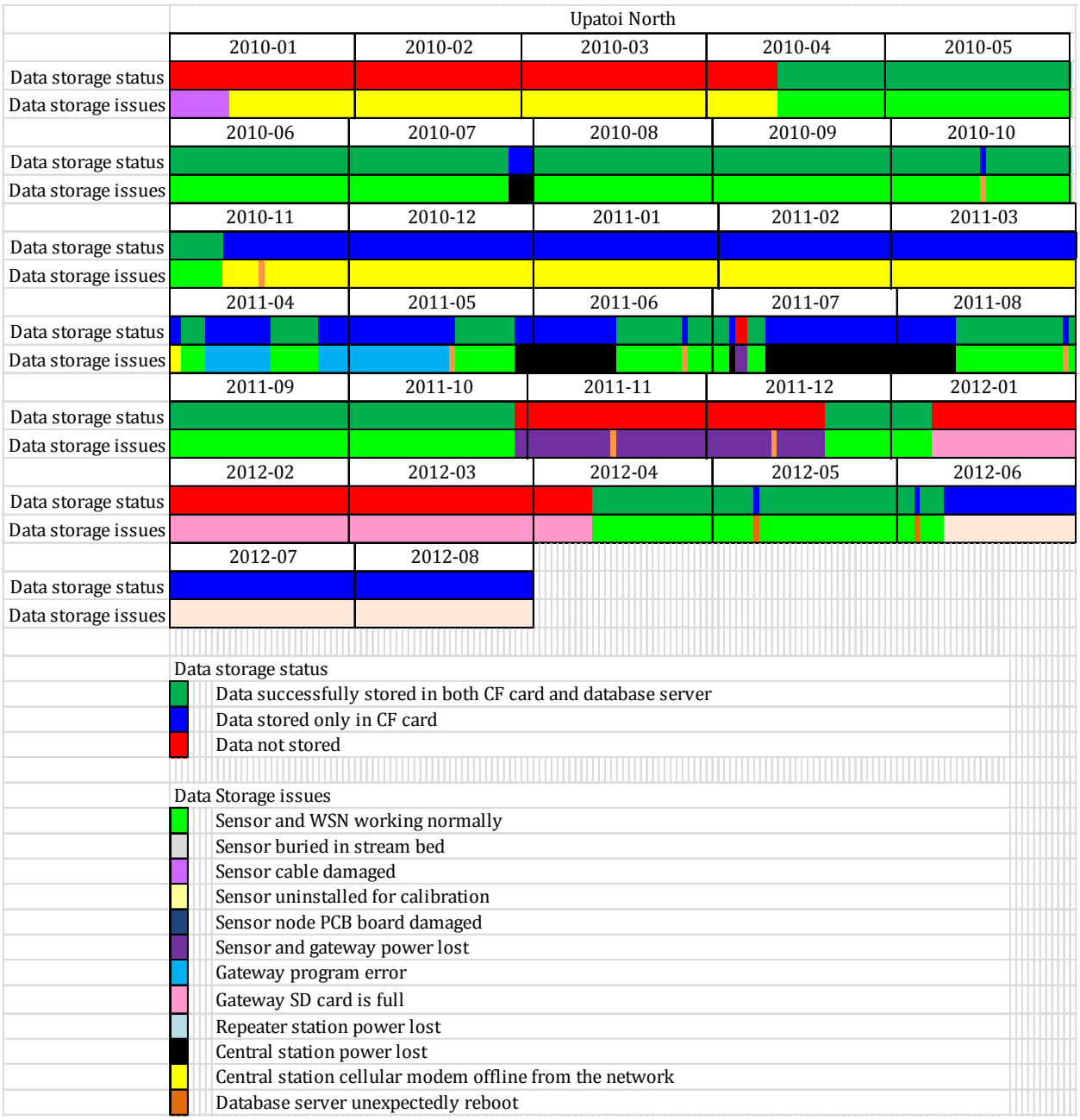

Figure 5. Sensor working history – Upatoi North

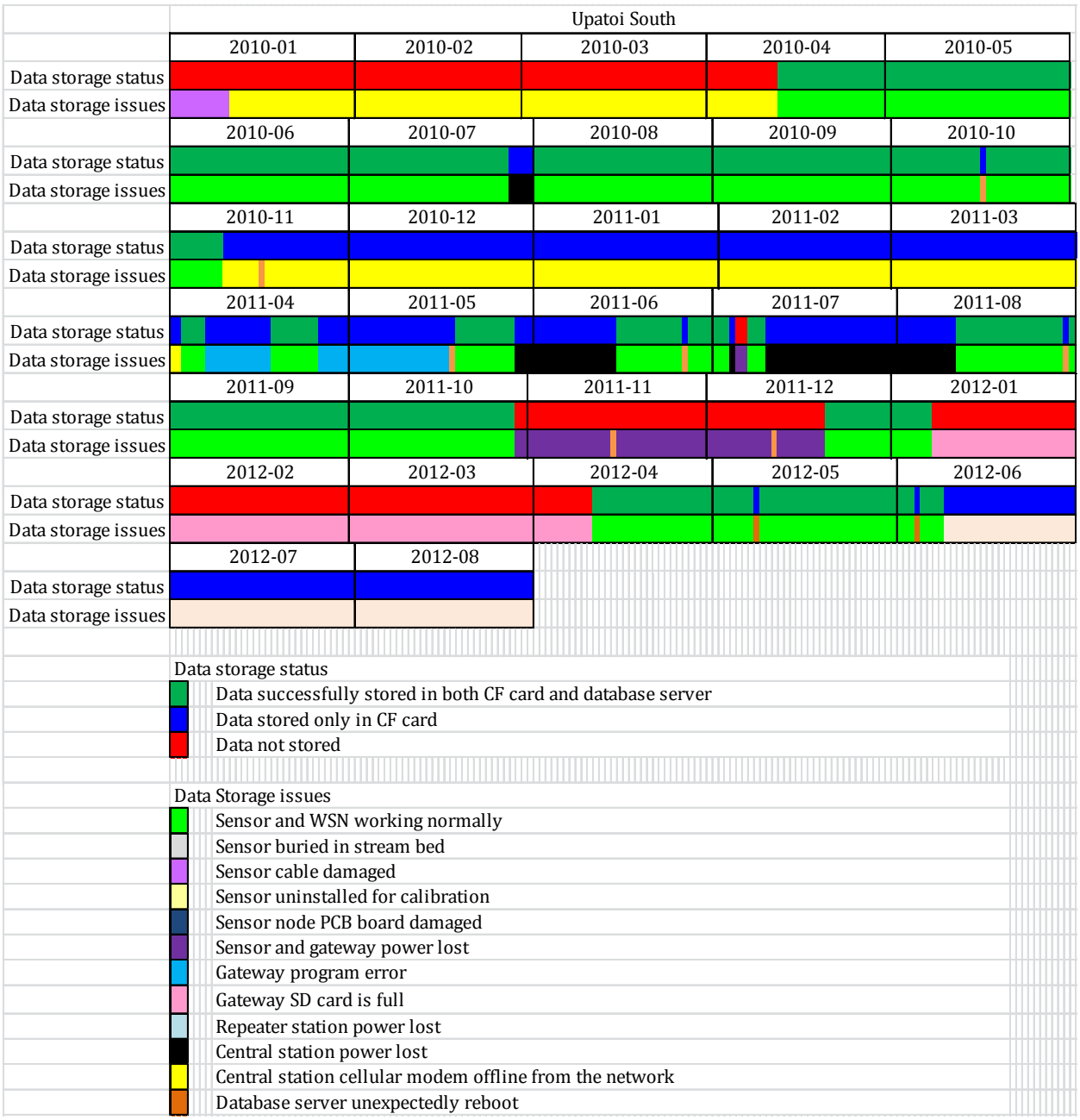

Figure 6. Sensor working history – Upatoi South

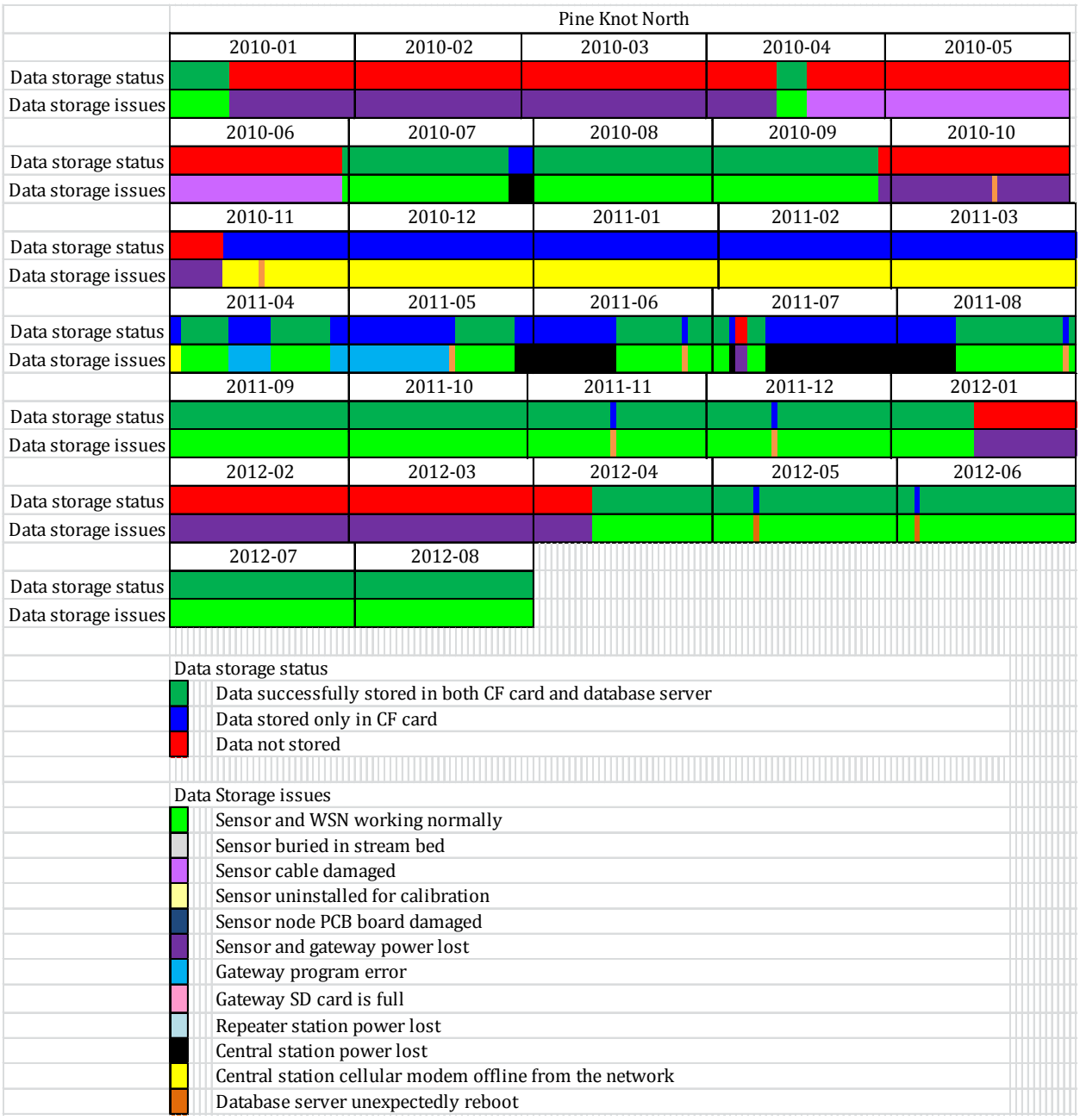

Figure 7. Sensor working history – Pine Knot North

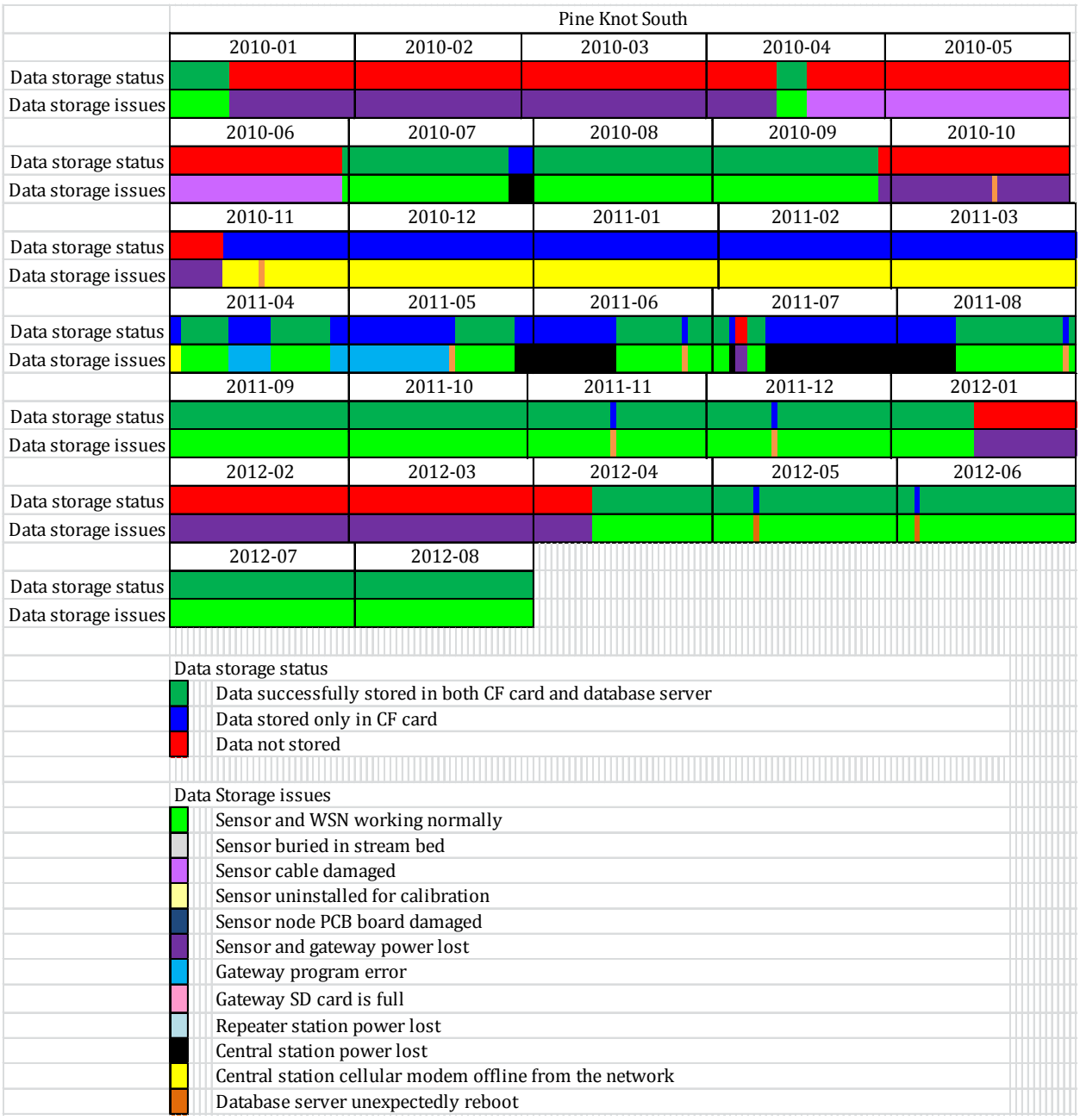

Figure 8. Sensor working history – Pine Knot South

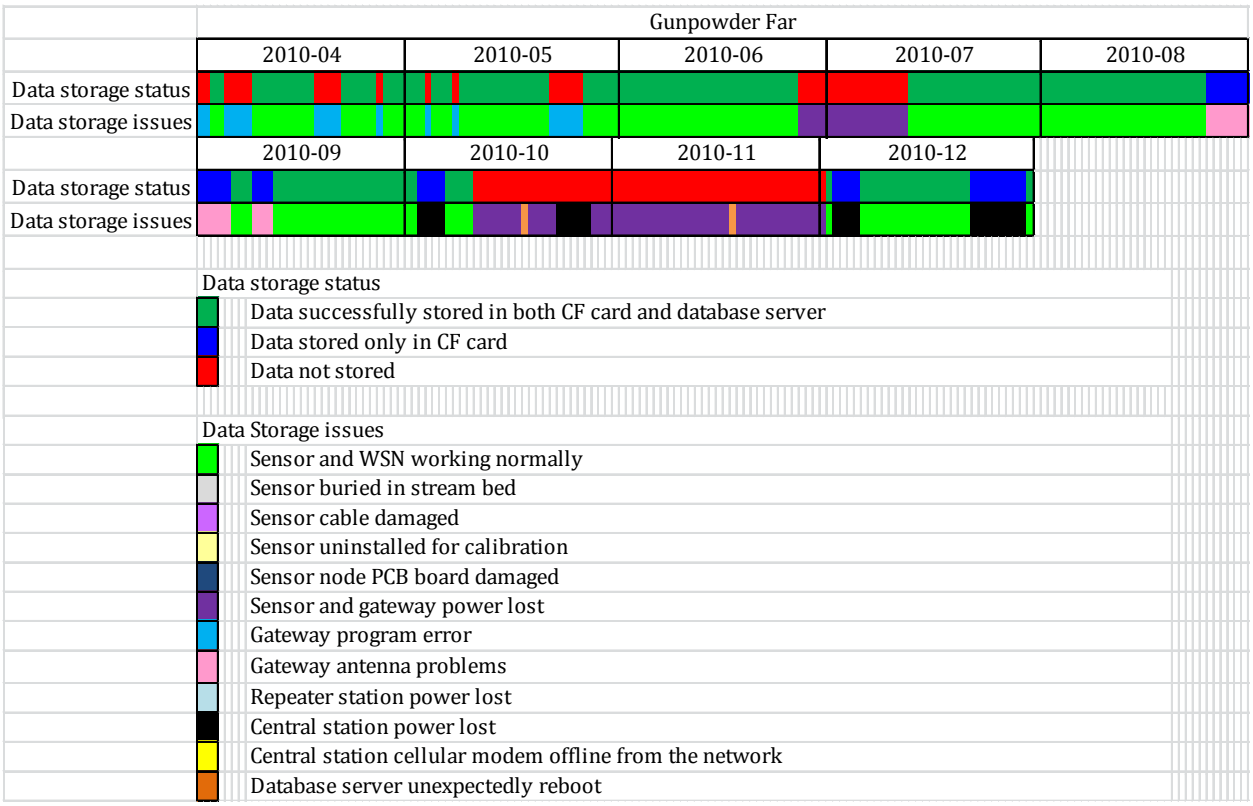

Figure 9. Sensor working history – Gunpowder Far

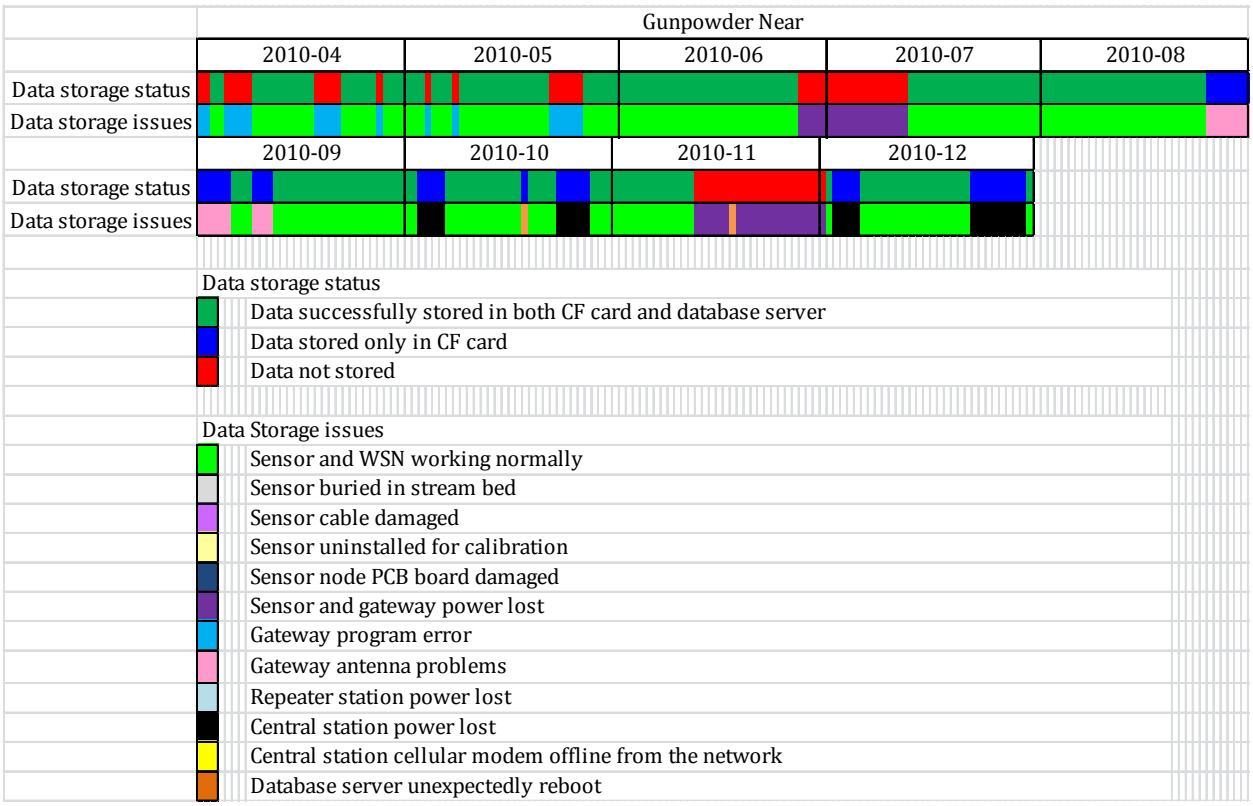

Figure 10. Sensor working history – Gunpowder Near

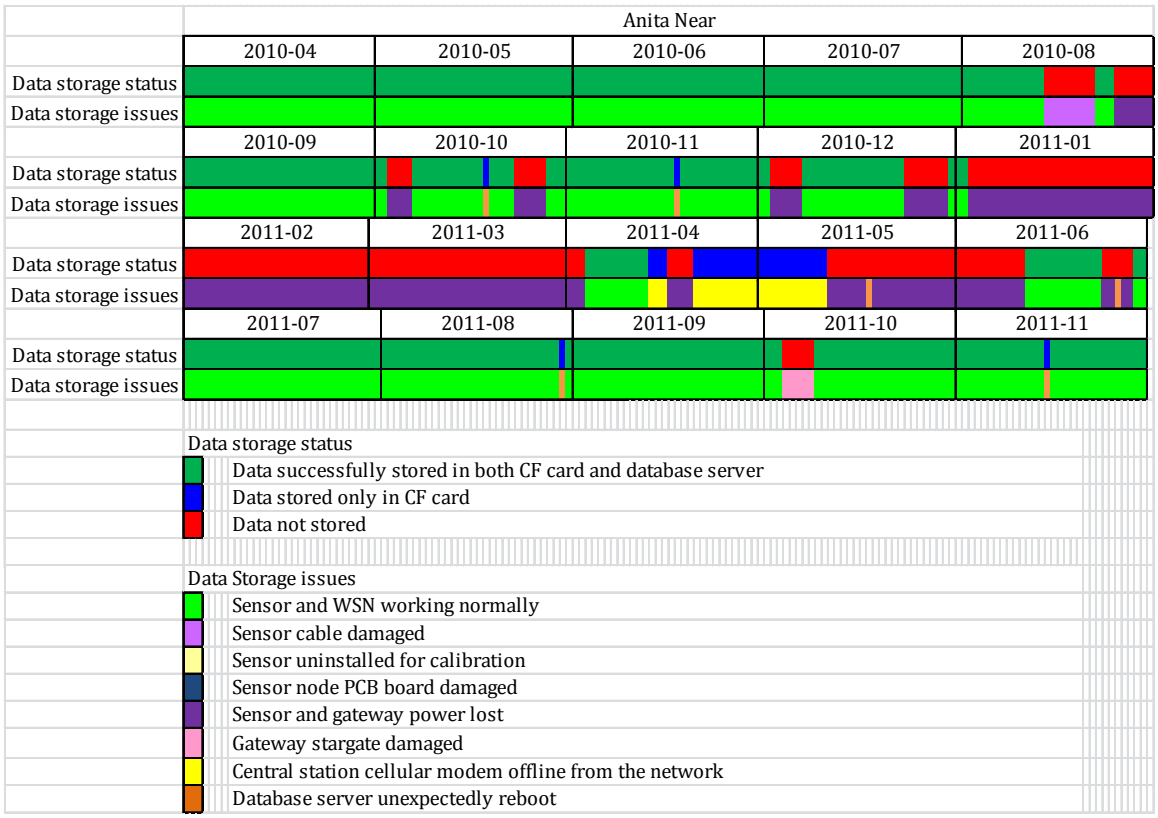

Figure 11. Sensor working history – Anita Near

Figure 12. Sensor working history – Anita Far

Appendix C: A sampler for Fast Calibration of SSC Sensor

INTRODUCTION

The calibration model developed by Bigham (2012) for the suspended sediment sensor installed in three different sites, namely Fort Riley-KS, Fort Benning-GA and Aberdeen Proving Ground-MD, showed a good linear relationship between the suspended sediment concentration and the three different signals- IR45, OR45 and OR180. However, most of the sensors were calibrated at a narrow range of sediment concentrations (i. e. less than 1000 mg/L), while others lacked concentrations in the middle range.

Suspended sediment concentration is dependent on the presence or absence of rain before or during the sampling time. When there is no rain, the suspended sediment concentration is close to zero, and concentration increases as the intensity and the duration of rainfall increases. Because of the difficulty in having sample with a wide range of concentration level, a calibration setup was made.

OBJECTIVES

The main objective of this study is to calibrate each sensor installed in the creeks found in Fort Benning, Georgia and Fort Riley, Kansas. The specific objectives include:

1. to develop and evaluate a set-up for calibration of the sediment sensor;
2. to develop linear models for predicting suspended sediment concentration; and
3. to determine the best linear model for the sediment sensor

MATERIALS AND METHODOLOGY

Calibration Set-up

A setup for calibration of the sensor was fabricated to somewhat control the suspended sediment concentration levels. The idea is for this setup to contain the water with the desired concentration and let the sensor measure the voltage reading. The setup has some provision for collection of water sample for the determination of actual suspended sediment concentration. This concentration will then be compared with the voltage reading at each sampling time for developing the calibration model.

Figure 1 shows the calibration setup which is composed of the pump set, the sensor holder, rubber lock, sediment feeder, sampling point, water replenishing point, flexible hoses, PVC pipes and fittings. Table 1 shows the specification/description of the different parts.

The setup has a capacity of 29 L of water. The water just recirculates and sediment concentration can be varied by adding sediment at the sediment feeder. Water sample can be obtained through the sampling point. During water sample collection, the amount of water in the setup decreases. To make the volume of water almost constant, water is being replenished at some point.

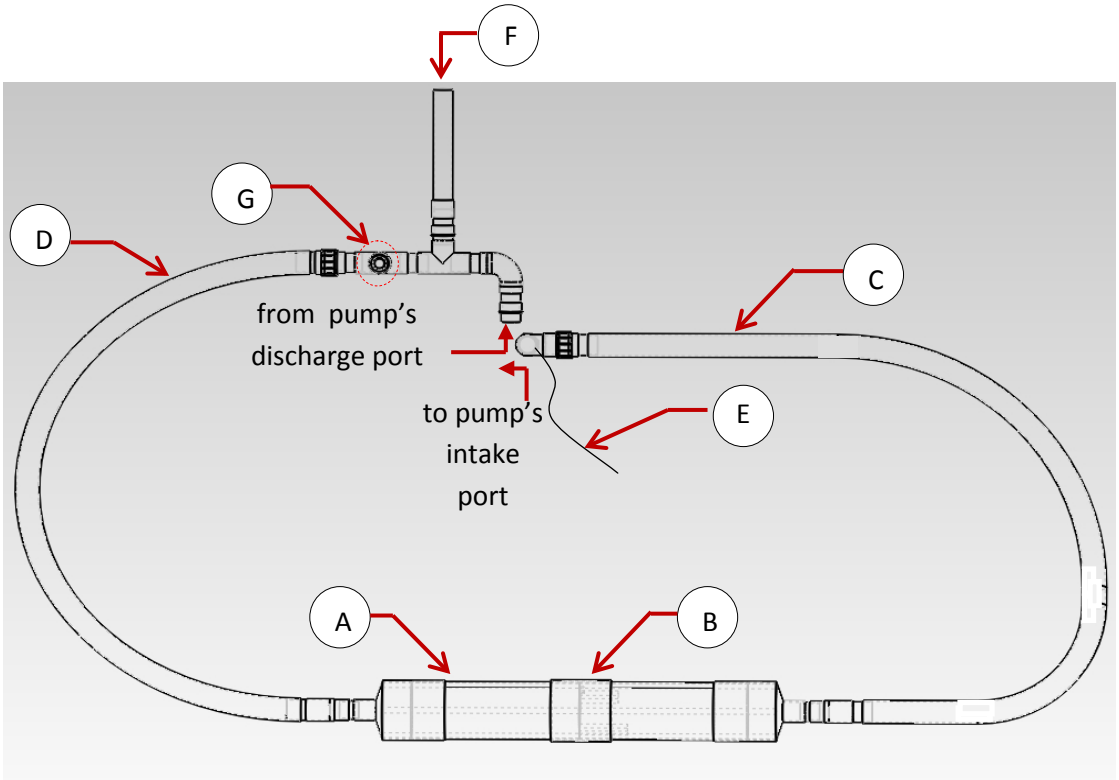

Figure 1. Sediment sensor calibration set-up assembly. (A)main duct/sensor holder assembly; (B) rubber lock; (C) and (D) flexiblle hose; (E) water replenishing point; (F) sediment feeder; (G) sampling point; (H) pump set

Table 1. Parts and description of the calibration set-up

Parts	*Description*
(A) Main duct/sensor holder assembly	two parts: left and right; each part is a 21" long Ø6"PVC with bell end
(B) Rubber lock	6.5" long rubber tube to secure the sensor holder assembly
(C) and (D) Flexible hose	Ø2" flexible hose, 90" long
(E) Water replenishing point	a point in the intake pipe where a 0.5" plastic tube is connected and gets water from the stream; ball valve is used for control
(F) Sediment feeder	Ø2" PVC pipe which serves as entry of sediment being added an at the same time, the pressure head
(G) Sampling point	A point in the setup where water samples are collected; a pastic ball valve is used for control
(H) pump set	5.0hp gasoline engine; Ø2" pump

Pre-calibration Testing

Before using the set-up in actual calibration of the sensors installed in the different sites, pre-testing was done. This involved running an experiment to test whether this setup can produce signals that are reasonable.

Calibration Procedure

The sensor to be tested was inserted and secured first in the sensor holder. Then, water from the stream was added until the setup is completely filled with water. In some instances, the pipes were agitated to ensure that there is no air trapped in the pipes. Trapped air produced some turbulence in the water flow and resulted to a significant amount of noise in the signal. When the setup is completely filled with water, engine was started and ran at about 3000 rpm. Sediment, which was collected from the site, was added gradually to increase the concentration level. Sampling took place after a minute elapsed from the time sediment was added. Four subsamples were collected in a 120-ml plastic bottles for each concentration level. The time of each sampling was noted for comparison with the voltage reading of the sensor.

Actual suspended sediment concentration (SSC) was determined by following the EPA method 160.2. The procedure involved weighing, filtration and oven drying. Suspended sediment concentration was determined by dividing the dry weight of sediment to the volume of water.

The signal generated by the sensor was processed by filtering with the use of butterworth filter in MATLAB. For each sampling time, 15-second averaging was done prior to sampling time. The relationship of these filtered signals with the actual sediment concentration was determined using REG procedure of SAS. The best model was determined using a backward elimination and max R^2 method of SAS.

FIELD CALIBRATION

Little Kitten

Forty-eight grab samples with varying concentrations were collected from this site. The actual sediment concentration of each water sample was determined. Fifteen-second averaging was done to the sensor's reading (IR45, OR45, OR180) corresponding to each water sample. Table 2 summarizes the suspended sediment concentration (SSC in mg/L) and the corresponding processed signals for IR45, OR45 and OR180.

The range of SSC for this calibration is 23 to 5,824 mg/L which is much wider than the previous calibration done by Bigham (2012). It must be noted that as concentration level increases, IR45 and OR45 signals increase, and OR180 signal decreases. At saturation, voltage for IR45 and OR45 is 2500mV, and for OR180, it is 0mV. From the table, it can be seen that two of the signals, IR45 and OR180, almost reached saturation.

Regression was done for SSC and each sensor's signal using the REG procedure of SAS 9.1.3. Table 3 summarizes the output of the linear regression done for the three sensor signals considering one variable at a time. Figures 2 to 4 show the points and the predicted SSC for each signal. All models have high coefficient of determination with IR45 being the highest (R^2 = 0.9801) and OR180, the lowest (R^2 = 0.8778). The latter has the lowest R^2 because the points tend to follow a logarithmic trend due to the nature of its signal that becomes saturated as

concentration increases (Figure 4). This model using OR180 to predict SSC can be improved by log transformation before regression or by lowering the upper range of the concentration, such that the signal for OR180 does not reached saturation. But, based on the p-values of SAS, the models and the parameter estimates are all acceptable at 95% level of confidence.

Table 2. Calibration data for the sediment sensor in Little Kitten.

SSC mg/L	IR45 mV	OR45 mV	OR180 mV	SSC mg/L	IR45 mV	OR45 mV	OR180 mV
46	578	513	1812	4250	1964	1587	189
33	471	355	1755	4155	2007	1607	187
23	358	281	1612	4000	1979	1623	187
54	288	317	1965	4030	1978	1608	190
1032	505	498	1404	5042	2161	1706	142
775	506	595	1246	4497	2165	1716	143
888	547	668	1323	4371	2157	1709	145
777	545	581	1223	4208	2153	1714	145
1588	813	800	932	5088	2337	1774	117
1510	806	832	874	4916	2344	1789	115
1552	837	867	894	4826	2355	1801	115
1428	804	826	880	4702	2344	1808	115
2467	1156	1054	581	5824	2469	1835	95
2237	1147	1084	559	5054	2476	1837	93
2357	1174	1095	570	5174	2473	1847	96
2255	1168	1109	545	5008	2462	1851	76
3223	1468	1295	392	5504	2499	1875	77
2813	1471	1343	373	5230	2496	1877	77
2702	1454	1332	377	5197	2501	1889	80
2845	1464	1338	367	5019	2499	1876	80
3787	1730	1453	266	5594	2499	1909	68
3526	1758	1463	256	5560	2498	1901	69
3329	1757	1497	253	5324	2499	1898	70
3504	1757	1499	247	4982	2493	1908	72

Table 3. Summary of SAS one-variable linear regression of Little Kitten's sediment sensor

Source	*df*	*Parameter estimate*	*p-value*	*Root MSE*	R^2
IR45 vs SSC	1	x	<0.0001	255.80279	0.9801
Intercept	1	-548.97179	<0.0001	x	x
IR45 (slope)	1	2.34735	<0.0001	x	x
OR45 vs SSC	1	x	<0.0001	295.76277	0.9734
Intercept	1	-1297.85912	<0.0001	x	x
OR45 (slope)	1	3.42174	<0.0001	x	x
OR180 vs SSC	1	x	<0.0001	633.55980	0.8778

Intercept	1	4895.63288	<0.0001	x	x

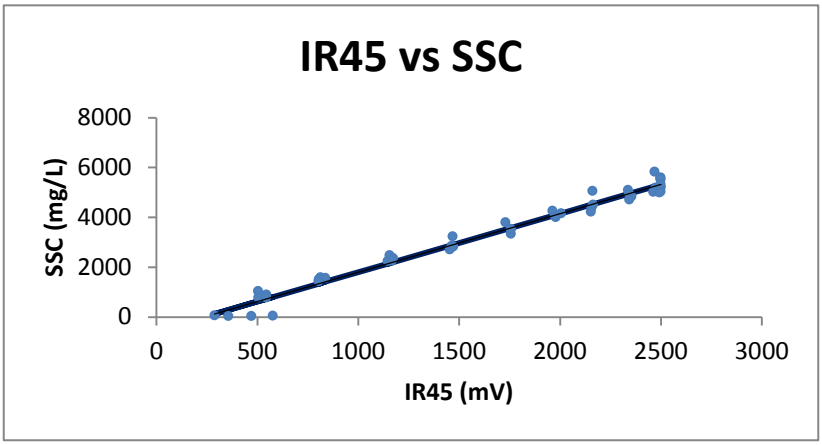

OR180 (slope)	1	-3.09968	<0.0001	x	x

Figure 2. SSC linear model of the sensor in Little Kitten using IR45 signal

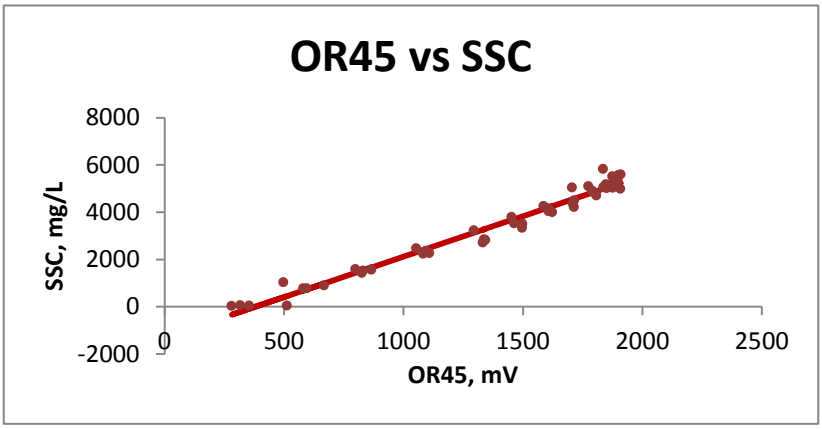

Figure 3. SSC linear model of the sensor in Little Kitten using OR45 signal

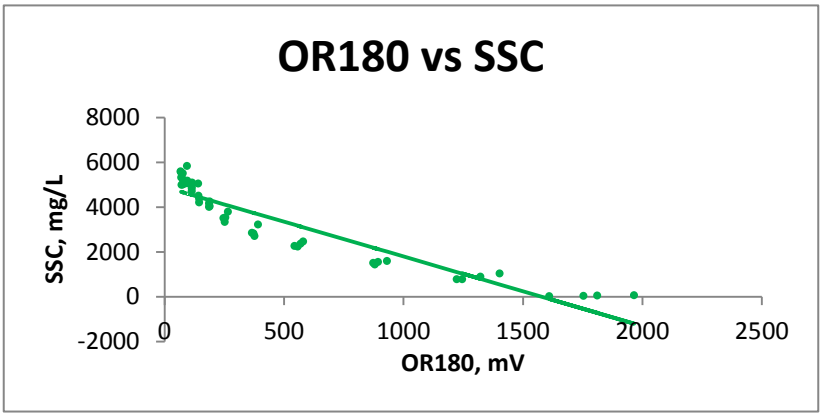

Figure 4. SSC linear model of the sensor in Little Kitten using OR180 signal

The uncertainties of these prediction models for this sensor were ± 512 mg/L , ± 592 mg/L , ± 1,267 mg/L for IR45, OR45 and OR180, respectively, for concentrations between 23 to 5,824 mg/L. These uncertainties were relatively low when compared to the maximum range it can predict SSC.

Two-variable and three-variable linear models were also tried in SAS to determine the possibility of having a better calibration model. In general, all models developed for this sensor in Little Kitten were found to be not good in predicting SSC at lower concentration levels. All of them exhibited a linear trend except for the one- variable model using OR180 signal. Comparison between the predicted SSC of the best model, which uses IR45 and OR180 as predictors, and the actual SSC for Little Kitten sensor is shown in Figure 5.

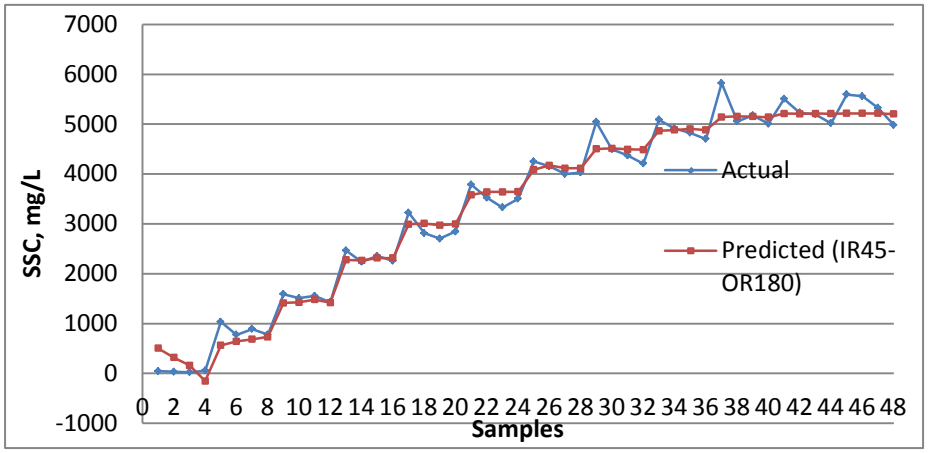

Figure 5. Comparison between the predicted SSC of IR45-OR180 model and actual SSC of Little Kitten creek.

Data from grab samples taken during demonstration at the Little Kitten site were fitted to the predicition models. Figure 6 shows the results.

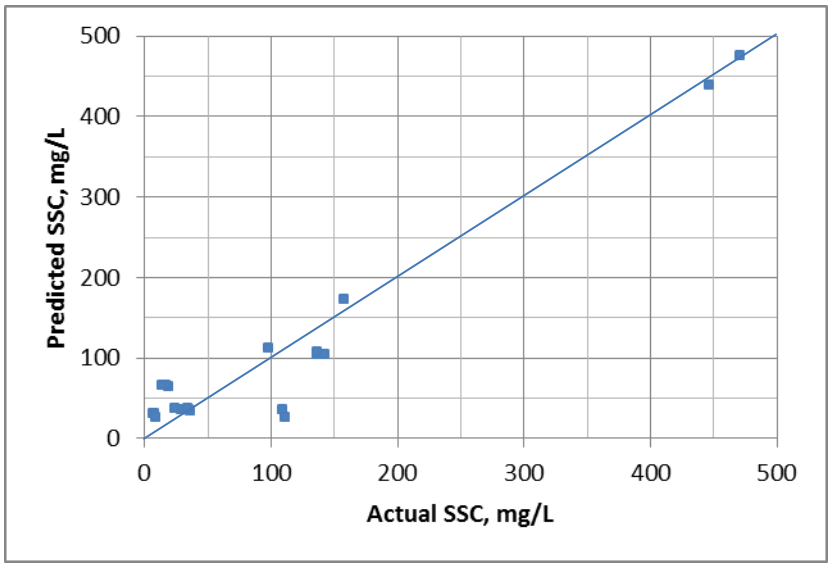

Figure 6. Comparison between the SSC predicted using the IR45 model and actual grab samples taken at the Little Kitten site.

Wildcat Bridge

Fifty-six grab samples with varying concentrations were collected from this site. The range of SSC for this calibration is 52 to 13,954 mg/L which is much wider than the previous calibration done by Bigham (2012).

Regression was done for SSC and each sensor's signal, and Table 4 summarizes the output of the one-variable linear regression. Based from their coefficient of determinations, the best one-variable model is the one using IR45 as predictor for SSC with R^2 value of 0.7267, followed by that of OR180 with R^2 =0.7178 and OR45 with R^2 = 0.6396.

Table 4. Summary of SAS one-variable linear regression of Little Kitten's sediment sensor.

Source	Df	Parameter estimate	p-value	Root MSE	R^2
IR45 vs SSC	1	x	<0.0001	1571.55433	0.7267
Intercept	1	-2598.53875	<0.0001	x	x
IR45 (slope)	1	5.80134	<0.0001	x	x
OR45 vs SSC	1	x	<0.0001	1804.63580	0.6396
Intercept	1	-4580.79243	0.0002	x	x
OR45 (slope)	1	20.80920	<0.0001	x	x
OR180 vs SSC	1	x	<0.0001	1596.69692	0.7178
Intercept	1	8504.37531	<0.0001	x	x
OR180(slope)	1	-7.25181	<0.0001	x	x

The one-variable linear models for predicting SSC in Wildcat Bridge were illustrated in Figures 7 to 9. Compared to the sensor in Little Kitten, the R^2 of the models using the three different signals individually were lower in this site. It can be observed that at higher concentrations

(above 7,000 mg/L), the points do not follow a linear trend. The points tend to cluster which made the R^2 for these models to be relatively low and their uncertainties to be more than $\pm$3,000 mg/L. Notice that the data points wherein the concentration is 7000mg/L cluster at a voltage range of 1800 - 2000 mV for IR45 and approaches 0mV for OR180. Maybe the sensor is already saturated at a concentration of 7000 mg/L. Bigham (2012) stated in his study that the maximum voltage signal for the sensors was set to 1800mV. On the contrary, IR45 of all the sites exceeded this value and some approaches 2500mV, which was the maximum value set in the PCB board, as it reaches saturation.

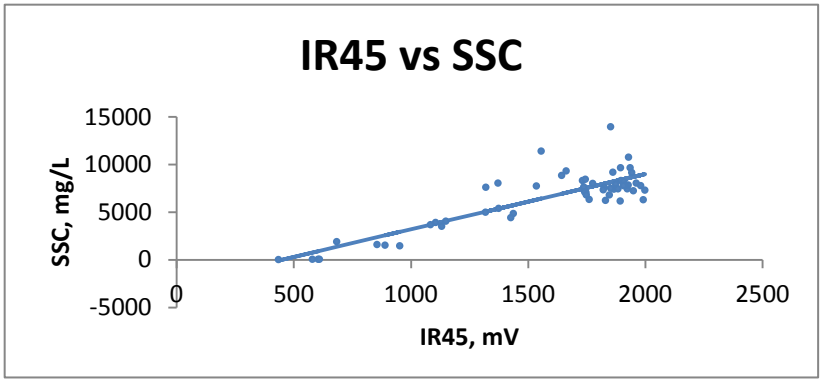

Figure 7. SSC linear model of the sensor in Wildcat Bridge using IR45 signal.

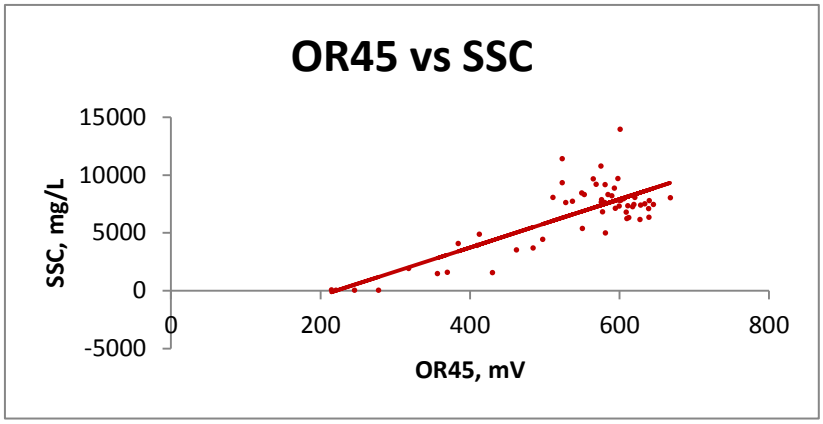

Figure 8. SSC linear model of the sensor in Wildcat Bridge using OR45 signal.

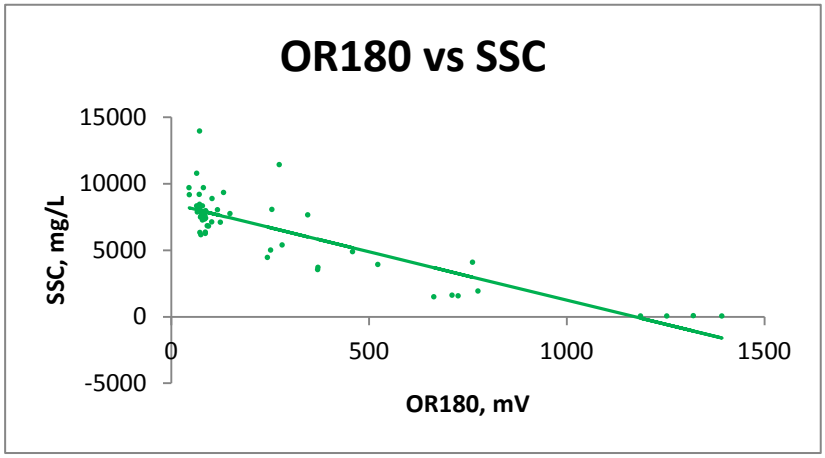

Figure 9. SSC linear model of the sensor in Wildcat Bridge using OR180 signal.

For multiple variable linear models (Table 5), the three-variable linear model has the highest coefficient of determination (R^2 = 0.7531) but SAS backward selection again identified the two-variable model, which uses IR45 and OR180 as predictors, to be the best model (R^2 = 0.7448). Figure 10 shows the comparison between the actual and predicted SSC of the best linear model. This model can be further improved by removing the concentrations higher than 10,000 mg/L which can be considered as outliers.

Table 5. Two-variable and three-variable calibration model for the sensor in Wildcat Bridge.

Model	Variables	Equation*	Root MSE*	R^2
2-variable	IR45-OR45 vs SSC	SSC = 5.6*IR45 + 0.8*OR45 – 2719.6	1586.0	0.7268
	IR45-OR180 vs SSC	SSC = 3.3*IR45 – 3.4*OR180 + 2296.7	1532.6	0.7448
	OR45-OR180 vs SSC	SSC = -2.0*OR45 – 7.9*OR180 – 9771.8	1610.1	0.7184
3-variable	All vs SSC	SSC = 4.0*IR45 – 8.3*OR45 – 5.1*OR180 + 6102.3	1522.2	0.7531

*SSC and Root MSE in mg/L; IR45, OR45 and OR180 in mV

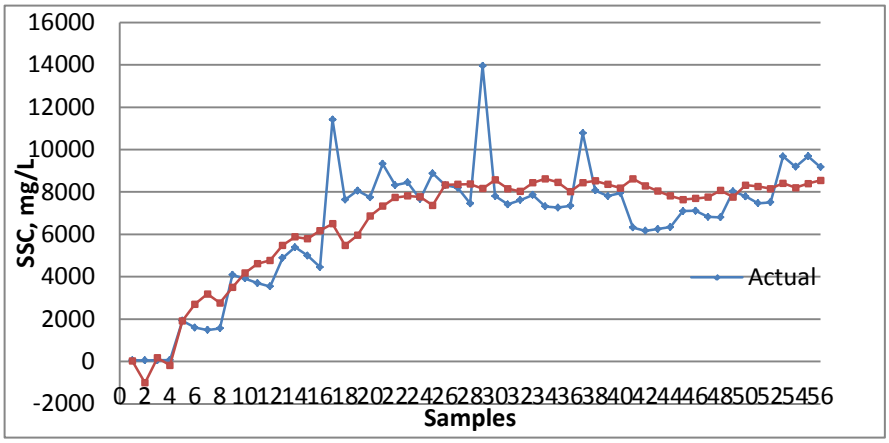

Figure 10. Comparison between the predicted SSC of IR45-OR180 model and actual SSC of Wildcat Bridge Creek.

Pine Knot North

Forty-eight grab samples were collected from this site, but only thirty-six of these were collected used in the calibration procedure. The first subsample for each concentration level was discarded due to very high actual concentration as compared to the other three subsamples. The sediment from this site is dominated by sand and silt particles and once the first subsample was collected, a big drop in sediment concentration was observed for all concentration levels. The range of SSC for this calibration is 83 to 8,209 mg/L which is off the range that of previous calibration done by Bigham (2012).

The results of one-variable linear regression for this site were summarized in Table 6. The best one-variable model is the one using IR45 as predictor with R^2 value of 0.7267, followed by that of OR180 with R^2 =0.7178 and OR45 with R^2 = 0.6396. Figures 11 to 13 shows the three one-variable linear models.

Table 6. Summary of SAS one-variable linear regression of Pine Knot North's sediment sensor.

Source	Df	Parameter estimate	p-value	Root MSE	R^2
IR45 vs SSC	1	x	<0.0001	1339.14470	0.6559
Intercept	1	-6021.90056	<0.0001	X	x
IR45 (slope)	1	6.98331	<0.0001	X	x
OR45 vs SSC	1	x	<0.0001	1411.52520	0.6177
Intercept	1	-4021.65428	0.0002	X	x
OR45(slope)	1	15.14467	<0.0001	X	x
OR180 vs SSC	1	x	<0.0001	1433.50875	0.6057
Intercept	1	6890.63771	<0.0001	X	x
OR180(slope)	1	-4.32958	<0.0001	X	x

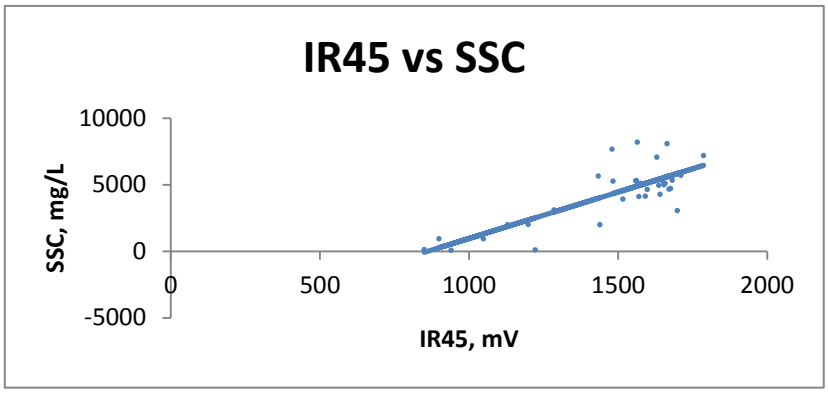

Figure 11. SSC linear model of the sensor in Pine Knot North using IR45 signal.

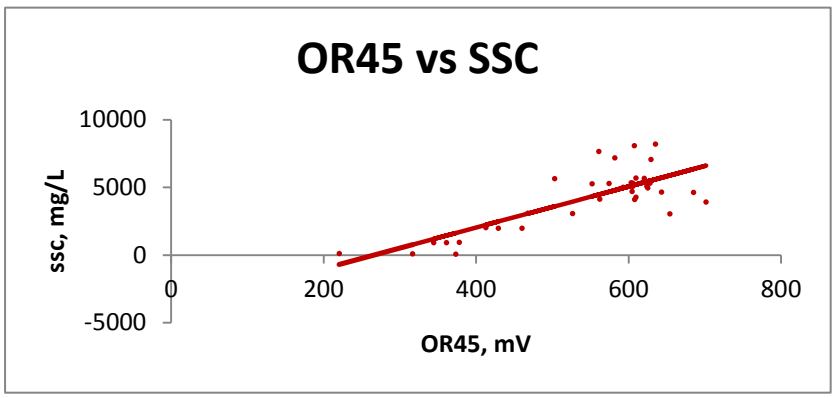

Figure 12. SSC linear model of the sensor in Pine Knot North using OR45 signal.

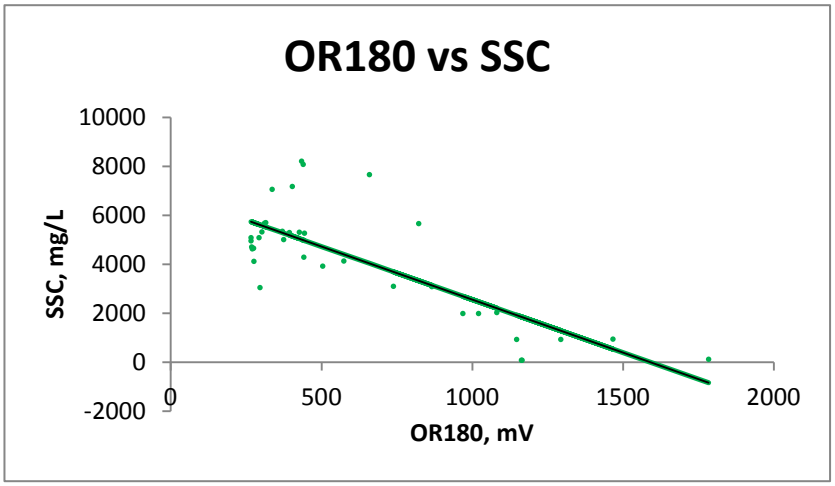

Figure 13. SSC linear model of the sensor in Pine Knot North using OR180 signal.

Multiple-variable regression was also done in SAS and the results were tabulated in Table 7. Best model was determined using the backward selection method of SAS. The one-variable model using IR45 as predictor was the best model for this site. Although R^2 of the three-variable model and the two-variable model using IR45 and OR45 were higher, the effect on Root MSE was not that significant as compared to the one-variable IR45 model.

Table 7. Two-variable and three-variable calibration model for the sensor in Pine Knot North.

Model	Variables	Equation*	Root MSE*	R^2
2-variable	IR45-OR45 vs SSC	SSC = 4.7*IR45 + 5.5*OR45 – 5730.5	1331.2	0.6700
	IR45-OR180 vs SSC	SSC = 5.8*IR45 – 0.78*OR180 – 3878.4	1354.9	0.6581
	OR45-OR180 vs SSC	SSC = 9.2*OR45 – 1.8*OR180 + 364.2	1412.1	0.6286
3-variable	All vs SSC	SSC = 5.4*IR45 + 7.1*OR45 + 0.9*OR180 – 8056.6	1348.5	0.6716

*SSC and Root MSE in mg/L; IR45, OR45 and OR180 in mV

Pine Knot South

The first subsample for each concentration level was discarded due to very high actual concentration as compared to the other three subsamples. Out of the forty-eight samples, thirty-six samples were left and were used in the calibration procedure. The sediment from this site is the same in Pine Knot North because these two sites are in a single stream. The range of SSC for this calibration is 890 to 34,500 mg/L which is outside the range of the previous calibration done by Bigham (2012).

The results of one-variable linear regression for this site were summarized in Table 8. The best one-variable model is the one using OR45 as predictor with R^2 value of 0.6833, followed by that of IR45 with R^2 =0.6729 and OR45 with R^2 = 0.6523. Figures 14 to 16 show the three one-

variable linear models. The uncertainties of these models are much higher than the other sites exceeding ±10,000 mg/L.

Table 8. Summary of SAS one-variable linear regression of Pine Knot South's sediment sensor.

Source	*df*	*Parameter estimate*	*p-value*	*Root MSE*	R^2
IR45 vs SSC	1	x	<0.0001	5024.56624	0.6729
Intercept	1	-14354	0.0002	x	x
IR45 (slope)	1	15.13724	<0.0001	x	x
OR45 vs SSC	1	x	<0.0001	4944.21176	0.6833
Intercept	1	-10580	0.0009	x	x
OR45 (slope)	1	53.39945	<0.0001	x	x
OR180 vs SSC	1	x	<0.0001	5180.27728	0.6523
Intercept	1	21057	<0.0001		x
OR180 (slope)	1	-17.98099	<0.0001	x	x

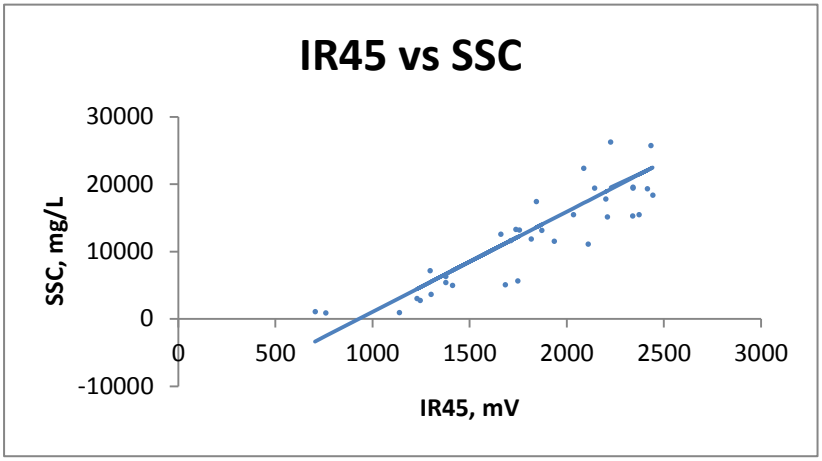

Figure 14. SSC linear model of the sensor in Pine Knot South using IR45 signal.

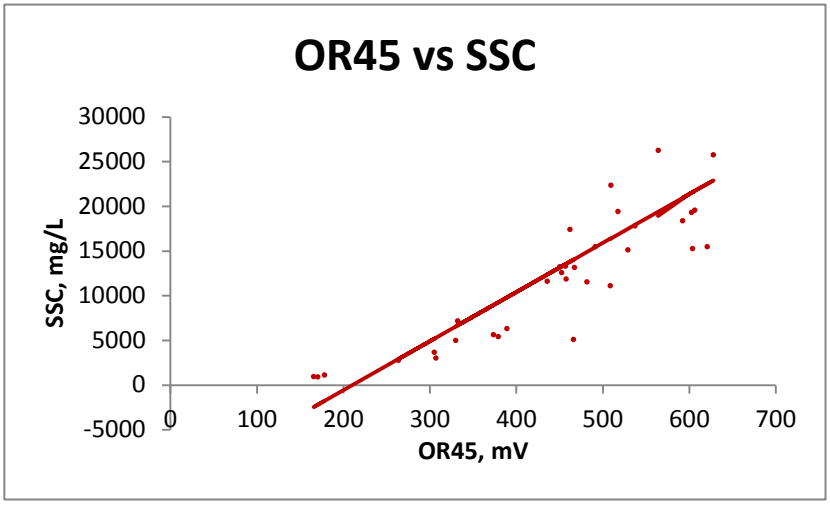

Figure 15. SSC linear model of the sensor in Pine Knot South using OR45 signal.

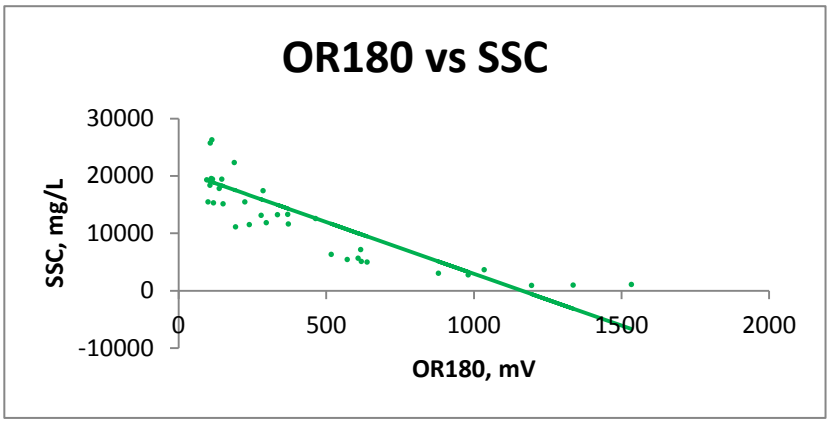

Figure 16. SSC linear model of the sensor in Pine Knot South using OR180 signal.

Multiple-variable regression was also done in SAS and the results were tabulated in Table 9. The best model using the backward selection regression of SAS was the one-variable model using IR45. But, if the basis of the selection is R^2 and Root MSE alone, the best one-variable model should be that one using OR45, and the best two-variable model is the one using IR45 and OR180 as predictors. The three-variable model R^2 does not vary significantly with that of the best two-variable model.

Table 9. Two-variable and three-variable calibration model for the sensor in Pine Knot South.

Model	Variables	Equation*	Root MSE*	R^2
2-variable	IR45-OR45 vs SSC	SSC 6.0*IR45 + 33.2*OR45 – 12449	4964.4	0.6901
	IR45-OR180 vs SSC	SSC = 9.2*IR45 – 7.9*OR180 – 16.6	4927.2	0.6947
	OR45-OR180 vs SSC	SSC = 42.1*OR45 – 4.0*OR180 – 3795.7	4997.9	0.6859
3-variable	All vs SSC	SSC = 7.4*IR45 + 11.5*OR45 – 6.1*OR180 – 2691.9	4996.3	0.6956

*SSC and Root MSE in mg/L; IR45, OR45 and OR180 in mV

Upatoi Norh

Thirty-six samples were also considered in the calibration procedure for this site. Like Pine Knot, the sediment from this site is dominated by sand and silt particles. The calibration range this time done was between 430 to 31,600 mg/L.

For the sensor in this site, only IR45 signal is usable. The other two signals did not respond to the varying concentrations. Regression was done and the output of SAS regression is summarized in Table 10 and the model is illustrated in Figure 17. The coefficient of determination for this site is fairly high (R^2=0.8420) and can be improved further by not including the samples after IR45 reached saturation.

Table 10. Summary of SAS one-variable linear regression of Upatoi North's sediment sensor.

Source	Df	Parameter estimate	p-value	Root MSE	R^2
IR45 vs SSC	1	x	<0.0001	3629.81693	0.8420
Intercept	1	-5742.97494	0.0007	X	x
IR45 (slope)	1	11.82973	<0.0001	X	x

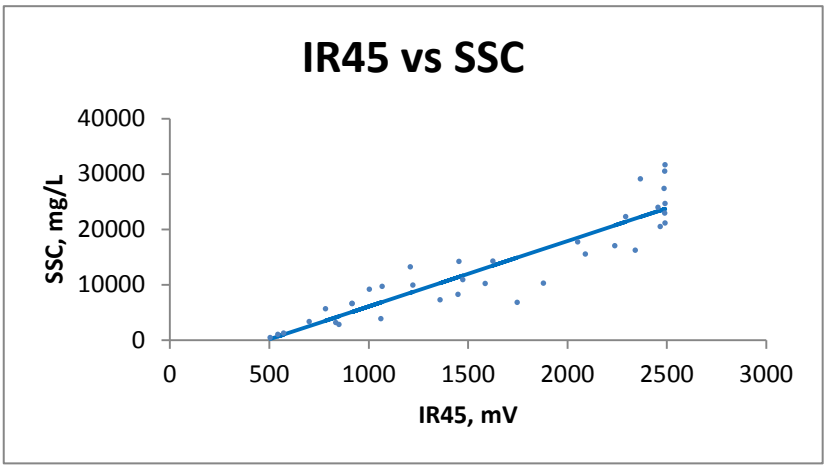

Figure 17. SSC linear model of the sensor in Upatoi North using IR45 signal.

Upatoi South

Forty-two samples were collected and considered in the calibration for this site. Table 11 summarizes the suspended sediment concentration and the corresponding processed signals for IR45, OR45 and OR180. The calibration range was between 1,000 to 25,100 mg/L which is again outside the range of naturally occurring suspended sediment concentration in Upatoi creek.

Results of SAS one-variable linear regression were summarized in Table 14. Among the three signals, OR45 model had the highest coefficient of determination (R^2 = 0.7749) followed by the two signals (OR45 and OR180) with R^2 not different from each other. Figures 18 to 20 show the three one-variable linear models for predicting SSC.

Table 11. Summary of SAS one-variable linear regression of Upatoi South's sediment sensor.

Source	*df*	*Parameter estimate*	*p-value*	*Root MSE*	*R^2*
IR45 vs SSC	1	x	<0.0001	3278.15299	0.6778
Intercept	1	-4953.80384	0.0021	x	X
OR45 (slope)	1	17.68047	<0.0001	x	X
OR45 vs SSC	1	x	<0.0001	2740.26096	0.7749
Intercept	1	-2635.90344	0.0124	x	X
IR45 (slope)	1	24.99422	<0.0001	x	X
OR180 vs SSC	1	x	<0.0001	3324.23015	0.6687
Intercept	1	20288	<0.0001	x	X
OR180 (slope)	1	-13.25151	<0.0001	x	X

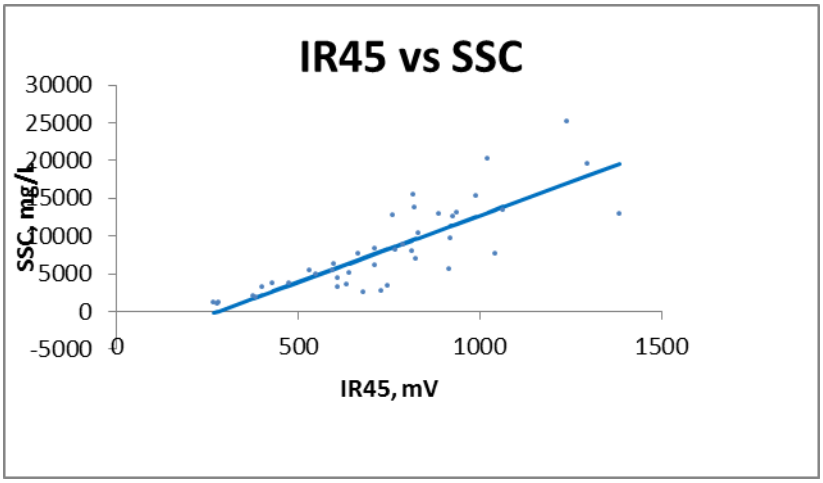

Figure 18. SSC linear model of the sensor in Upatoi South using IR45 signal.

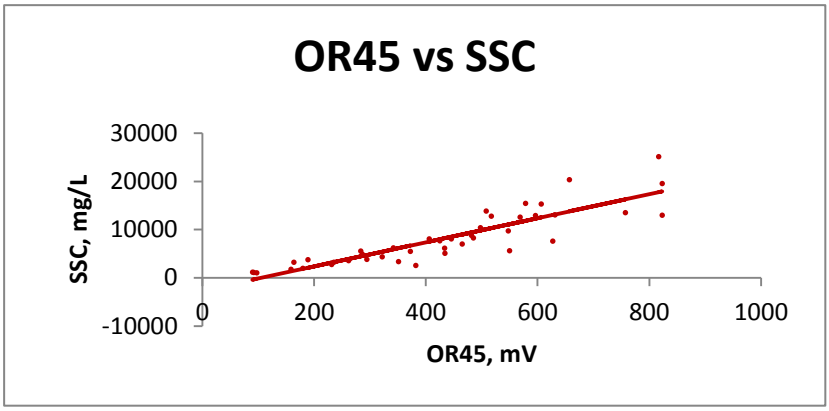

Figure 19. SSC linear model of the sensor in Upatoi South using OR45 signal.

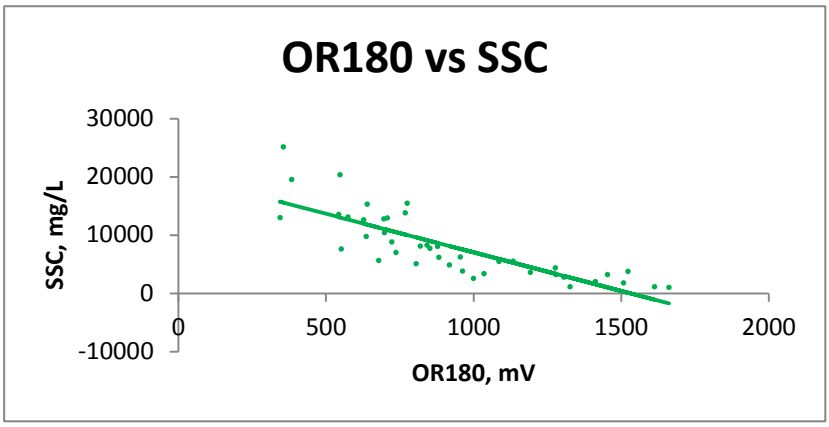

Figure 20. SSC linear model of the sensor in Upatoi South using OR180 signal.

Results of multiple-variable linear regression were summarized in Table 14. The best two-variable linear model is the one using OR45 and OR180 as predictors with a coefficient of determination value of 0.7801. In backward elimination method of SAS the one-variable model using OR45 is not significantly different from the two-variable model using OR45 and OR180, which suggest that in predicting SSC of Upatoi South, OR45 alone is sufficient.

Table 14. Two-variable and three-variable calibration model for the sensor in Upatoi South

Model	**Variables**	**Equation***	**Root MSE***	**R^2**
2-variable	IR45-OR45 vs SSC	SSC = -4.6*IR45 + 30.8*OR45 – 1732.2	2750.5	0.7788
	IR45-OR180 vs SSC	SSC = 9.9*IR45 – 6.5*OR180 + 6791.8	3166.0	0.7070
	OR45-OR180 vs SSC	SSC = 31.5*OR45 + 3.9*OR180 – 9054.5	2742.4	0.7801
3-variable	All vs SSC	SSC = -5.1*IR45 + 38.5*OR45 + 4.2*OR180 – 8555.1	2747.9	0.7849

*SSC and Root MSE in mg/L; IR45, OR45 and OR180 in mV